Tara Ní Néill

DEVELOPMENT OF MIRNA THERAPEUTICS TARGETING INTERVERTEBRAL DISC DEGENERATION

Trinity College Dublin, February 2026

A thesis submitted to Trinity College Dublin, the University of Dublin in partial fulfilment of the requirements for the degree of

Doctor of Philosophy

Supervisor: Professor Conor T. Buckley

Internal Examiner: Professor Daniel J. Kelly

External Examiner: Professor Devina Purmessur

Declaration

I declare that this thesis has not been submitted as an exercise for a degree at this or any other university and it is entirely my own work. I confirm that the work has been completed in full compliance with relevant university policies, including the Academic Integrity policy, the Trinity Policy on Good Research Practice, and the guidance on AI and GenAI in Teaching, Learning, Assessment and Research.

I agree to deposit this thesis in the University's open access institutional repository or allow the Library to do so on my behalf, subject to Irish Copyright Legislation and Trinity College Library conditions of use and acknowledgement.

I consent to the examiner retaining a copy of the thesis beyond the examining period, should they so wish (EU GDPR May 2018).

Tara Ní Néill

Dublin, February 2026

Summary

Low back pain is one of the leading causes of disability worldwide, with its prevalence continuing to rise. Intervertebral disc (IVD) degeneration, particularly that of the central nucleus pulposus (NP) region, is widely considered a primary contributor to this condition. However, current treatment strategies are largely conservative and do not address the underlying disruption in tissue homeostasis that drives the degenerative cascade. This imbalance is characterised by progressive loss and disorganisation of key extracellular matrix (ECM) components, accompanied by heightened inflammatory and catabolic activity within the disc microenvironment. MicroRNAs (miRNAs) regulate the expression of multiple target genes simultaneously, making them attractive candidates for therapeutic modulation of complex degenerative pathways. This thesis therefore aimed to investigate miRNA-based strategies to develop a translationally relevant injectable therapy capable of exerting a multimodal effect: suppressing inflammation while promoting regenerative ECM synthesis.

Initially, miRNAs identified from the literature were systematically screened in monolayer cultures to determine their suitability for IVD delivery, with a focus on anti-catabolic and pro-matrix effects. In parallel, two cell-penetrating peptides (CPPs) were evaluated to optimise delivery to the nucleus pulposus (NP). To enhance therapeutic efficacy, selected miRNAs were co-delivered in pairs to assess potential synergistic effects. To gain a better understanding of the effects following miRNA delivery, ex vivo organ culture models were employed. This initial screening suggest a synergistic effect when delivering the miRNAs in pairs rather than isolation, particularly in relation to the development of an anti-catabolic niche identified in rat IVD organs. Notably, these investigations identified a dual-miRNA pairing most suitable for further investigations, providing a framework to build upon in the subsequent chapters.

The second objective explored adjunct stimulation strategies by combining dual-miRNA treatment with human platelet lysate (HPL), a clinically established regenerative biologic in orthopaedics and musculoskeletal medicine. Alongside the incorporation of ex vivo organ culture models, a biomimetic extracellular matrix (ECM) NP gel analogue was employed to recapitulate the disc microenvironment in vitro. This NP cell-laden analogue incorporated cells derived from degenerated patient NP tissue, thereby offering vital clinical insight into cell response. Central to the results here was the sustained maintenance of the anti-catabolic niche generated by dual-miRNA delivery. Moreover, HPL supplementation enhanced the protein expression of ECM markers, suggesting a shift towards a pro-regenerative effect. Importantly, both culture systems exhibited comparable treatment responses, reinforcing the translational potential of this approach and supporting the development of a scalable, high-throughput platform incorporating human cells to screen potential therapeutics.

Recognising that cell loss is a hallmark of disc degeneration, the third aim compared dual-miRNA stimulation in native NP cells and bone marrow-derived stem cells (BMSCs) to determine the most appropriate cellular target for IVD therapy. Utilising increasingly complex culture systems divergent responses were revealed between the cell populations. Notably, BMSCs exhibited a pro-catabolic response following dual-miRNA transfection in two- and three-dimensional cultures. This effect was mitigated in ex vivo organ culture, demonstrating the importance of physiologically relevant culture systems. Overall, dual-miRNA transfected NP cells demonstrated superiority to BMSCs through the enhancement of ECM markers and suppression of inflammatory and catabolic markers. These findings suggest NP cells as a more appropriate delivery strategy for dual-miRNA-based IVD therapies.

Finally, for the first time, the optimised dual-miRNA formulation was evaluated in a preclinical large animal model of mild IVD degeneration to assess safety, efficacy, and translational feasibility. It was observed that dual-miRNA enhanced ECM marker expression while concurrently suppressing inflammatory and catabolic signalling pathways. In contrast, delivery of NP cells, both naïve and dual-miRNA-transfected, was associated with metabolic disruption, compromised matrix integrity, and exacerbation of degenerative features. Taken together, the results presented here highlight the critical influence of the disc microenvironment while considering cell-based therapeutic strategies. Furthermore, they reveal the promise of a novel dual-miRNA treatment in a clinically relevant in vivo model of mild IVD degeneration.

Collectively, this thesis demonstrates the promise of miRNA-based therapeutics as a component of injectable treatments for IVD degeneration. By investigating their use alone, in combination, and alongside regenerative adjuncts such as HPL and cellular targets, and by validating findings in physiologically relevant in vitro and preclinical models, this thesis provides a strong foundation for the clinical translation of miRNA-driven therapies to restore disc homeostasis and treat degeneration of the IVD.

Acknowledgements

Firstly, I would like to sincerely thank my supervisor Conor, for your continued and valued support over the last few years. Throughout the entire process and the challenges it has presented you have always been there with a fresh outlook and perspective, without which I'm not sure we'd be at this point, and I'm truly grateful for your guidance and mentorship. I would like to extend my thanks to Prof. Danny Kelly and Prof. Michael Monaghan for serving on my doctoral committee and their invaluable insights throughout the years. I would also like to thank my external examiner Prof. Devina Purmessur for taking the time to read this thesis and travel to examine it, I really appreciate it.

None of this work would have been possible without help and collaboration, both within and without TBSI. For the animal work, Audrey, Martha, Mark, and Laavanya for all the rat help. In UCD, thank you honestly to all the team, but especially Pieter, Margot, Michael, and Sarah. For all the human work involving the Mater Misericordiae University Hospital, thank you to Joe and Stacey. Thank you, Simon, for all the help and support in TBSI. To Caroline, Fergal, and James, thank you for the valuable collaboration throughout the project.

The Buckley lab and TCBE has had some amazing members over the last few years, to whom I'm eternally grateful, not just from a research perspective but a personal. I will hopefully see most of you soon to tell you all in person, so this will be brief. Marcos, thank you for taking me under your wing and cracking jokes. Tug, for that first initial tour and impromptu lab tech class, I couldn't have asked for a better introduction to the lab, and out of hours companion. Jake it's been an absolute pleasure; you kept us all going. Jijo myself and the Buckley lab would be lost without you. Niamh, I couldn't have wished for a better person to start on the PhD journey with, and it's been an absolute pleasure to share the ups, downs, and meltdowns with you. Thank you really and truly to Morgan, Mimma, Matthia, Marcin (all M's?). For all the good times, hard times, and pints in between, I'm so fortunate to have met you all and for you to be part of my life.

Finally, though they are the most important, they are often the most forgotten, my family, without whose love and backing nothing would be possible. To my Mam, for being the most supportive and amazing person I know, you believe in me when I falter and have no belief left. My Dad, whose a calm in the storm, always offering guidance and knowing the right thing to say. Dáire, a complete rock in comparison to my flapping. To my granny and grandad, who have supported during this journey, I'm sure you probably didn't need a housemate, but I want you to know I'll be always grateful. Last and most certainly not least, thank you Andrew for everything. Listening to my rants and spirals, you could probably recite this thesis in and of itself at this point. Throughout this whole time, you've been a constant source of joy, love, and light in the darkest of days, I'm truly fortunate.

Table of Contents

List of Figures

List of Tables

Nomenclature

2D Two-dimensional

3D Three-dimensional

AB Alcian blue

ACAN Aggrecan

ADAMTS A disintegrin and metalloprotease with thrombospondin motifs

AF Annulus fibrosis

AGO Argonaute

APAF1 Apoptotic peptidase activating factor

AREC Animal Research Ethics Subcommittee

BBC BCL2 Binding component

BDNF Brain-derived neurotrophic factor

BMP Bone morphogenicf protein

BMSC Bone marrow derived stem cell

BSA Bovine serum albumin

cABC Chondtroitinase ABC

CEP Cartilage endplate

COL1 Collagen type I

COL2 Collagen type II

CPP Cell penetrating peptide

CS Chondroitin sulphate

CT Computer tomography

CXCL12 C-X-C Motif chemokine ligand 12

DAB Diaminobenzidine

Df Diclofenac

DHI Disc height index

dw dry weight

ECM Extracellular matrix

EGF Epidermal growth factor

ERK Extracellular signal-related kinase

EthD-1 Ethidium homodimer

EU European Union

EV Extracellular vesicle

FASLG Fas ligand

FBS Foetal bovine serum

FGF Fibroblastic growth factor

FLR GET peptide FGF2B-LK12-8R

FOXF1 Forkhead box F1

FSE Fast spin echo

GAG Glycosaminoglycan

GCSF Granulocyte-colony stimulating factors

GDF Growth differentiation factor

GET GAG-binding enhanced transduction

GF Growth factor

GJA Gap junction protein alpha

GO Gene ontology

GTP Guanosine triphosphate

H&E Haematoxylin and eosin

HA Hyaluronic acid

HAc Acetic acid

HG High glucose

HPL Human platelet lysate

HPRA Health Products Regulatory Authority

HRP Hydrogen peroxide

IDD Intervertebral disc degeneration

IL Interleukin

IL-1RA Interleukin-1 receptor antagonist

IMS Industrial methylated spirits

IPSC Induced pluripotent stem cell

ITGB1 Integrin-beta-1

IVD Intervertebral disc

KO Knock out

KRT19 Keratin 19

L Lumbar

LacZ Beta-galactosidase

LAP Lithium phenyl-2, 4, 6-trimethylbenzoylphosphinate

LBP Low back pain

LG Low glucose

LPS Lipopolysaccharide

MA Methacrylic anhydride

MAPK Mitogen activated protein kinase

miRNA microRNA

MMP Matrix metalloproteinases

MPC Mesenchymal precursor cell

mRNA messenger RNA

mESC Murine embryonic stem cell

MRI Magnetic resonance imaging

MYD88 Myeloid differentiation primary response protein 88

NF-κB Nuclear factor kappa-light-chain-enhancer

NGF Nerve growth factor

NLRP1 Nod-like receptor Pyrin domain containing 1

NP Nucleus pulposus

NSAID Non-steroidal anti-inflammatory drug

NS Non-significant

NT Non-transfected

N:P NitrogenPhosphate

OA Osteoarthritis

OCT Optimum cutting temperature

ODI Oswestry disability index

PBS Phosphate buffered saline

PBMC Peripheral blood mononuclear cells

PDGF Platelet-dervied growth factor

PEG Polyethylene glycol

PEI Polyethyleneimine

PFA Paraformaldehyde

PGL Proteoglycans

P13K Phosphoinositide 3-kinase

PL Platelet lysate

PPI Protein interaction network

PR Picrosirius red

pDNA Plasmid DNA

RCT Randomised clinical trial

RALA Cationic 30mer amphipathic peptide

RISC RNA-induced silencing complex

ROI Region of interest

ROS Reactive oxygen species

RT Room temperature

RTqPCR Reverse transcription quantitative polymerase chain reaction

SLAM Suspended layer additive manufacturing

siRNA Silencing RNA

SIRT Sirtuin

SOX9 Sry-Box TF 9

STRING Search Tool for the Retreival of Interacting Genes

SVF Stromal vascular fraction

T Thoracic

TBHP Tert-Butyl hydroperoxide

TGF Transforming growth factor

TF Transcription factor

TIMP Tissue inhibitor of matrix metalloproteinase

TNF Tumour necrosis factor

TNFR Tumour necrosis factor receptor

UCD University College Dublin

US United States

VAS Visual analogue score

VEGF Vascular endothelial growth factor

WT Wild type

ww wet weight

XPAN Expansion media

Publications

First-Author Journal Articles

Ní Néill, T., Barcellona M.N., Wilson, N., O'Brien, F.J., Dixon, J.E., Curtin, C.M., Buckley, C.T (2024) "In vitro and ex vivo screening of microRNA combinations with enhanced cell penetrating peptides to stimulate intervertebral disc regeneration". *JOR Spine*, 7(2) doi: 10.1002/jsp2.1366

Contribution: Contributed substantially to the conception and design of the work. Performed the acquisition and interpretation of literature, data analysis, presentation and interpretation of results, drafting the article, critical revision, and final approval.

Ní Néill, T., Wilson, N., McDonnell, J.M., O'Brien, F.J., Dixon, J.E., Brama, P.A.J., Curtin, C.M., Buckley, C.T (2026) "Comparative analysis of dual-miRNA mediated stimulation of nucleus pulposus and bone marrow derived stem cells for intervertebral disc repair". *JOR Spine, 9(2).* doi: 10.1002/jsp2.70198

Contribution: Made significant contributions to the conception and design of the work. Conducted the literature review, data acquisition and analysis, interpreted and presented the findings, drafted the manuscript, performed critical revisions, and provided final approval of the version to be published.

Ní Néill, T., Wilson N., Thomas J., McDonnell, J.M., Darwish, S.L., Butler, J.S., O'Brien, F.J., Dixon, J.E., Curtin, C.M., Buckley, C.T (2026) "Restoring Disc Matrix Homeostasis: Dual-miRNA and Human Platelet Lysate as a Novel Therapeutic Strategy". *Materials Today Bio 38:103190.* doi: 10.1016/j.mtbio.2026.103190

Contribution: Played a key role in the conception and design of the study. Carried out the literature review, data collection and analysis, interpreted and presented the results, prepared the manuscript draft, undertook critical revisions, and approved the final version for publication.

Co-Authored Journal Articles

McDonnell, E.E., Barcellona M.N., Wilson, N., **Ní Néill, T.**, Brama, P.A., Cunniffe, G., Darwish, S., Butler, J.S., Buckley, C.T. (2023) " Preclinical to clinical translation for intervertebral

disc repair: Effects of species-specific scale, metabolism, and matrix synthesis rates on cell-based regeneration." *JOR Spine*, doi: 10.1002/jsp2.1279

Contribution: Contributed to the acquisition of laboratory samples, critically revised the article, and approved the final version.

Barcellona M.N., **Ní Néill, T.**, O'Brien, F.J., Dixon, J.E., Curtin, C.M., Buckley, C.T. (2024) "Modulation of inflammation and regeneration in the intervertebral disc using enhanced cell-penetrating peptides for microRNA delivery". *Advanced NanoBiomed Research*, doi: 10.1002/anbr.202300112

Contribution: Contributed to collection of laboratory samples and data, analysis, interpretation of results, critically revised and approved the final draft.

McDonnell, E.E., **Ní Néill, T.**, Wilson, N., Darwish, S.L., Butler, J.S., Buckley, C.T. (2024) "In silico modelling the potential clinical effect of growth factor treatment on the metabolism of human nucleus pulposus cells." *JOR Spine*, doi: 10.1002/jsp2.1352

Contribution: Contributed to the acquisition of laboratory data, analysis, and interpretation. Critically revised and approved the final draft of the manuscript.

Wilson, N., **Ní Néill, T.,** McDonnell, J.M., McDonnel, E.E., Brama, P.A.J., Buckley, C.T. (2026) "Influence of the intervertebral disc microenvironment on matrix synthesis and metabolism in goat nucleus pulposus cells." *JOR Spine*, doi: 10.1002/jsp2.70160

Contribution: Contributed to the acquisition of laboratory data, analysis, and interpretation. Critically revised and approved the final draft of the manuscript.

Maggio, M., Martins, C.S., Almasri, R., Petrousek, S., Brunet, M.Y., Madden, L.A., Gorgun, C., **Ní Néill, T.,** Buckley, C.T., O'Driscoll, L., Hoey, D.A. (2026) "Extracellular vesicle-mediated crosstalk in bone: miRNA-150-5p as a mechanosensitive regulator of osteoclastogenesis." *In preparation, Molecular Therapy.*

Contribution: Contributed to the acquisition of laboratory data, specifically the transfection experiments where miRNA-150-5p was delivered in vitro. Critically revised the manuscript and approved the final draft.

Wilson, N., **Ní Néill, T.,** McDonnell, J.M., McDonnel, E.E., Darwish, S.L., Butler, J.S., ., Buckley, C.T (2026) "Defining the Human Nucleus Pulposus Microenvironment and Its Impact on Cell Matrix Synthesis and Metabolic Activity. " *In review, JOR Spine.*

Contribution: Contributed to the collection, analysis, and interpretation of laboratory data. Critically reviewed, revised, and approved the final version of the manuscript.

Conferences and symposia

Podium Presentations

1. **Ní Néill T.,** Wilson, N., McDonnell, J.M., Brama, P.A.J., O'Brien, F.J., Dixon, J.E., Curtin, C.M., Buckley, C.T. *miRNA-pair delivery supported by platelet lysate to restore NP cell homeostasis.* In: School of Engineering Research Symposium, Dublin, Ireland, 3rd December 2025.
2. Wilson, N., **Ní Néill T.,** McDonnell, J.M., Darwish, S., Butler, J.S., Buckley, C.T., *Human intervertebral disc microenvironment: Profiling and in vitro cellular response.* In: Irish Spine Society Annual Meeting, Galway, Ireland, 18th October 2025.
3. Thomas, J., **Ní Néill T.,** Wilson, N., McDonnell, J.M., Brama, P.A.J., Buckley, C.T., *Next-generation injectable hydrogel for nucleus pulposus replacement and disc repair.* In: Irish Spine Society Annual Meeting, Galway, Ireland, 18th October 2025.
4. **Ní Néill T.,** Wilson, N., McDonnell, J.M., O'Brien, F.J., Dixon, J.E., Curtin, C.M., Buckley, C.T. *Targeting homeostasis restoration in nucleus pulposus cells of the intervertebral discs via miRNA-paired delivery supported by human platelet lysate.* In: European Chapter of the Tissue Engineering Research Society (TERMIS), Freiburg, Germany, 19th-23rd May 2025.
5. Wilson, N., **Ní Néill T.,** McDonnell, J.M., Darwish, S., Butler, J., Buckley, C.T. *Characterisation of the human intervertebral disc microenvironment and recapitulated in vitro cellular response.* In: European Chapter of the Tissue Engineering Research Society (TERMIS), Freiburg, Germany, 19th-23rd May 2025.
6. McDonnell, J.M., Thomas, J., Wilson, N., **Ní Néill T.,** Brama, P.A.J., Butler, J., Buckley, C.T. *Leptin induces extracellular matrix stiffness changes which induce cartilage endplate matrix composition and cellular senescence.* In: European Chapter of the Tissue Engineering Research Society (TERMIS), Freiburg, Germany, 19th-23rd May 2025.
7. Maggio, M., Martins, C., Almasri, R., Petrousek, S., Brunet, M.Y., **Ní Néill, T.,** Buckley, C.T., O'Driscoll, L., Hoey, D.A. *Bone-derived extracellular vesicles as emerging anti-catabolic therapeutics for bone regeneration.* In: European Chapter of the Tissue Engineering Research Society (TERMIS), Freiburg, Germany, 19th-23rd May 2025.
8. Maggio, M., Martins, C., Almasri, R., Petrousek, S., Brunet, M.Y., **Ní Néill, T.,** Buckley, C.T., O'Driscoll, L., Hoey, D.A. *Mesenchymal-derived bone cells regulated osteoclastogenesis via an extracellular vesicle-mediated mechanism.* In: International Society for Extracellular Vesicle, Vienna, Austria, 24th-27th April 2025.
9. Maggio, M., Martins, C., Almasri, R., Petrousek, S., Brunet, M.Y., **Ní Néill, T.,** Buckley, C.T., O'Driscoll, L., Hoey, D.A *Mesenchymal-derived bone cells regulate osteoclastogenesis via an extracellular vesicle-mediated mechanism that is dependent on the stage of mesenchymal*

lineage commitment and the mechanical environment. In: Proceedings of the Orthopaedic Research Society (ORS) Annual Meeting, Phoenix, USA, February 7th-11th 2025.

10. **Ní Néill T.,** Wilson, N., McDonnell, J.M., Brama, P.A.J., O'Brien, F.J., Dixon, J.E., Curtin, C.M., Buckley, C.T. *Advancing intervertebral disc regeneration: A comparative study of dual miRNA stimulated nucleus pulposus and bone marrow-derived stem cells.* In: Proceedings of the 30th Annual Conference of the section of Bioengineering of the Royal Academy of Medicine in Ireland, Athlone, Ireland, January 4th-5th 2025.
11. Wilson, N., **Ní Néill T.,** McDonnell, J.M., Darwish, S., Butler, J., Buckley, C.T. *Comparative analysis of in vivo and ex vivo models for microenvironmental effects of intervertebral disc degeneration.* In: Proceedings of the 30th Annual Conference of the section of Bioengineering of the Royal Academy of Medicine in Ireland, Athlone, Ireland, January 4th-5th 2025.
12. Maggio, M., Martins, C., Almasri, R., Petrousek, S., Brunet, M.Y., **Ní Néill, T.,** Buckley, C.T., O'Driscoll, L., Hoey, D.A. *Bone-derived vesicles and associated miRNAs: Unravelling novel nanotherapeutics for bone regeneration.* In: Proceedings of the 30th Annual Conference of the section of Bioengineering of the Royal Academy of Medicine in Ireland, Athlone, Ireland, January 4th-5th 2025.
13. Mc Donnell, J.M., Wilson, N., **Ní Néill T.,** Brama, P.A.J., Butler, J., Buckley, C.T. *The role of leptin on cartilage endplate matrix synthesis and reactive oxygen species generation.* In: Proceedings of the 7th Orthopaedic Research Society Philadelphia Spine Research Society, Pennsylvania, 10th-14th November 2024.
14. **Ní Néill T.,** Barcellona M.N., O'Brien, F.J., Dixon, J.E., Curtin, C.M., Buckley, C.T *microRNA screening in the nucleus pulposus of the intervertebral disc to drive regenerative factors.* In: School of Engineering Research Symposium, Dublin, Ireland, 26th October 2023.
15. **Ní Néill T.,** Barcellona M.N., O'Brien, F.J., Dixon, J.E., Curtin, C.M., Buckley, C.T *microRNA screening of regenerative factors in the nucleus pulposus of the intervertebral disc using cell penetrating peptide delivery.* In: European Chapter of the Tissue Engineering Research Society (TERMIS), Manchester, UK, 28th-31st March 2023
16. **Ní Néill T.,** Barcellona M.N., O'Brien, F.J., Dixon, J.E., Curtin, C.M., Buckley, C.T. *Investigation of the effect of microRNA transfection on healthy and unhealthy rat nucleus pulposus cells.* In: Proceedings of the 28th Annual Conference of the section of Bioengineering of the Royal Academy of Medicine in Ireland, Meath, Ireland, 27th-28th January 2023.
17. McDonell J.M., **Ní Néill T.,** Wilson, N., Barcellona M.N., Buckley, C.T. *Lumbar disc disease in females: Exploring the oestrogen-iron relationship and its effect on vertebral cartilaginous endplate cells.* In: Proceedings of the 28th Annual Conference of the section of Bioengineering of the Royal Academy of Medicine in Ireland, Meath, Ireland, 27th-28th January 2023.
18. McDonnell, E.E., Barcellona M.N., Wilson, N. **Ní Néill, T**., Brama, P.A.J., Cunniffe, G., Darwish, S., Butler, J.S., Buckley, C.T. *From preclinical to clinical translation of intervertebral*

disc cell-based regeneration: In-silico modelling to elucidate the effects of species-specific scale, metabolism, and matrix synthesis rates. In: Proceedings of the 28th Annual Conference of the section of Bioengineering of the Royal Academy of Medicine in Ireland, Meath, Ireland, 27th-28th January 2023

19. **Ní Néill T.,** Barcellona M.N., O'Brien, F.J., Dixon, J.E., Curtin, C.M., Buckley, C.T. *microRNA modulation for nucleus pulposus regeneration in the intervertebral disc.* In: Proceedings of the 28th Annual Conference of the section of Bioengineering of the Royal Academy of Medicine in Ireland, Galway, Ireland, 20th-21st May 2022.
20. **Ní Néill T.,** Barcellona M.N., O'Brien, F.J., Dixon, J.E., Curtin, C.M., Buckley, C.T. *microRNA modulation of regenerative factors in nucleus pulposus cells of the intervertebral disc.* In: Proceedings of the 6th Orthopaedic Research Society Philadelphia Spine Research Society, Pennsylvania, 6th-10th November 2022.

Poster Presentations

1. **Ní Néill T.,** Wilson, N., McDonnell, J.M., Brama, P.A.J., O'Brien, F.J., Dixon, J.E., Curtin, C.M., Buckley, C.T. *microRNA strategies for low back pain therapies: A cellular engineering approach.* In: Irish Spine Society Annual Meeting, Galway, Ireland, 18th October 2025.
2. **Ní Néill T.,** Wilson, N., McDonnell, J.M., Darwish, S., Butler, J.S., O'Brien, F.J., Dixon, J.E., Curtin, C.M., Buckley, C.T. *Targeting disc degeneration through miRNA delivery supported by human platelet lysate.* In: Irish Spine Society Annual Meeting, Galway, Ireland, 18th October 2025.
3. Wilson, N., **Ní Néill T.,** McDonnell, J.M., McDonnell, E.E., Brama, P.A.J., Buckley, C.T. *The influence of the nucleus pulposus microenvironment on cellular matrix synthesis and metabolic rates.* In: Irish Spine Society Annual Meeting, Galway, Ireland, 18th October 2025.
4. **Ní Néill T.,** Wilson, N., McDonnell, J.M., Brama, P.A.J., O'Brien, F.J., Dixon, J.E., Curtin, C.M., Buckley, C.T. *microRNA strategies to target low back pain: A cellular engineering approach.* In: 28th Sir Bernard Crossland Symposium, University College Dublin, 4th-5th September 2025.
5. **Ní Néill T.,** Wilson, N., McDonnell, Brama, P.A.J., O'Brien, F.J., Dixon, J.E., Curtin, C.M., Buckley, C.T. *Comparative analysis of miRNA-enhanced nucleus pulposus and bone marrow stem cell therapies for intervertebral disc regeneration.* In: Trinity Biomedical Sciences Institute Research Symposium, Dublin, Ireland, 11th December 2024.
6. **Ní Néill T.,** Wilson, N., McDonnell, Brama, P.A.J., O'Brien, F.J., Dixon, J.E., Curtin, C.M., Buckley, C.T. *Enhancing intervertebral disc regeneration: Comparative analysis of miRNA-enhanced cell therapies using nucleus pulposus and bone marrow-derived stem cells.* In:

Proceedings of the 7th Orthopaedic Research Society Philadelphia Spine Research Society, Pennsylvania, 10th-14th November 2024.

7. Wilson, N., **Ní Néill T.,** McDonnell, J., Darwish, S., Butler, J., Buckley, C.T. *Microenvironmental profiling of human nucleus pulposus tissue for regeneration of the intervertebral disc.* In: Proceedings of the 7th Orthopaedic Research Society Philadelphia Spine Research Society, Pennsylvania, 10th-14th November 2024.
8. Barcellona M.N., **Ní Néill T.,** O'Brien, F.J., Dixon, J.E., Curtin, C.M., Buckley, C.T. *Non-viral cell penetrating peptides for miRNA delivery and modulation of nucleus pulposus cell phenotype.* In: AMBER Advancing Materials for Impact Conference, Dublin, Ireland, 15th-16th April 2024.
9. McDonnell, E.E., Barcellona M.N., Wilson, N. **Ní Néill, T**., Brama, P.A.J., Cunniffe, G., Darwish, S., Butler, J.S., Buckley, C.T. *From Preclinical to clinical translation of intervertebral disc cell-based regeneration-Effects of species-specific scale, metabolism, and matrix synthesis rates.* In: Proceedings of the 6th Orthopaedic Research Society Philadelphia Spine Research Society, Pennsylvania, 6th-10th November 2022.
10. Barcellona M.N., **Ní Néill T.,** O'Brien, F.J., Dixon, J.E., Curtin, C.M., Buckley, C.T. *non-viral cell penetrating peptides for miRNAdelivery and regulation of NP cell phenotype.* In: Proceedings of the 6th Orthopaedic Research Society Philadelphia Spine Research Society, Pennsylvania, 6th-10th November 2022.
11. **Ní Néill T.,** Barcellona M.N., O'Brien, F.J., Dixon, J.E., Curtin, C.M., Buckley, C.T. *microRNA screening for regenerative modulation of nucleus pulposus cells of the intervertebral disc with non-viral cell penetrating peptides.* In: Trinity Centre for Bioengineering Research Day, Dublin, Ireland, 6th December 2022.

Awards and Distinctions

1. **1st PLACE RAPID FIRE PRESENTATION**

   December 2025: *Trinity Centre for Biomedical Engineering*
2. **2nd PLACE POSTER PRESENTATION 28TH SIR BERNARD CROSSLAND SYMPOSIUM**

   September 2025: *28th Sir Bernard Crossland Symposium*
3. **BEST POSTER FOR A SENIOR RESEARCHER**

   Dec 2024: *Trinity Centre for Biomedical Engineering*
4. **1ST PLACE ORAL PRESENTATION TERMIS 2023**

   March 2023: *Student and Young Investigator Section (SYIS), Tissue Engineering and Regenerative Medicine Society, Manchester, UK*
5. **BEST PODIUM PRESENTATION NEXT GENERATION TREATMENTS, ORS-PSRS**

November 2022: *Orthopaedic Research Society, Philadelphia Spine Research Society, Pennsylvania*

Chapter 1. Introduction

1.1 Research Motivation – The need for injectable therapies

The incidence of low back pain (LBP) is rising, with an estimated 600 million people affected worldwide. This represents a growing socioeconomic burden, particularly in ageing populations, where €240 million is spent annually in the European Union (EU) alone. One of the predominant causative factors in LBP is degeneration of the intervertebral disc (IVD), primarily the central nucleus pulposus (NP). Treatments for LBP are primarily conservative in nature, involving physiotherapy and pain management, progressing to spinal surgeries when degeneration increases in severity. [1] Surgical interventions are becoming more commonplace, with over half a million discectomies performed annually in the United States (US).[2,3] Also in the US, single-level spinal fusions have seen a rise of 776% from 2000 to 2019, with this number projected to double by 2050.[4] Surgical procedures offer short term relief, however the effect is not sustained, indicating a need for more effective therapeutic options.[5] Injectable therapies aim to halt the degradative cascade before reaching the point of surgery, restoring functional balance to the IVD, though as yet none are commercially available.

At a biochemical level, degeneration of the NP is characterised by the degradation of the glycosaminoglycan (GAG)-rich extracellular matrix (ECM) and its key components. The disruption to the catabolic : anabolic homeostasis results in a loss of matrix-related transcription factors (TFs) such as Sry-Box TF 9 (SOX9), and proteins, for example, aggrecan and collagen type II. [6,7] Concurrently there is an escalation in levels of matrix degrading enzymes, namely members of the matrix metalloproteinases (MMP) and a disintegrin and metalloprotease with thrombospondin motifs (ADAMTS) families. [8-12] Restoring the intradiscal microenvironment to homeostatic balance has been the goal of numerous therapeutic attempts over the years. The introduction of growth factors, biomaterials, cell populations, and nucleic acids have gained interest over the last twenty years.

microRNAs (miRNAs), short non-coding nucleic acids, can regulate thousands of distinct genetic targets and therefore their protein outcomes, in a non-heritable manner.[13,14] Given their small size, their delivery can be more efficient than larger protein or messenger RNA (mRNA) cargoes, and their biological action requires delivery to the cell cytoplasm rather than the nucleus. Numerous vehicles have been developed, both viral and non-viral in origin. Non-viral vectors are particularly attractive due to lower immunogenicity and reduced risk of rejection, while still maintaining functional efficacy.[15,16] One such group are cell penetrating peptides (CPPs), a specific class of nanoparticle defined by their size of between 5-30 amino acids, with inherent membrane translocation sequences.[17,18] These particles can be amphiphilic and cationic in nature, fostering

cellular uptake, be it endocytic or non-endocytic, with internalisation dependent upon optimum charge ratios.

Alongside nucleic acids, the introduction of a healthy cell population that could bolster matrix production while replenishing the resident degenerated population has been widely explored. Primarily, NP and bone marrow derived stem cells (BMSCs) have been investigated, with some proceeding to human clinical trial. Discgenics (IVD cells), and Mesoblast Ltd (stem cells) have reached in-human trials, demonstrating safety but also some clinical improvements.[19-21] However, debate as to which cell type, cell number required, and whether the sufficient regeneration can be achieved without supplementary stimulation. Therefore, it is the aim of this thesis to investigate injectable miRNA therapies, exploring their potential alone and with additional human platelet lysate (HPL) and cellular stimuli.

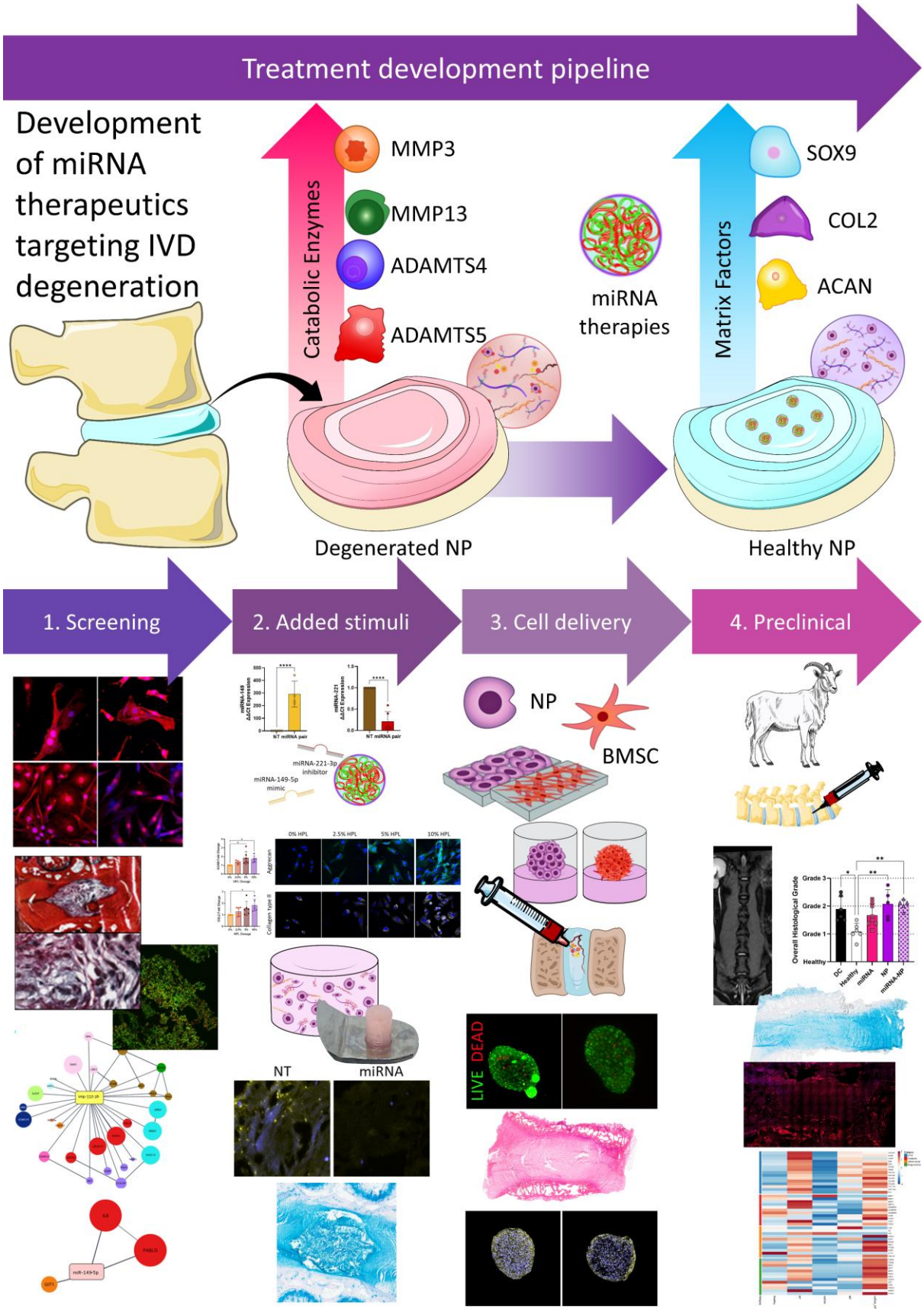

Figure 1.1 Schematic overview of the development pipeline of miRNA-based therapeutics targeting intervertebral disc degeneration. Candidate miRNAs were screened and validated,

additional stimuli explored, incorporated into cell-based delivery strategies, and preclinical evaluation in a large animal model of mild degeneration, potential miRNA treatments were evaluated to support translation towards an injectable restorative treatment.

1.2 Thesis Objectives

Considering the need for homeostatic rebalance to counteract the degenerative cascade within the IVD, this thesis examines injectable miRNA-based therapies for IVD degeneration. Primarily, stimulation with miRNAs makes up the central remit, however additional supplementation, with and without cells is explored. Given the importance of relevant preclinical models in the assessment of potential treatments, this thesis employs in vitro, ex vivo, and in vivo models of disease. Alongside miRNA stimulation alone, further supplementation approaches such as human platelet lysate (HPL) are explored as a cell-free approach with the aim of boosting the regenerative capacity of the native NP cells. The suitability of two cell populations of miRNA-transfected cells were assessed in relation to their restorative and anti-catabolic activity. Finally, the safety and efficacy of an identified therapeutic dual-miRNA and dual-miRNA transfected cells are examined in a large animal model of mild degeneration. Taken together, this work investigates injectable miRNA-based strategies to modulate regeneration and catabolism in the disc pre-clinically, and can be broken down into four main objectives, outlined below.

1. To screen miRNA combinations with enhanced cell penetrating peptides in vitro and ex vivo.

miRNAs exist in multitudes, with thousands of potentially beneficial miRNAs known to modulate functions involved in extracellular matrix development and inflammatory pathways. In the IVD field alone over 50 miRNAs have been identified as being directly involved in degenerative functions,[22] although the true number is likely much higher, therefore an initial screening was required to narrow the options. Chapter 4 of this thesis highlights the screening of four miRNAs selected from the literature due to their augmentation of matrix markers and silencing of inflammatory cytokines. Initial screenings explore these miRNAs in isolation, however, develops into six miRNA pairs with the aim of exploring potentially synergistic activities. This chapter provides a framework to identify functional changes with miRNA pairs with a particular focus on ex vivo models of disease, with the aim of identifying a pair with meaningful potential to target degeneration of the IVD.

2. To explore adjunct miRNA supplementation with human platelet lysate.

While miRNA-only delivery has great potential in disease management, especially in modulation of catabolic activity, the possibility of further supplementing regenerative processes should be explored. HPL is a growth factor and anti-inflammatory cytokine rich material derived from platelets, being actively examined clinically in orthopaedic and musculoskeletal fields. In Chapter 5 the therapeutic dual-miRNA from Chapter 4 is investigated in combination with HPL, aiming to maintain the anti-catabolic activity of the dual-miRNA whilst driving the expression of ECM markers. This work examines the possibility of a cell-free injectable therapy as a multi-pronged approach to IVD degeneration, with the aim of silencing catabolic factors concurrent with laying the building blocks for matrix rejuvenation.

3. To investigate the most beneficial cell source for miRNA-stimulation for IVD delivery.

Cell therapies have long-since been explored as a means of restoring the depleted native cell population of the degenerated IVD. However, there is no consensus in the field as to the most appropriate therapeutic cell source to deliver, with NP cells and stem cells of various origins being the most abundantly studied. Chapter 6 of this work provides a comparative analysis of NP and BMSCs post-dual-miRNA transfection with the aim of elucidating the most suitable therapeutic cells population for delivery to the IVD. Alongside this it examine whether there are benefit to the inclusion of cells in an injectable therapy, or if dual-miRNA delivery alone would elicit potent enough effects.

4. To assess the safety and efficacy of miRNA and miRNA-cell transplantation in a large animal model.

Key to progression past pre-clinical evaluation is to demonstrate the safety and efficacy of any potential therapeutic. In Chapter 7, the previously identified dual-miRNA is delivered in isolation, alongside dual-miRNA-stimulated cells and non-transfected cells in a caprine model of mild IVD degeneration. Goat IVDs bear geometrical and size similarities to human, making them a suitable and translatable animal model of disc degeneration. The aims of this work are to demonstrate not only that the injectable therapies are well tolerated, but also to examine biochemical, histological, morphological, and immunological effects of the treatments in a large animal model of mild IVD degeneration.

Chapter 2. Literature Review

2.1 Normal intervertebral disc function

Low back pain (LBP) is a growing economical and sociological concern, with an estimated 80% of people being affected throughout their lifetimes, and with increasingly aged populations LBP will likely become more prevalent. [23] One of the most common causative agents of LBP is degeneration of the IVD. Contained within the vertebral bodies of the spinal column it is comprised of three main cellular regions: the NP, annulus fibrosis (AF), and cartilage endplate (CEP) as illustrated in Figure 2.1. [24] The IVD confers flexibility, mechanical loading capacity, and allows for a range of spinal motion, with the three main elements functioning in tandem to maintain these functions. [25] The CEP, as the outer border of the avascular IVD, plays a role in nutrient diffusion to the inner disc region. [26] Bounded by the CEP, the AF composes 15 to 25 concentric collagen type I fibrous lamellae, imbuing the IVD with the ability to withstand torsional strain and swelling pressure from the NP. [27] Morphologically NP cells are rounded, similar to articular chondrocytes [28], and sparsely populate the region, numbering approximately $4x10^6$ cells/cm^3. [29] During development humans are endowed with notochordal cells, large, vacuolated cells associated with proteoglycan synthesis [30], though upon reaching adulthood it is widely accepted that these cells are diminished either entirely or to a significant degree. [31]

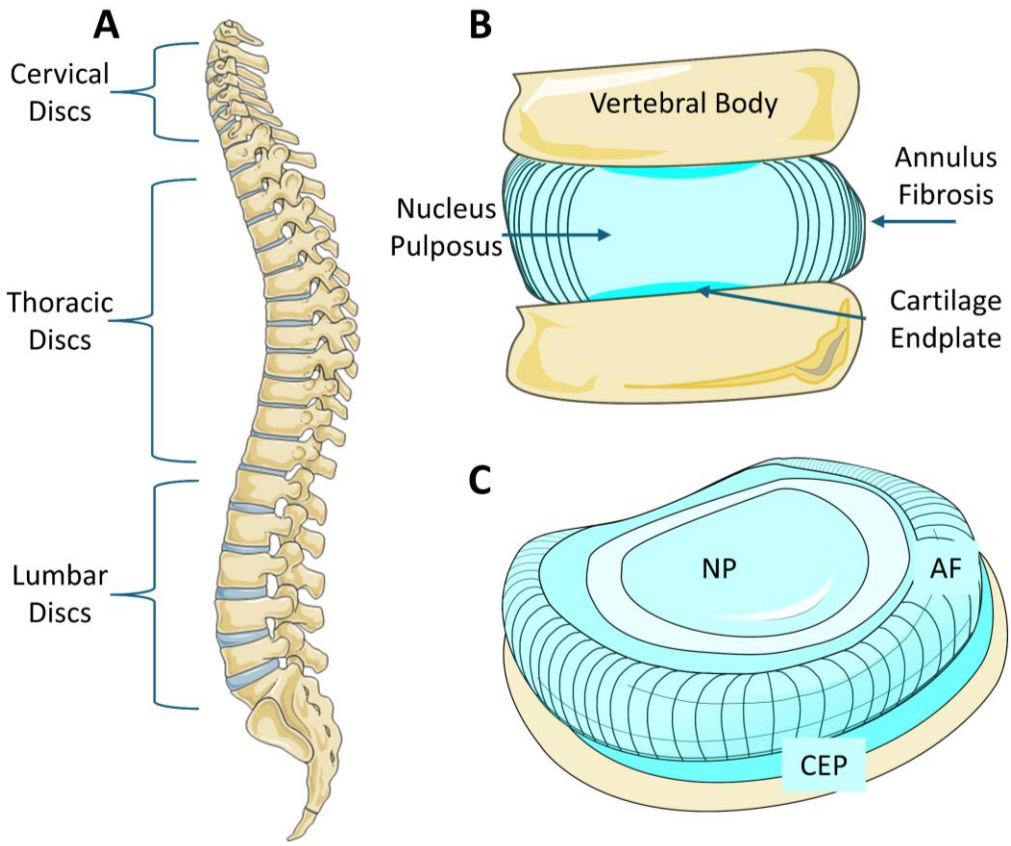

Figure 2.1 Structure of the Intervertebral Disc. (A) Spine from the axial direction, outlining the key elements of the intervertebral disc. (B) Mid-sagittal representation of the intervertebral disc, outlining the key tissues. (C) Schematic of the IVD.

The highly hydrated NP of the disc is predominately composed of collagen type II and proteoglycans, which make up 20% and 50% of the dried weight respectively. [8] Proteoglycans with negatively charged glycosaminoglycan (GAG) side chains assist the disc in remaining hydrated, as they can partake in reversible deformation. [32] Aggrecan is one of the most abundant proteoglycans in the ECM of the disc [9], and contains GAG chains such as chondroitin and keratan sulphate that maintain the hydration required for load bearing by osmotic pressure. [33] The avascular nature of the disc corresponds to a hypoxic and hyperosmotic area, with a carefully maintained ECM anabolic : catabolic balance. [34] Anabolic growth factors (GFs) include the transforming growth factor (TGF)-β superfamily, bone morphogenic protein (BMP) family, and tissue inhibitor of matrix metalloproteinase (TIMP)-2 [35,36], with catabolic factors represented by enzyme families such as the MMPs and ADAMTS [37] which degrade the ECM.

2.2 Intervertebral disc degeneration

Diminished GAG content leads to a loss in the ability to absorb compressive loads resulting in reduced disc height and can lead to nerve compression and pain. [38] Loss of GAGs is believed to be a key driver in early stage IVD degeneration [23], which leads to a reduction of the NP, beginning a degenerative cascade, destabilising the anabolic : catabolic homeostasis of the disc, as defined in Figure 2.2. Alongside increases in mRNA and protein expression of ECM degrading enzymes from the MMP and ADAMTS families [10,11], decreases in discogenic markers such as aggrecan, collagen type II, and the chondrogenic transcription factor SRY-Box Transcription Factor 9 (SOX9) [6,7] are seen. The MMP family is made up of zinc-dependent proteolytic enzymes that cleave collagens, thereby increasing ECM turnover and degradation. Elevated levels of MMP's have been associated with degenerative disc disorder, with MMP-1, -3, -10, -13 [39] and -12 [40] upregulated in patients with degenerated discs. The ADAMTS family function in cleaving proteoglycans, with ADAMTS-4 and -5, classed as major aggrecanases, being of particular interest in IVD degeneration due to their aggrecan degrading ability. [12,41]

Concurrent to this, increases in pro-inflammatory cytokines, at both the gene and protein level are seen, including tumour necrosis factor (TNF)-α and the interleukin (IL) family, further driving the homeostatic imbalance through inflammatory pathway activation. Gene expression of both TNFα and IL-1β has been demonstrated to be prolific in degenerated patient samples, 100% and 96%, respectively, which is greater than the proportion in non-degenerated samples, 63% and 13%, respectively. [42] TNF-α primarily elicits effects through receptor TNFR1- and TNFR2-dependent pathways, both of which can have a myriad of downstream effects, though the majority have been found to be destructive in degenerative conditions. [43] TNFR1 is thought to be the primary driver of TNF signalling, being implicated in mitogen activated protein kinase (MAPK) kinase kinase-3 activation, where following phosphorylation and degradation steps, nuclear factor kappa-light-chain-enhancer of activated B cells (NF-κB) is released, which has been linked to apoptosis promotion via p50 and p60. [44] TNFR1 stimulation can also initiate a caspase cascade that further drive apoptosis thorough death-inducing signalling complexes. [45] TNFR2, though considered anti-apoptotic as it does not contain a death domain, has been found to induce cytotoxicity when co-expressed with TNFR1, suggesting a crosstalk mechanism between the two receptors that could further drive cell death. [46]

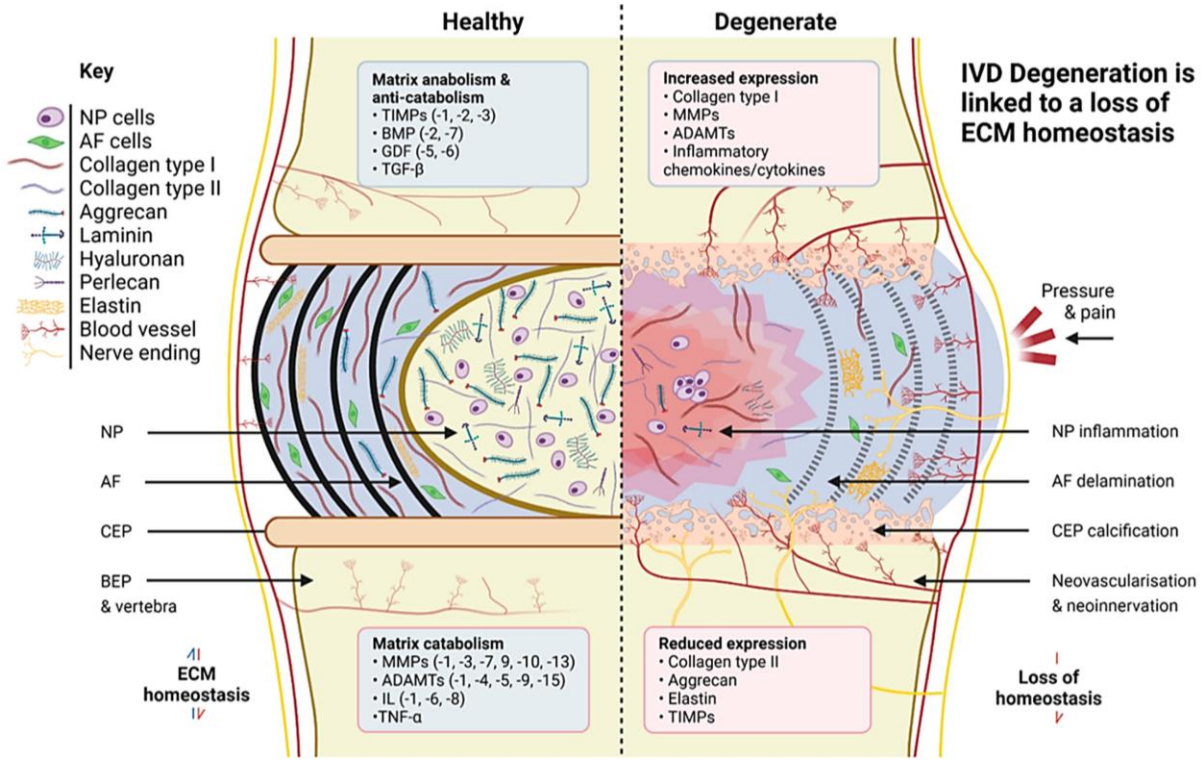

Figure 2.2 Comparison of anabolic : catabolic homeostasis and imbalance in the disc. The healthy disc is balanced with regards to expression of anabolic and catabolic factors, whereas with the progression of degeneration the balance is shifted. A degenerate phenotype reveals itself as increases in the fibrotic collagen Type 1, matrix degrading enzymes, and pro-inflammatory cytokines and chemokines. Taken from [6]

The IL-1 family of cytokines has shown increased expression in degenerate discs compared to non-degenerate, both in human and animal models [47-49], with IL-1β particularly investigated. One of the hallmarks of disc degeneration is the progressive vascularisation and innervation of the disc, whereby the over-expression of GFs such as vascular endothelial growth factor (VEGF), nerve growth factor (NGF) and brain-derived neurotrophic factor (BDNF) contribute to these processes. [50,51] IL-1β stimulation has been shown to upregulate these factors in human IVD tissues, placing it as a potentially crucial mediator of disc degeneration. [52]

These cytokines can also impact upon disc degradation through their ECM remodelling capabilities, including their effects on the expression of the MMP and ADAMTS families, and downregulation of discogenic factors, aggrecan, collagen type II, and SOX9. Bovine NP cells stimulated with TNF-α had significantly increased gene expression levels of MMP3, ADAMTS-4, -5, and IL-6 and -8, with the expression of collagen type II significantly downregulated. [53] These findings were mirrored in progression to a bovine organ culture model whereby gene expression of ADAMTS-4, -5, MMP3, IL-6 , and -8 were all increased, with aggrecan and collagen type II

expression decreased. IL-1β has likewise been implicated in similar trends, Sun *et al* found that human NP cells had increases at both gene and protein levels of MMP3, MMP13, ADAMTS4, and ADAMTS5 under normoxic and physioxic culture conditions. [54] A separate study found in human NP cells, markedly reduced gene expression of aggrecan, collagen type II, and SOX9, alongside reduction in the protein expression of COL2 following IL-1β stimulation. [55] These different influences on the IVD represent the multi-faceted aetiology of degeneration, demonstrating how potential therapeutics would preferably have a similarly multi-pronged effect, by targeting regenerative factors, degradative enzymes, and inflammatory cytokines in order to be effective in treating degeneration.

2.3 Current therapies

Currently the gold standard of treatment for LBP and IDD involves physiotherapy and pain management. [1] Should the degeneration worsen in severity, treatment options are limited to surgical interventions such as discectomy or spinal fusion, which in the short-term offers relief, however over the course of subsequent years this relief falters, with functional relief limited, particularly in the case of spinal fusion. [5] At this point, further surgeries may not be appropriate, likewise, therapeutic intervention at this point would likely be ineffective, as the degeneration has passed beyond a point of functional reparation, with the resident cell population diminished. With this in mind, novel therapeutics are being actively explored and trialled to be delivered before the onset of this severe degeneration, including but not limited to growth factors, gene delivery, cell delivery, and nucleic acids. For the purpose of this thesis, these will be broadly split into cell free and cell therapies.

2.3.1 Growth Factors

When attempting to alter NP cell behaviour towards a regenerative phenotype, GF stimulation has been identified as a promising method, with a number of specific families often implicated. Members of the bone morphogenic factor (BMP) family have shown particular promise. BMP-7 has been demonstrated as increasing proteoglycan (PG) content in a rabbit model of annular puncture disc degeneration. [56] Another member of the BMP family, growth differentiation factor-5 (GDF-5), has been identified as pro-chondrogenic and capable of stimulating ECM production in a rat model of IVD degeneration. [57] Recent in silico modelling has also identified a possible donor-specific response to GDF-5 administration, suggesting a more personalised medicine approach to GF delivery may be required. [58] Transforming growth factor-beta (TGF-β) is well established in disc and cartilage fields as being pro-chondrogenic, capable of driving ECM generation, [59] and has

been shown to have an anti-catabolic effect in TNF-α challenged NP cells. [60] However, issues with dosing and the need for sustained released have led to alternative sources of growth factors. [61]

In an attempt to further promote anabolic pathways, combinatorial GF delivery has garnered much attention in musculoskeletal fields. The incorporation of platelet lysates (PLs) has particularly been often utilised to strong effects. These lysates are derived from plasma and rich in GFs have been shown to promote the production of key matrix components. [59,62-65] These effects are likely due to the high levels of members of the TGF superfamily, vascular endothelial growth factor (VEGF), platelet-derived growth factor (PDGF), fibroblastic growth factor (FGF), and epidermal growth factor (EGF). [66,67] In the IVD field, a preliminary prospective trial found significant improvements to the visual analogue score (VAS) and Oswestry Disability Index (ODI) in nearly half of patients 6 months after receiving a single injection of platelet rich plasma. [68] Further studies have observed a significantly reduction in patients' pain and improvements to function at a follow-up period of 8 weeks post-lysate administration. [69]

2.3.2 Gene and nucleic acid therapies

Gene therapy has been heralded as a new frontier in treatment development for a range of conditions and disorders since it's advent in the 1960's [70] and progression to human clinical trials in the 1990's. [71] Here, the aim is to introduce genetic material, in the form of a nucleic acid such as DNA or RNA, into the patient's cells to modify function in several potential ways: 1.) by driving the expression of the introduced gene, 2.) by inhibiting expression of a target gene, or 3.) by altering the behaviour of the target gene. [72] The effectiveness of this hinges upon the ability to deliver it to the nucleus of the cell in the case of DNA, and the cytoplasm in relation to RNA, in a non-heritable manner. Additional to this is the delivery of smaller nucleic acids, such as miRNAs and siRNAs, either directly or as cargo engineered in extracellular vesicles (EVs).

One of the key motivations of gene therapies was to elicit the promising effects of GFs without the clinically unfeasible need for sustained delivery. Initial in vitro studies demonstrated the ability to transfer beta-galactosidase (LacZ) and interleukin-1 receptor antagonist (IL-1RA) genes through a viral-mediated approach in chondrocytic disc cells.[73] The transfected cells initiated production of IL-1RA protein, demonstrating the clinical potential of this approach. The first in vivo study in 1998 delivered an adenovirus encoding the LacZ gene to rabbit IVDs, resulting in sustained delivery for at least 12 weeks. [74] Gene delivery has been utilised for successful delivery of pro-anabolic [75-77] and anti-catabolic factors [78-80], alongside "gene cocktails" combining both approaches. [81-84] However promising, it must be noted that expectations as to gene delivery

providing a curative approach to IVD degeneration have been somewhat tempered through concerns over patient safety. Pilot studies have identified potential issues around dosing-associated cytotoxicity and the overproduction of the target protein, which may likewise have adverse effects. [85]

While investigations into gene therapies to target IVD degeneration continue [86,87], there has been a shift towards the delivery of RNAs, miRNAs (which will be discussed in the following section) or EVs, which are generally better tolerated. EVs represent a heterogenous population of nanoparticles that function as intracellular communication mediators, though the transfer of molecular cargo between cells.[88] This cargo is comprised of target-specific molecules, for instance proteins, lipids, DNA, and a variety of RNAs [89], making them an attractive strategy with the potential of targeted reprogramming of the degenerated cell population. Engineering of these nanoparticles can impart additional benefits, examples include regenerative cues such as forkhead-box F1 (FOXF1) [90,91], surface peptides to increase target specificity [92,93], and pluripotency markers to stimulate phenotypic changes to the target cells. [94]

2.3.3 microRNAs

In recent years miRNAs have gained traction as a therapeutic approach in the field of tissue regeneration, by post-transcriptional modulation of mRNA targets and protein expression. These short (20-22 nucleotides in length), endogenous, non-coding RNAs have been shown to be plentiful in humans, with the annotation software miRbase estimating 2,675 fully defined mature miRNA sequences currently. [95] Amongst those classified, their mRNA targets are numbered in their thousands, over 45,000 miRNA target sites are selectively conserved amongst mammalian genomes, with single miRNAs having potentially numerous targets. [96] It has been speculated that they could bypass the drawbacks associated with the use of GFs, such as the short half-life and need for repeat injections. [97] Alongside their potential therapeutic functions, they have also been postulated as being ideal biomarkers for early diagnosis of many diseases including degeneration of the IVD, as their expression has been found to drastically alter in diseased versus non-diseased states. [98]

With regards to their biogenesis and function, miRNAs are transcribed to a primary miRNA (pri-miRNA), undergoing enzyme processing to produce a nucleotide hairpin, the pre-miRNA, which is exported to the cell cytoplasm and further enzymatically cleaved. This cleavage generates guide and passenger strands, the guide being loaded into the Argonaute (AGO) protein containing RNA-induced silencing complex (RISC), which facilitates binding to the target mRNA by arranging it in a helical confirmation. [99] A more detailed overview of this process is outlined in Figure 2.3.

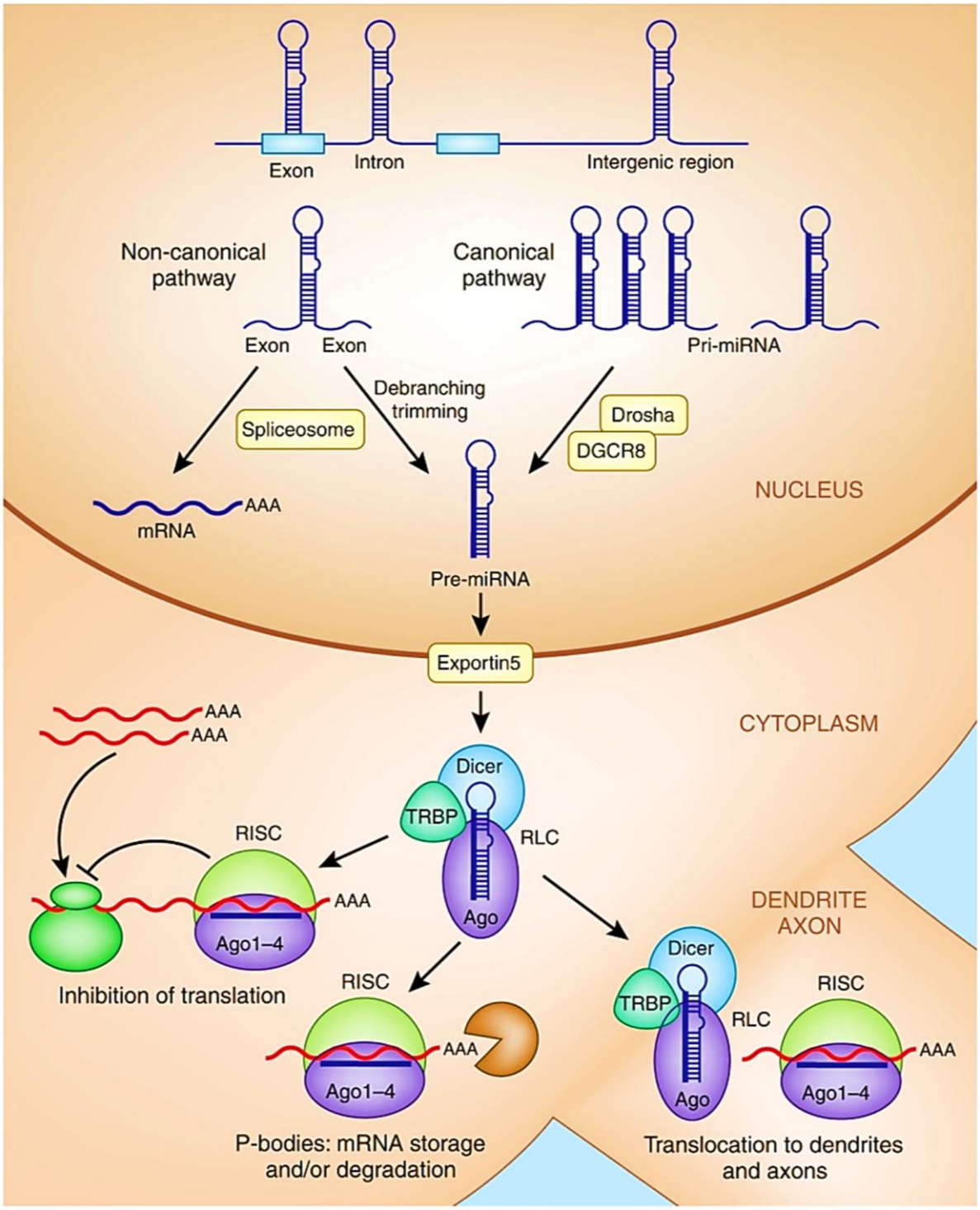

Figure 2.3 The biogenesis and action of mRNA silencing by miRNAs. The transcribed miRNA gene, a pri-miR, undergoes nuclear processing prior to export to the cytoplasm. In the cytoplasm, the pre-miRNA is cleaved by Dicer and loaded onto an Argonaute (Ago) protein that houses the RNA-induced silencing complex (RISC). By arranging the miRNA in a helical conformation, binding to the target mRNA can occur. DGCR8 = DiGeorge Syndrome Critical Region Gene 8, TRBP: Tar (HIV-1) RNA-binding protein, adapted from [100]

miRNAs function in the repression of target mRNA expression through RISC-mediated silencing, there are two methods by which this can occur, by mRNA decay, or through gene expression silencing, with the mechanism guided by the complementarity of the miRNA to the target mRNA. [14] mRNA degradation is accountable for between 66-90% of miRNA-related silencing [101], where the miRNA guides the target towards a 5'-3' mRNA decay pathway, where through deadenylation and decapping of the mRNA they are targeted by exonucleases and degraded. [102] Gene expression silencing is thought to be initiated by inhibiting the first step of translation by impeding the action of initiation factors eIF4A-I and eIF4A-II, blocking the formation of the rIF4F translation initiation complex. [103] Traditionally it was accepted that miRNAs functioned only in the repression of targets, however there is evidence of upregulation in direct, where the miRNA activates the target mRNA, or indirect, where there is a loss of repression, both of which the outcome is an increase to protein expression. [104] This activation has been linked to specific cell cycle states, during quiescence [105], or in response to cues related to cell cycle arrest. [106] With regards to therapeutic approaches, often miRNA function is divided into two distinct groups, the first being miRNA antagonists acting as inhibitors of the endogenous miR. The second, or replacement approach, utilises miRNA mimics that function in mimicking the action of the endogenous miRNA.[107] Introduction of nucleic acids over 30 nucleotides in length activates the IFN pathway as an antiviral defence mechanism [108], however this pathway initiation is bypassed due to the shorter length of miRNAs. This modulation of gene expression and lack of innate immune response could be taken advantage of therapeutically and has been explored in a range of fields, though as the focus of this thesis is the IVD, examples from that field will be centred on in section 2.4.6.

2.4.4 microRNA delivery

Given the hydrophilic nature of the backbone of nucleic acids, a vector is needed to cross the cell membrane; to do this the primary routes can be divided into two approaches: viral and non-viral. Viral vectors, though efficient, have become less widely used as vectors for nucleic acid delivery due to concerns with immunogenicity, insertional mutagenesis and the possibility of oncogene activation, making way for the next generation of non-viral approaches. [15,109-111] Non-viral vectors encompass a broader aspect of genetic material delivery than their viral counterparts, making use of a range of physical approaches such as electroporation or sonoporation, alongside the physicochemical alternatives such as lipids, nanoparticles, and cationic polymers.

Lipofection, commonly referred to as lipid or liposome-based transfection, is a commonly utilised technique, whereby a liposome encircles the genetic material to be delivered to the cell,

forming a lipoplex through electrostatic interactions that can be transported into the cell via fusion with the cell membrane or endocytosis. [112] The commercial availability of different lipofection reagents has led to its frequent use, with various iterations of Lipofectamine™ (Invitrogen), Escort™ (Merck), Transfectamine™ (AAT Bioquest), and DharmaFECT™ (Dharmacon) as examples. Paired to their ready availability, these regents are easy to use, relatively quick, and provide effective transfection of a wide range of cell types, reflected in its wide use in disc literature. [113-115] However, this method has been associated with acute toxicity, and induction of inflammatory and apoptotic responses, which could be exasperated in in vivo settings. [116,117]

From the initial breakthrough of lipid-based gene delivery in the 1980's, polymeric nanoparticles represent a more modern incarnation of delivery vectors, allowing the conjugation of genetic material with a given polymer. The polymers in question can range from the synthetic, such as poly(L-lysine) and polyethyleneimine (PEI), to the natural, for example chitosan, gelatine, and dextran. Often these polymers can be improved with modifications. PEI in its unmodified state is cytotoxic to cells due to its non-cleavable structure and membrane damaging effects [118], however modifications with polyethylene glycol (PEG) have shown improvements to its cytotoxicity while maintaining effective transfection in human cell lines. [119] This lends polymers like this to "personalisation", and the possibility of modifying them to one's individual needs and the material they wish to deliver. Natural nanoparticles offer reduced immunogenicity and biocompatibility, making them an attractive option for gene therapy. Chitosan has been found to share these attributes and has been used for the safe delivery of plasmid DNA (pDNA), oligonucleotides, and silencing RNA (siRNA). [120] Moreover, it's use as a biomaterial opens other avenues when developing treatments for regenerative medicine.

Cell penetrating peptides (CPPs) are a specific class of nanoparticle, generally defined by their small size of between 5-30 amino acids, with inherent membrane translocation sequences, and can be amphiphilic and cationic in nature. [121] CPP uptake by the cell target can be nonendocytic or endocytic, depending upon the structure of the CPP itself, along with the internalised molecule, this internalisation being dependent upon optimal charge ratios. [122] The synthetic α-helix GALA peptide, consisting of a glutamic acid-alanine-leucine-alanine repeat was initially designed to bind the lipid bilayer membranes at acidic pH, inducing membrane fusion and leakage of the encapsulated molecules. [123] GALA was initially touted as a vector for delivery of genetic material, and while efficient in disrupting the lipid bilayer and delivering the nucleic acid in vitro, there was a build-up of the complexes within the endosome, reducing the delivery efficacy. [124] This led to further incarnations of GALA, which will be introduced in Chapter 4. A different family of CPPs worth noting are the GAG-binding enhanced transduction (GET) peptides. This class of cationic peptide contains a heparin binding domain, which makes up the GET system when paired with a membrane-docking peptide. [125] This system has been successfully utilised for not only the transport of nucleic

acids, but also enzymes, proteins, and nanoparticles, without affecting cell viability in a range of cell types in vivo, for example both human (h) and murine embryonic stem cells (mESCs), the murine fibroblastic cell lines NIH/3T3, and human induced pluripotent stem cells (hIPSCs). [126] The structure of GET peptides allows for improved intracellular transduction when CPPs are coupled with a GAG-binding peptide, given the ubiquity of GAGs in the IVD, this could be of particular use when aiming to deliver therapeutic nucleic acids to the disc itself. Overall, the methods of delivery for genetic material varies, with advantages and drawbacks associated with all.

2.4.5 microRNA applications in intervertebral disc regeneration

In studies of IDD, miRNAs have been gaining ground as potential therapeutics, in terms of both stimulating regeneration of the disc and exerting anti-catabolic effects. One such miRNA is miRNA-338-3p, which was found to be significantly upregulated in the NP tissue of patients with IDD, with increased expression of the miRNA positively correlated to the extent of degeneration. [127] In this study, human NP cells transfected were transfected with mimics and inhibitors of miRNA-338-3p, with those transfected with the inhibitors showing significant protein level increases in discogenic factors COL2 and ACAN, and decreases in catabolic factors MMP9 and ADAMTS4, with the inverse true for those transfected with miRNA mimic. This study also demonstrated a halting of degeneration in an IDD induced mouse model following delivery of miRNA-338-3p, recommending its possible use as a therapeutic. Evidence from this study indicated that miRNA-338-3p was exerting these positive effects on the disc through modulation of the MAPK/extracellular signal-regulated kinase (ERK) pathway via targeting of sirtuin 6 (SIRT6). The MAPK/ERK pathway has been implicated in IDD, where its activation drives disc degeneration through ECM decay, apoptosis, induction of inflammatory cascades, and increases in oxidative stress that further diminish the IVD. [128] Negative regulation of this pathway has shown reductions in IDD [129,130], and miRNAs targeting this pathway could warrant further investigation.

Given the initial low cell number in the disc, the subsequent loss that occurs due to IDD can have detrimental effects, especially for cell therapies that target the resident cell population. miRNA-125-5p was found to be upregulated at the gene level in the NP tissue of patients undergoing discectomy, with *in vitro* experiments suggesting that inhibition of miRNA-125-5p not only down-regulates the release of IL-1β, but also reduces apoptosis factors apoptotic peptidase activating factor 1 (APAF1), and the caspases 3, 7, and 9. [114] Silencing of apoptotic pathways could be a useful tool in disc rejuvenation, maintaining the cell population so that it can be acted upon with other therapeutics that will stimulate its repair. miRNA-17-3p has been shown to have a similar reductive effect on caspases 3, 7, and 9, while concurrently reducing the protein expression of catabolic factors MMP-3 and -13 and ADAMTS-4 and -5, and increasing the expression of COL2

and ACAN in human NP cells. [131] Combined with anti-apoptotic and ECM homeostatic factors, the importance of inflammatory cytokines and their regulation should also be considered, miRNA-206 was found in human NP cells to decrease the gene expression of gap junction protein alpha 1 (GJA1), leading to suppression of inflammatory factors IL-1β, TNF-α, and IL-6. [132] The downregulation of such factors could aid in the restoration of the disc microenvironment, providing a more suitable niche for cellular stimulation.

As introduced here, the effects of miRNAs within the IVD can be varied and far-reaching, with a vast number of possibly therapeutic miRNAs to choose to investigate, each with different targets and effects, whether that be pro-discogenic, anti-catabolic, anti-inflammatory, or perhaps anti-apoptotic. Taking advantage of these mechanisms of action could provide the basis for a treatment of IDD, whether that be with the use of a single miR, or perhaps combining them to have a greater over-arching impact on the cellular processes mentioned here.

2.5 Cell strategies for intervertebral disc regenerative therapies

The introduction of cells to the NP region would ideally look to repair and regenerate while having an advantageous anti-inflammatory effect, to this end the number of cell-based therapies available are slim. Numerous studies are carried out with extensive in vitro and in vivo yearly within the disc community, though few of these proceed further towards pre-clinical evaluation. Those that do are often at risk of entering the "valley of death", which represents the transition from preclinical stages to human trial evaluation. The avascular, nutrient deplete, and hypoxic disc microenvironment is challenging in terms of the introduction of new cells, with the choice of cell being of great importance alongside the pre-treatment they undergo. A small percentage of cell-based therapies have advanced to clinical trial and will be introduced here.

As discussed, stem cells of various origins could be appropriate candidates for cell therapies, as they have the capacity to differentiate into a given cell lineage when exposed to the correct cues. Mesoblast Ltd. propose the use of allogeneic, immunoselected adipose-derived mesenchymal precursor cells (MPCs) to stimulate the resident disc tissue while imparting an anti-inflammatory effect. Prior to human studies, an ovine *in vivo* study was carried out, with high (0.5 million) or low (0.1 million) MPC doses administered in a pentosan polysulphate hydrogel to an induced degeneration model. 36 weeks post-administration biochemical analysis revealed enhanced sGAG and collagen levels, more so in the lower dose than higher, with loss of disc height reduced to the most extent also in the lower dose group. [133] The upregulation of matrix synthesis in the lower dose rather than higher may be related to the limited nutrient capacity in the native disc, whereby too high a cell number is unsustainable, and should be borne in mind when developing such

therapeutic strategies. In a first in human Phase 1b/2a participants were given high (18 million) or low (6 million) MPC doses encapsulated in hyaluronic (HA) gels and were evaluated up to 36 months. In both groups, participants saw improvements to pain response tests at both dosages, with the no notable changes, be that improved or worsened, to the Modified Pfirrmann score as assessed by magnetic resonance imaging (MRI). [21] As the first in human trial, the main objective was to guarantee safety of the product, though the improvements in pain response is a welcome result, and the potential of these therapeutic MPCs is currently under phase 3 investigation with a larger sample size (NCT02412735). Furthermore, longer follow-up periods could elucidate the effect in a more substantial manner, in particular if compared to non-intervention or the traditional routes of surgery that can exasperate the degeneration.

The appropriation of native NP cells and their subsequent differentiation into multipotent lineages is the strategy put forward by Discgenics. These cells, dubbed “discogenic cells”, were isolated from human donors and injected into needle puncture injured rabbit discs to be examined 8 weeks later for regenerative capacity. [19] Disc height increased in all groups receiving cells, with increased deposition of both sGAGs and collagens in comparison to animals administered a sham control. A study carried out of high (15 million) and low (1.5 million) discogenic cells in chondrodystrophic beagle dogs with induced degeneration found that these discogenic cells conferred a similar reduction to diminished disc height, with histological grading displaying overall improvements in comparison to the sham group, however not to the control. [20] Interestingly, once again the lower dose of cells was more efficacious in the reduction of disc height worsening, once again demonstrating the importance of cell number when designing therapeutics. Finally, the safety and efficacy of the IDCT (Discogenic Cells + Sodium Hyaluronate vehicle), Rebunoputemcel, is currently under investigation in a Phase I/II clinical trial, where high (9 million) or low (3 million) discogenic cells will be injected into patients with lumbar disc degeneration (NCT03955315), with results to follow.

2.6 Preclinical models of intervertebral disc degeneration

Key to translatable therapeutics is the incorporation of clinically relevant models of IVD degeneration, which increase in complexity from initial monolayer screenings. Of particular relevance to this thesis are ex vivo organ culture models which preclude in vivo applications. These models offer the potential to recapitulate the complex IVD microenvironment, thereby providing a meaningful framework to not only study disease progression, but also promising therapies.

2.6.1 Ex vivo organ culture

The implementation of the most biologically relevant models will provide the best foundation for translational clinical benefit. In this regard, *ex* vivo organ culture systems possess the capacity of bridging the gap between initial *in vitro* screenings and *in* vivo animal models, which are coming under increasing scrutiny, including regulatory pressure in the application of the 3Rs. [134] In an IVD context, the use of an entire organ also imparts a more physiologically relevant niche upon which to test therapeutics, with the native ECM providing paracrine signals that may aid in the effectiveness of an intervention, and which are difficult to accurately recapitulate in vitro. [135] Furthermore, diurnal loading can be applied to applied to recapitulate the daily strain that the IVD experiences. This compression acts a pump through which pressure transports solutes to and from the disc, alongside providing stimuli to the resident cells. [136] A range of different species are utilised for these systems, with bovine proving the most common, making up 42% of all ex vivo organ culture publications in recent years. [137] Induction of degenerative changes to the disc is primarily carried out with pro-inflammatory cytokines [138], or enzymatically, often with chondroitinase ABC (cABC), which cleaved proteoglycans (PGs). [139]

Demonstrating the utility of *ex vivo* organ culture, Teixeria *et al* made use of an inflammatory cytokine challenged bovine explant culture system with which to test the efficacy of the anti-inflammatory drug diclofenac (Df), and MSCs encapsulated within a gel, for restoring disc homeostasis. [140] Df administration resulted in decreased gene expression of IL-6, MMP-1 and MMP-3, with ACAN expression increasing. The MSC group demonstrated reductions to IL-6 and IL-8 though to a lesser degree. A study using organs from miR-146a knock out (KO) mice sought to elucidate the anti-inflammatory effect of miRNA-146a. [141] Both wild type (WT) and KO discs were cultured in the presence or absence of IL-1, with histological analysis revealing a sharp decline in GAGs in KO mice following cytokine stimulation, combined with significant increases of MMP-13 and ADAMTS-5 immuno-positive cells, suggesting a role for this miR in the modulation of inflammatory responses. An example of gene therapy under investigation in an organ culture model comes from Bucher and colleagues, where MSCs transfected with BMP14 were administered to a bovine disc in culture, and demonstrated some return to the native GAG/DNA ratio in the disc after a week. [142] Finally, another benefit to organ culture systems is the tunability to apply different loading patterns, which better represent those experienced in humans in comparison the quadrupeds most frequently used as animal models. Different modes of compression and loading will result in the transduction of cell responses, with large magnitude loading (above 1MPa) having a detrimental effect on the cell population, and those lower than 1MPa being less deleterious. [143] Overall, ex vivo organ culture offers a meaningful approach to maximise the potential of a therapeutic prior to progression to a preclinical animal model, where aspects of the IVD that cannot be fully represented in an in vitro setting can be better reproduced.

2.6.2 Large animal models of IVD degeneration

While a useful tool as outlined above, organ culture will not fully replace the use of animal models as of yet in the pipeline for development of therapeutics, with testing a key point in the clinical translation of a therapeutic. Large animal models for IDD include caprine, ovine, and chondrodystrophic canines [144], with these models having the advantage of the absence of notochordal cells in adulthood and a similar sized and shaped discs to humans. An in vivo study utilising these animals has advantages over organ culture, one being the ability to evaluate a therapeutic over a longer time period, better reproducing the complexity of a human and identifying potential systemic effects stemming from immune responses and crosstalk with neighbouring tissues. Moreover, IDD can be a slow, progressive disease, and extended time periods to see reparative actions are not out of the question. Crosstalk between the IVD and adjacent tissues could result in the activation of pathways that would not be accounted for in other models, such as pain pathways or biomarkers associated with pain. [145] The degeneration of these models is often induced to mimic a certain degree of degeneration, whether physically or chemically to model the diseased state. [146]

Goat models of IDD have the advantage of similar disc and cellular morphology, along with biochemical composition to human cells [147], making them an attractive option for preclinical testing. Gullbrand *et al* established an induced model of goat degeneration through chemonucleolysis with cABC, demonstrating progressive loss of disc height, increases to the Pfirrmann grade, supported by histological grading, and changes to biomechanical traits such as increases in compressive range of motion and decreases in elastic modulus which correspond to degenerated discs in humans. [148] This induced degeneration model was further shown to significantly increase the number of cells immuno-positive for MMP-13, ADAMTS-4, TNF-α, and IL-1β, representing the inflamed milieu that is associated with IDD. [149] Models such as this are therefore of use to test the efficacy of therapeutics, as they can recapitulate the disc microenvironment, providing a framework to assess developed products.

2.7 Summary and clinical significance

This thesis examines the development of injectable miRNA therapeutics for treatment of IVD degeneration. This need stems from a lack of treatment options outside of conservative or surgical interventions, with neither option addressing the underlying biological dysfunction. In this thesis, miRNAs identified from the literature as being pro-regenerative were selected to systematically evaluate their ability to modulate the catabolic response while stimulating matrix

protein synthesis. Further examination was conducted by combining the miRNAs in pairs to identify whether a synergistic response could be achieved by their co-delivery. In parallel, two CPPs were employed to investigate whether there was an optimal carrier, particularly with regards to the NP region of the IVD. While dual-miRNA delivery proved effective in suppressing catabolic activity, regenerative effects could be improved upon. Consequently, additional supplementary options were explored to deliver in tandem with a therapeutic miRNA-pair, such as HPL, which has been employed clinically in the orthopaedic field and demonstrated great promise in stimulating a regenerative response. Dual-miRNA stimulation was investigated in the two most commonly used cell populations, NP cells and BMSCs, to determine the most appropriate cell type for delivery to the IVD following dual-miRNA transfection. Throughout these studies ex vivo organ culture models were utilised to closely replicate degenerative disc conditions, thereby providing a platform for evaluating potential of the proposed therapeutics. Finally, the optimised injectable miRNA therapeutic was evaluated preclinically in a large animal model of mild IVD degeneration to determine its safety, efficacy and potential for further translational development. Collectively, this work sought to harness the therapeutic potential of miRNA therapeutics for IVD regeneration, whilst exploring complementary strategies to further enhance or augment the regenerative response. This research holds important clinical value, as the prevalence of IVD degeneration continues to increase annually, with no effective interventions currently available to address or treat the underlying causes of degeneration.

Chapter 3. General Methods

3.1 Cell Isolation and Monolayer Expansion

3.1.1 Rat nucleus pulposus

Rat tissue was obtained from discarded tissue of animals that underwent procedures in the Comparative Medicine Unit (CMU) of Trinity College Dublin following approval by the animal research ethics committee (AREC) of Trinity College Dublin and the Health Products Regulatory Authority (HPRA) in Ireland (Approval - AE19136/P149). NP cells were harvested under sterile conditions from adult, skeletally mature, female Wistar rats (10-20 weeks) immediately following euthanasia, with 3 tails pooled to represent a donor. Due to the ease of access and high prevalence of use in IVD degeneration studies [150], caudal discs were employed for all cell culture studies. NP tissue was enzymatically digested simultaneously with pronase (70 U/mL, Millipore, Merck Life Science Ltd., U.K.) and collagenase type II (400 U/mL Molecular Probes, Bio-Sciences, Ireland) for 6 hours at 37°C at 10 r.p.m. Once cells were digested to a single cell level, they were plated in flasks for expansion at a density of $5x10^3$ cells/cm^3. Cells were expanded in expansion media (XPAN) comprised of low glucose Dulbecco's Modified Eagle Medium (LG DMEM, Sigma-Aldrich, Merck Life Science Ltd., U.K.), 2% penicillin/streptomycin (Pen/Strep), and 10% Foetal Bovine Serum (FBS, all Invitrogen, Bio-Sciences Ltd., Ireland). NP cells were used between passage 1 and 3, as no morphological changes were visually observed.

3.1.2 Goat nucleus pulposus

In accordance with the principles of the 3R's and to minimise animal use, goat NP cells were obtained from discarded material from animals used in a separate study approved by the University College Dublin Animal Research Ethics Committee (AREC-P-19-17) and the Irish Healthy Products Regulatory Authority (HPRA AW18982/P142). Briefly, motion segments of the lumbar spine were isolated to allow for NP tissue dissection. The tissue was enzymatically digested in serum free low glucose DMEM (LG DMEM, Sigma-Aldrich) containing pronase (100 U/mL, Millipore) and collagenase Type II (300 U/mL, Gibco) supplemented with 2% penicillin/streptomycin (pen/strep, Gibco) and 2.5 mg/mL Amphotericin B (Sigma-Aldrich). Digestion was carried out at 37°C with gentle agitation (10 r.p.m) until single cells were released. Cells were seeded at a density of 5 $x10^3$ cells/cm^2 and maintained in XPAN media at physioxic (5% O_2 and 5% CO_2) oxygen levels. NP cells were used experimentally between passage 1 and 3.

3.1.3 Goat bone marrow derived stem cells

Bone marrow derived stem cells (BMSCs) were isolated from the scapula, likewise they were obtained from discarded tissue from animals used in a separate study approved by the University College Dublin Animal Research Ethics Committee (AREC-P-19-17) and the Irish Healthy Products Regulatory Authority (HPRA AW18982/P142). Bone marrow was aspirated from the scapula with a 16G needle and subjected to sequential centrifugation and filtration steps. Cells were seeded at a density of 23 x 10^6/T175 flask to promote colony formation and cultured for 72 hours. Red blood cells were then removed by washing with phosphate buffered saline (PBS, Sigma). BMSCs were cultured in XPAN media under physioxic conditions (5% O_2 and 5% CO_2), with all experiments performed between passage 1 and 4.

3.1.4 Human nucleus pulposus

Human NP cells were isolated from disc tissue collected with informed consent from patients undergoing discectomy procedures, approved by the Mater Misericordiae University Hospital IRB (Ref 1/378/2229) and Trinity College Dublin (TCDFSTEMSREC/15032021/Buckley). To ensure no contaminants were present, tissue was incubated overnight in serum free (SF) Dulbecco's Modified Eagle Medium – low glucose (DMEM LG, Sigma-Aldrich) with 2% penicillin/streptomycin (P/S, Gibco), 100 µg/mL kanamycin sulphate (Gibco), and 2.5 mg/mL Amphotericin B (Sigma-Aldrich). NP tissue was dissected from the remaining disc tissue under sterile conditions and digested enzymatically with 100 U/mL pronase and 300 U/mL collagenase type II. Following trituration to obtain a single cell suspension cells were plated at a density of 5 x 10^3 cells/cm^3 and expanded to confluency in expansion media (XPAN), containing DMEM LG supplemented with 2% P/S and 10% foetal bovine serum (FBS, all Gibco). Cells were maintained at physioxic (5% O_2) conditions in a humidified atmosphere at 37°C, with media measuring between 300 and 325 mOsm, correlating to the osmolarity of a degenerated disc.[151]

3.2 microRNA

3.2.1 microRNA complexation

miRNA complexes were generated through electrostatic interactions of FLR (Dixon Laboratory, University of Nottingham, U.K.) at predefined Nitrogen : Phosphate (N:P) charge ratios of 5, [17,152] and RALA (GenScript, Netherlands) at an N:P ratio of 10, [153,154] for miRNA mimics-140-5p & 149-5p, and 141-3p & 221-3p inhibitors (all miRNAs were purchased from Horizon

Discovery, U.K.). For assessment of dual-miRNA delivery, the following miRNA pairings were formed: miRNA-140-5p mimic + 141-3p inhibitor, 140-5p + 149-5p mimics, 140-5p mimic + 221-3p inhibitor, 141-3p inhibitor + 149-5p mimic, 141-3p +221-3p inhibitors, and 149-5p mimic + 221-3p inhibitor. A negative miRNA scramble control was likewise formed under the same conditions. For all monolayer experiments an miRNA concentration of 10 ng/µl was used, with 25 ng/µl utilised for experiments in ex vivo organ culture. Complexes were formed for 30 minutes at room temperature prior to cell and organ delivery.

3.3 Ex vivo Organ Culture

3.3.1 Rat ex vivo organ culture

The top three caudal discs were isolated from rat tails, removing the skin and tendons to allow for easier access to the disc section. To avoid swelling of the NP, the CEP and vertebral elements were left intact. Following successive washes in povidone iodine (Duggan Veterinary Supplies Ltd., Ireland) and 70% industrial methylated spirt (IMS) the discs were incubated in LG DMEM, supplemented with 2% Pen/Strep, 0.2% Primocin (InvivoGen), and 0.25µg/mL Amphotericin B (Sigma-Aldrich, Merck Life Sciences Ltd., Ireland) for 24 hours, before culture for 7 days in XPAN at physioxic (5% O_2) to more accurately simulate the native IVD. At day 7, discs were injected with 2µL of 0.025U chondroitinase ABC (cABC, Sigma-Aldrich, Merck Life Sciences Ltd., Ireland) using a 30G needle and degeneration allowed to progress for 7 days. 2µl of treatments were delivered directly into the NP region via a 30G needle.

3.3 Quantitative Biochemical Analysis

3.3.1 Determination of DNA content

Samples were digested for 18 hours at 60°C in 100mM Sodium Phosphate/5 mM Na_2EDTA Buffer, with 3.88 U/mL papain enzyme and 5mM L-Cysteine (both Sigma-Aldrich, Merck Life Science Ltd., Ireland). Media samples were pooled and stored at -80°C prior to lyophilisation following a standard freeze-drying protocol (500 mTorr, -10°C, 16 – 18h, Harvest Right™, USA) and incubated in activated papain solution as above. DNA content was assessed using Hoechst Bisbenzimide 33258 dye assay (DNA QF Kit, Sigma-Aldrich, Merck Life Science Ltd., Ireland.) with a calf thymus DNA standard.

3.3.2 Quantification of sulphated glycosaminoglycans

Determination of sulphated glycosaminoglycans (sGAGs) was carried out using the dimethylmethylene blue binding assay (DMMB) (Blyscan, Biocolor Ltd., Northern Ireland) with a chondroitin sulphate (CS) standard.

3.3.3 Assessment of total collagens

Total collagen content was assessed through hydroxyproline measurement, with samples hydrolysed in concentrated hydrochloric acid (38% HCl) at 110°C for 18 hours. A chloramine-T assay was performed and collagen content was estimated using a hydroxyproline:collagen ratio of 1:7.69. [155]

3.4 Qualitative Histological Assessment

3.4.1 Cell fixation in monolayer

Cells in monolayer were fixed in 4% paraformaldehyde (PFA) for 12 minutes, followed by washing in PBS.

3.4.2 Whole organ fixation

Rat discs were fixed overnight in 4% PFA at 4°C and decalcified in decalcification solution-lite (Sigma-Aldrich, Merck Life Sciences, Ireland) until soft (~7 days).

Goat discs were fixed for 48 hours in 4% PFA at 4°C, decalcification solution-lite was employed to decalcify solutions until soft, taking approximately 6 weeks.

3.4.3 Sample dehydration for wax embedding

Following fixation, samples were dehydrated sequentially in increasing ethanol solutions and paraffin wax embedded prior to sectioning on a microtome (Leica).

3.4.4 Sample preparation for cryosectioning

To preserve structural integrity, samples such as goat whole motion segments and NP-ECM analogue gels were immersed in 30% sucrose as a cryoprotectant post-fixation. This was followed by embedding in optimal cutting temperature (OCT) compound, and being snap-frozen in liquid nitrogen, with sections obtained on a Leica CM3050 S cryostat.

3.4.5 Histological staining

Histological staining was performed as follows: haematoxylin and eosin (H&E) for cellularity, picrosirius red (PR) for collagen, and alcian blue (AB) for sGAG deposition. Sections were imaged on an Aperio AT2 Slide Scanner (Leica).

3.5 Immunohistochemical Staining

3.5.1 Sample preparation for monolayer and sectioned samples

For samples in monolayer, cell membranes were permeabilised in 0.1% Triton X-100 for 20 minutes, and non-specific binding was blocked with 1% bovine serum albumin in PBS for 30 minutes (BSA, all Sigma-Aldrich, Merck Life Science Ltd., U.K.). Primary antibody solutions were applied overnight at 4°C, with a concentration matched IgG control used for all staining. Species-matched AlexaFluor secondary antibodies were incubated for 1.5 hours, with nuclear counterstaining with Hoechst Bisbenzimide 33258 (Sigma-Aldrich).

Following the relevant antigen retrieval method, wax embedded samples were likewise permeabilised with 0.1% Triton X-100 for 20 minutes and blocked for 1 hours in 5% BSA in PBS. Primary and secondary antibodies were applied as for monolayer samples.

3.6 Statistical Analysis

Statistical analysis was carried out using GraphPad Prism (version 10.4.0). Outlier ROUT tests were performed for each dataset, and data were tested for normality. Comparisons between two groups were performed using unpaired t-tests. For analysis between groups of three or more, a one-way ANOVA with Tukey's post-hoc test was performed. In instances where there was a significant difference between group means, a Brown-Forsyth and Welch ANOVA test was employed. For comparisons between non-normally distributed data the Kruskal-Wallis test followed by Dunn's multiple comparisons test was used, with data displayed as median ±

interquartile range. When examining differences between groups at more than one timepoint, a two-way ANOVA with Tukey's post-hoc test was utilised. p-values below 0.05 were considered statistically significant. All experiments included a minimum of three independent biological replicates represented as individual datapoints in the graphs, with graphical data presented as mean ± standard deviation.

Chapter 4. In Vitro and Ex Vivo Screening of microRNA Combinations with Enhanced Cell Penetrating Peptides to Stimulate Intervertebral Disc Regeneration

A significant portion of this chapter has been previously published in **Ní Néill T.,** Barcellona M.N., Wilson N., O'Brien, F.J., Dixon, J.E., Curtin, C.M., Buckley, C.T (2024) "In vitro and ex vivo screening of microRNA combinations with enhanced cell penetrating peptides to stimulate intervertebral disc regeneration". *JOR Spine*, 7(2) doi: 10.1002/jsp2.1366

Contribution: Contributed substantially to the conception and design of the work. Performed the acquisition and interpretation of literature, data analysis, presentation and interpretation of results, drafting the article, critical revision, and final manuscript approval.

4.1 Introduction

The introduction of regenerative nucleic acids has gained ground over the last decade, with microRNAs (miRNAs) offering the potential to treat a range of disorders. [156-159] miRNAs function in the post-transcriptional regulation of target genes, of which for each miRNA hundreds of targets are applicable, [95,96] and this activity results in the stimulation or dampening of protein expression. [101,102,104] From a regenerative standpoint, 4 pro-discogenic miRNAs were selected that have demonstrated therapeutic potential, both in terms of predicted targets and those experimentally validated in the literature, namely: miRNA-140-5p mimic, miRNA-141-3p inhibitor, miRNA-149-5p mimic, and miRNA-221-3p inhibitor.

miRNA-140-5p has been shown to have a positive impact on driving chondrogenesis in models of osteoarthritis (OA), with similar key markers as those observed in discogenesis; SOX9, aggrecan, and collagen type II, [160,161] and in catabolic enzyme expression, specifically ADAMTS5 and MMP13, [162,163] indicating its potential usage in a regenerative capacity in the disc. The presence of miRNA-141 has been implicated as a driver of catabolic degeneration in human NP cells, stimulating ADAMTS5 and MMP13 expression. [164,165] Xu et al observed that by inhibiting miRNA-141 there was a return towards healthy levels of collagen II and aggrecan deposition, with decreases in gene expression of ADAMTS and MMP family members. [166] The transduction of rat NP cells cultured in cytokine-stimulated media with miRNA-149-5p restored gene and protein expression of aggrecan and collagen type II towards non-stimulated, healthy levels. [167] In chondrocytes, a study by Wang et al found evidence indicating an anti-apoptotic role and silencing of MMP13, [168] which could aid in the stimulation of NP cells towards a regenerative behaviour. Finally, the silencing of miRNA-221 has been linked to enhancement of a discogenic-like phenotype for human NP cells in

vitro. [169,170] Dubbed chondroprotective, the inhibition of this miRNA may function in driving the deposition of ECM-related markers. Taken together, there is experimental evidence to suggest the applicability of these miRNAs for IVD regeneration.

To exploit this regenerative potential of miRNAs, a method of delivery must be chosen to taxi these miRNAs into the cells. Though efficacious, the viral delivery of nucleic acids has decreased in popularity due to safety concerns and immunogenicity. [15,109,110] To this end, non-viral cell penetrating peptides (CPPs) that retain internalisation capabilities while proving less stimulatory of the immune system are being explored. In this study, two CPPs were identified for investigation, cationic 30mer amphipathic peptide (RALA) and GAG-binding enhanced transduction (GET) peptide FGF2B-LK12-8R (FLR), both of which function by complexing nucleic acids through electrostatic interactions. RALA, an amphipathic cationic peptide, has arginine residues incorporated throughout the structure to enhance the cationic charge and improve membrane transduction and internalisation. [18,171,172] A modified GAG-binding enhanced transduction (GET) peptide, FLR contains a fibroblast growth factor 2 heparin-binding domain that facilitates homing to the cell membrane conjugated to an amphipathic and cationic peptide seequence. [125,152]

The overall objective of this chapter was to screen the regenerative potential of four indivually delivered and six miRNA pairings in vitro and in an ex vivo organ culture model, while simultaneously assessing the suitability of CPPs for miRNA delivery to the NP region.

4.2 Materials and Methods

4.2.1 Monolayer transfection of rat nucleus pulposus cells

For immunofluorescence of protein markers cells were seeded at a density of $1x10^4$ in 18-well µ-well slides (Ibidi GMBH, Germany) and allowed to attach for 24 hours prior to transfection. For biochemical analysis of aggrecan and collagen production, NP cells were seeded at $1x10^5$ in 6 well plates, again allowing 24 hours for attachment. In all cases, complexes were formed for 30 minutes at room temperature (RT) as described above in serum free OptiMEM (Invitrogen, Bio-Sciences Ltd., Ireland). Complexes were added to cells following a phosphate buffered saline (PBS) wash and transfection allowed to proceed for 5 to 6 hours at 37°C. At the end of incubation, complexes were removed, and cells cultured for 3 days for immunofluorescence analysis, and 14 days for biochemical analysis with media changes performed biweekly where appropriate. For all transfection experiments a non-transfected (NT) control receiving OptiMEM alone was utilised. Preliminary transfection efficiency had previously been shown in the Buckley lab by flow

cytometry as being above 90% for RALA and FLR at a dose of 10 ng/µl, with viability 24 hours post-transfection above 80% as assessed by Calcein staining. To ensure transfection was not impacting on ECM protein production, a negative mimic control (Horizon Discovery, U.K.) was employed as per manufacturer's instructions. For monolayer cultures, between 3 and 5 independent biological replicates were performed, as indicated in the Figure legends. Table 4.1 outlines the specific cell culture experimental set-up for each experiment. For ease of culture, all initial screenings were carried out under normoxic (20% O_2) conditions in a humidified atmosphere at 37°C.

Table 4. 1 Experimental outline of nucleus pulposus cell monolayer experiments.

Assay	Single/ Dual miRNA	Time Point	Plate Size	Seeding Density	Cytokine Insult	Output
Immunofluorescence	Single	3 days	18-well µ-well slide (Ibidi)	$1x10^4$	No	Protein: aggrecan, collagen type II
Immunofluorescence	Dual	3 days	18-well µ-well slide (Ibidi)	$1x10^4$	Yes	Protein: aggrecan, collagen type II
Immunofluorescence	Dual	3 days	18-well µ-well slide (Ibidi)	$1x10^4$	Yes	Protein: ADAMTS5, MMP13
Biochemical Quantification	Dual	14 days	6-well	$1x10^5$	Yes	DNA, sGAGs, collagen

4.2.2 Proinflammatory cytokine challenge

To better represent physiological conditions a cytokine challenge was employed for assessing dual miRNA transfections. 24 hours post-seeding, cells were starved of serum for 24 hours and subsequently insulted with TNF-α (50 ng/mL) and IL-1β (10 ng/mL) for a further 24 hours as previously described. [173,174] After 24 hours of incubation, cytokine media was removed, cells were washed with PBS and miRNA-vector complexes were incubated as previously described.

4.2.3 Immunohistochemistry of monolayer cultures

Primary antibody solutions: rabbit-anti-collagen II (PA599159), rabbit-anti-aggrecan (MA532695), rabbit-anti-ADAMTS5 (PA532142), and mouse-anti-MMP13 (MA514247, all Invitrogen, Bio-Sciences Ltd., Ireland), were incubated overnight at 4°C. A concentration-matched IgG control was used for all staining. Species-matched AlexaFluor secondary antibodies: goat anti-rabbit 488 (ab150077, Abcam, U.K.) and goat anti-mouse 488 (A11001, Invitrogen, Bio-Sciences Ltd., Ireland) were incubated for 1.5 hours, with nuclear counterstaining with Hoechst Bisbenzimide 33258 (Sigma-Aldrich, Merck Life Sciences Ltd., U.K.). Images for each independent biological replicate were captured in triplicate on a Leica SP8 Scanning Confocal Microscope (Lecia Microsystems, Germany), with analysis of protein expression quantified using a custom CellProfiler pipeline (CellProfiler 4.2.1), which measures the signal intensity and normalises per cell number. Fluorescence intensity was normalised to NT control to determine the degree of fold change between groups, with 3-5 independent biological replicates performed.

4.2.4 Rat ex vivo organ culture

The top three caudal discs were isolated from rat tails, removing the skin and tendons to allow for easier access to the disc section. To avoid swelling of the NP, the CEP and vertebral elements were left intact. Following successive washes in povidone iodine (Duggan Veterinary Supplies Ltd., Ireland) and 70% industrial methylated spirt (IMS) the discs were incubated in LG DMEM, supplemented with 2% Pen/Strep, 0.2% Primocin (InvivoGen), and 0.25µg/mL Amphotericin B (Sigma-Aldrich, Merck Life Sciences Ltd., Ireland) for 24 hours, before culture for 7 days in XPAN at physioxic (5% O_2) to more accurately simulate the native IVD. At day 7, discs were injected with 2µL of 0.025U chondroitinase ABC (cABC, Sigma-Aldrich, Merck Life Sciences Ltd., Ireland) using a 30G needle and degeneration allowed to progress for 7 days.

Complexes of the miRNA combinations were formed for 30 minutes at a concentration of 25ng/µL and 2µl was delivered directly into the NP region. 14 days post-transfection the discs were fixed overnight in 4% PFA and decalcified in decalcification solution-lite (Sigma-Aldrich, Merck Life Sciences, Ireland) until soft (~7 days). Each experiment was performed independently with 3 biological replicates. NP cell viability was assessed by live/dead staining with Calcein AM (Biotium) and Ethidium homodimer (Sigma-Aldrich, Merck Life Sciences Ltd., Ireland) for 4 independent biological replicates and imaged on a Leica SP8 Scanning Confocal Microscope (Leica Microsystems, Germany).

4.2.5 Immunocytochemistry

Disc sections were sliced in the sagittal orientation to a 10µm thickness on a microtome (Leica Microsystems, Germany). Antigen retrieval was carried out using 35 U/mL pronase at 37°C for 30 minutes, followed by membrane permeabilisation with 0.1% Triton X-100 and blocking for 1 hour with 5% BSA in PBS. Primary antibody solutions for rabbit-anti-SOX9, rabbit-anti-ADAMTS5 (PA532142, Invitrogen, Bio-Sciences Ltd., Ireland), and mouse-anti-MMP13 (MA514247, Invitrogen, Bio-Sciences Ltd., Ireland) were prepared in 1% BSA in PBS, with a concentration-matched IgG control, and incubated overnight at 4°C. Species-matched AlexaFluor secondary antibodies: goat anti-rabbit 488 (ab150077, Abcam, U.K) and goat anti-mouse 488 (A11001, Invitrogen, Bio-Sciences Ltd., Ireland) were incubated for 1.5 hours at room temperature, with nuclear counterstaining using Hoechst Bisbenzimide 33258 (Sigma-Aldrich, Merck Life Sciences, Ireland). Samples were mounted with Fluoromount Aqueous Mounting Media (Sigma-Aldrich, Merck Life Sciences, Ireland) and imaged on a Leica SP8 Scanning Confocal Microscope. To assess protein expression, regions of interest (ROIs) of equal size were captured and fluorescence measured. The corrected total cell fluorescence was then determined as follows: Integrated Density – (Area of Selected Cell Mean * Mean Fluorescence of Background Readings). All read outs were normalised to the NT control to express fold changes of protein expression.

4.2.6 Bioinformatics analysis

To further investigate the roles of miRNA-149-5p mimic and miRNA-221-3p inhibitor in the degeneration of the IVD, strongly evidenced miRNA-gene interactions (those identified through reporter assays, Western blotting, or quantitative polymerase chain reaction (qPCR)) were determined using the online repositories miRNATarBase, [175] and MIENTURNET. [176] A miRNA-gene target list was achieved with a cut-off of $p < 0.05$. The lists for both miRNAs were visualised in Cytoscape, Version 3.10, [177] and enriched utilising the Gene Ontology Biological Process Tool,

removing redundant results. Relevant pathways were isolated, and protein-protein interaction (PPI) networks were visualised through the Search Tool for the Retrieval of Interacting Genes (STRING) database, [178,179] employing a 0.8 confidence score cut-off. Nodes were displayed as being larger with higher levels of expression in the extracellular space, given the importance of ECM production in the IVD. The datasets obtained from miRTarBase and MIENTURNET are available in the Supplemental Information.

4.3 Results

4.3.1 Delivery of individual miRNAs demonstrated favourable influence on the modulation of extracellular matrix proteins in monolayer culture

As identified from literature, the four selected miRNAs, miRNA mimics 140-5p and 149-5p, and inhibitors of miRNAs 141-3p and 221-3p, were delivered individually to NP cells in monolayer by both RALA and FLR vectors, and their effect on regenerative ECM markers aggrecan and collagen II was assessed. Immunofluorescence quantification demonstrated transfection with miRNA-140 mimic significantly enhanced aggrecan deposition following transfection with FLR ($p=0.015$), and collagen II protein production was significantly increased by RALA delivery ($p=0.014$), with a positive trend for FLR ($p=0.081$) (Fig. 4.1 A, B). Some increases were also exhibited for miRNA-149 mimic (Fig. 4.1 C, D) and miRNA-221-inhibitor (Fig. 4.1 E, F), although these were not found to be statistically significant. RALA-miRNA-221-3p inhibitor stimulated significant aggrecan expression ($p=0.046$), with collagen II showing increases (Fig. 4.1 G, H). Generally, improvements to matrix protein expression were approximately 1.5 to 2-fold range in comparison to the NT control.

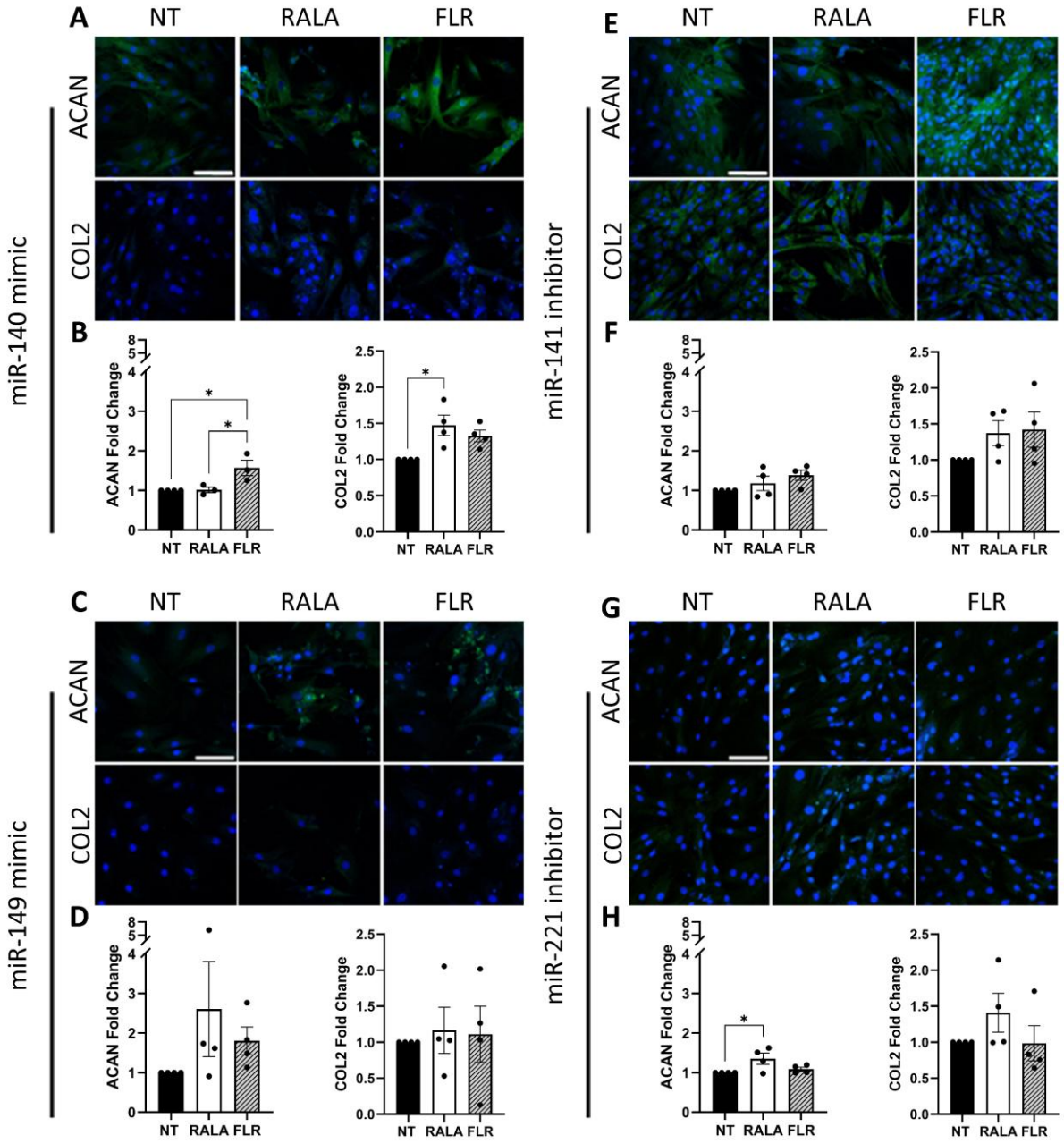

Figure 4.1 Transfection of rat nucleus pulposus cells with individual miRNA mimics and inhibitors with cell penetrating peptides demonstrated positive trends towards increased matrix production in monolayer culture. (A&B) miRNA 140 mimic transfection significantly increased aggrecan (ACAN) and collagen type II (COL2) protein expression, (C&D) 149 mimic, (E&F) 141 inhibitor and (G&H) 221 inhibitor demonstrated instances of increased protein expression of ACAN and COL2 three days post-transfection. * ($p<0.05$) indicates statistical significance, $N \geq 3$. Scale bars are 100 μm.

4.3.2 Transfection of therapeutic dual-miRNA enhanced the deposition of matrix proteins in 2D monolayer culture

While some upward trends were identified from individual miRNA delivery, it was next explored if a combinatorial approach may amplify the regenerative response while also dampening the catabolic cascade associated with degeneration. Here, all groups, including NT controls were stimulated with pro-inflammatory cytokines to induce catabolic enzyme production in order to evaluate how miRNA pairings could influence the promotion of matrix proteins and the suppression of degradative catabolic factors. With regards to aggrecan production, miRNA-140 mimic + miRNA-141 inhibitor markedly improved protein expression (RALA-group $p=0.002$, FLR-group $p=0.045$), with RALA-miRNA inhibitors 141 + 221 demonstrating similar promise ($p=0.046$, Fig. 4.2 A, B). FLR-miRNA mimics 140 + 149 approached significance ($p=0.051$) for aggrecan deposition. Amongst the remaining three combined groups, increases approaching a 4-fold increase were observed, in comparison to approaching 1.5 to 2-fold with single miRNA transfections, signifying the enhanced potential of dual miRNA delivery. Immunofluorescence analysis of collagen displayed less altered protein expression, though increases approached a mean 5-fold increase for a number of groups, such as miRNA mimics 140+149, miRNA-141 inhibitor+miRNA-149 mimic, miRNA inhibitors 141+221, and miRNA-149 mimic and 221 inhibitors (Fig. 4.2 C, D), again this was enhanced compared to the delivery of individual miRNAs (Fig. 4.1 A-H).

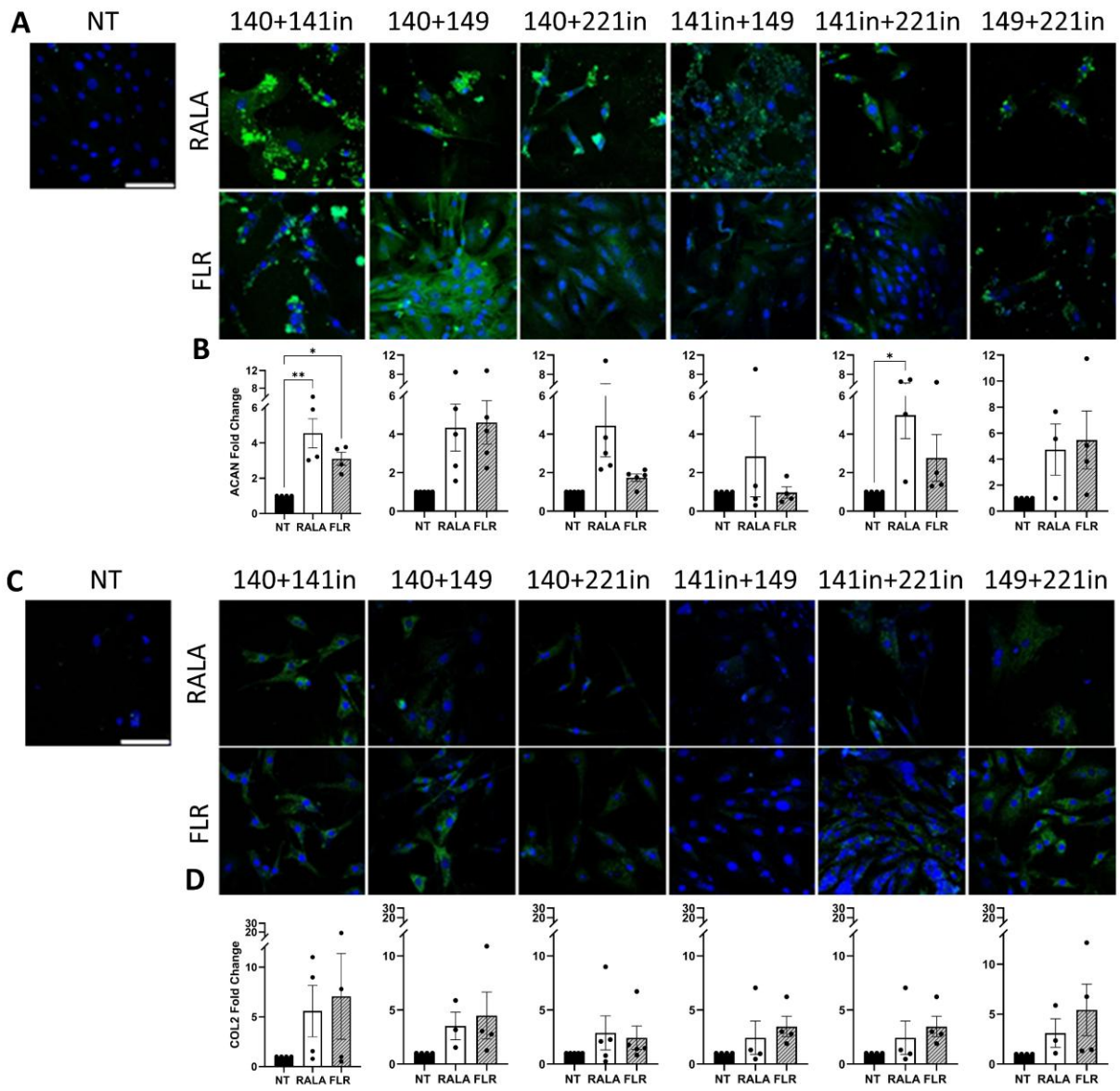

Figure 4. 2 Delivery of miRNAs pairings with cell penetrating peptide mediated delivery increased extracellular matrix protein deposition in rat nucleus pulposus monolayer culture. (A&B) Immunofluorescence analysis 3 days post-transfection exhibited increases in aggrecan (ACAN) expression for miRNA-140-mimic + miRNA-141-inhibitor, and miRNA-141-inhibitor + miRNA-221-inhibitor. Deposition of aggrecan demonstrated some positive trends toward increased deposition after 14 days in monolayer culture. (C&D) Collagen type II (COL2) protein expression demonstrated similar non-significant increases in production at 3 days post-transfection. * ($p<0.05$), ** ($p<0.01$) indicates statistical significance, $N \geq 4$. NT: Non-transfected. Scale bars are 100 µm.

Upon ascertaining that delivery of a negative control scramble miRNA did not significantly alter DNA, sGAG, or collagen content (Fig. 4.3 A), biochemical analysis was performed on each miRNA-pairing. No significant differences were found between the NT control and transfected

groups (Fig. 4.3 B). Collagen deposition in 2D culture demonstrated limited changes in comparison to NT groups (Fig. 4.3 C), potentially representing the unsuitability of monolayer culture systems for identification of ECM factors and their modulation.

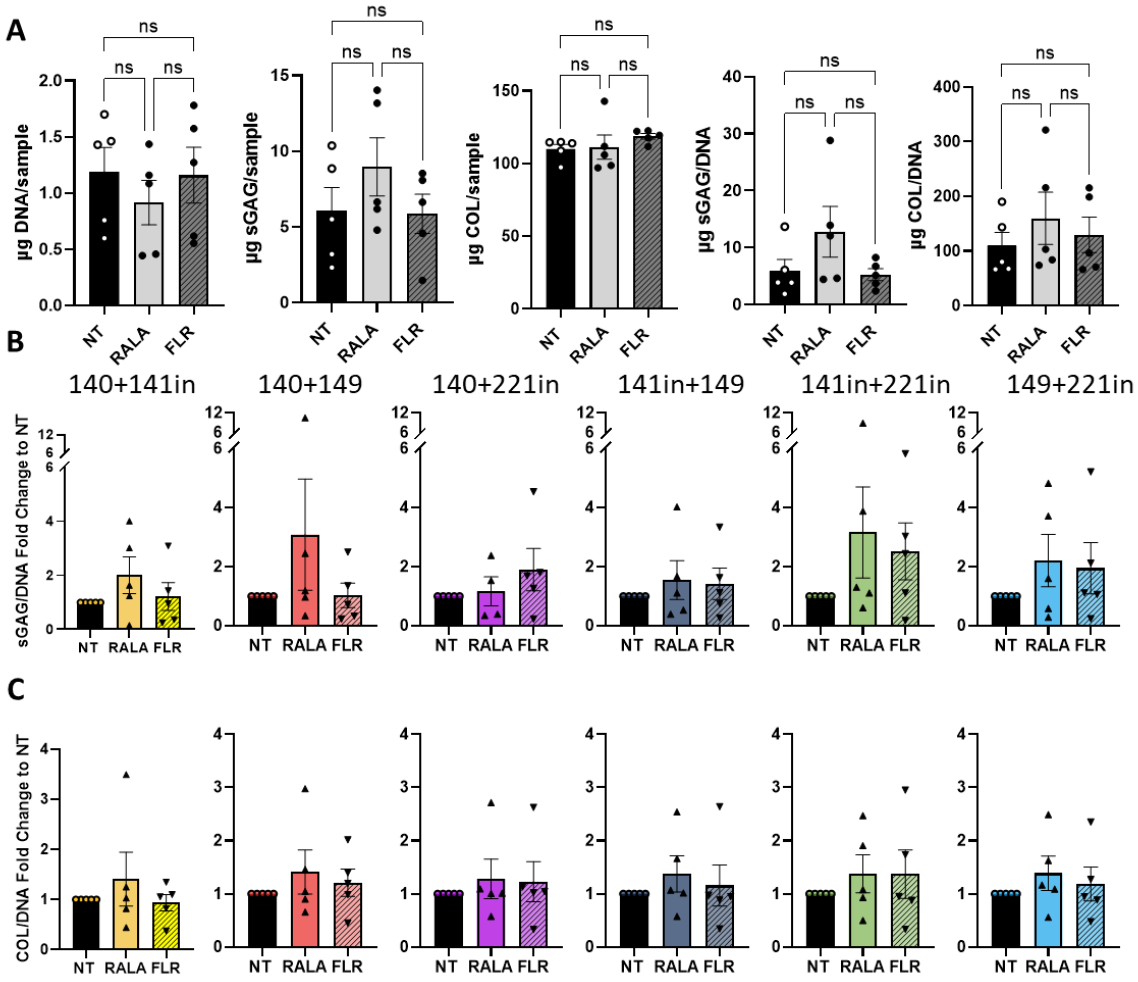

Figure 4.3 Biochemical analysis of rat nucleus pulposus monolayer cultures following vector-scramble miRNA and vector-miRNA pairing delivery. (A) Delivery of a negative control miRNA showed no significant changes to biochemical quantification 14 days post-transfection. (B) Sulphated glycosaminoglycans (sGAG) and (C) collagen (COL). Data is displayed as sGAG or COL normalised to DNA content and the non-transfected (NT) control. N =5, ns: non-significant.

4.3.3 Impact of dual-vector-miRNA delivery on catabolic enzyme expression in monolayer culture

As mentioned, cytokine stimulation was included for all groups to drive catabolic enzymes such as ADAMTS5 and MMP13 and screen the prospective downregulation of dual-miRNA delivery. RALA-mediated delivery substantially increased ADAMTS5 above that of the NT and/or

FLR groups, in the case of miRNA groupings 140 + 149 mimics, miRNA-140 mimic + miRNA-221 inhibitor, miRNA inhibitors 141+221, and miRNA-149 mimic + 221 inhibitor (Fig. 4.4 A, B). Similar increases were identified for MMP13 in particular for miRNA-140 mimic + miRNA-141 inhibitor, and miRNA mimics 140 + 149 (p=0.069), and to a greater extent in the RALA groups (Fig. 4.4 C, D).

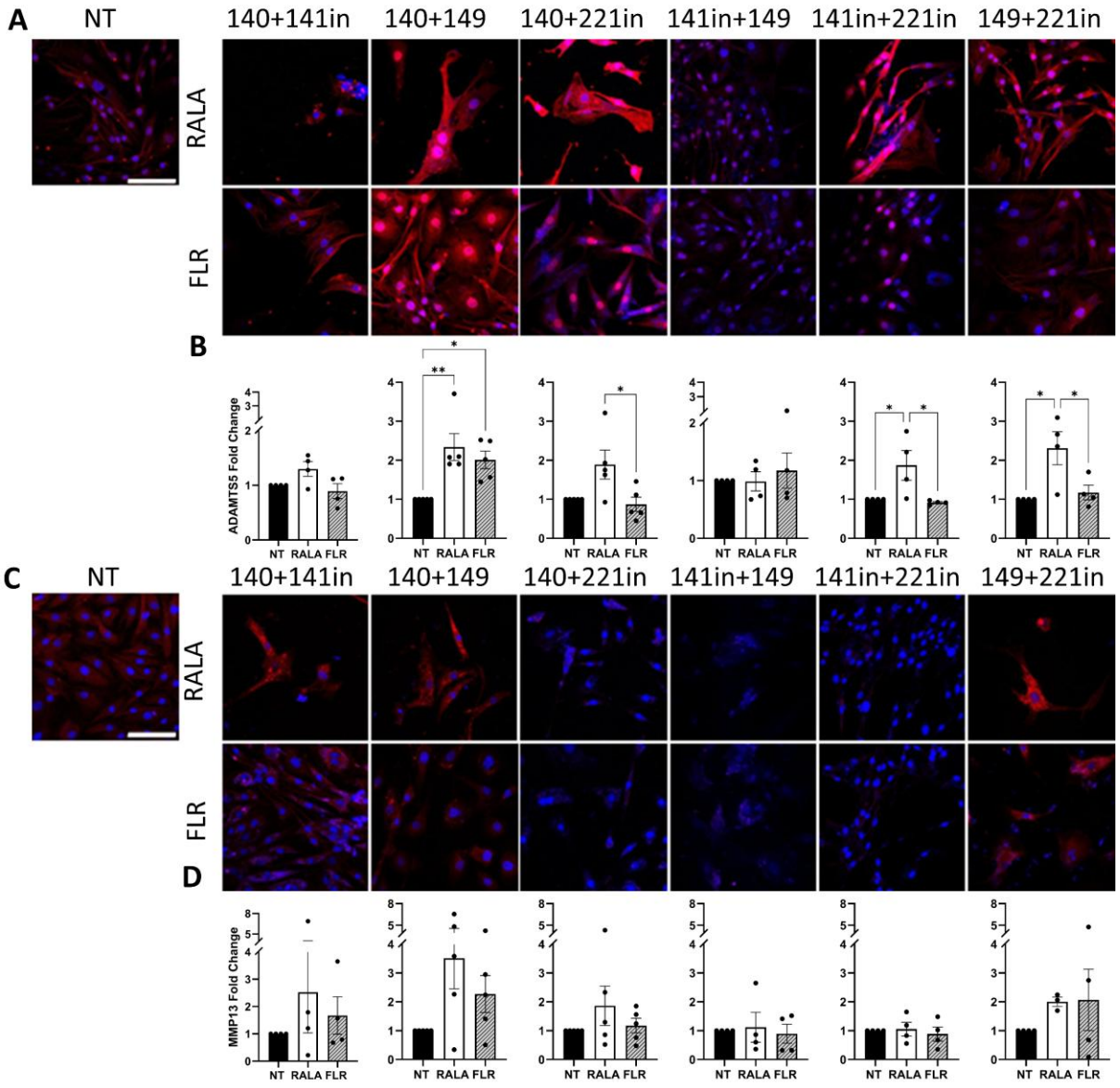

Figure 4.4 Effect of vector-miRNA pairings on the production of catabolic enzymes in rat nucleus pulposus monolayer culture. (A&B) ADAMTS5 expression three days post-transfection was significantly increased for miRNA-140 + miRNA-149 mimics, miRNA-140 mimic + miRNA-221-inhibitor, miRNA-141-inhibitor + miRNA-221-inhibitor, and miRNA-149 mimic + miRNA-221-inhibitor in comparison to non-transfected (NT) and FLR transfected cells. (C&D) MMP13 protein expression showed some instances of increases though none to a significant degree.

*p<0.05, **p<0.01 indicates statistical significance, N=4-5 independent biological replicates. Scale bars are 100 μm.

4.3.4 Dual-Vector-miRNAs fostered a regenerative niche in rat ex vivo organ culture

Histological appraisal of sGAG presence revealed marked increases in a number of the groups, such as RALA-miRNA-140 mimic + miRNA-221 inhibitor and miRNA-141 + miRNA-221 inhibitor. Transfection using FLR led to increased sGAG deposition for miRNA-140 mimic + miRNA-141 inhibitor, and miRNA-140 + 149 mimics. Overall, the strongest staining was shown for miRNA-149 mimic + miRNA-221 inhibitor, with the FLR group supporting the largest increase in sGAG staining (Fig. 4.5 A). A significant increase in the key transcription factor SOX9 was observed following RALA-miRNA-140 + 149 mimics delivery in comparison to both the healthy and NT control, with evidence of increasing expression in the other groups for both vector-mediated transfections (Fig. 4.5 B, C).

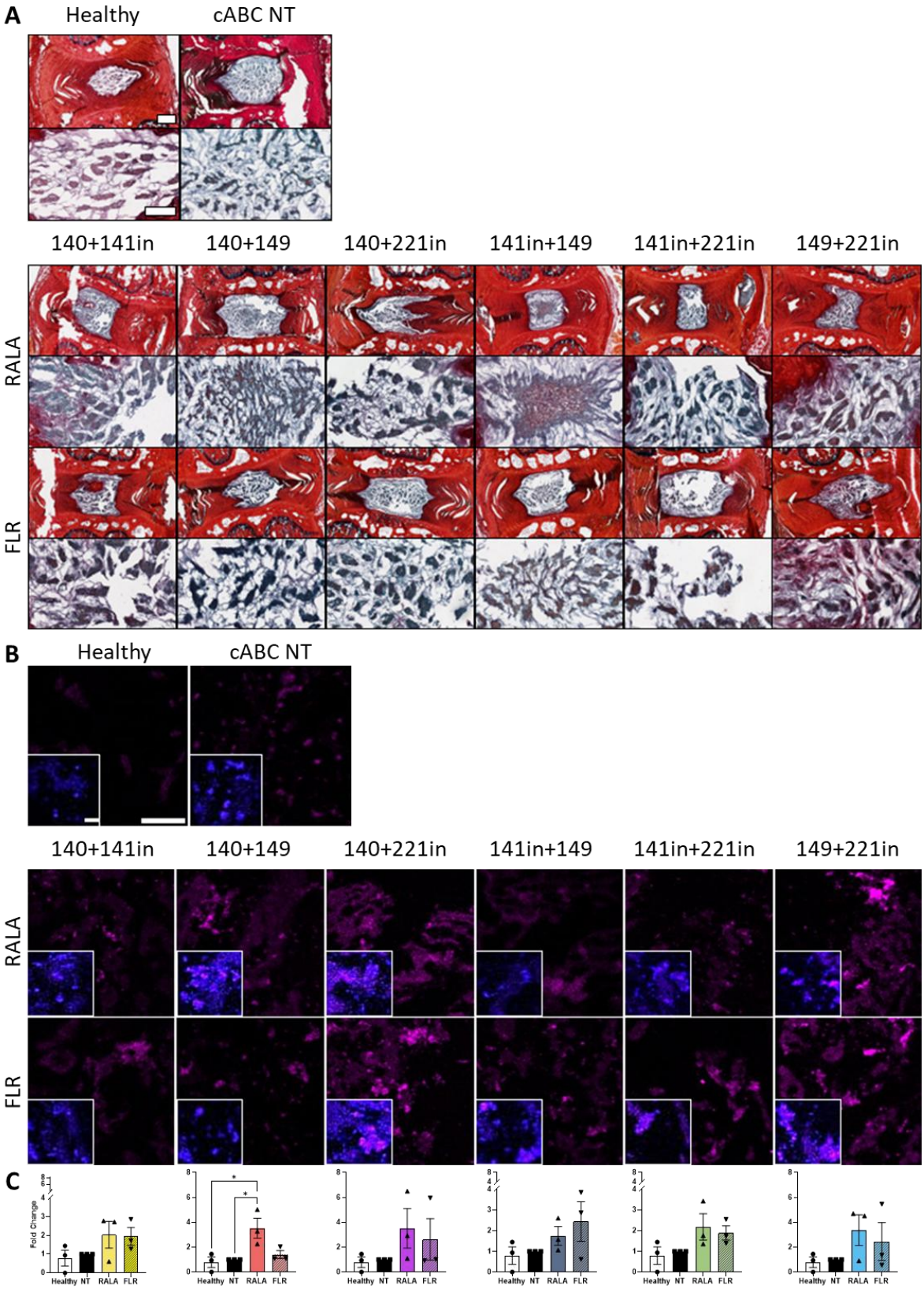

Figure 4. 5 Histological staining of miRNA pairings delivered with cell penetrating peptides (RALA and FLR) in ex vivo rat caudal organ cultures 14 days post-transfection demonstrated instances of increases to glycosaminoglycan (GAG) and transcription factor SOX9.(A)

Collagen was detected with picrosirius red staining (red), and (GAG) presence with alcian blue (blue/purple). There is evidence of increased GAG deposition in comparison to the controls in groups 140+141-in, 140+149, and 141-in+149, with more intense GAG staining observed for FLR 149+221-in. (B) Antibody labelling of SOX9 (magenta) revealed elevated expression levels across the majority of groups with a significant upregulation after transfection with RALA-miRNA-140+149. (C) Semi-quantitative analysis of SOX9 expression. * ($p<0.05$) indicates statistical significance, N=3 independent biological replicates. Healthy controls did not receive cABC treatment, with non-transfected (NT) controls degenerated with cABC and injected with a sham PBS injection. Scale bar for histology images of whole discs is 500 µm, images of GAG staining are 150 µm. Scale bar for fluorescence images is 100µm. Scale bar for insets with nuclear (blue) staining are 20 µm.

In addition to increases in sGAGs, an encouraging suppression of key ECM-degrading proteins was evidenced with immunofluorescence imaging in the FLR-miRNA-149 mimic + miRNA-221 inhibitor group A significant decrease in ADAMTS5 ($p=0.036$) protein expression was identified (Fig. 4.6 A, B).

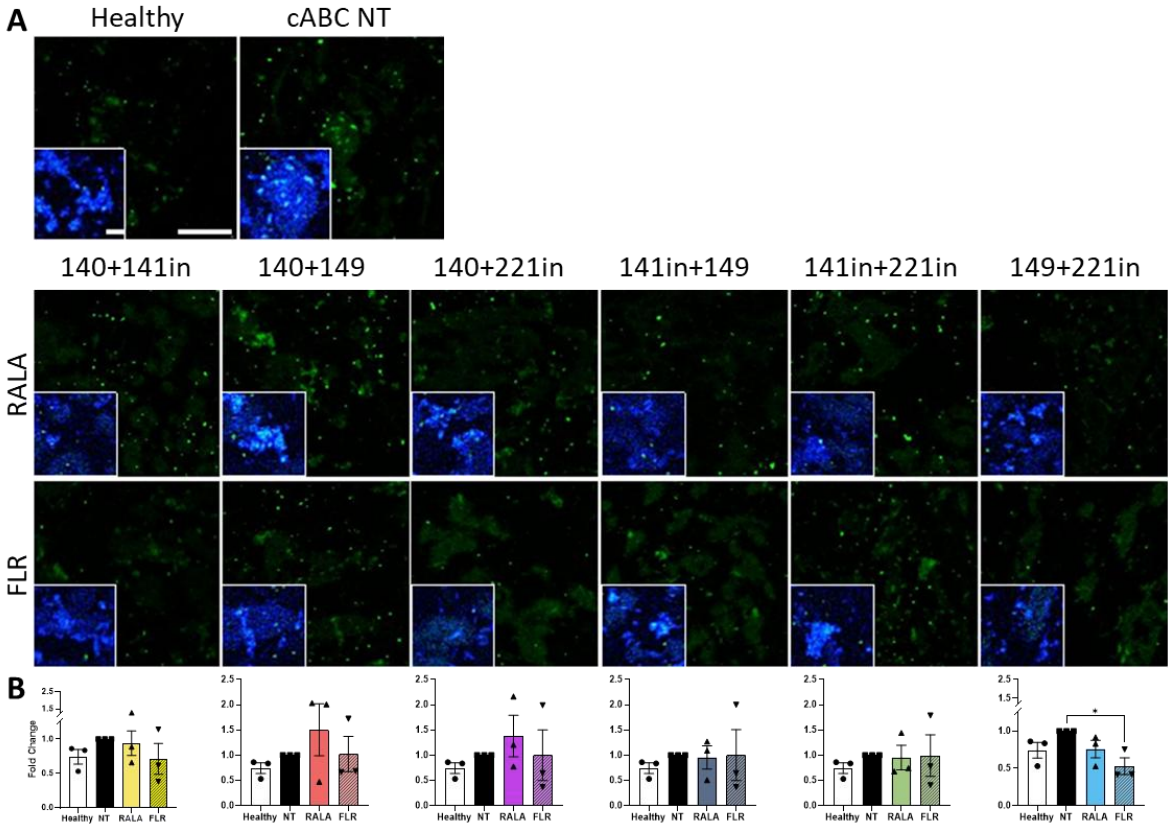

Figure 4. 6 Combined delivery of FLR-miRNA-149 mimic and miRNA-221-inhibitor markedly decreased protein expression of the catabolic enzyme ADAMTS5 in rat caudal

organ cultures 14 days post-transfection. (A) Immunolabelling for ADAMTS5 (green) demonstrated significantly reduced expression following transfection of miRNA-149 mimic and miRNA-221-inhibitor using FLR, lower than that of the non-transfected (NT) control. (B) * ($p<0.05$) indicates statistical significance, N=3 independent biological replicates. Scale bar is 100 µm. Scale bar for insets with nuclear (blue) staining are 20 µm.

The reduction in ADAMTS5 protein release was concomitant with a marked reduction in MMP13 ($p=0.001$) (Fig. 4.7 A, B). In both cases, the fold change were equivalent to expression in the healthy, non-degenerated discs. Interestingly, mirroring somewhat what was observed in monolayer, RALA-miRNA-140 mimic + miRNA-221 inhibitor elevated MMP13 expression and was found to be significant ($p=0.022$).

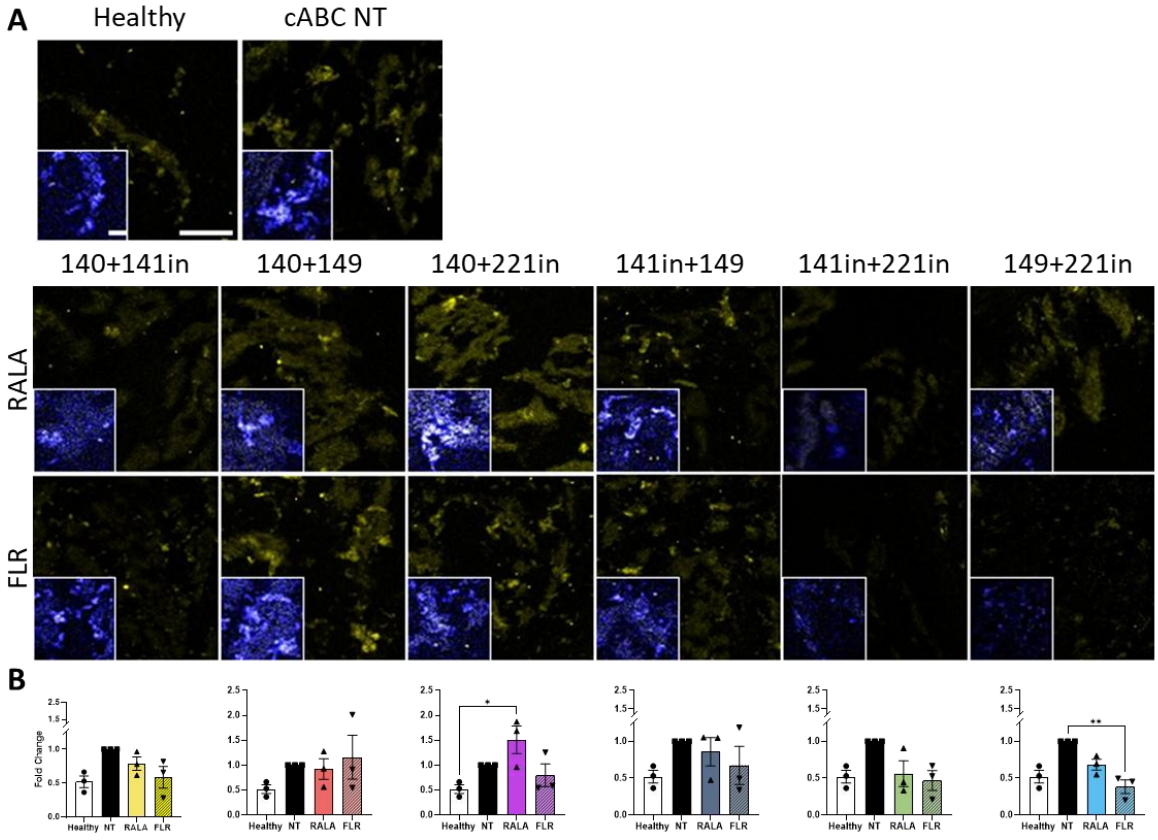

Figure 4. 7 FLR-miRNA-149 mimic and miRNA-221-inhibitor combined delivery significantly reduced protein expression of the catabolic enzyme MMP13 in rat caudal ex vivo organ culture explants 14 days post-transfection. (A) Immunofluorescence detected significantly reduced MMP13 (yellow) expression following transfection of FLR-miRNA-149 mimic and miRNA-221-inhibitor in comparison to the non-transfected (NT) control. (B) RALA-mediated miRNA-140 mimic and miRNA-221-inhibitor transfection significantly increased MMP13

production. * ($p<0.05$) ** ($p<0.01$) indicates statistical significance, N=3 independent biological replicates. Scale bar is 100 µm. Scale bar for insets with nuclear (blue) staining are 20 µm.

As the most promising of the screened dual-miRNAs NP viability following 21 days in culture was assessed. Viability was found to be 48.32% for the healthy control, 47.51% for the NT control, and 49.16% for the vector-dual-miRNA treatment, with no significant differences between groups (Fig 4.8).

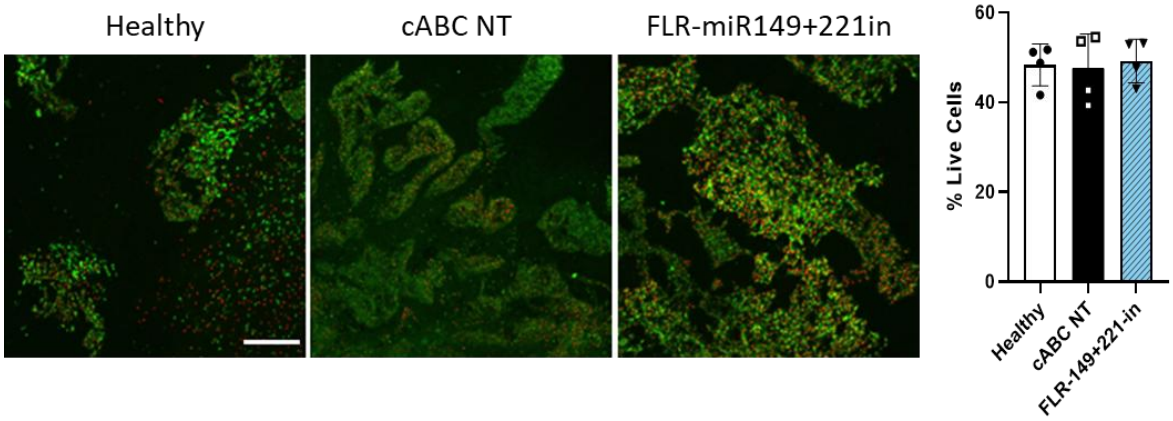

Figure 4.8 Cell viability of rat caudal NP tissue following 21 days of ex vivo organ culture. A. Representative images of maximum projection of z-stacks of Calcein AM (green, live) and Ethidium homodimer (red, dead) staining. B. Viability assessment of live and dead cells. Healthy discs were non-degenerated. Chondroitinase ABC (cABC), NT and FLR-miRNA-149+221-in groups were mildly degenerated with cABC for 7 days prior to Sham or miRNA-pair treatment. Scale bar is 150 µm. N=4.

4.3.5 Enrichment analysis identified distinct pathways and targets that interact with miRNA-149-5p mimic and miRNA-221-3p inhibitor

To further investigate the mechanism behind miRNA-149-5p mimic and miRNA-221-3p inhibitor in the downregulation of catabolic factors and stimulation of anabolic factors in the IVD, bioinformatic tools were utilised. A total of 54 strongly validated enriched targets were identified for the two miRNAs. miRNA-149-5p mimic was significantly implicated in a number of relevant pathways, including Response to Lipopolysaccharide (LPS), Execution Phase of Apoptosis, Response to Peptidoglycan, and Regulation of Signal Transduction (Fig.4.9 A-D). A table of all gene name abbreviations is provided in Appendix B.1.

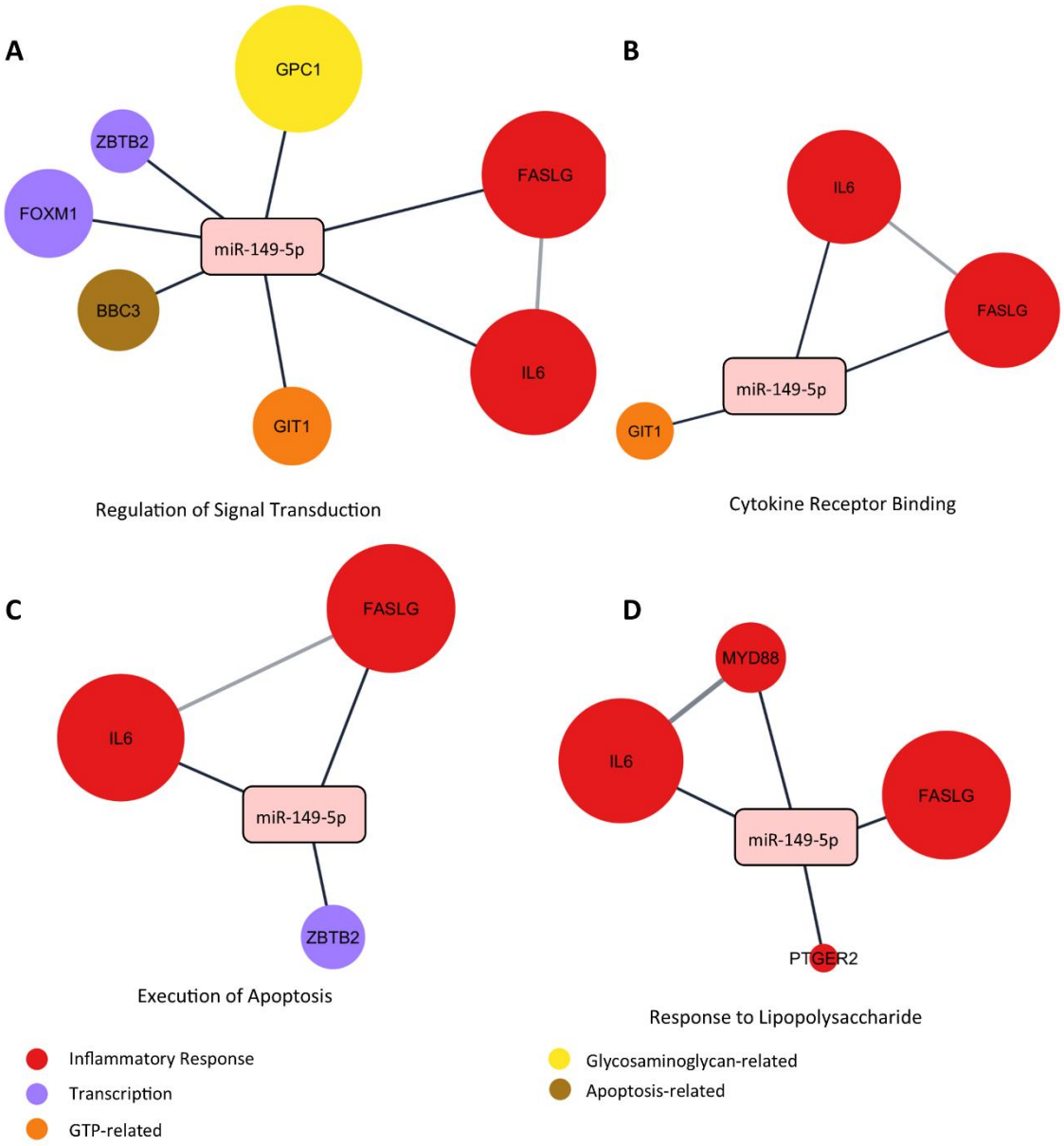

Figure 4. 9 Gene ontology (GO) pathway enrichment analysis of miRNA-149-5p and experimentally validated protein targets. (A) Regulation of Signal Transduction. (B) Cytokine Receptor Binding. (C) Execution of Apoptosis. (D) Response to Lipopolysaccharide. Expression levels within the extracellular compartment are visually presented, where larger nodes correspond to greater degree of expression within the extracellular space. Nodes are connected if an interaction is known to occur. Network constructed in Cytoscape Version 3.10. GTP: Guanosine triphosphate.

Conversely, miRNA-221-3p was enriched for pathways that relate to IDD, including Response to Hypoxia, Signal Transduction, Response to Cytokine, and Regulation of Protein Serine/Threonine Kinase Activity (Fig. 4.10 A-D). Interestingly, except for BCL2 Binding Component 3 (BBC3), there was no overlap in the target protein interactions, with both miRNAs having distinct targets and pathways with which they interact. A full list of abbreviated gene terms is provided in Appendix B.2.

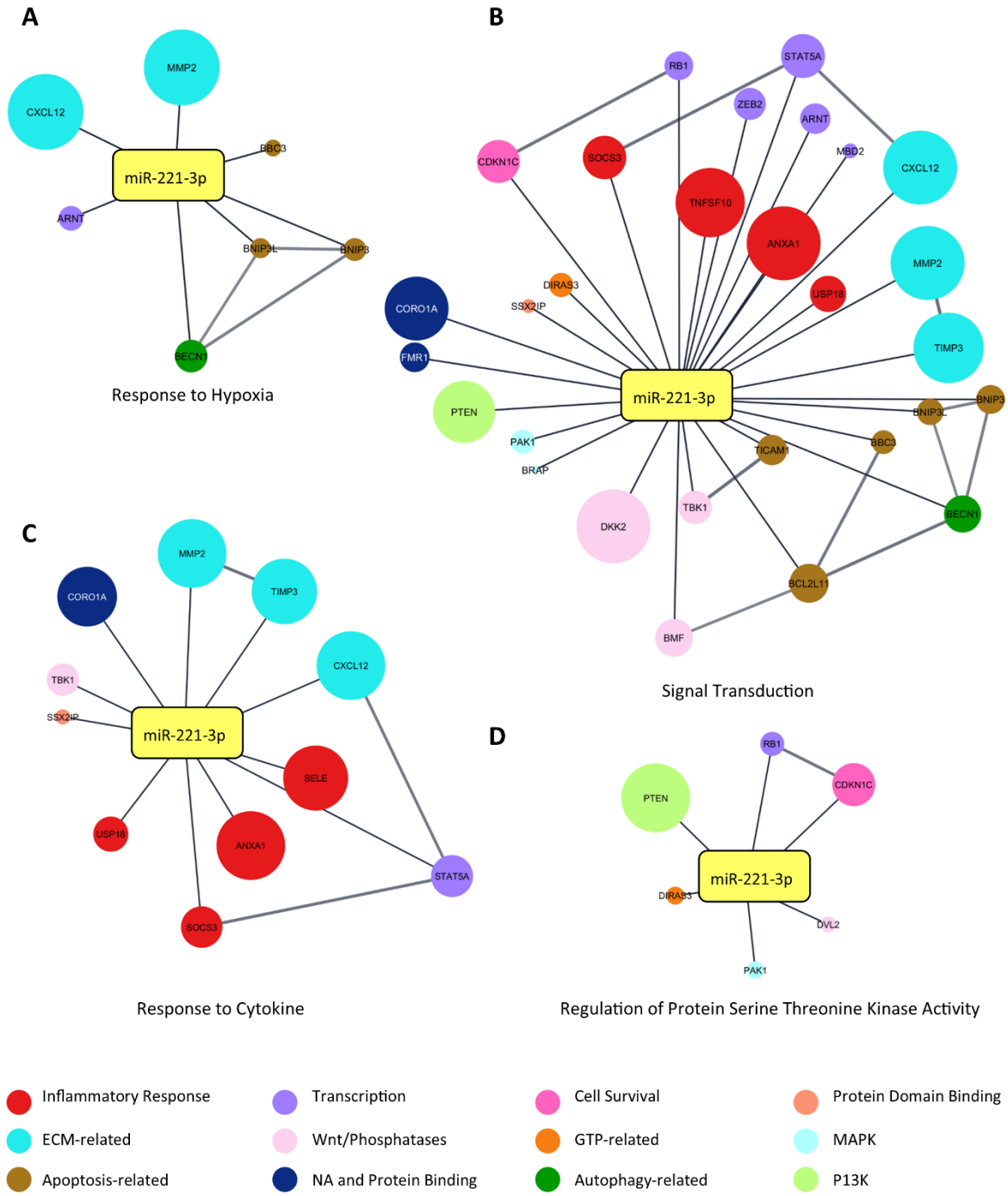

Figure 4. 10 Gene ontology (GO) pathway enrichment analysis of miRNA-221-3p and experimentally validated protein targets. (A) Response to Hypoxia. (B) Signal Transduction. (C) Response to Cytokine. (D) Regulation of Protein Serine Threonine Kinase Activity. Expression levels within the extracellular compartment are visually presented, where larger nodes correspond to greater degree of expression within the extracellular space. Nodes are connected if an interaction is known to occur. Network constructed in Cytoscape Version 3.10. NA: Nucleic acid, GTP:

Guanosine triphosphate, MAPK: Mitogen-activated protein kinases, P13K: Phosphoinositide 3-kinase.

4.4 Discussion

The introduction of non-virally delivered nucleic acids is an attractive therapeutic avenue, whereby key proteins and pathways can be regulated in a manner that drives regeneration or suppresses catabolic factors. For IVD treatment, this chapter highlights the potential of dual miRNA delivery when combined with CPPs and demonstrated that FLR-miRNA-149-5p mimic + miRNA-221-3p inhibitor stimulated the production of sGAGs and ECM proteins, while encouraging the downregulation of matrix degrading enzymes (ADAMTS5 and MMP3). Although there were promising results observed in monolayer culture, the adoption of an ex vivo organ culture model underscored the significance of using biologically relevant models. In this model, a notable reduction in catabolic enzyme activity was observed, further emphasising its relevance and potential.

Within monolayer investigations, increases in aggrecan and type II collagen protein expression above 4-fold in the miRNA pair groupings were identified, suggesting that dual-transfection is amplifying the regenerative response. In vitro protein expression increases following miRNA delivery above 1.5-fold of both aggrecan, and collagen type II have been linked to improvements to disc height index (DHI), GAG production, and restoration of the catabolic : anabolic balance in rodent models. [127,165] The potential and efficacy of dual-miRNA pairings has also been observed in other fields. In the context of diabetic wounds, Wang and colleagues identified that while transfection using miRNAs-129 and -335 individually promoted healing, when delivered in tandem this effect was strengthened. [180] In a similar manner, it was identified that dual delivery of let-7b and miRNA-34a reduced the proliferation of non-small cell lung cancer lines to a greater degree than single delivery alone, subsequently reducing tumour size. [181] Building on a 2009 study, [182] Mariner et al differentiated human MSCs towards an osteogenic lineage with co-delivery of miRNA-148b mimic and miRNA-489 inhibitor, to a greater extent than individual delivery. [183] Loading of collagen-nanohydroxyapatite scaffolds with a combination of miRNA-210 mimic and miRNA-16 inhibitor resulted in significantly increased vascularisation and bone density in a rat calvarial defect model, further indicating the potential of dual miRNA delivery. [184] These examples offer insight into the potential strengthening of positive stimuli with the correct combination of miRNAs and their cooperative impact.

In relation to the expression of catabolic proteins in monolayer, ADAMTS5 expression was, for the majority of the miRNA-pair groups, enhanced in the RALA groups, with FLR-transfected

combinations at times being significantly reduced in comparison. A similar, though not as pronounced effect was seen for MMP13. The FLR CPP was designed to include a GAG-binding peptide which fosters interaction with the lipid bilayer of the target cell and enhances cellular uptake of the given cargo. [126] Potentially, the homing effect of FLR to GAG-rich domains, which is abundant in the NP, facilitated targeted delivery of the miRNA-pairings, resulting in more efficient downregulation of ADAMTS5 and MMP13. The monolayer parameters of these screening experiments should be taken into consideration however, and the inherent lack of a protective ECM. [185] These conditions may have exacerbated the effect of the cytokine challenge, whereby any potential anabolic effect of the vector-miRNA-pairings may have been reduced. The variability identified may lie in the inherent inter-donor differences, with rats being from different donors and preparations. Added to this, cells used for in vitro studies often lose their circadian synchronicity, which may impact upon their responses to treatments, [186,187] prompting further investigations in a more relevant ex vivo organ culture model. A limitation of the 2D screenings was the implementation of normoxic culture conditions, which may have impacted upon matrix production and influenced the phenotype of NP cells, however, for ex vivo organ culture experiments physioxic oxygen levels were adopted.

Similar to the 2D experiments, when examining ex vivo organ cultures, elevated deposition of ADAMTS5 and MMP13 in the RALA groups compared to the FLR groups was observed. For most FLR-miRNA pairings, a decrease in enzyme production was detected, which was comparable to the levels seen in the non-degenerated, healthy control group. However, the strongest decreases for both ADAMTS5 and MMP3 were identified in the FLR-miRNA-149-5p mimic + miRNA-221-3p group. Increases in the expression of the key transcription factor SOX9 were identified in all groups, with the strongest degree of sGAG deposition observed histologically in the FLR-miRNA-149-5p mimic + miRNA-221-3p inhibitor group. Deemed an anti-chondrogenic miRNA, the inhibition of miRNA-221-3p has been shown to promote chondrogenesis through stimulation of aggrecan and collagen type II production. [188,189] Recently, the application of acetone extracts from Violina pumpkin leaves to IVD cells demonstrated the suppression of miRNA-221 expression and promoted the restoration of a healthy disc phenotype. This was notably characterised by a significant increase in the levels of aggrecan, collagen type II, and SOX9, in conjunction with enhanced resilience to damage induced by reactive oxygen species (ROS). [190] miRNA-149-5p was identified as a promoter of discogenic behaviour under LPS-stimulated culture conditions. [167] Its role in positively regulating the inflammatory response has been extensively documented in disease models of OA. [191,192] Elevated levels of pro-inflammatory cytokines, specifically IL-1β and TNF-α, are observed in degenerated discs, exacerbating the catabolic cascade. [43,53,193,194] To further elucidate the potential of FLR-miRNA-149-5p mimic + miRNA-221-3p inhibitor, future investigations will integrate anti-inflammatory mechanisms and their role in IVD degeneration.

The enhanced modulation of regenerative outcomes with dual-miRNA delivery may be explained by the targeting of distinct sets of pathways by both miRNA-149-5p mimic + miRNA-221-3p inhibitor. Through the analysis of enriched and experimentally validated miRNA-target interactions, various pathways and targets of both miRNA-149-5p mimic and miRNA-221-3p inhibitor were identified. miRNA-149-5p was primarily associated with a role in inflammatory processes, such as validated interactions with interleukin-6 (IL-6), Fas Ligand (FASLG), and myeloid differentiation primary response protein 88 (MyD88), all of which were highly expressed in the extracellular compartment. A meta-analysis conducted by Deng et al demonstrated a significant increase in IL-6 protein expression in patients with IDD compared to controls. [195] Additionally, a separate study established a correlation between IL-6 concentration and LBP. [196] Clinically, the incidence of reported pain and higher levels of IL-6 has been identified, [197] suggesting the importance of this cytokine in the degenerative cascade involved in IDD and the associated clinical relevance. As a member of the TNF family, polymorphisms in FASLG have been associated to degeneration of the IVD, [198] with FASLG driving NP cell apoptosis through the binding of FAS and recruitment of pro-inflammatory cytokines. [199,200] The toll-like receptor MyD88 has previously been linked with miRNA-149 in LPS-stimulation, whereby its silencing facilitated a dampening of the inflammatory milieu and stimulated a return towards a healthy expression of aggrecan and collagen type II. [167] MyD88 expression has been identified as being driven by pro-inflammatory cytokines in the disc [201] along with the immune response in cardiovascular and neurological disorders. [202,203] Considering the role of inflammation in IDD, the potential of miRNA-149-5p to mitigate these effects holds significant promise.

As a chondrogenesis-related miRNA, miRNA-221-3p was enriched for ECM-related pathways, with highly expressed targets in MMP2, Tissue Inhibitor of Metalloproteinase 3 (TIMP3), and C-X-C Motif Chemokine Ligand 12 (CXCL12) within the extracellular space. As matrix degrading enzyme promoters and inhibitors, respectively, a dysregulation of members of the MMP and TIMP families exacerbates the catabolic imbalance at the crux of IDD. [11,37] MMP2 specifically acts through the degradation and remodelling of collagens, [204] and polymorphisms in the gene have been associated with a statistically significant increase in the risk of developing IDD. [205] TIMP3 is unique among the TIMP family as it can suppress all MMPs, and a range of ADAMTS, including -4 and -5 which are of particular relevance to IDD. [12,41,206] A recent study identified a suppression of the discogenic pain marker Substance P following stimulation with TIMP3 in a rodent model, possibly through a reduction in vascularisation. [207] The upregulation of TIMP3 could therefore serve a therapeutic role when seeking regenerative therapies. Serum levels of the chemokine CXCL12, also referred to as stromal cell-derived factor 1 (SDF-1), have been found to be elevated with more severe levels of IVD degeneration and associated pain. [208] A connection has been identified between a dose-dependent effect of CXCL12 upon MMP2 protein expression in

cartilage endplate (CEP) cells, however, when delivered directly to the NP region in a rat tail model facilitated an increase in proteoglycan deposition, possibly via a stem cell homing mechanism. [209] Contrary to this amelioration of degeneration in the NP, CXCL12 has predominantly been linked to inflammation-induced apoptosis and matrix destruction. [210-212] Given the potential relationships between TIMP3, MMP2, and CXCL12, their interactions with miRNA-221-3p may prove advantageous in restoring regenerative function to the damaged IVD.

Finally, this chapter highlights the importance of adopting an appropriate and relevant study model, particularly when working within the three-dimensional constraints of the native ECM. While monolayer investigations evidenced some trends, more meaningful results were demonstrated in the ex vivo organ culture model. In the context of the IVD, NP cells readily lose their native phenotype when cultured in monolayer. [213] Furthermore, rats belong to the subsection of species that retain an NP progenitor notochordal cell population throughout adulthood. However, previous work has identified the reduction of notochordal porcine cells upon passaging, whereby NP and notochordal cells were indistinguishable from one another [214]. In the rat ex vivo organ culture model, notochordal cells will be present and constitute up to 30% of the NP cell population. However, injury in the form of degeneration diminishes this number. [215] Notochordal cells have been linked to regenerative potential [30,216], and their presence may have aided in some of the positive changes identified following miRNA delivery. Nonetheless, utilising the entire organ imparts a more physiologically relevant niche upon which to assess therapeutics, with the native ECM providing paracrine signalling to better replicate those reported in vivo. [135] Furthermore, ex vivo culture systems better reconstitute the metabolic microenvironment, offering more realistic systems to explore potential therapeutics. [137] The inclusion of a whole organ also offers the potential of employing loading pressure that more closely resembles the native mechanical stimuli experienced to gain deeper insights into potential treatment outcomes. [136]

The reduction shown in pro-catabolic enzymes possibly signifies the beginning of the creation of a microenvironmental niche with reduced catabolic activity that would facilitate regeneration. The salient biochemical characteristics of the degenerated NP are defined by a destabilisation of homeostasis causing reductions in vital discogenic proteins such as aggrecan and type II collagen, stimulation of degradative enzymes, including members of the ADAMTS and MMP families, and an increased inflammatory response. [217-219] The importance of ameliorating this degradative cascade has been well documented. [34,37,39,220,221] There could potentially be an inflammatory response to the carrier; however, such a reaction has not previously been reported for RALA or FLR. [172,222] Additionally, inflammation at the site of the injection could occur, as has been documented in in vivo rodent models. [223,224] The marked reduction in ADAMTST5 and MMP13 identified in the ex vivo organ culture for FLR-miRNA-149-5p mimic + 221-3p inhibitor may signify a calming of this catabolic environment, creating a niche whereby regenerative effects can

proceed, as observed with the increased sGAG deposition. This promising result demonstrates how the delivery of exogenous therapeutic vector-miRNA pairings can influence and engineer a suitable microenvironment to facilitate the return towards a homeostatic balance.

4.5 Conclusion

Through screening 6 potentially regenerative miRNA pairings delivered by employing two CPPs, FLR-miRNA-149-5p mimic + miRNA-221-3p inhibitor pairing was identified as being the most suitable for the deposition of sGAGs, and simultaneous dampening of pro-catabolic factors. A bioinformatics approach to analyse the experimentally validated targets of these two miRNAs demonstrated distinct targets and pathways that may be beneficial for IVD regeneration, with dual delivery amplifying those expected when delivered in isolation. Overall, this chapter suggests a therapeutic vector-miRNA pairing that may foster regeneration by the creation of an anti-catabolic niche within the IVD.

Chapter 5. Restoring Disc Matrix Homeostasis: Dual-miRNA and Human Platelet Lysate as a Novel Therapeutic Strategy

A significant portion of this chapter has been previously published in **Ní Néill, T.,** Wilson N., Thomas J., McDonnell, J.M., Darwish, S.L., Butler, J.S., O'Brien, F.J., Dixon, J.E., Curtin, C.M., Buckley, C.T (2026) "Restoring Disc Matrix Homeostasis: Dual-miRNA and Human Platelet Lysate as a Novel Therapeutic Strategy". *Materials Today Bio 38:103190.* doi: 10.1016/j.mtbio.2026.103190

Contribution: Played a key role in the conception and design of the study. Carried out the literature review, data collection and analysis, interpreted and presented the results, prepared the manuscript draft, undertook critical revisions, and approved the final version for publication.

5.1 Introduction

A multitude of regenerative medicine approaches have been trialled to tackle degeneration of the IVD, including cell therapies,[225-227] biomaterial augmentation,[228-230] and growth factor (GF) delivery.[58,231-233] In pre-clinical models, GF supplementation appears to be promising and beneficial, but the long-term efficacy has been limited, particularly due to single-dose durability and short half-life.[234-236] Building on this, instead of incorporating a single factor, using a cocktail may offer a multi-pronged strategy to enhance regenerative outcomes. Platelet lysate, derived from plasma, is enriched with multiple GFs including but not limited to members of the transforming growth factor (TGF) family, platelet-derived growth factor (PDGF), and vascular endothelial growth factor (VEGF).[59] Originally used as a serum substitute in cell culture[237], platelet lysate has demonstrated extracellular matrix (ECM) enhancing potential in the field of orthopaedics, including the upregulation of key components such as aggrecan and collagen type II, both in vitro and in vivo.[62-65]

Human platelet lysate (HPL) delivery has been explored clinically in the treatment of numerous musculoskeletal conditions, involving tissues with limited intrinsic healing potential, similar to the IVD. In the IVD field, a preliminary prospective trial reported that 47% of patients had significant improvements to the visual analogue score (VAS) and Oswestry Disability Index (ODI) 6 months-post single platelet rich plasma injection.[68] A prospective double-blind randomised clinical trial (RCT) evaluated a single intradiscal lysate injection in patients with chronic low back pain, reporting statistically significant improvements in pain, function, and patient satisfaction compared to the control group 8 weeks post-treatment.[238] Akeda and colleagues also reported

significant improvements to patient VAS scores following a single intradiscal injection of platelet-rich plasma, though, interestingly no improvements in disc height index were observed.[239] However, it should be noted that evidence from the disc field is sparse, detailing changes to pain scores but often no structural or mechanical changes. Importantly, none of these studies have reported adverse effects associated with lysate administration, highlighting its safety and translational potential as a low risk, first-line therapeutic option in orthopaedics.

Effective IVD therapies will likely augment and promote ECM production while mitigating the inflammatory and catabolic responses. Incorporating an anti-catabolic factor offers a multimodal strategy whereby inflammation is suppressed, allowing matrix regeneration to proceed. Given the promising anti-catabolic action of miRNA delivery and the regenerative potential of platelet lysate, this chapter proposed supplementing the dual-miRNA identified in Chapter 4 to enhance matrix production. The primary objective of this work was to investigate the potential of dual-miRNA delivery supplemented with HPL in a range of culture models and species, to identify whether the anti-catabolic effect was maintained whilst driving the production of ECM proteins. It was hypothesised that the combined delivery of miRNA-pair-149-5p mimic and 221-3p inhibitor and HPL may stimulate the repair process, offering a novel prospective treatment for IVD degeneration.

5.2 Materials and Methods

5.2.1 Human donor characteristics

Five human NP donors were utilised for encapsulation in an NP-ECM gel analogue, with donor information detailed in Table 5.1.

Table 5. 1 Demographic and clinical characteristics of human donors used for in vitro studies

Donor	Gender	Age	Smoker (Y/N)	Pfirrmann Grade
1	F	24	No	3
2	M	44	Former – 15 years	2
3	F	29	No	2
4	M	57	No	3
5	F	33	No	3

5..2.2 Human platelet lysate dosage study in monolayer

Rat NP cells were seeded in microwell chamber slides (ibidi GmbH) at a density of 5 x 10^3 cells per well in XPAN, where attachment was allowed to proceed overnight and subsequently washed with phosphate buffered saline (PBS). Media was added, either SF DMEM LG alone or supplemented with 2.5, 5, or 10% HPL (StemCell Technologies, Canada). Cells were cultured for 3 days and fixed in 4% paraformaldehyde (PFA) for 12 minutes followed by assessment of aggrecan and collagen type II protein expression. The extent of cell proliferation was assessed by counting the nuclei from each group. For all studies a minimum of three independent biological replicates were performed, with a minimum of duplicate technical replicates. Biological replicates are indicated by individual data points in the graphs.

5.2.3 Confirmation of miRNA over- and under-expression via RT-qPCR

To confirm the successful delivery of miRNA-149-5p mimic and miRNA-221-3p inhibitor, rat NP cells were seeded at 10 x 10^4 in 48-well plates and allowed to attach overnight. miRNA complexes of 10ng/µl miRNA-149-5p mimic and miRNA-221-3p inhibitor (both Dharmacon) with the FLR peptide (Dixon Lab, Nottingham) were formed via electrostatic interactions in OptiMEM reduced serum media (Gibco) for 30 minutes. Cells were washed with PBS to remove residual serum and transfected for 6 hours at 37°C at 5% O_2. Post-transfection wells were replenished with XPAN media and cultured for 3 days for analysis of miRNA over- and under-expression. Total RNA was extracted using QIAzol reagent and the miRNeasy kit (Qiagen) according to manufacturer's instructions. The miRCURY LNA reverse transcription kit and validated miRCURY LNA SYBR Green PCR assays were utilised to assess levels of miRNA-149-5p and miRNA-221-3p (all Qiagen). Relative expression levels were normalised to the endogenous 18S ribosomal RNA and calculated using the 2(-ΔΔCt) method to compare expression levels between non-transfected (NT) and transfected cells.

5.2.4 miRNA pair delivery supplemented with HPL in monolayer

Upon fixing the HPL dosage, the effect of dual-miRNA delivery augmented with HPL was examined. NP cells were seeded at a density of 5 x 10^3 cells in microwell chamber slides (ibidi GmbH) and allowed to attach overnight. Transfection was performed as described above, where following transfection SF DMEM LG media, or DMEM LG + 10% HPL media was applied to cells, which were cultured for 3 days for protein analysis of ECM markers, aggrecan and collagen type II, alongside proliferation analysis. Stimulation of matrix degrading enzymes was achieved through

a cytokine challenge 24 hours post-transfection of 50 ng/mL TNF-α and 10 ng/mL IL-1β (both Fisher Scientific). Cells were insulted for 24 hours whereupon media was replaced as described above and culture proceeded for 3 days.

5.2.5 Assessment of miRNA and HPL treatment in rat ex vivo organ culture

To confirm the viscosity of HPL would not adversely affect miRNA uptake, a fluorescently-tagged miRNA miRDy547 (Dharmacon) was first employed. Following degeneration, miRDy547 complexes (25 ng/µl) were prepared by incubating with FLR in OptiMEM for 30 minutes at room temperature. Where applicable, 10% HPL was subsequently incorporated and 2 µl of the mixture was delivered to rat discs. Uptake of the fluorescently tagged miRNA was assessed after 7 days of culture. Treatments were prepared and administered in 2 µl volumes using a 30G needle. The non-transfected (NT) control received OptiMEM as the vehicle, while the HPL-only group received 10% HPL prepared in the same vehicle. FLR-miRNA-149-5p mimic and miRNA-221-3p inhibitor dual complexes were prepared at a concentration of 25 ng/µl in OptiMEM and incubated for 30 minutes at room temperature. miRNA complexes were directly injected for the miRNA-only group, whereas the for the miRNA + HPL group, 10% HPL was added to the complexes prior to injection. Treatments were maintained in culture for14 days with biweekly media exchanges. Collected media were pooled to assess GAG released during the culture period. At the end of culture, discs were fixed overnight with 4% PFA at 4°C for histological evaluation, or the NP region excised for, biocompatibility, biochemical, and cytokine quantification.

5.2.6 NP-ECM, NP-ECM-MA, and CS-MA preparation

To simulate ex vivo organ culture while incorporating patient-derived cells, an NP analogue was developed for in vitro culture. Fresh bovine NP tissue was dissected and finely diced into approximately 2mm fragments. The tissue was then pretreated with 0.2 M NaOH for 24h at 4 °C under constant rotation to assist with subsequent tissue digestion. The tissue was washed with PBS sequentially prior to freeze drying and cryo-milled with a cryogenic grinder (6775 Freezer/Mill, SPEX SamplePrep) to obtain a fine NP-ECM powder. Nucleic acids were removed through treatment with Benzonase nuclease (2U/mL, Sigma-Aldrich) in Tris Buffer. Solubilisation was carried out with activated pepsin solution (30 mg/20 mg of ECM powder) in 0.5 M acetic acid (HAc) for 48 hours at room temperature under constant rotation. Salt precipitation was performed using 0.9 M NaCl followed by dialysis against deionised water with 12-14 kDa MWCO dialysis membrane at 4°C. Dialysis was carried out for 28 hours with water changes twice daily. The dialysate was freeze dried under standard conditions (500 mTorr, -10°C, 16 – 18h, Harvest Right™).

Methacrylate (MA) groups were added to the NP-ECM to facilitate photo-crosslinking. To begin, NP-ECM was solubilised in 2.5 mg/mL 0.5M HAc overnight at 4°C with vigorous agitation, whereupon the pH was adjusted to 7.5. Protected from light, methacrylic anhydride was added at a dose of 20 µl per 100 mg of NP-ECM in a dropwise fashion and stirred overnight at 4°C. NP-ECM-MA was dialysed in 12-14 kDa MWCO membrane, initially against 1% v/v HAc for 3 days at 4°C, followed by deionised water for a further 3 days. For each dialysis step, the required solution was changed twice per day. The retained NP-ECM-MA was freeze-dried and stored at -20°C prior to gel preparation. For the functionalisation of chondroitin sulphate (CS), sodium salt (Biosynth) was dissolved in deionised water (20 mg/mL), with 1 mL/mL of methacrylic anhydride added dropwise under constant stirring and protected from light. The pH of the solution was adjusted to 8 and allowed to stir at room temperature for 3 hours, followed by overnight at 4°C. The unreacted methacrylic anhydride (MA) was precipitated out of solution by the addition of a 4-fold excess of ethanol, and the ethanol washing step was repeated three times. CS-MA was resuspended in deionised water, dialysed for 3 days against 1% HAc and 3 days against deionised water, followed by freeze-drying to obtain a CS-MA powder.

5.2.7 Preparation of human NP cell-laden NP-ECM-MA CS-MA analogues

To prepare the tissue ink, NP-ECM-MA (15% w/v) and CS-MA (10% w/v) powders were weighed and solubilised in XPAN media for 48 hours at 4°C. Prior to cell incorporation, the solutions were mixed at 1:1 ratio to yield a final concentration of 7.5% w/v NP-ECM-MA and 5% w/v CS-MA, neutralised with 5M NaOH, and sterilised by ultraviolet (UV) radiation for 15 mins. Human NP cells from patient samples ranging from mild to moderately degenerated discs were expanded and utilised experimentally by Passage 3. Cells were incorporated into the gels through mixing at a concentration of 2.5 x 10^6 cells/mL, which relates to approximately the total number of NP cells found in a degenerated disc.[240] 0.25% v/v lithium phenyl-2, 4, 6-trimethylbenzoylphosphinate (LAP, Sigma-Aldrich) was employed as the photo-initiator and the mixture was injected into 50 µL moulds and crosslinked for 1 minute under blue light (405 nm). The formed gels were cultured in 4% agarose wells prepared in 48 well plates, each containing an internal well that housed individual gels to facilitate easier injection delivery for subsequent experiments. Culture conditions were maintained in XPAN media at 5% O_2 in a humidified incubator at 37°C.

5.2.8 Evaluation of miRNA and HPL treatment using a human cell-laden NP-ECM gel analogue

An overview of the experimental outline for NP cell-laden ECM analogues is presented in Figure 5.1. To induce a mildly catabolic and GAG-degrading response comparable to that observed in the rat ex vivo organ culture model, human NP cell-laden gel analogues were injected with 2µl of 0.025U cABC and cultured to allow for 7 days to allow degeneration to proceed. Following this, degenerated groups were treated with either the vehicle (NT control), FLR-miRNA-149-5p mimic + miRNA-221-3p inhibitor (miRNA pair), 10% HPL, or 10% HPL + miRNA pair and cultured for a further 14 days. As an additional healthy control, one group of gels was not treated with cABC for the 21 days culture period. Media changes were performed twice weekly, with the collected media pooled at each time point for biochemical analysis of leached ECM components and ELISA assessment of inflammatory markers. Whole gels were also reserved for biochemical analysis, while those designated for histology were fixed in 4% PFA overnight at 4°C.

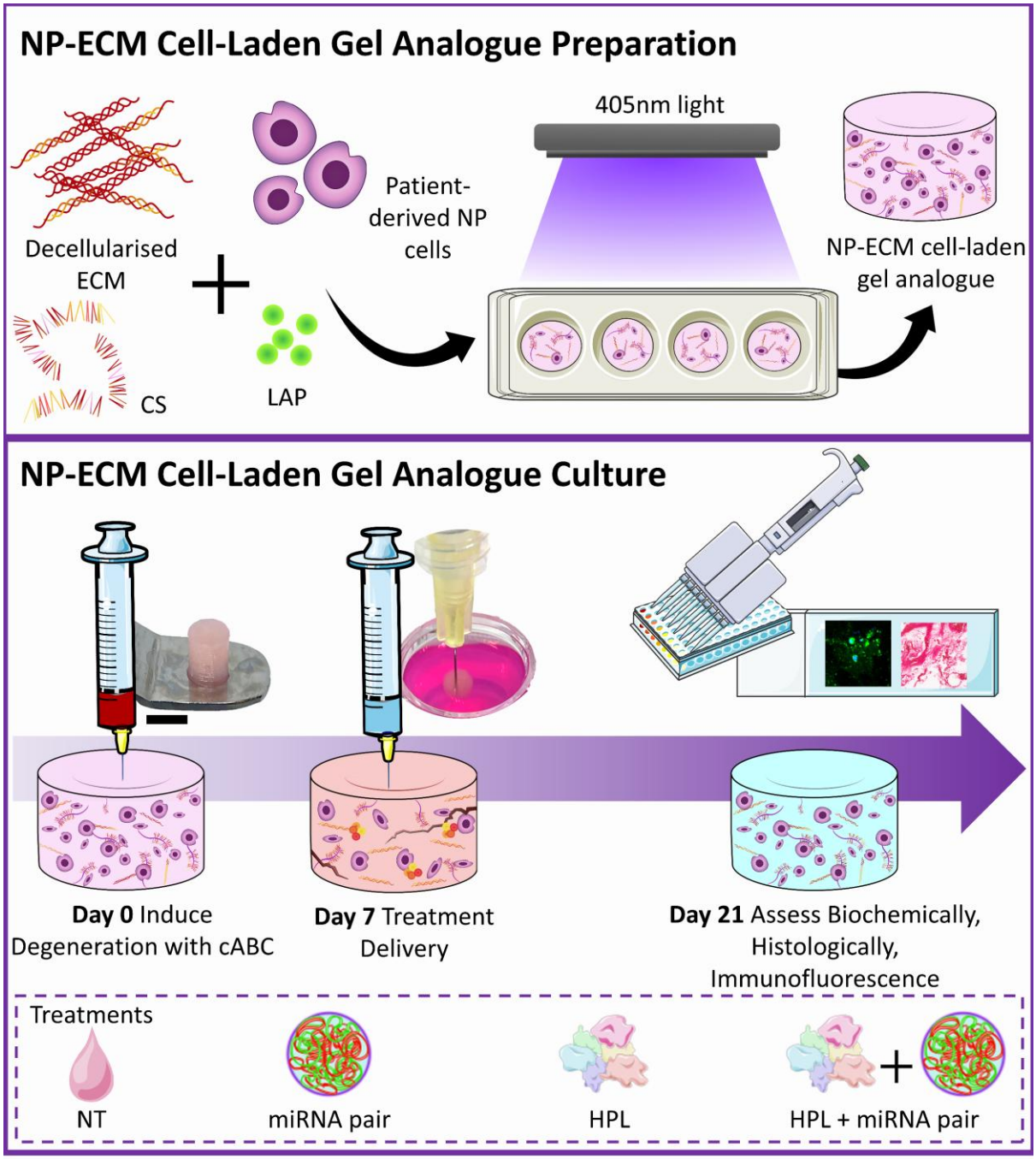

Figure 5.1 Experimental outline for generating human cell-laden nucleus pulposus (NP)-extracellular matrix (ECM) gel analogues. Gel analogues were prepared as described in Section 2.8, and degeneration was induced in samples designated for treatment with chondroitinase ABC (cABC) which cleaves sulphated glycosaminoglycans (sGAG) and triggers a catabolic response. Healthy, non-degenerated controls were included in all experiments. On day 7, gel analogues were injected with the respective treatments and cultured until day 21, when they were analysed biochemically, histologically, and via immunofluorescence for specific anabolic and catabolic markers. Abbreviations: CS, Chondroitin sulphate; LAP, lithium phenyl-2, 4, 6-trimethylbenzoylphosphinate; NT, Non-transfected. Scale bar = 5mm.

5.2.9 Assessment of rat ex vivo organ and NP analogue culture biocompatibility

At the culture endpoints, the entire NP tissue was dissected from rat ex vivo organ culture motion segments. The viability of both NP tissue and NP-ECM gels was assessed through staining with 2 µM Calcein AM and 4 µM ethidium bromide (EtBR) for 1 hour at 37°C. Samples were imaged on a Leica SP8 scanning confocal microscope, where a z-stack of the entire NP tissue or NP analogue was taken. Acquired images were analysed using ImageJ software (version 1.54p) to identify the live and dead cell populations.

5.3 Results

5.3.1 Confirmation of HPL dosage and miRNA expression in rat nucleus pulposus monolayer culture

Critical to the experimental framework was ascertaining the effect of HPL supplementation on a rat NP cell population (Fig. 5.2). Both 5 and 10% HPL significantly increased aggrecan protein expression (Fig. 5.2A & B, $p = 0.011$ and 0.039, respectively), with collagen type II similarly being upregulated at the 10% dose (Fig. 5.2C & D, $p = 0.017$). The addition of HPL at all concentrations enhanced cell proliferation, with the strongest effect observed at 10% (Fig. 5.2E & F, $p = <0.0001$). Therefore, 10% HPL supplementation was selected for subsequent experiments. Successful over-expression of miRNA-149-5p was confirmed by RT-qPCR post-transfection with a significant increase compared to the NT control (Fig. 5.2G, $p <0.0001$). The silencing of miRNA-221-3p was also demonstrated, with its expression significantly downregulated compared to the control (Fig. 5.2H, $p <0.0001$).

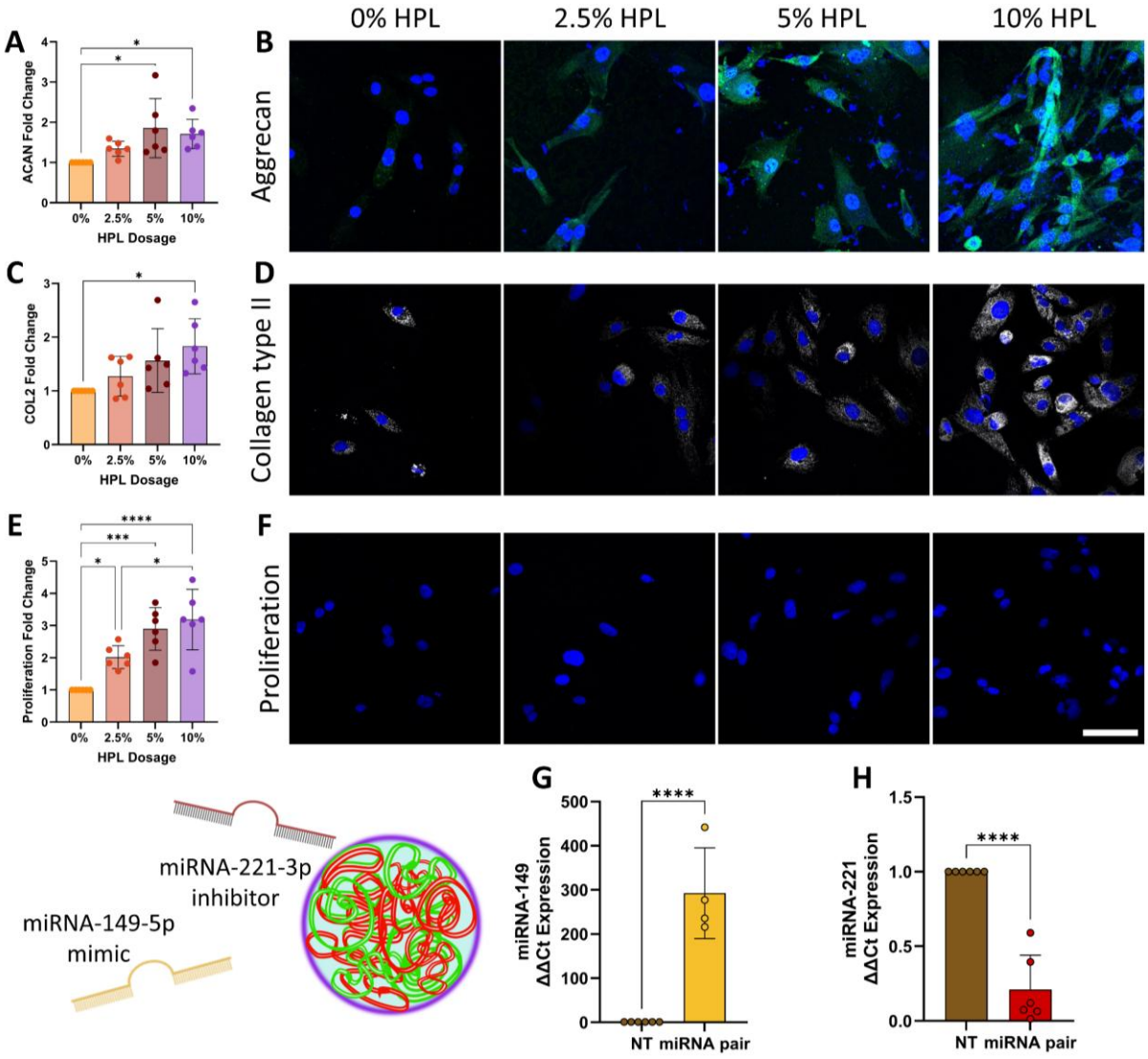

Figure 5.2 Increasing doses of human platelet lysate (HPL) increased extracellular matrix markers, alongside cell proliferation in rat nucleus pulposus (NP) monolayer culture. Protein expression was quantified via immunofluorescence, with representative images displayed for (A & B) aggrecan and (C & D) collagen type II. (E & F) Proliferation was assessed through DAPI staining and quantification of nuclei. (G & H) RT-qPCR was used to assess the expression of miRNA-149 and miRNA-221 3 days post-transfection. N = 6 independent biological donors, immunofluorescence data normalised to 0% HPL control, RT-qPCR to the non-transfected (NT) control. * $p < 0.05$, *** $p < 0.001$, **** $p < 0.0001$ indicates statistical differences. Scale bar = 100 µm.

5.3.2 Dual-miRNA transfection combined with HPL supplementation increased protein expression of matrix markers while maintaining an anti-catabolic effect in rat monolayer culture

Upon establishing the most efficient HPL dose, the incorporation of the therapeutic dual-miRNA and the impact upon ECM protein markers was explored (Fig. 5.3). ECM production was enhanced in the miRNA + HPL group, with aggrecan protein levels significantly increased compared to the NT control (Fig. 5.3A & B, $p = 0.017$). Production of collagen type II also increased in the miRNA + HPL group (Fig. 5.3C & D, $p = 0.049$). Furthermore, proliferation increased over 3-fold following miRNA-pair transfection combined with HPL supplementation (Fig. 5.3E & F, $p = 0.003$ vs NT, $p = 0.002$ vs miRNA only). Alcian blue staining of sGAGs supported these findings, with deeper staining evident in the miRNA + HPL group compared to all other treatments and NT control (Fig. 5.3G).

Targeting the catabolic milieu is essential for tackling IVD degeneration. Therefore, the protein expression of two frequently upregulated degradative enzymes, ADAMTS5 and MMP13, were assessed following cytokine challenge. ADAMTS5 was significantly downregulated in the miRNA pair group (Fig. 5.3H & I, $p = 0.031$ vs NT), with the combination of HPL further bolstering this effect ($p = 0.005$ vs NT). MMP13 expression was significantly reduced across all treatments, with dual-miRNA alone producing the strongest effect when compared to the control (Fig. 5.3J & K, $p = 0.0007$). HPL supplementation exerted a comparable effect, suppressing MMP13 expression ($p = 0.032$ for HPL only and $p = 0.016$ for miRNA + HPL in relation to NT). No significant changes in proliferation were observed, likely due to the cytokine challenge (Fig. 5.3L & M). However, an upward trend similar to the non- challenged cytokine group was observed.

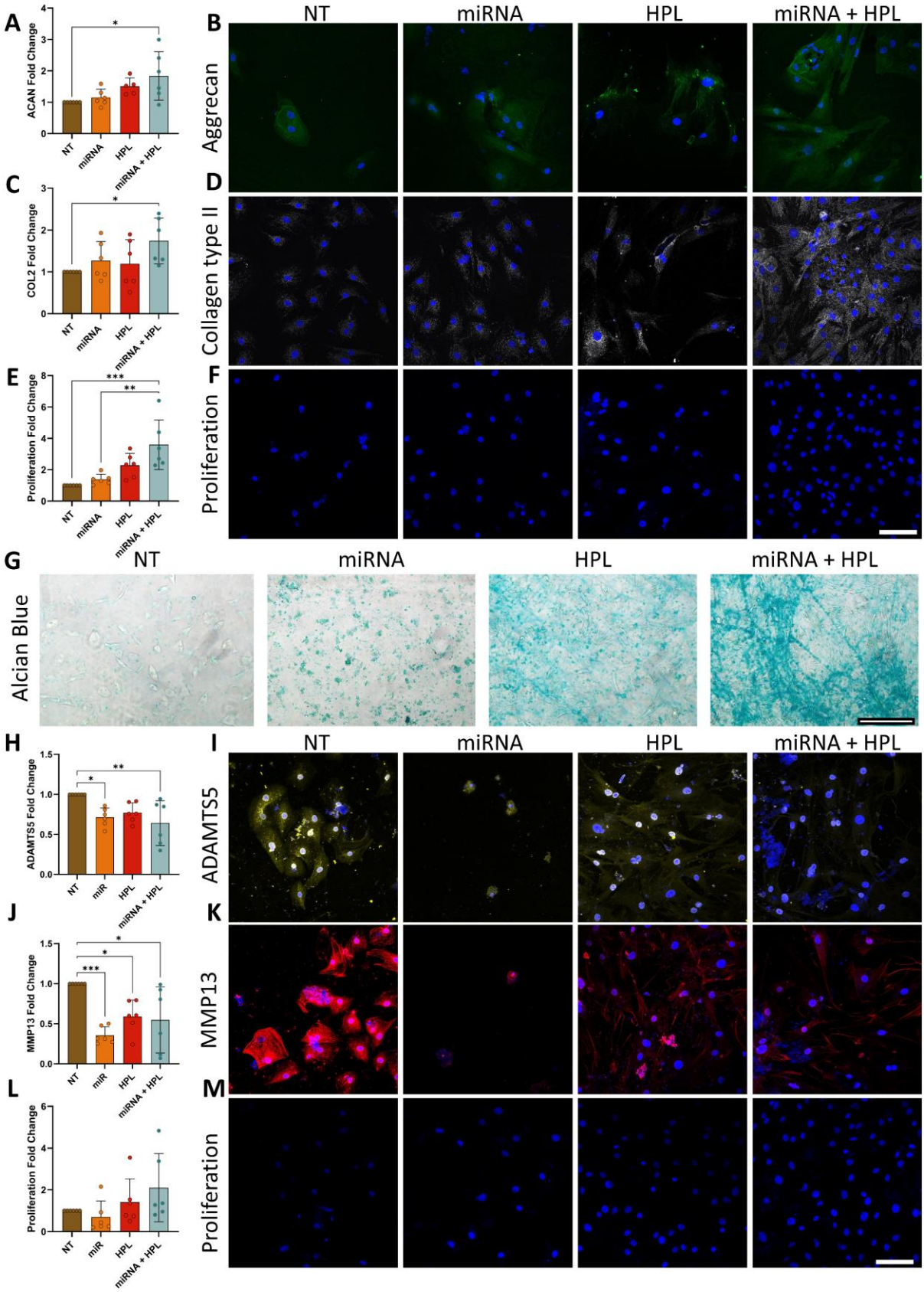

Figure 5.3 Examination of extracellular matrix (ECM) discogenic and degrading factors in rat nucleus pulposus monolayer cultures demonstrated enhanced expression of regenerative proteins and downregulation of catabolic markers. ECM markers assessed using

immunofluorescence staining with representative images for (A & B) aggrecan and (C & D) collagen type II. (E & F) Proliferation was assessed through DAPI staining and quantification of nuclei. (G) Representative images of Alcian blue staining evaluated the total accumulation of sGAGs. (H & I) Catabolic protein expression for ADAMTS5 and (J & K) MMP13, alongside (L & M) proliferation post-cytokine challenge. N = 6 independent biological donors, data normalised to 0% HPL control.* $p < 0.05$, ** $p < 0.01$, *** $p < 0.001$ indicates statistical differences. Scale bars = 100 µm.

5.3.3 Dual-miRNA combined with HPL enhanced production of matrix constituents in a rat ex vivo organ culture model

The effects of miRNA and HPL treatment were subsequently evaluated in a more physiologically relevant microenvironment using mildly degenerated rat ex vivo disc organs. NP cell viability was preserved throughout the culture period, as determined by live/dead staining, with no marked changes evident in DNA content between the groups (Fig. 5.4 A - D). Histological analysis revealed that cABC treatment visibly disrupted the NP matrix, with tears evident in all stains compared to the intact healthy control. The viscosity of HPL did not impede miRNA delivery as demonstrated by the uptake of fluorescently labelled miRDy547, which remained localised within the cells following 7 days in culture (Fig. 5.4 E & F).

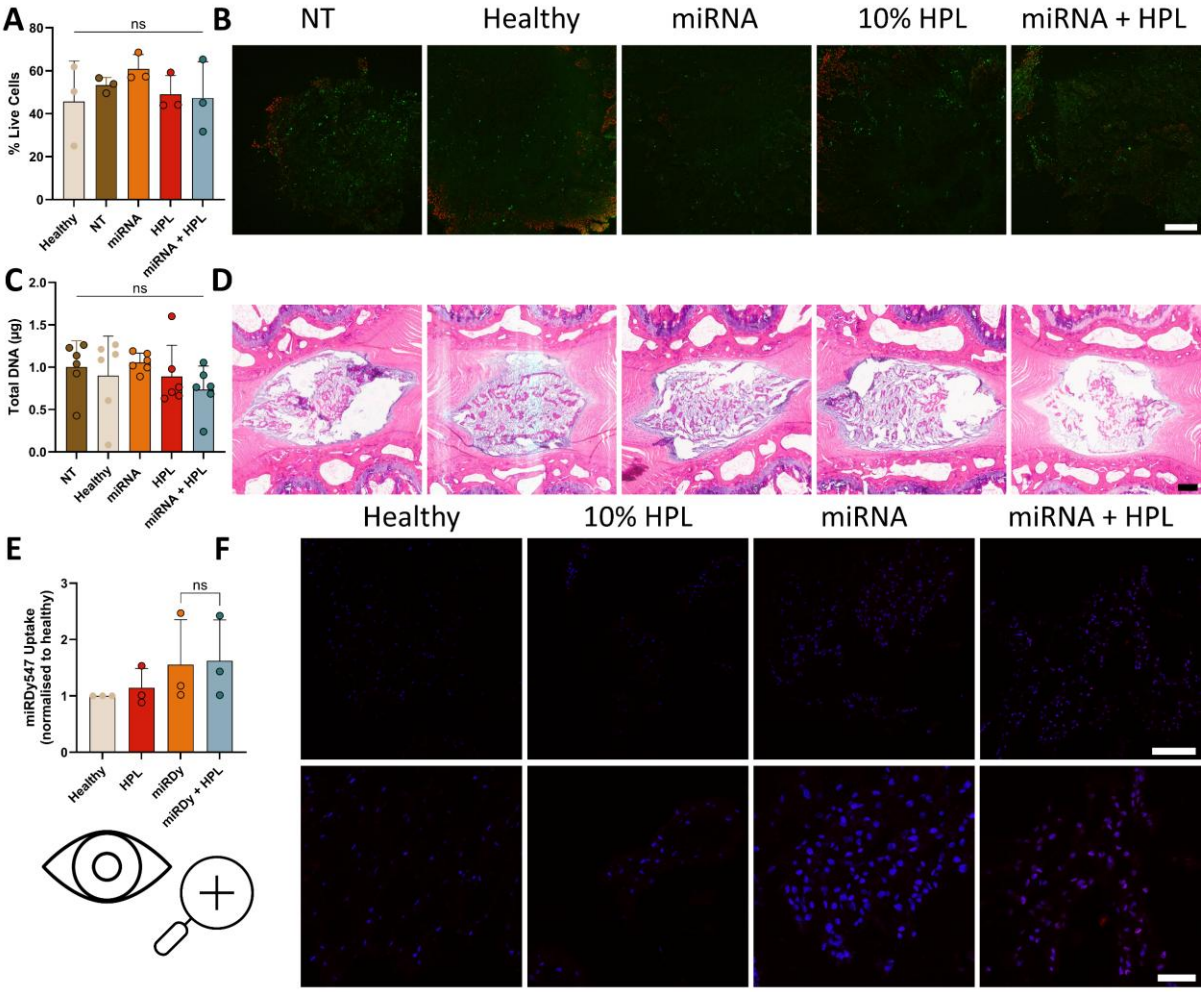

Figure 5.4 Cell viability and miRNA uptake in rat ex vivo organ cultures. (A) Organ culture viability as assessed by (B) live/dead staining following 21 days of culture. (C) Total DNA was quantified biochemically and cellular morphology by evaluated using (D) haematoxylin and eosin staining. (E & F) Uptake of the fluorescently labelled miRDy547 was measured after 7 days of culture, in isolation or with the supplementation of 10% HPL. N = ≥ 3 independent biological donors. Live/dead scale bar = 200 µm, histology scale bar = 500 µm, miRDy547 uptake scale bar = 100 µm for overall image, 150 µm for magnified image

To assess the potential of the potential treatments in promoting ECM components, total collagen and specific collagen markers were analysed. Overall collagen levels in the NP remained unchanged following treatments (Fig. 5.5A & B). Collagen type I, associated with a fibrotic phenotype, was significantly upregulated in the 10% HPL only group (Fig. 5.5C & D, $p = 0.028$). Consistent with findings from monolayer cultures, collagen type II was markedly increased following miRNA + HPL treatment relative to the NT control (Fig. 5.5E & F, $p = 0.047$).

Stimulation of sGAG production is critical for achieving regenerative potential in the disc. Biochemical evaluation revealed that sGAG levels in the miRNA + HPL group increased more than 2-fold compared to the NT control (Fig. 5.5G & H). To further explore this, key early- and late-stage proteins in the ECM were measured. SOX9 protein expression was significantly upregulated 2-fold by miRNA + HPL treatment relative to the degenerated control (Fig. 5.5I & J, $p = 0.019$). Consistent with monolayer findings, the late-stage protein aggrecan was also significantly enhanced by miRNA + HPL treatment (Fig. 5.5K & L, $p = 0.048$ vs NT), suggesting a shift towards sGAG-rich matrix production.

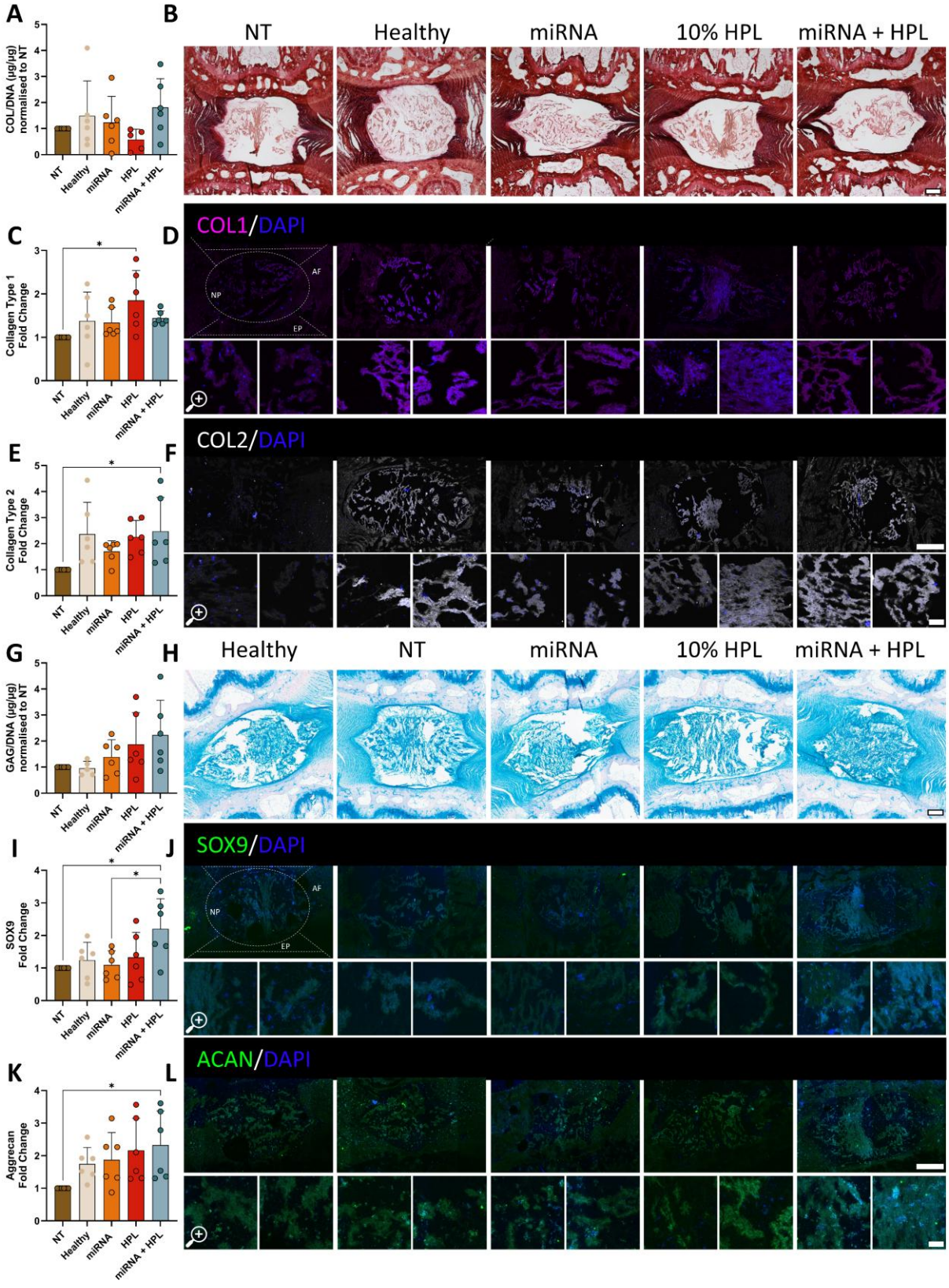

Figure 5.5 Biochemical and histological evaluation in a rat ex vivo organ culture model of mild disc degeneration demonstrated upregulation of extracellular matrix (ECM) constituents. (A) Collagen content was measured biochemically and normalised to DNA content and non-treated (NT) control, with (B) Picrosirius red staining. (C & D) Specific markers were

quantified using immunofluorescence, displayed alongside representative images for collagen type I and (E & F) collagen type II. (G) sGAGs were investigated quantitatively via a biochemical assay and qualitatively with (H) Alcian blue staining. (I & J) SOX9 an early-stage discogenic marker and (K & L) aggrecan a late-stage marker were evaluated by antibody staining. N = 6 independent biological donors, data normalised to NT control. * $p < 0.05$ indicates statistical differences. Histology scale bars = 500 µm, main immunofluorescence images = 400 µm, magnified image = 50 µm. NP = nucleus pulposus, AF = annulus fibrosis, CEP = cartilaginous endplate.

Assessment of sGAG release into the culture media at each timepoint revealed no significant differences between groups, indicating that excess sGAGs were retained within the NP region (Fig. 5.6 A & B).

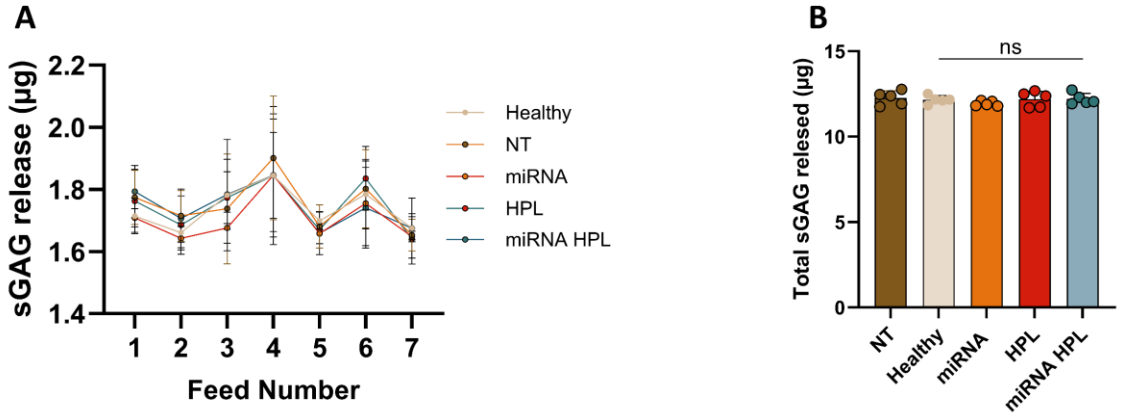

Figure 5.6 Sulphated glycosaminoglycans (sGAGs) released into the media during rat ex vivo organ cultures. (A) sGAG levels at each feeding showed no significant differences and (B) Total sGAG release was also not significantly different. N = 5 independent biological donors.

5.3.4 Dual-miRNA transfection effectively suppressed catabolic markers in an ex vivo organ culture model

Effective therapeutic targeting of IVD degeneration is likely to be enhanced by further reducing or dampening the catabolic milieu thereby providing a permissive environment for regeneration to occur. In this study clear evidence of catabolic suppression was demonstrated, with all treatment groups returning to levels comparable to the non-treated healthy control. All treatments significantly downregulated ADAMTS4 and ADAMTS5 protein expression when compared to the NT control, with the strongest silencing observed in the miRNA + HPL group (Fig. 5.7A -D, $p = 0.009$ for ADAMTS4, and $p < 0.0001$ for ADAMTS5, respectively). Furthermore, dual-miRNA

treatment mirrored previous findings from this thesis and laboratory, [241,242] showing a substantial reduction, over 50%, in both MMP3 and MMP13 protein expression compared to the NT control (Fig. 5.7E-H, p = 0.04 and p = 0.05, respectively).

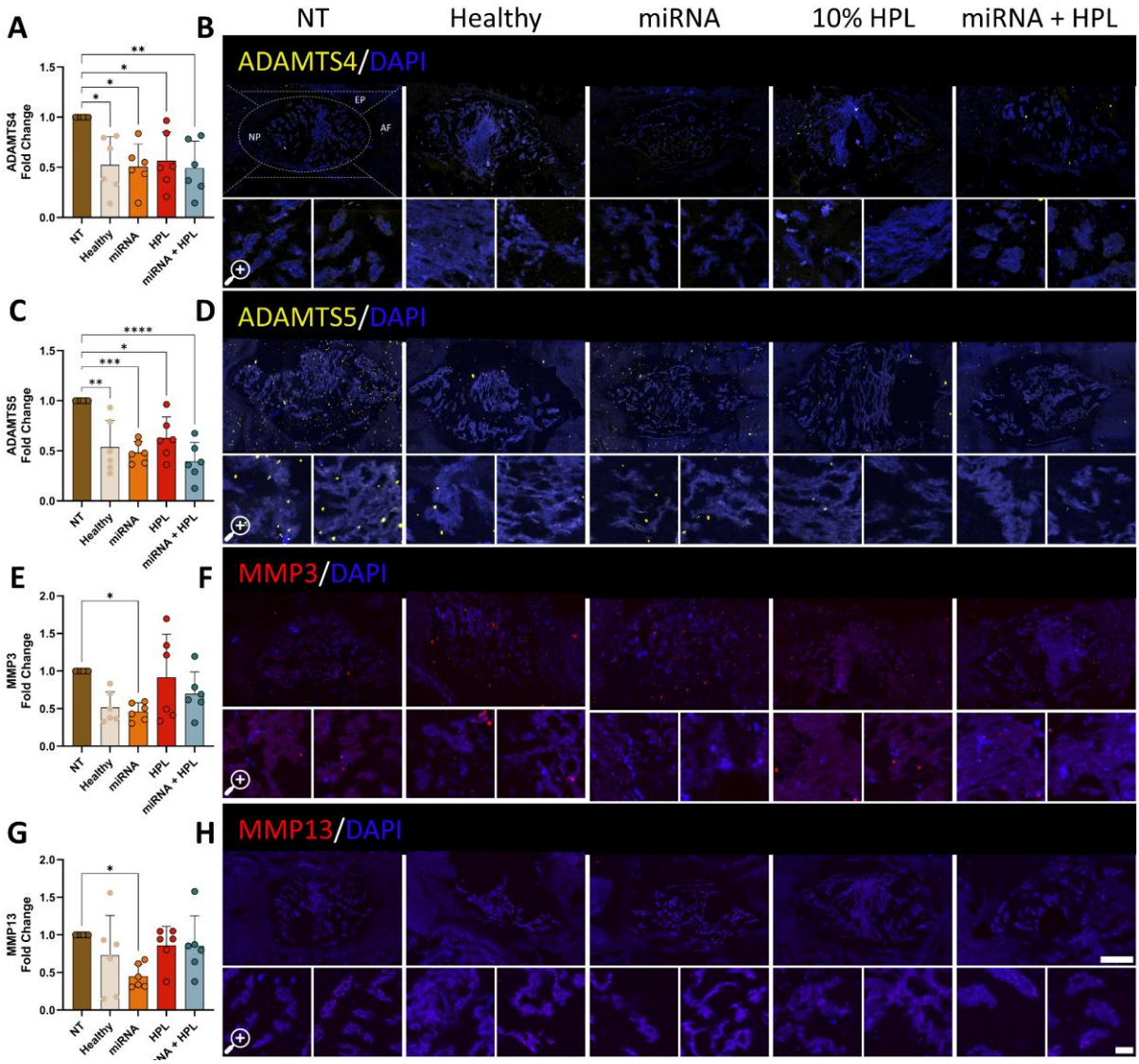

Figure 5. 7 Downregulation of protein expression of catabolic ECM degrading factors in a rat ex vivo organ culture model of mild degeneration following treatment with miRNA pair and 10% HPL. Representative immunofluorescence images of (A&B) ADAMTS4 (C&D) ADAMTS5 (E&F) MMP3, and (G&H) MMP13 protein expression. N = 6 independent biological donors, data normalised to NT control. * $p < 0.05$, ** $p < 0.01$, *** $p < 0.001$, **** $p < 0.0001$ indicates statistical differences. Main image scale bar = 400 µm, magnified image = 50 µm. NP = nucleus pulposus, AF = annulus fibrosis, CEP = cartilaginous endplate.

5.3.5 Co-delivery of the dual-miRNA combined with HPL enhanced the expression of matrix markers in human NP cell-laden analogues

Assessment of human patient-derived NP cell responses to miRNA and HPL delivery revealed promising anabolic effects. Following three weeks of culture, cell viability was comparable to that of the healthy control across all treatment groups, with the highest viability observed in the miRNA HPL groups ($p = 0.006$ compared to NT control, Fig. 5.8 A-D). DNA content remained consistent across all groups, confirming the biocompatibility of the model.

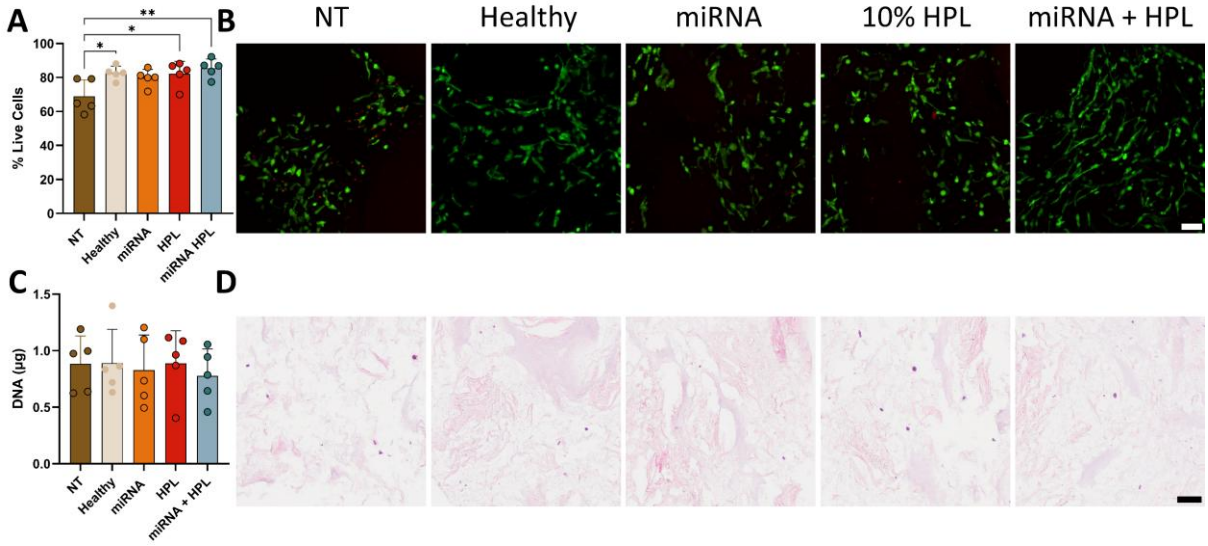

Figure 5. 8 Cell viability and proliferation of patient NP-laden NP analogues following 21 days of culture. (A & B) Viability was quantified with live/dead staining, (C & D) DNA content and representative haematoxylin and eosin staining. * $p < 0.05$, ** $p < 0.01$ indicates statistical differences. N = 5 independent biological donors. Scale bars = 100 µm.

Total collagen content did not appreciably increase by the end of culture as confirmed biochemically and histologically via Picrosirius red staining, nor was collagen type I (Fig. 5.9A-D). In contrast, collagen type II was significantly upregulated following HPL supplementation, with a mean 1.8-fold increase compared to the NT control ($p = 0.007$). Treatment with miRNA + HPL further elevated collagen type II levels, resulting in a 2-fold increase (Fig. 5.9E-F, $p = 0.0009$). Consistent with the findings in rat organ cultures, an upward trend in sGAG production following miRNA + HPL treatment was observed, as evidenced by the DMMB assay and Alcian blue staining (Fig. 5.9G-H, $p = 0.07$). Furthermore, a marked increase in ECM factors with the delivery of miRNA + HPL was observed, namely SOX9 with more than a 2.5-fold change when compared to the NT control (Fig. 5.9I-J, $p = 0.008$). miRNA + HPL treatment also enhanced aggrecan production, with an average 2.6-fold increase compared with the NT control (Fig. 5.9K-L, p =

0.023). Overall, the expression patterns of matrix constituents closely mirrored those observed in the rat ex vivo organ culture, reinforcing the relevance of this NP-ECM analogue model as a representative ex vivo model.

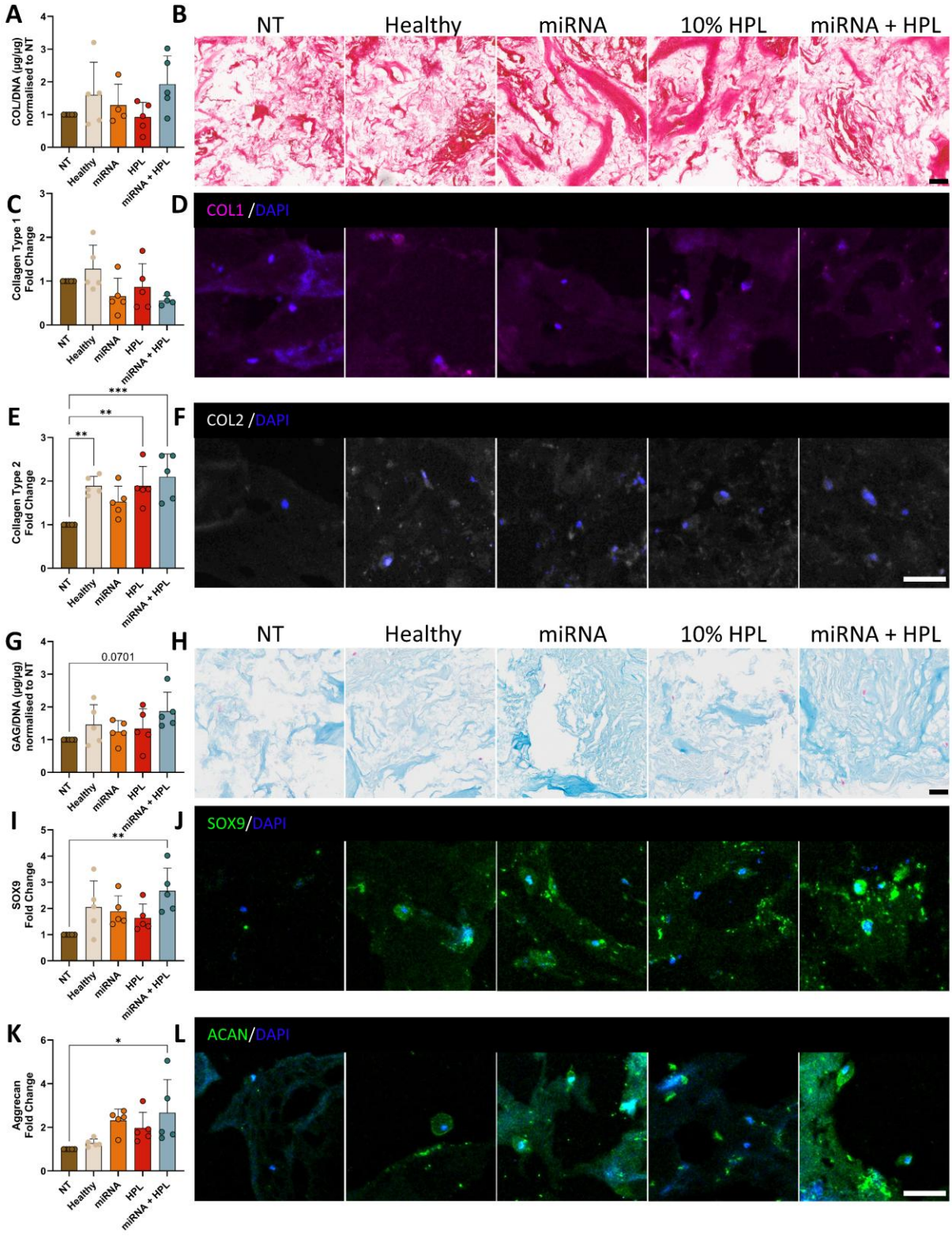

Figure 5. 9 Co-delivery of the miRNA-pair combined with HPL enhanced the expression of matrix markers in a chondroitinase ABC degenerated human cell-laden NP-ECM gel analogue. (A) Total collagen levels were analysed biochemically and (B) histologically with Picrosirius red staining. (C & D) Collagen type I and (E & F) collagen type II protein expression was determined using antibody staining. (G) Total sulphated glycosaminoglycans (sGAGs) were

assessed biochemically and with (H) Alcian blue staining. (I & J) Protein expression of SOX9 and (K & L) aggrecan was evaluated using immunofluorescence staining. N = 5 independent biological donors, all data normalised to NT control. * $p < 0.05$, ** $p < 0.01$, *** $p < 0.001$ indicates statistical differences. Representative histological images scale bar = 100 µm, representative histology staining scale bar 50µm, immunofluorescence images scale bar = 50 µm.

5.3.6 Dual-miRNA + HPL treatment attenuated catabolic enzyme expression of human NP cells cultured in an NP cell-laden analogue

Modulating the response of NP cells to degeneration is essential for developing effective treatments and studies using patient-derived cells provide deeper insights into therapeutic potential. As expected, treatment with cABC induced the highest protein levels of aggrecanases ADAMTS4 and ADAMTS5, and collagenases MMP3 and MMP13, reflecting the homeostatic imbalance characteristic of IVD degeneration. ADAMTS4 expression was reduced by over 50% compared to the NT control following either miRNA only or miRNA + HPL delivery (Fig. 5.10A-B, $p < 0.0001$ for both). Interestingly, the inclusion of miRNA-149-5p mimic and 221-3p inhibitor exerted an enhanced protective effect. ADAMTS4 expression was significantly diminished in both miRNA groups compared to HPL alone (Fig. 5.10A-B, $p = 0.009$ miRNA vs HPL, and $p = 0.019$ miRNA + HPL vs HPL). A similar pattern was observed for ADAMTS5, with both miRNA and miRNA + HPL treatments resulting in substantial decreases compared to the NT control (Fig. 5.10C-D, $p = 0.002$ for miRNA, and $p = 0.008$ for miRNA + HPL). Consistently, miRNA delivery produced a significant inhibitory effect compared to HPL treatment alone (Fig. 5.10C-D, $p = 0.029$). MMP3 expression was reduced by over 50% following miRNA treatment (Fig. 5.10E-F, $p = 0.002$ vs NT). Similarly, miRNA + HPL treatment significantly inhibited MMP3 in comparison to the NT control (Fig. 5.10E-F, $p = 0.003$), while HPL only treatment did not exhibit a beneficial effect. Treatment with miRNA + HPL suppressed MMP13 production compared with the NT control (Fig. 5.10G-H, $p = 0.035$), whereas miRNA only treatment showed a non-significant downward trend (Fig. 5.10G-H, $p = 0.078$). The observed alignment between the rat ex vivo organ response and patient-derived NP cells cultured in an NP analogue suggests that this system may serve as a relevant 3D in vitro model for evaluating patient-specific responses to novel treatments.

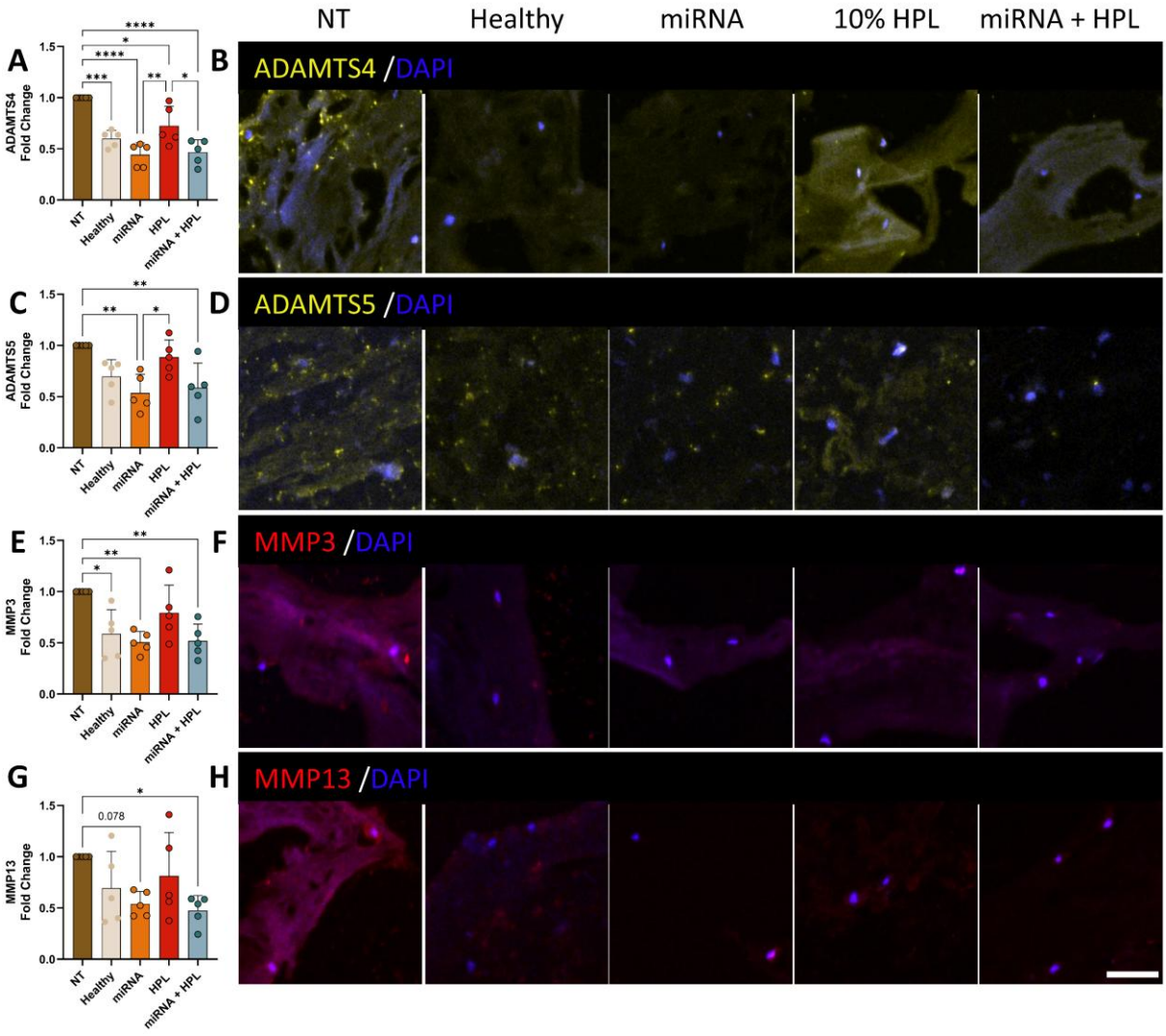

Figure 5. 10 Co-delivery of the miRNA-pair combined with HPL supressed matrix degrading enzyme expression in a chondroitinase ABC degenerated human cell-laden NP-ECM gel analogue. Following three weeks of culture, immunocytochemistry was performed to measure levels of the aggrecanases (A & B) ADAMTS4 and (C & D) ADAMTS5, and the collagenases (E & F) MMP3 and (G & H) MMP13. N = 5 independent biological donors, all data normalised to NT control. * $p < 0.05$, ** $p < 0.01$, *** $p < 0.001$, **** $p < 0.0001$ indicates statistical differences. Scale bar = 50 µm.

5.4 Discussion

Treatment of IVD degeneration, a multifaceted condition, likely requires a multi-pronged approach, to silence degradative and inflammatory processes while promoting matrix synthesis. miRNA-based therapies have shown considerable promise, and the dual delivery of FLR-miRNA-149-5p and a miRNA-221-3p inhibitor identified in Chapter 4 exerts a strong anti-catabolic effect

on resident NP cells.[241,242] However, while encouraging, the observed anabolic response requires additional enhancement to achieve a meaningful regenerative outcome. Platelet lysates with their multitude of GFs, cytokines, and chemokines have demonstrated the ability to stimulate ECM deposition in vitro and improve patient outcomes in vivo.[239,243] In this study, combined dual-miRNA and HPL delivery to assess its potential as a novel therapeutic for IVD degeneration was investigated. The anti-catabolic effect established in Chapter 4 through FLR-miRNA-149-5p and miRNA-221-3p inhibitor delivery in both rat and human models of mild IVD degeneration. Notably, HPL supplementation promoted the expression of discogenic markers in both rat ex vivo organ culture and patient-derived cells cultured in an NP-analogue. Collectively, these findings indicate that combined dual-miRNA and HPL administration facilitates a homeostatic rebalance conducive to the formation of a restorative niche in models of IVD degeneration.

A central feature of IVD degeneration is the dysregulation and exacerbation of the inflammatory and catabolic milieu. miRNA-149-5p has demonstrated potent anti-inflammatory effects in both in vitro and in vivo studies and likely contributed to the reduced degradative enzyme response observed in this work. Qin et al delivered miRNA-149 to NP cells in a lipopolysaccharide (LPS)-induced model of inflammation. Consistent with the findings presented here, they reported a significantly reduction in MMP3 and ADAMTS4 expression at both the gene and protein levels.[167] Chondrocytes share close morphological and functional similarities with NP cells making their treatment responses relevant to IVD research. In this context, TNF-α treated chondrocytes transfected with miRNA-149 rescued cell viability relative to non-treated controls, while also reducing levels of interleukin (IL)-1β, IL-6, and IL-18 in vitro.[244] In a murine OA model, miRNA-149 treatment reduced arthritis severity reflected in improved Mankin scores, and was associated with marked decreases in the inflammatory cytokines tumour necrosis factor (TNF)-α, IL-1β, and IL-6 compared with negative controls. [245] Both TNF-α and IL-1β are key regulators of MMP and ADAMTS expression that exacerbate IVD degeneration.[43,53,54,174] The inclusion of miRNA-149-5p in the therapeutic miRNA-pair may explain the suppression of degradative enzyme expression observed in the presented culture systems.

Interestingly, HPL delivery alone did not exhibit this anti-catabolic effect, requiring the incorporation of the dual-miRNA. Backly and colleagues reported that, in keratinocytes, lysate-mediated enhancement of wound healing is preceded by a transient inflammatory response accompanied by cytokine recruitment.[246] Furthermore, Pereira et al found that chondrocytes treated with lysates exhibited an inflammatory response when cultured in the presence of IL-1α, with a more pronounced effect than IL-1α stimulation alone.[247] In the ex vivo organ and NP analogue culture systems, it was observed that dual-miRNA and dual-miRNA + HPL were more effective at supressing the expression of catabolic factors than HPL supplementation alone. Expression of ADAMTS and MMP family members in the disc is closely associated with inflammatory signalling, and is stimulated by key regulators such as TNF-α and IL-1β.[43,194] The responses observed here

may therefore reflect an initial inflammatory reaction triggered by HPL delivery that had not yet abated by the end of the culture period.

While the above studies focus on shorter timepoints, more pronounced anti-inflammatory effects may only become evident over longer study durations. Studies in cartilage, similar to the NP due to its avascular nature, biochemical composition, and mechanical loadbearing have demonstrated this response as being shorter term. In vivo implantation of a platelet lysate hydrogel scaffold for cartilage repair in rabbits resulted in significantly higher populations of anti-inflammatory M2 macrophages compared to the inflammatory M1 macrophages up to 42 days post-implantation.[248] This has been reflected clinically in OA, with Filardo et al reporting increased post-injection swelling and pain in lysate-treated patients compared to controls.[249] Khoshbin and colleagues likewise reported significantly more occurrences of adverse events, including post-injection swelling and pain in their lysate group over controls in the treatment of OA.[250] In both cases these events were transient, which may suggest a temporal elevated inflammatory response that was not captured in the relatively shorter culture times.

A key objective of this work was to enhance the effect of the dual-miRNA in relation to the promotion of anabolic factors. A synergistic effect was observed when combining the dual-miRNA with HPL, resulting in greater upregulation of matrix markers than with dual-miRNA delivery. HPL is enriched with GFs, containing over 1400 proteins, highlighting its regenerative potential.[251] Amongst these, members of the TGF superfamily, VEGF, PDGF, fibroblastic growth factor (FGF), epidermal growth factor (EGF), and bone morphogenic proteins (BMPs) are often over-represented.[66,67,252] Similarly to the promotion of matrix factors identified in this work, platelet-related treatments have shown promising regenerative effects in NP cells, with one study reporting that 2.5% PRP upregulated the expression of collagen type II, aggrecan, and SOX9 in rat NP cells. [253] A recent study demonstrated significant increases in aggrecan and collagen type II protein expression following pure PRP treatment in IL-1β challenged rat NP cells, consistent with the findings presented here. [254] Likewise, in a porcine ex vivo organ culture model, delivery of PRP resulted in significantly increased GAGs when compared to the degenerated control.[255] The inclusion of a GF cocktail HPL in combination with the immunomodulatory effect of the dual-miRNA likely promoted the expression of factors such as aggrecan, SOX9, and collagen type II reported here.

Inhibition of miRNA-221 has been associated with enhanced matrix marker expression, as demonstrated in a recent study where stem cell-laden, miRNA-221 activated hydrogels showed significant increases in sGAG and collagen type II levels after 21 days of chondrogenic culture.[256] miRNA-221 has been shown to directly target and downregulate tissue inhibitor of metalloproteinase-2 (TIMP-2), a key regulator of the MMP family, leading to amplified MMP expression in degenerative conditions. However, silencing miRNA-221 in fibroblastic cells isolated from the spinal ligamentum flavum restores TIMP-2 expression and corrects aberrant ECM

degradation allowing aggrecan and collagen type II production to resume.[257] In this work similar patterns were observed, although some positive effects were noted when the dual-miRNA or HPL was delivered alone, the strongest effects occurred when they were combined. Consistent with the previous study in Chapter 4, significant increases in collagen type II protein expression following treatment with dual-miRNA and HPL were observed. Additionally, both rat and human culture systems showed an upward trend in sGAG production, along with significant increases to SOX9 and aggrecan, key precursors of the mature protein. Taken together, these findings suggest a synergistic effect whereby co-delivery of dual-miRNA and HPL enhances matrix marker expression more effectively than either treatment alone.

Alongside investigating the combined delivery of a therapeutic dual-miRNA and HPL, a biomimetic ECM 3D culture system suitable for studying IVD degeneration was developed. In vitro systems that closely replicate physiological conditions are crucial to gain a deeper understanding of cellular responses to treatments. NP cells exhibit differential expression of discogenic markers depending on whether they are cultured in 2D or 3D systems, with 3D culture promoting increased expression of NP-like and chondrogenic markers, indicative of a more representative phentotype[258] [259] To better represent physiological conditions, a decellularised NP-ECM matrix mimicking the matrix composition of a mildly degenerated Pfirrmann Grade 3 disc was employed as a culture system for human NP cells, allowing the study to model the structural environment of a degenerated matrix.

While decellularised matrices or biologically similar constituents have shown promise as therapeutics in the IVD field,[229,230,260-262] in this work the versatility of using a decellularised NP-ECM matrix as an in vitro biomimetic culture environment was demonstrated. Complementary to this work, Yuan and colleagues reported that fibroblasts seeded atop rabbit-derived NP matrix exhibited significantly enhanced collagen type II expression. Furthermore, they observed a strong reduction in collagen type I expression, suggesting a shift away from the fibroblastic phenotype.[263] Rashidi and colleagues demonstrated differences in NP cell morphology and surface marker expression in biomimetic age-related collagen-proteoglycan gels.[264] Cells cultured in gels resembling aged matrix demonstrated increased integrin-beta-1 (ITGB1), indicative of degenerated discs.[265] Peng et al employed bone marrow derived stem cells (BMSCs) seeded on decellularised NP gels, whereby they identified significant upregulation of protein expression of collagen type II, aggrecan, and the NP markers CD24, and keratin 19 (KRT19) when cultured in 3D, suggesting that the NP gels were supporting a pro-regenerative NP-like response.[266] In this culture system not only was a tuneable, viable 3D ECM niche for cell encapsulation provided, similar to that of degenerated NP tissue, but also evidence to demonstrate its utility as an in vitro means of trialling therapeutics.

Alongside this, the results are comparable between ex vivo organ culture and NP-ECM-analogue systems, highlighting their utility as ex vivo and in vitro models of intervertebral disc degeneration. Ex vivo organ culture represents one of the most physiologically relevant systems

available for pre-clinical evaluation of developing treatments. Although straightforward to implement, the provision of an ECM niche for cells may be valuable for interrogating cellular responses to a range of potential treatments. Furthermore, it provides a 3D culture system that can be populated with patient-derived cells, thereby enhancing the translatability of prospective therapeutics. cABC is well established in promoting not only the degeneration of sGAGs but the upregulation of matrix degrading proteins ex vivo and in large animal models. [148,267,268] The inclusion of a cABC challenge induces a catabolic response indicative of the degenerated disc microenvironment, modelled here by the upregulation of members of the ADAMTS and MMP families. Finally, the system is tuneable, with ECM and CS composition adjustable to model different grades of degeneration, allowing greater exploratory capability.

Notwithstanding the strengths of the approaches employed in this work, several limitations warrant consideration. Catabolic enzyme expression was evaluated semi-quantitatively through staining; however more robust conclusions could be drawn from quantitative assessment of pro-inflammatory cytokines. Unfortunately, this was not feasible with the current culture set-up for both rat and human models, as ELISA readouts fell below the measurable assay range. Measurements from human discectomy tissue are typically in the pg / mL level for factors such as TNF-α and IL-1β. [269-271] To achieve these measurable levels would likely require either non-physiological cell numbers or and artificially high inflammatory stimulus, neither of which reflects the human IVD or would be relevant for translating the combined dual-miRNA + HPL treatment. This study included a limited number of human donors which prevents stratification by Pfirrmann grade but is sufficient for this exploratory work. Ex vivo organ culture and an NP-gel analogue culture models were employed, both of which lack in vivo tissue interactions but are useful for studying cellular responses to potential treatments.

In summary, a novel dual-FLR-miRNA and HPL therapy for the treatment of mild IVD degeneration across multiple species and culture systems was evaluated. The therapy demonstrated pro-regenerative and anti-catabolic effects in both rat and human NP models, highlighting its potential to supress matrix degradation while promoting matrix marker expression. Alongside this, a tuneable culture system representative of the microenvironmental ECM niche typically found within the IVD was developed, which showed responses comparable to ex vivo organ culture. Together, these findings offer a promising avenue for the treatment of low back pain.

5.5 Conclusion

Development of injectable therapeutics to treat degeneration of the IVD is a challenging endeavour, requiring the suppression of catabolic factors concurrent to restoration of the degenerated ECM. In this chapter, FLR-miRNA-149-5p mimic and 221-3p inhibitor supplemented with HPL restored homeostatic balance in rat and human NP cells through suppression of matrix

degrading factors implicated in progressive IVD deterioration (MMP and ADAMTS families). Alongside this, the promotion of regenerative marker expression, factors known to be required for the rebuilding of the ECM (SOX9, aggrecan, and collagen type II) was demonstrated. Using a tuneable human culture model system that recapitulates a mildly degenerated disc microenvironment, consistent responses were observed with ex vivo animal derived organ cultures, supporting the translational relevance of this approach. Collectively, these findings highlight a promising novel approach to target early-stage IVD degeneration and low back pain through a single injectable therapy modulating the expression of key markers in the degenerative cascade.

Chapter 6. Comparative analysis of dual-miRNA mediated stimulation of nucleus pulposus and bone marrow derived stem cells for intervertebral disc repair

A significant portion of this work is published in **Ní Néill, T.,** Wilson, N., McDonnell, J.M., O'Brien, F.J., Dixon, J.E., Brama, P.A.J., Curtin, C.M., Buckley, C.T (2026) "Comparative analysis of dual-miRNA mediated stimulation of nucleus pulposus and bone marrow derived stem cells for intervertebral disc repair". *JOR Spine, 9(2).* doi: 10.1002/jsp2.70198

Contribution: Made significant contributions to the conception and design of the work. Conducted the literature review, data acquisition and analysis, interpreted and presented the findings, drafted the manuscript, performed critical revisions, and provided final approval of the version to be published.

6.1 Introduction

While miRNA delivery and transfection has shown promise as a therapeutic strategy for injured or damaged tissues, the synergistic potential of combining it with cell-based approaches remains to be fully explored. Supplementing the injury site with viable cells would not only restore the tissue cell density but also promote paracrine interactions that support tissue homeostasis. Research to date has focused primarily on two principle cell populations as part of cell-based regeneration strategies for disc repair, resident -NP cells, and bone marrow-derived mesenchymal stem cells (BMSCs), with both cell types offering distinct benefits and drawbacks. NP cells are particularly well suited to the disc milieu due to their inherent tolerance of acidic pH, nutrient poor environment, and altered osmotic conditions.[151,272,273] NP progenitor cells are currently being explored as a therapeutic source in human clinical trials conducted by Discgenics (NCT03955315 Japan, NCT03347708, United States), following preclinical studies in rabbits that demonstrated marked improvements in disc height index (DHI) after 8 weeks of cell treatment.[19] However, other studies have found that while NP cell transplantation does improve disc height, it remains below that of the healthy controls at the study end point, suggesting partial rather than full regeneration.[20,274,275]

From 1994 to 2020 BMSCs were the most frequently transplanted cell type[276], valued due to their ability to differentiate towards a discogenic phenotype in vitro.[277] While their plasticity provides a potential advantage, the amount of matrix produced may be insufficient to elicit a

regenerative response or restore lost disc height.[278] In an uninjured rabbit model, delivery of BMSCs significantly increased aggrecan and collagen type II gene expression, and sulphated (s)GAGs at the 6 month endpoint.[279] Delivery of BMSCs to a goat model of injured IVDs saw significant increases in proteoglycans compared to their hydrogel control, however no changes in collagen content or MRI score were identified.[280] A recent meta-analysis investigating the effects of stem cell delivery reported positive outcomes in disc height restoration in rat models. However, this effect was not observed in ovine models, where no significant differences were found between control and stem cell groups, suggesting potential species-specific responses [281] or effects related to the larger anatomical scale of ovine discs. Nonetheless, the therapeutic potential of BMSCs should not be overlooked given their multipotent capacity. The objective of this study was to investigate the effects of dual-miRNA stimulation on caprine NP cells and BMSCs in vitro and ex vivo, assessing the regenerative and anti-catabolic potential of these transfected cell populations to determine their suitability for cell transplantation into degenerated IVDs.

6.2 Materials and methods

6.2.1 Primary cell culture

In accordance with the principles of the 3R's and to minimise animal use, goat nucleus pulposus (NP) and bone marrow derived stem cells (BMSCs) were obtained from discarded material from animals used in a separate study approved by the University College Dublin Animal Research Ethics Committee (AREC-P-19-17) and the Irish Healthy Products Regulatory Authority (HPRA AW18982/P142). Briefly, motion segments of the lumbar spine were isolated to allow for NP tissue dissection. The tissue was enzymatically digested in serum free low glucose DMEM (LG DMEM, Sigma-Aldrich) containing pronase (100 U/mL, Millipore) and collagenase Type II (300 U/mL, Gibco) supplemented with 2% penicillin/streptomycin (pen/strep, Gibco) and 2.5 mg/mL Amphotericin B (Sigma-Aldrich). Digestion was carried out at 37°C with gentle agitation (10 r.p.m) until single cells were released. To isolate BMSCs, bone marrow was aspirated from the scapula with a 16G needle and subjected to sequential centrifugation and filtration steps. Cells were seeded at a density of 23 x 10^6/T175 to promote colony formation and cultured for 72 hours. Red blood cells were then removed by washing with phosphate buffered saline (PBS, Sigma). Both cell types were cultured in LG DMEM as before supplemented with 10% foetal bovine serum (FBS, Gibco), referred to as expansion (XPAN) media, under physioxic conditions (5% O_2 and 5% CO_2) until passage 1, after which they were either used immediately for experiments or cryopreserved in liquid nitrogen (LN_2). NP cells were used up to passage 3, and BMSCs up to passage 4 for all experiments. All experiments were performed under physioxic conditions unless otherwise stated.

6.2.2 Tripotentiality determination of BMSCs

To assess the multilineage potential of isolated BMSCs, cells were treated with chondrogenic, adipogenic, and osteogenic medias as previously described. [282-284] Briefly, for chondrogenic differentiation, following expansion in XPAN, cell aggregates comprising of 2.5 x 10^5 cells were formed by centrifugation. The aggregates were then cultured for 21 days in a chemically defined medium (CDM), consisting of high glucose (HG) DMEM + GlutaMAX, 2% Pen/Strep (both Gibco), 2.5 mg/mL Amphotericin B (Sigma-Aldrich), 5 mM sodium pyruvate, 40 µg/mL L-Proline, 1.5 mg/mL bovine serum albumin (BSA, all Sigma-Aldrich). For chondrogenic induction, the CDM was further supplemented with 1X insulin transferrin selenium (ITS, Gibco), 10 ng/mL TGF-β3 (PeproTech), 100 nM dexamethasone, 50 µg/mL L-ascorbic acid-2-phosphate and 4.7 mg/mL linoleic acid (all Sigma-Aldrich). Adipogenic differentiation was induced in monolayer by seeding cells at a density of 1 x 10^3 cells/cm^2 and supplementing XPAN media with 100 nM dexamethasone, 0.5 mM IBMX, and 50 µM indomethacin (all Sigma-Aldrich). Osteogenic differentiation was performed similarly, with media instead supplemented with 100 nM dexamethasone, 10 mM β-glycerol phosphate, and 14.5 µg/mL L-ascorbic acid-2-phosphate (All Sigma-Aldrich). Differentiation outcomes were assessed with Alcian blue staining for chondrogenesis, Oil-Red-O for adipogenesis, and Alizarin red for osteogenesis. Results showing positive staining following chondrogenic, adipogenic, and osteogenic induction are presented in Figure 6.1.

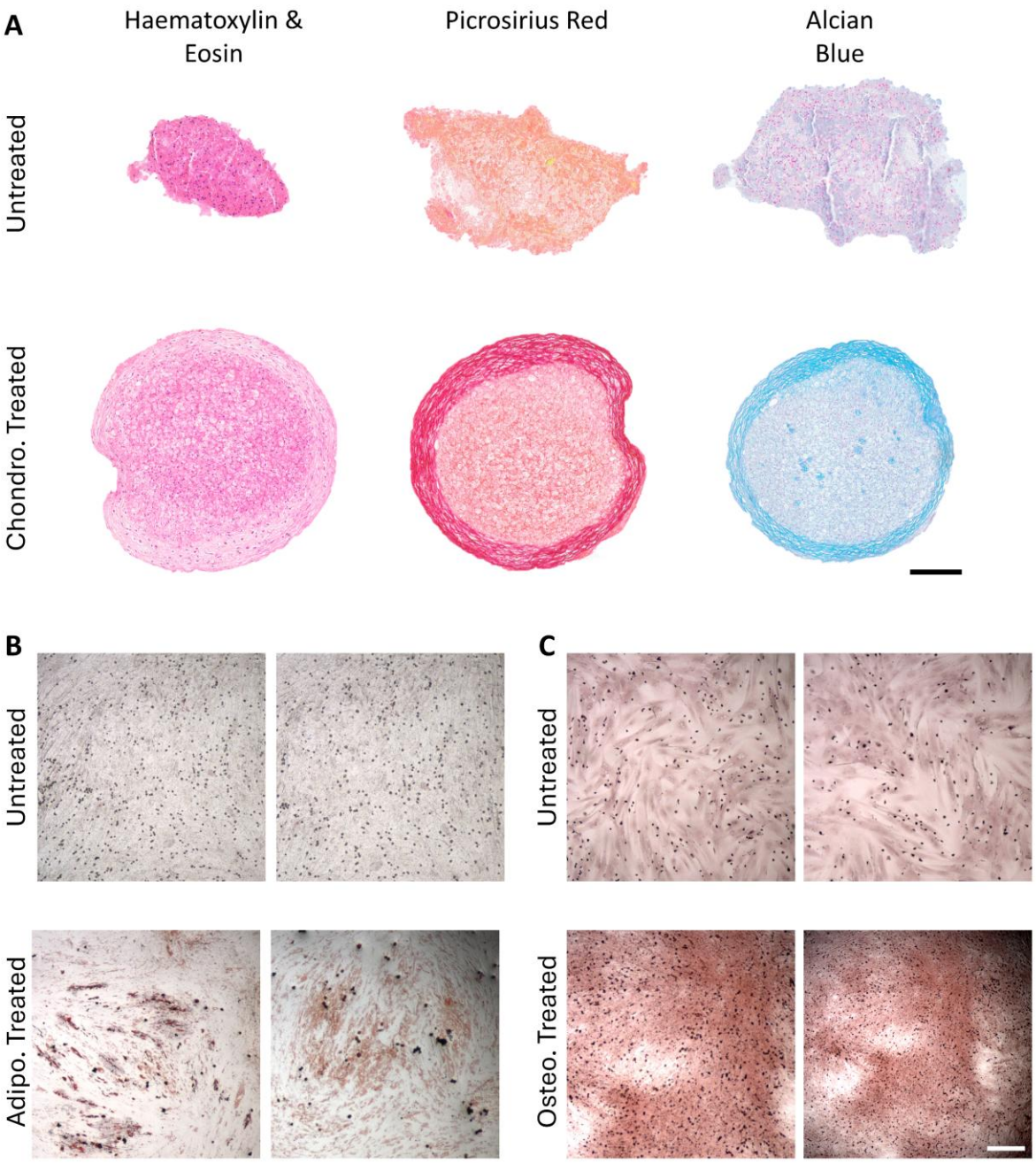

Figure 6.1 Representative images of tri-potentiality assessment of bone marrow-derived stem cells. (A) Chondrogenic (chondro.) supplementation of pellet cultures demonstrated pellets with more structural integrity, alongside enhanced collagen and sulphated glycosaminoglycan (sGAG) production, as determined by Picrosirius red and Alcian Blue staining. (B) Following supplementation with adipogenic (adipo.) supplements, increased Oil-Red O staining was achieved compared to untreated groups. (C) Supplementation with osteogenic (osteo.) media supplements resulted in increased Alizarin red staining representing increased calcium deposition. N = 3 biological replicates. All scale bars 200 μm.

6.2.3 Determination of transfection efficiency in monolayer NP and BMSC cultures

To achieve efficient miRNA transfection, a fluorescently labelled miRNA, miRDy547 (Dharmacon) was delivered to both cell types in monolayer culture using the FLR peptide, an arginine modified form of the glycosaminoglycan-binding enhanced transduction (GET) peptide (Dixon Lab, Nottingham). [152,285] Briefly, cells were seeded at a density of 5 x 10^3 in µ-Slide 18 well chamber slides (ibidi, GmbH) and allowed to attach overnight. Subsequently, to stimulate future experimental conditions, cells were serum starved for 24 hours and subjected to a cytokine challenge with TNF-α (50 ng/mL) and IL-1β (10 ng/mL, both Fischer Scientific) for 24 hours. miRNA complexes were prepared at increasing doses from 0 to 25 ng/µl in OptiMEM reduced serum media (Gibco), maintaining a charge ratio of N:P 5. Complexes were allowed to form via electrostatic interactions for 30 minutes at room temperature before being added to the cells. Transfection was allowed to proceed for 6 hours at 5% O_2 at 37°C, upon which the complexes were removed and cultured in XPAN for 3 days. Cells were either fixed in 4% paraformaldehyde (PFA) for 12 minutes for immunofluorescence or trypsinised for flow cytometric analysis using a LSRFortessa Flow cytometer, with nuclear counterstaining performed using Hoechst 33324 (Merck Life Sciences Ltd.) in both assays. For all transfection experiments a non-transfected (NT) control was included.

6.3.4 Assessment of protein marker expression following dual-miRNA delivery in monolayer culture

Protein expression of specific markers in monolayer culture following miRNA transfection was performed. Cells were seeded as previously described, with cytokine treatment applied as described in Section 2.3 for analysis of catabolic markers, while cultures without a cytokine challenge were used to assess anabolic protein expression. FLR complexes were formed with either a scrambled control miRNA (Dharmacon), or dual-miRNA149-5p mimic and miRNA-221-3p inhibitor at a concentration of 10 ng/µl. Protein expression was analysed 3 days post-transfection via immunofluorescence following antibody staining. To further examine the effects of transfection, NP cells and BMSCs were seeded in 6-well plates at a concentration of 10 x 10^4 cells per well. Following overnight attachment, cells were exposed to serum starvation and a cytokine challenge as before. FLR-scrambled miRNA complexes (10 ng/µl) were delivered and incubated for 6 hours. Cells were maintained in XPAN media for 14 days with biweekly media changes, and biochemical analyses were performed at the end of the culture period.

6.3.5 Microtissue culture of miRNA transfected NP and BMSCs

To assess the effects of dual-miRNA transfection in a more physiologically relevant 3D systems microtissues were generated from NP cells and BMSCs. Cells were seeded at a density of 1 x 10^6 in 6-well plates. After overnight attachment, cells underwent serum starvation followed by cytokine treatment, both for 24 hours as described above. Transfection proceeded for 6 hours using 10 ng/µl of complexes containing either FLR-scramble miRNA or FLR-miRNA-149-5p mimic combined with miRNA-221-3p inhibitor and cells were allowed to recover overnight. The following day, microtissues containing 5 x 10^4 cells each were formed following centrifugation at 800g for 10 minutes in sterile agarose coated 48-well plates. Media exchanges were performed twice weekly, with collected media pooled to allow for quantification of sGAG release during the culture period. Microtissues were maintained for either 3 or 14 days. At the relevant timepoints, 2 and 3 microtissues were pooled for biochemical analysis, and additional tissues were fixed for 30 minutes in 4% PFA at room temperature for histological evaluation.

6.2.6 Goat ex vivo organ culture and induction of mild degeneration

All goat tissue used for ex vivo organ culture was obtained with approval from the Animal Research Ethics Subcommittee (AREC), University College Dublin (UCD) (AREC-23-17-Brama). Spines were dissected and excess fascia was removed to expose the entire disc region, whereupon motion segments were excised containing vertebra-disc-vertebra**.** The segments were incubated overnight in LG DMEM supplemented with 2% Pen/Strep, 0.1 µl/mL Amphotericin B (Sigma), and 100 µg/mL Kanamycin Sulfate (Gibco). Each intact motion segment was then cultured in XPAN media in a custom-made bioreactor, under a pressure of 0.4 MPa, a value within the human and goat physiological range. [136,286] Mild degeneration was induced by injection of 200 µl of 2U chondroitinase ABC (cABC) via a 30G needle, and segments were maintained under these conditions for 14 days prior to treatment administration.

6.2.7 miRNA dosage for ex vivo organ culture delivery

Uptake of miRNA into mildly degenerated goat disc organs was evaluated using the fluorescently labelled miRDy547. Complexes of 10 and 25 ng/µl (200 µl per disc) were delivered via a 30G needle, with a sham OptiMEM (vehicle) NT control. Discs were cultured for 72 hours, after which the intact IVDs were excised, snap frozen in liquid nitrogen and embedded in optimal cutting temperature (OCT) compound (Fischer Scientific). Upon freezing, sections of 10 µm were cut in the sagittal orientation using a Leica CM 3050 S Cryostat. miRNA uptake to the cells was

assessed using a Leica SP8 scanning confocal microscope (Leica, Germany), with nuclei counterstained using Hoechst 33342.

6.2.8 Ex vivo organ culture treatment administration

Organ culture experiments were divided into five groups, as outlined in Table 1. A healthy control disc without cABC insult was included, while all other discs received cABC to induce mild degeneration. Treatment groups were administered as follows: The NT group received a sham injection of OptiMEM (vehicle). The miRNA-only group was injected with 200 µl of FLR-miRNA-149-5p mimic + miRNA-221-3p inhibitor complexes at a concentration of 25 ng/µl. For cell-based treatments, NP cells and BMSC were transfected with FLR-miRNA-149-5p mimic and miRNA-221-3p inhibitor as described previously. A total of 5.5 x 10^6 cells were delivered to each disc, a number predicted to restore goat matrix synthesis to a healthy level in vivo. [287] Prior to injection, both cell types were labelled with PKH-26 dye (Sigma) as per the manufacturer's instructions to allow visualisation. After termination of culture, NP tissue was dissected and removed from each disc, weighed, and stored at -70 °C. Tissues were freeze dried using a standard procedure (500 mTorr, -10°C, 16 – 18h, Harvest Right™, USA), re-weighed to determine hydration levels, and processed for biochemical evaluation. For histological evaluation, excess tissue and bone were removed, and discs were fixed in 4% PFA overnight at 4°C.

Table 6. 1 Treatment groups, description and details for ex vivo organ culture.

Group Name	Degeneration	Treatment Description	Treatment Details
Healthy	None	Non-degenerated healthy control	No treatment
Non-transfected (NT)	200 µl chondroitinase ABC (cABC)	Degenerated control,	200 µl Opti-MEM (vehicle) treated
miRNA-only	200 µl chondroitinase ABC (cABC)	FLR-dual-miRNA treated	200 µl FLR miRNA-149-5p + 221-3p inhibitor (25 ng/µl)
miRNA-NP	200 µl chondroitinase ABC (cABC)	FLR-dual-miRNA transfected nucleus pulposus (NP) cells	200 µl 5.5 x 10^6 NP cells transfected with FLR miRNA-149-5p + 221-3p inhibitor (10 ng/µl)

miRNA-BMSC	200 µl chondroitinase ABC (cABC)	FLR-dual-miRNA transfected bone marrow derived stem cells (BMSCs)	200 µl 5.5 x 10^6 BMSCs transfected with FLR miRNA-149-5p + 221-3p inhibitor (10 ng/µl)

6.2.9 Viability of microtissues and ex vivo organ culture

At days 3 and 14 of culture, microtissues were washed with PBS and incubated for 1 hour at 37°C in a staining solution consisting of 2 µM Calcein (Sigma-Aldrich) and 4 µM ethidium homodimer (EthD-1, SLS Scientific Laboratory Supplies). For evaluation of cell viability in ex vivo disc organ cultures, the intact disc was dissected from the vertebral bodies, washed with PBS and incubated for 1 hour at 37°C in the live/dead staining solution. Following aspiration of the staining solution and three washes of PBS the tissue was embedded in OCT and snap frozen in liquid nitrogen. Sections of 10 µm were acquired on a Leica 3050S Cryostat. Sections were imaged on a Leica SP8 confocal microscope to allow visualisation of live and dead cells (485 nm excitation, 530 nm emission for Calcein, 530 nm excitation, 645 nm emission for EthD-1). Images were analysed using ImageJ software (version 1.54p) to generate maximum-intensity projection z-stacks for quantification of live and dead cell populations.

6.2.10 Biochemical quantification of in vitro and ex vivo organ culture

For in vitro experiments pooled media was freeze dried as previously described, and both cells and media were digested for 18 hours at 60 °C in 100 mM Sodium Phosphate/ 5mM Na_2EDTA Buffer with 3.88 U/mL papain enzyme (all Merck Life Science Ltd.). Tissue samples from ex vivo organ cultures were weighed before and after freeze drying to assess hydration and were similarly digested with papain.

6.2.11 Histology and immunocytochemistry of in vitro and ex vivo organ culture

Following fixation, microtissues were embedded in 4% (w/v) agarose and sequentially dehydrated through graded ethanol solutions and embedding in paraffin wax. Sections of 7 µm thickness were prepared using a microtome (Leica Microsystems). Goat discs were decalcified in Decalcifying Solution-Lite (Merck Life Sciences Ltd.) for approximately 4 weeks, until softened, followed by incubation in 30% sucrose solution and OCT embedding. Sections of 10 µm were prepared using a Leica CM3050 S Cryostat.

For immunocytochemistry, due to being paraffin embedding, antigen retrieval on microtissue sections was performed in sodium citrate buffer (pH 6) heated to 100 °C in a pressure cooker for 1 minute. All antibodies used are detailed in Table . The corrected total cell fluorescence was quantified for regions of interest, (i.e. the microtissues or NP tissue), and normalised to cell number.

Table 6. 2 Primary and secondary antibodies utilised for immunocytochemistry.

Antigen	Species	Concentration	Supplier & Code
Aggrecan	Rabbit	1:250	Invitrogen, MA532695
Collagen type II	Rabbit	1:250	Invitrogen, PA599159
Collagen type IAI	Rabbit	1:150	Invitrogen, PA5-29569
SOX9	Rabbit	1:250	Invitrogen, PA586301
ADAMTS5	Rabbit	1:250	Invitrogen, PA532142
MMP13	Mouse	1:125	Invitrogen, MA514247
TNF-α	Rabbit	1:100	Invitrogen, PA519810
IL-1β	Rabbit	1:200	Invitrogen, P420B
Anti-Rabbit Alexa Fluor 488	Goat	1:500	Invitrogen, A27034
Anti-Mouse Alexa Fluor 488	Goat	1:2000	Invitrogen, A11001

6.3 Results

6.3.1 Efficient microRNA internalisation was achieved, and the scramble control showed no functional effects in NP cell or BMSC cultures

The success of miRNA therapy hinges upon effective nanoparticle delivery, while the vector employed should not adversely alter cell function. Efficient internalisation was achieved following FLR-miRDy547 transfection at concentrations above 5 ng/µl (Fig. 6.2A), with a plateau

reached at 10 ng/µl (mean NP 79.4% ± 6.0, mean BMSC 85.0% ± 10.5, $p \leq 0.0001$ for both NP and BMSC compared to 0 ng/µl, Fig. 6.2B). At the highest concentration of 25 ng/µl, NP cell number decreased significantly compared to the 10 ng/µl dose ($p = 0.016$), with BMSCs following a similar trend (5 ng/µl vs 25 ng/µl, $p = 0.085$), indicating a detrimental effect at elevated concentrations (Fig. 6.2C).

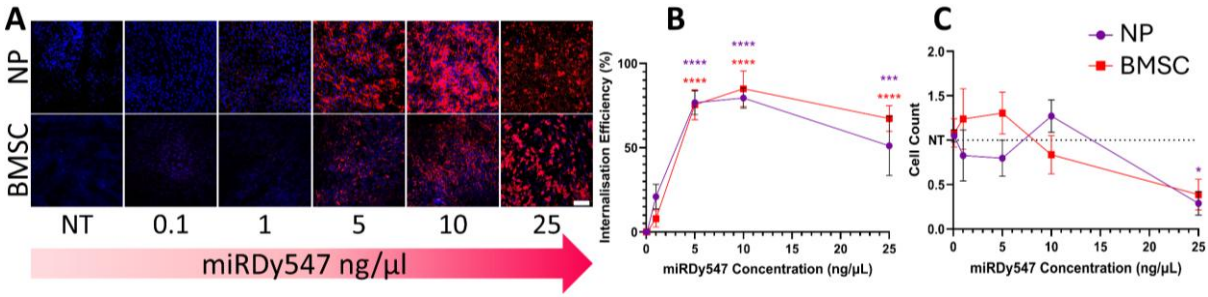

Figure 6. 2 Dosage study of FLR delivered fluorescently tagged miRDy547 in goat nucleus pulposus (NP) and bone marrow-derived stem cells (BMSC) 3 days post-transfection, showing a plateau in internalisation efficiency at 10 ng/µl for both cell types. (A) Representative images of miRDy547 internalisation. (B) Degree of miRDy547 internalisation efficiency (%) as assessed by flow cytometry. (C) Fold change in cell count normalised to non-transfected (NT) control. Statistical analysis- one-way ANOVA with Tukey's post hoc analysis. N = 3 independent biological donors. * $p < 0.05$, *** $p < 0.001$, **** $p < 0.0001$ indicates statistical significance. Scale bar = 200 µm.

FLR-scrambled miRNA transfection did not induce functional changes, with no significant differences in DNA, sulphated glycosaminoglycan (sGAG), or collagen levels in either two- or three-dimensional cultures (Fig. 6.3).

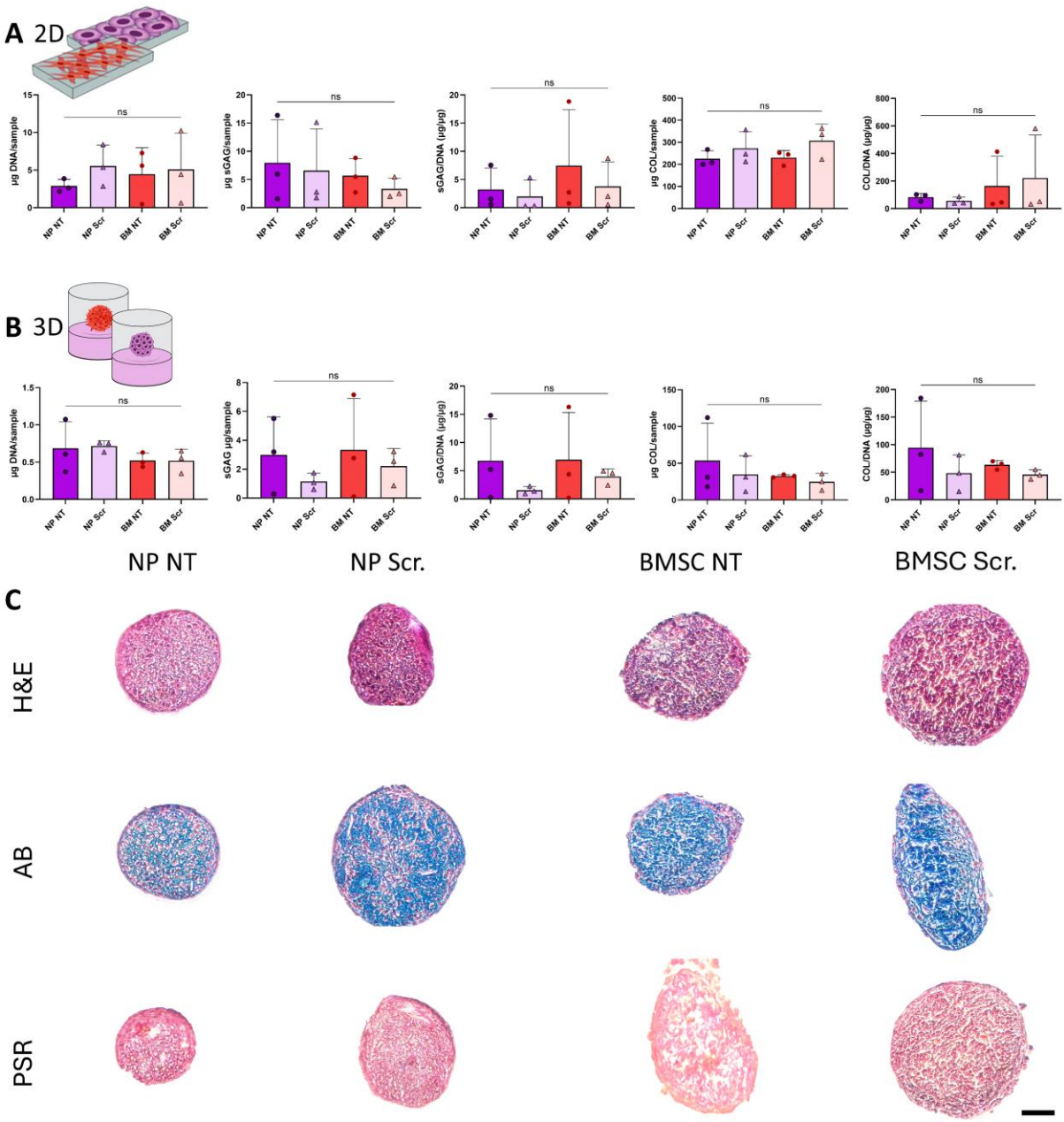

Figure 6.3 Functional assessment of scramble miRNA transfection on monolayer and 3D culture in goat nucleus pulposus (NP) and bone marrow-derived stem cells (BMSCs). (A) No changes were identified biochemically following scramble miRNA transfection, with DNA, sulphated glycosaminoglycan (sGAG), and collagen production assessed. (B) Biochemical analysis of three- dimensional culture likewise demonstrated no changes. (C) Representative images of histological staining for haematoxylin and eosin (H&E), Alcian blue (AB), and Picrosirius red (PR). Statistical test is one-way ANOVA with Tukey's post-hoc analysis. ns = non-significant. N = 3 independent biological replicates. Scale bars 50 µm.

6.3.2 Dual-miRNA delivery induced cell type-specific differences in matrix degrading enzyme expression in monolayer cultures

Driving ECM protein production while reducing catabolic activity is critical when assessing potential treatments targeting IVD degeneration. In monolayer culture, a modest upward trend in aggrecan protein expression was observed (Fig. 6.4 A & B BMSC $p = 0.0737$), while collagen type II was unchanged three days post-transfection for both cell types. However, following cytokine stimulation, the cell types exhibited distinct post-transfection responses. ADAMTS5 was significantly upregulated in transfected BMSCs compared to NP cells ($p < 0.001$), while transfected NP cells showed a significant decrease in expression relative to NT controls ($p = 0.015$). Similarly, MMP13 expression was increased in BMSCs and significantly higher than in NP cells ($p = 0.019$).

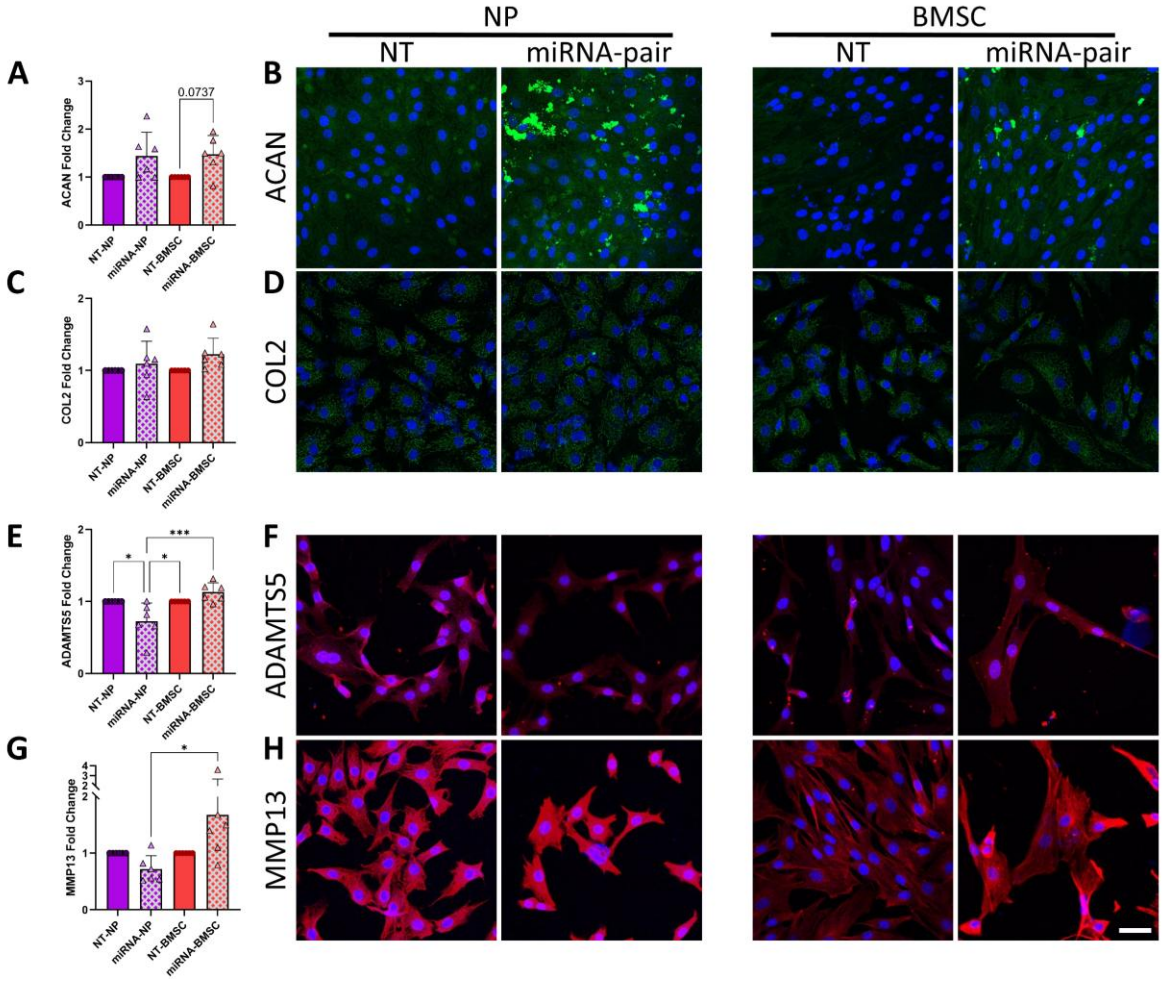

Figure 6.4 Comparison of extracellular matrix (ECM) markers, and catabolic enzymes three days post dual-miRNA transfection in goat nucleus pulposus (NP) and bone marrow-derived stem cells (BMSCs). Fluorescence intensity was quantified for aggrecan (A & B, ACAN), collagen type II (C & D, COL2), ADAMTS5 (E & F), and MMP13 (G & H) and normalised to the non-transfected (NT) control, with representative images presented for each condition. Statistical test is

one-way ANOVA with Tukey's post hoc analysis. N = 6 independent biological donors, * $p < 0.05$, ** $p < 0.01$, *** $p < 0.001$ indicates statistical significance. Scale bar = 50 µm.

6.3.3 Microtissues maintained strong viability throughout the culture period

To investigate the effect of dual-miRNA stimulation in a more relevant 3D model, it was first confirmed that viability was maintained throughout the culture period. DNA content increased for both NT-NP and miRNA-BMSC treated groups from day 3 to 14 (Fig. 6.5A & B $p = 0.0142$ and $p = 0.0081$, respectively). However, no differences were identified between any of the groups at the culture endpoint. Live/dead staining at both early and late timepoints confirmed these findings. Although a significant reduction in viability was observed in the NT-BMSC group compared to both NP groups (Fig. 6.5C & D, $p = 0.0067$ compared to NT-NP and $p = 0.0024$ compared to miRNA-NP), viability remained above 88% across all groups at both timepoints.

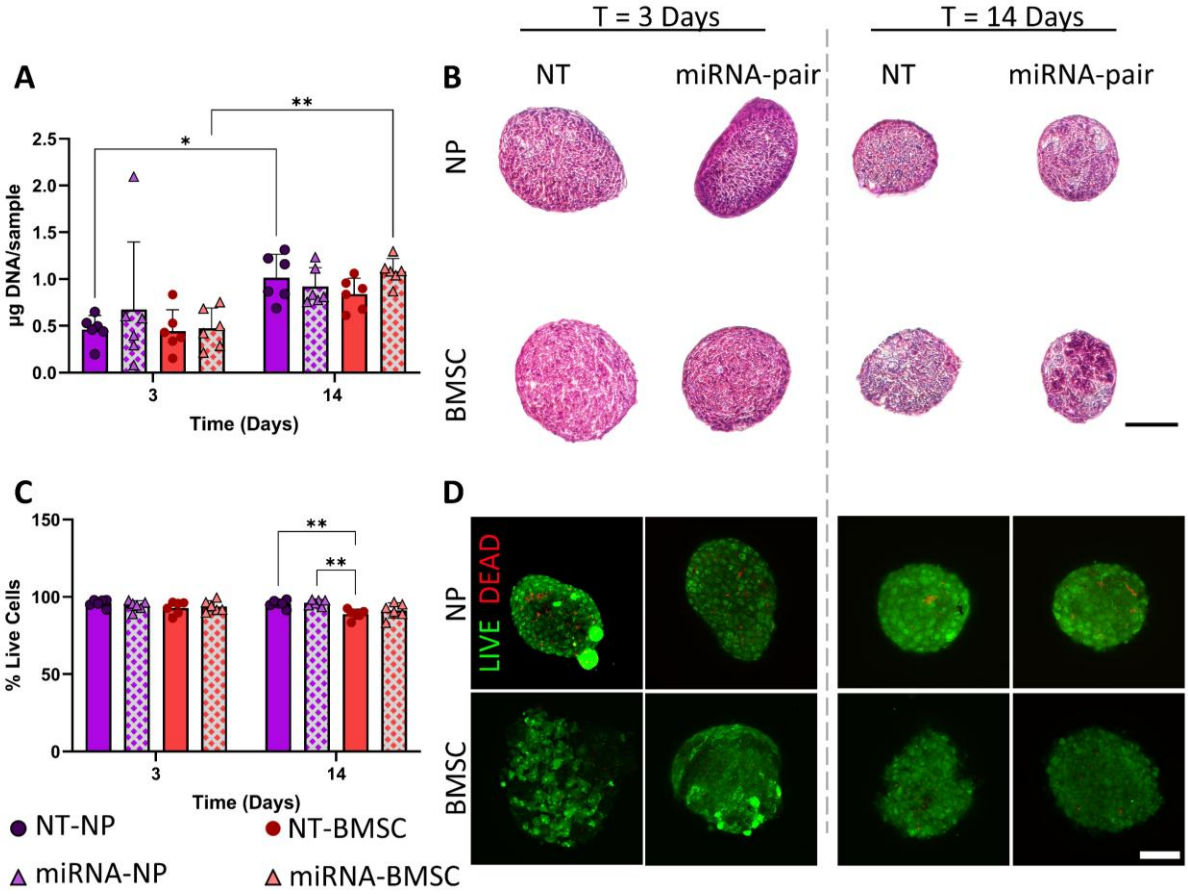

Figure 6.5 DNA quantification, representative Haematoxylin and Eosin (H&E) staining, and viability of non-transfected (NT) and FLR-miRNA-149 mimic + miRNA-221-inhibitor (dual-miRNA) 3D microtissues formed from nucleus pulposus (NP) and bone marrow-derived stem cells. (A) DNA content (µg DNA/sample) was quantified using a Hoechst Bisbenzimide assay. (B)

Representative H&E images of NP and BMSC microtissues. (C) Live cell viability (%) in microtissues was assessed employing live/dead staining. (D) Representative images of live/dead staining. Statistical test is a two-way ANOVA with Tukey's post-hoc analysis. N = 6 independent biological donors. * $p < 0.05$, ** $p < 0.01$ indicates statistical significance. Scale bars = 100 µm.

6.3.4 Dual-miRNA transfection promoted divergent upregulation of early and late-stage extracellular matrix markers in 3D cultures

Given the crucial role of GAGs in the formation of ECM, total sGAG production was assessed in microtissue cultures, alongside proteins of interest at early and late-stages. sGAG deposition, displayed as the total amount and normalised to DNA content, was significantly upregulated across all groups following two weeks of microtissue culture (Fig. 6.6A, B, C, $p < 0.0001$ for all groups). The total sGAGs deposited by miRNA-BMSCs were significantly higher than in NP groups (Fig. 6.6A $p = 0.0044$ vs NT-NP, and $p = 0.0009$ vs miRNA-NP). However, this effect between groups was abrogated after normalisation to DNA content, with significant differences remaining only between timepoints (Fig. 6.6B, C). Qualitatively this was reflected in increased GAG production as visualised by Alcian blue staining, with deeper staining observed at later timepoints across all groups (Fig. 6.6B). Immunofluorescence analysis revealed a significant increase in the early chondrogenic marker SOX9 in dual-miRNA transfected NP cells at the end of culture compared to NT controls (Fig. 6.6D. & E. $p = 0.0322$). Conversely, the later-stage proteoglycan ACAN was substantially upregulated in transfected BMSCs relative to transfected NP cells, and both NT controls (Fig. 6.6F. & G. $p = 0.0282$, $p = 0.0088$ respectively).

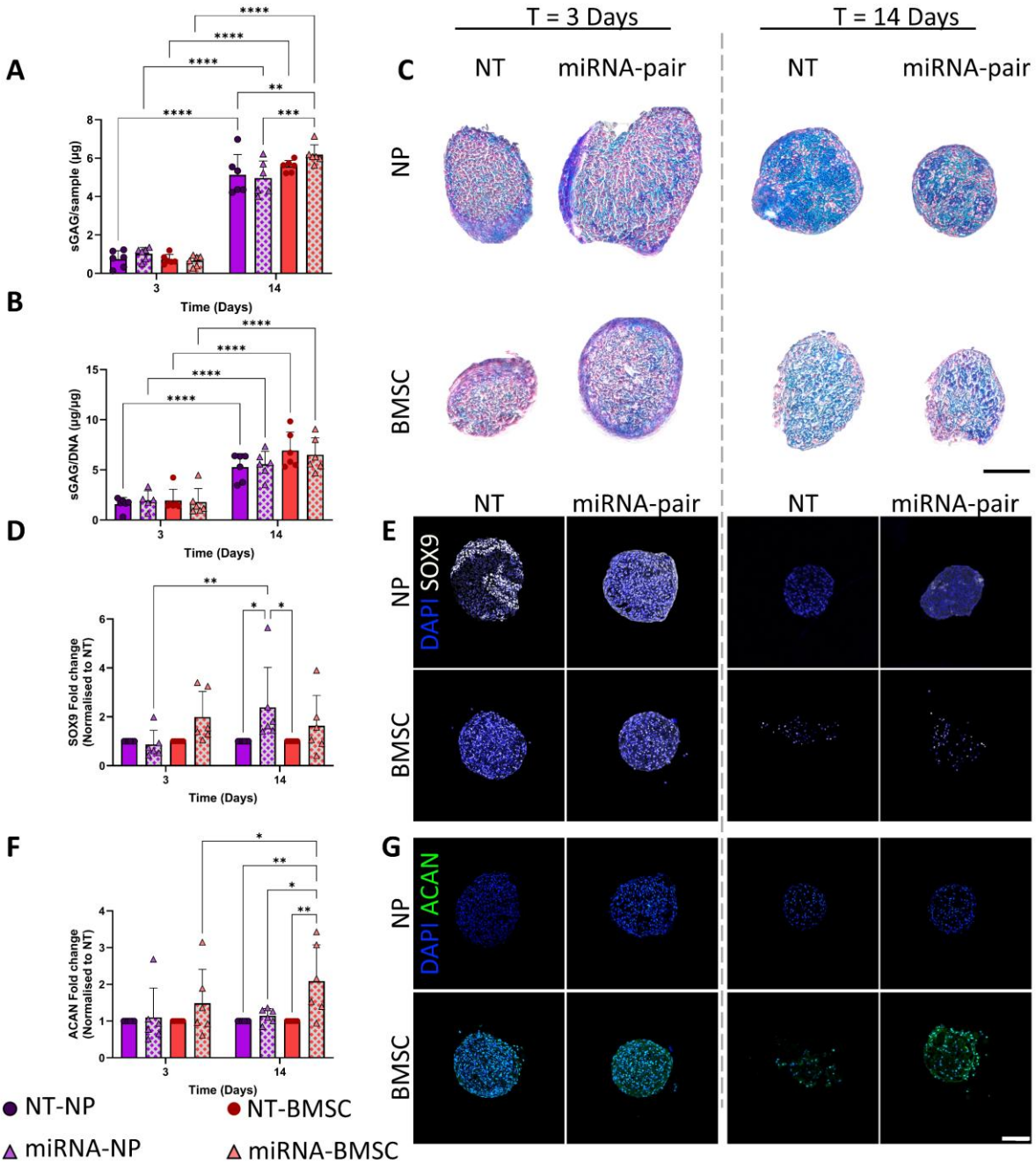

Figure 6.6 Biochemical quantification, histological, and immunocytochemistry analysis of matrix-specific markers of non-transfected (NT) and FLR-miRNA-149 mimic + miRNA-221-inhibitor (dual-miRNA) 3D microtissues formed from nucleus pulposus (NP) and bone marrow-derived stem cells (BMSCs) at timepoints 3 (T3) and 14 (T14) of culture. (A) Sulphated glycosaminoglycans (sGAGs) per sample (µg) and (B) normalised to DNA content (µg/µg) (C) Representative images of Alcian blue (AB) staining for sGAGs. (D) SOX9 protein expression was quantified using immunofluorescence, NP-transfected cells exhibited significant increases by day 14. (E) Representative images of SOX9 protein staining. (F) Aggrecan protein expression as quantified by immunofluorescence. By day 14, BMSCs exhibited significantly higher expression compared to all other groups (G) Representative images of aggrecan staining. Statistical

test is a two-way ANOVA with Tukey's post-hoc analysis. N = 6 independent biological donors, * $p < 0.05$, ** $p < 0.01$, *** $p < 0.001$, **** $p < 0.0001$ indicates statistical significance. Scale bars = 100 μm.

6.3.5 Dual-miRNA stimulation increased total collagen content and specific collagen markers in microtissue cultures

Alongside GAG formation, collagens, particularly collagen type II, are crucial for maintaining NP ECM integrity. Total collagen content increased as a function of time across all treatment groups except NT-NP (Fig. 6.7A & B $p \leq 0.05$). However, following normalisation to DNA content this effect was abolished (Fig. 6.7C), with no differences observed between any of the groups. Likewise, minor increases in Picrosirius red (PSR) staining intensity was observed in the transfected groups. miRNA-BMSCs exhibited increased expression of the more fibrotic collagen type I compared with NT controls (Fig. 6.7D & E, $p = 0.033$), while collagen type II showed a trend towards higher expression in the transfected BMSC group (Fig. 6.7F & G, $p = 0.1025$).

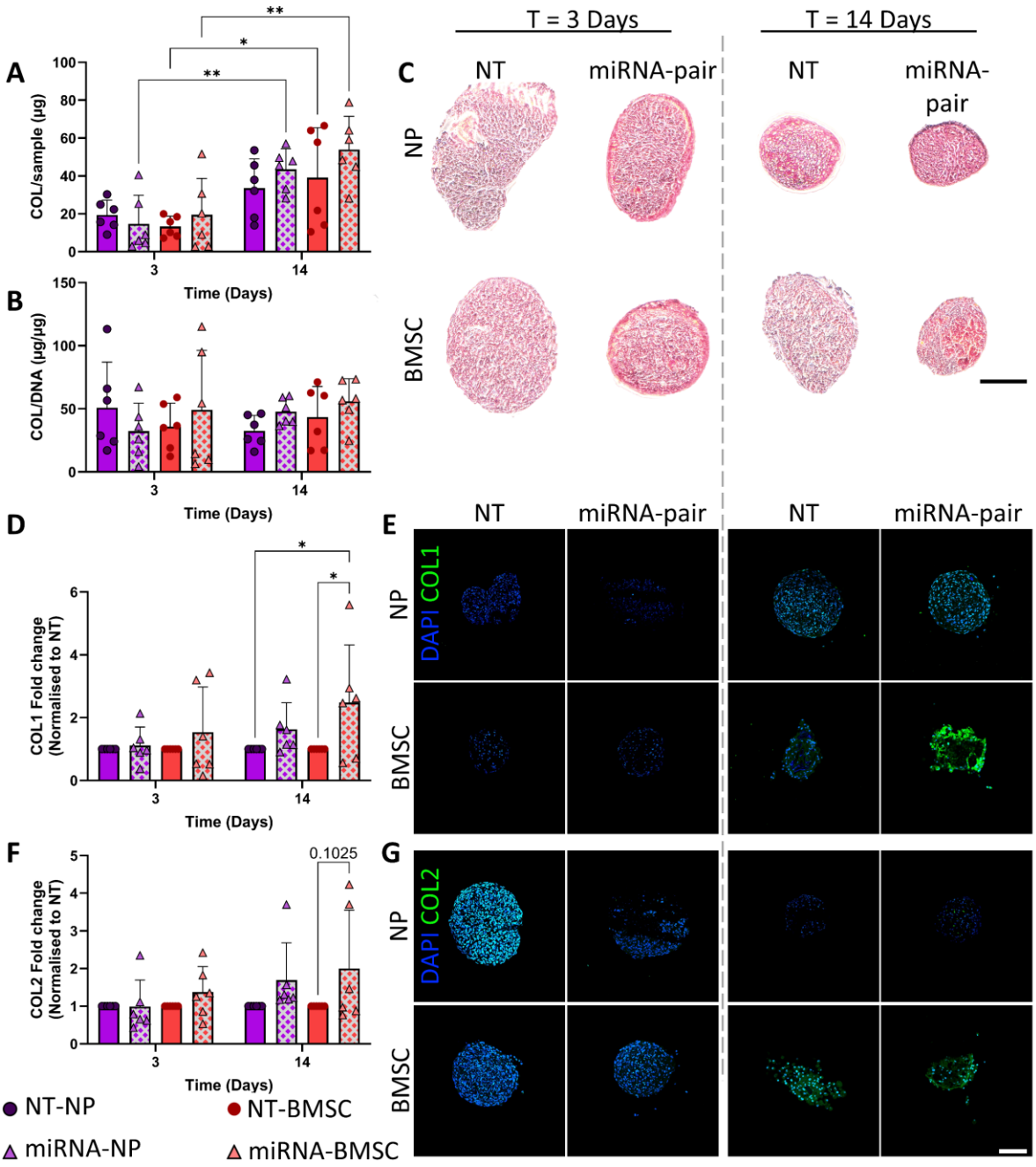

Figure 6.7 Biochemical quantification, histological, and immunocytochemistry analysis of collagen-specific markers of non-transfected (NT) and FLR-miRNA-149 mimic + miRNA-221-inhibitor (dual-miRNA) 3D microtissues formed from nucleus pulposus (NP) and bone marrow-derived stem cells. (A) Collagen content per sample (µg) and (B) normalised to DNA content (µg/µg). (C) Representative histological images of microtissues following Picrosirius Red staining for collagen. (D) Protein expression of COL1A1 and (E) representative immunofluorescent images for DAPI/COL1 (F) COL2A1 protein expression and (G) representative immunofluorescent images for DAPI/COL2 . Statistical test is a two-way ANOVA with Tukey's post-hoc analysis. N = 6 independent biological donors, * $p < 0.05$, ** $p < 0.01$ indicates statistical significance. Scale bars = 100 µm.

6.3.6 Dual-miRNA transfection induced differential catabolic and inflammatory responses between cell types

Restoring homeostatic balance in the degenerated IVD requires the suppression of catabolic and inflammatory mediators. Consistent with monolayer studies, ADAMTS5 expression was substantially elevated in transfected BMSC cells compared to both NT controls and miRNA-NP cells (Fig. 6.8A & B $p = 0.0236$ and $p = 0.0038$, respectively). In contrast to the 2D experiments, MMP13 expression in miRNA-BMSCs was strongly attenuated after 14 days in culture compared with controls (Fig. 6.8C & D $p < 0.0001$). As observed in monolayer studies, transfected NP cells demonstrated marked reductions in MMP13 expression ($p = 0.0158$). To gain deeper insight into inflammatory activity, IL-1β and TNF-α were assessed. IL-1β showed an upward trend in miRNA-BMSCs compared with miRNA-NP cells (Fig. 6.8E & F $p = 0.0746$). TNF-α levels demonstrated modest decreases overall, however transfected NP cells recovered from an initial spike at day 3 and showed a significant reduction by day 14 (Fig. 6.8G & F $p = 0.028$).

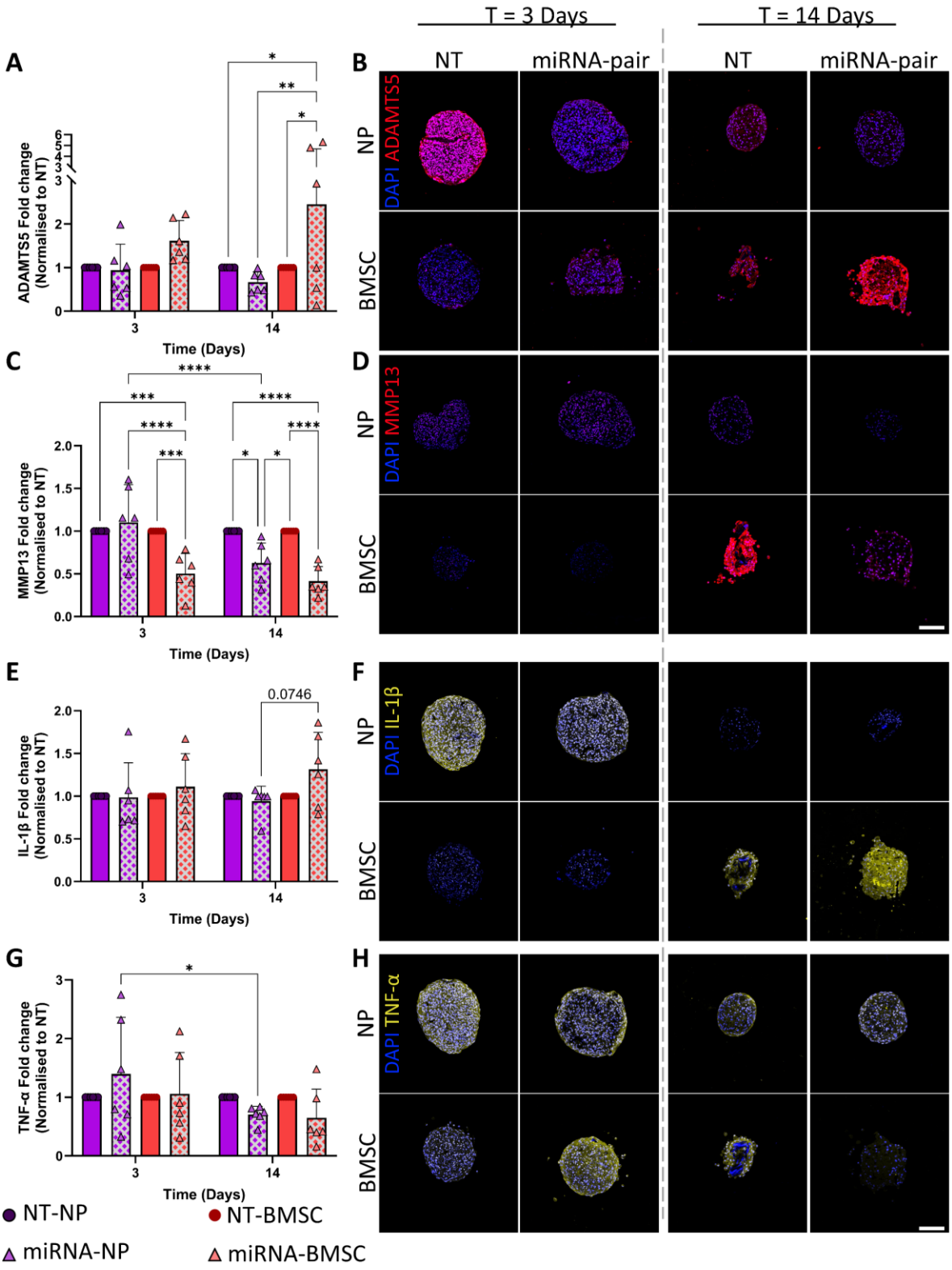

Figure 6.8 Immunofluorescence protein quantification and representative images of catabolic enzymes and pro-inflammatory cytokines in non-transfected (NT) and FLR-miRNA-149 mimic + miRNA-221-inhibitor (dual-miRNA) 3D microtissues formed from nucleus pulposus (NP) and bone marrow derived stem cells (BMSCs). (A & B) ADAMTS5 expression exhibited a significant increase in the BMSC-transfected group. (C & D) MMP13 protein expression was

reduced for both cell types (E & F) IL-1β showed no significant changes, however there was evidence of an upwards trend for the BMSC transfected groups. (G & H) TNF-α levels in dual-miRNA transfected NP cells significantly decreased by the end of the study. Statistical test is a two-way ANOVA with Tukey's post-hoc analysis. N = 6 independent biological donors, * $p < 0.05$, ** $p < 0.01$, *** $p < 0.001$, ****$p < 0.0001$ indicates statistical significance. Scale bars = 100 μm.

6.3.7 Dual-miRNA and transfected-cell delivery promoted discogenic protein expression while suppressing catabolic and inflammatory factors in an ex vivo organ culture

Ex vivo organ culture represents one of the most physiologically relevant models available in the disc field outside of in vivo models. The dose of 2U cABC was established through a pilot study to determine a mild rather than severe degree of degeneration (Fig. 6.9). There was demonstrated a reduction in sGAGs through Alcian Blue staining (Fig. 6.9A) and a significant increase in ADAMTS5 protein expression with 2U compared to the healthy control following 14 days of degeneration (Fig. 6.9C). It is important to note, that while the higher dose of 4U elicited a stronger response in relation to sGAG degeneration alongside MMP13 and ADAMTS5 expression, this magnitude of response is consistent with severe degeneration, outside the remit of the proposed treatments. Furthermore, it has been shown in vivo that degeneration will proceed throughout the study period,[268] therefore, a lower insult of 2U cABC is a more appropriate model of mild degeneration.

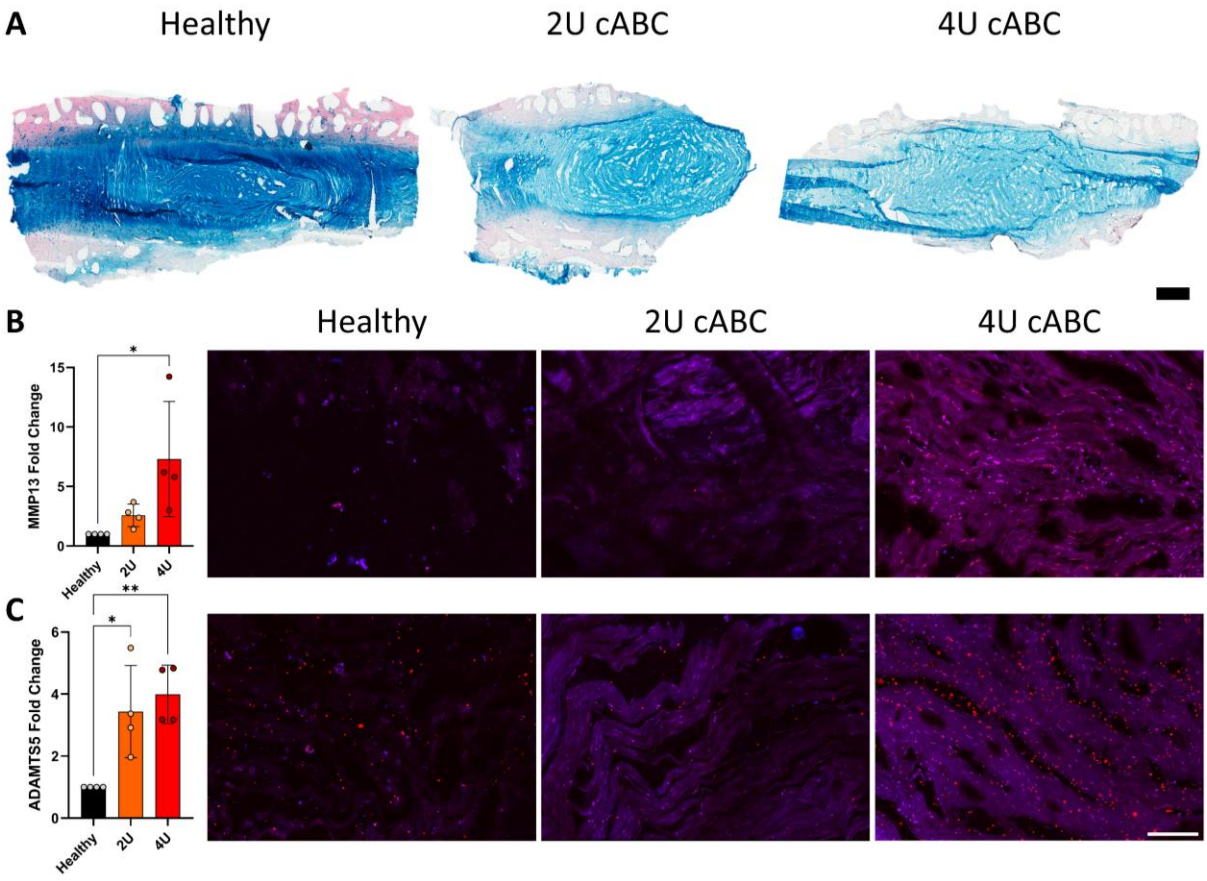

Figure 6.9 Goat ex vivo organ culture degeneration pilot to establish cABC dosage, following 14 days of cABC degeneration. (A) Representative Alcian blue staining for sulphated glycosaminoglycan (sGAG) deposition. Protein quantification normalised to healthy control and representative immunofluorescence images for catabolic proteins (B) MMP13, (C) ADAMTS5. Histology scale bar 3mm, immunofluorescence scale bar. Statistical test is one-way ANOVA with Tukey's post-hoc analysis, n = 4 technical replicates.

To ensure the suitability of the model, FLR-miRDy547 uptake was assessed in mildly degenerated goat IVDs, with a dose of 25 ng/µl selected for further studies due to its significant overexpression and retention within cells (Fig. 6.10A). Cell viability was unaffected by miRNA delivery (Fig. 6.10B). Following delivery, PKH26-labelled NP cells and BMSCs were confirmed to be retained within the NP region at the end of the culture period (Fig. 6.10C).

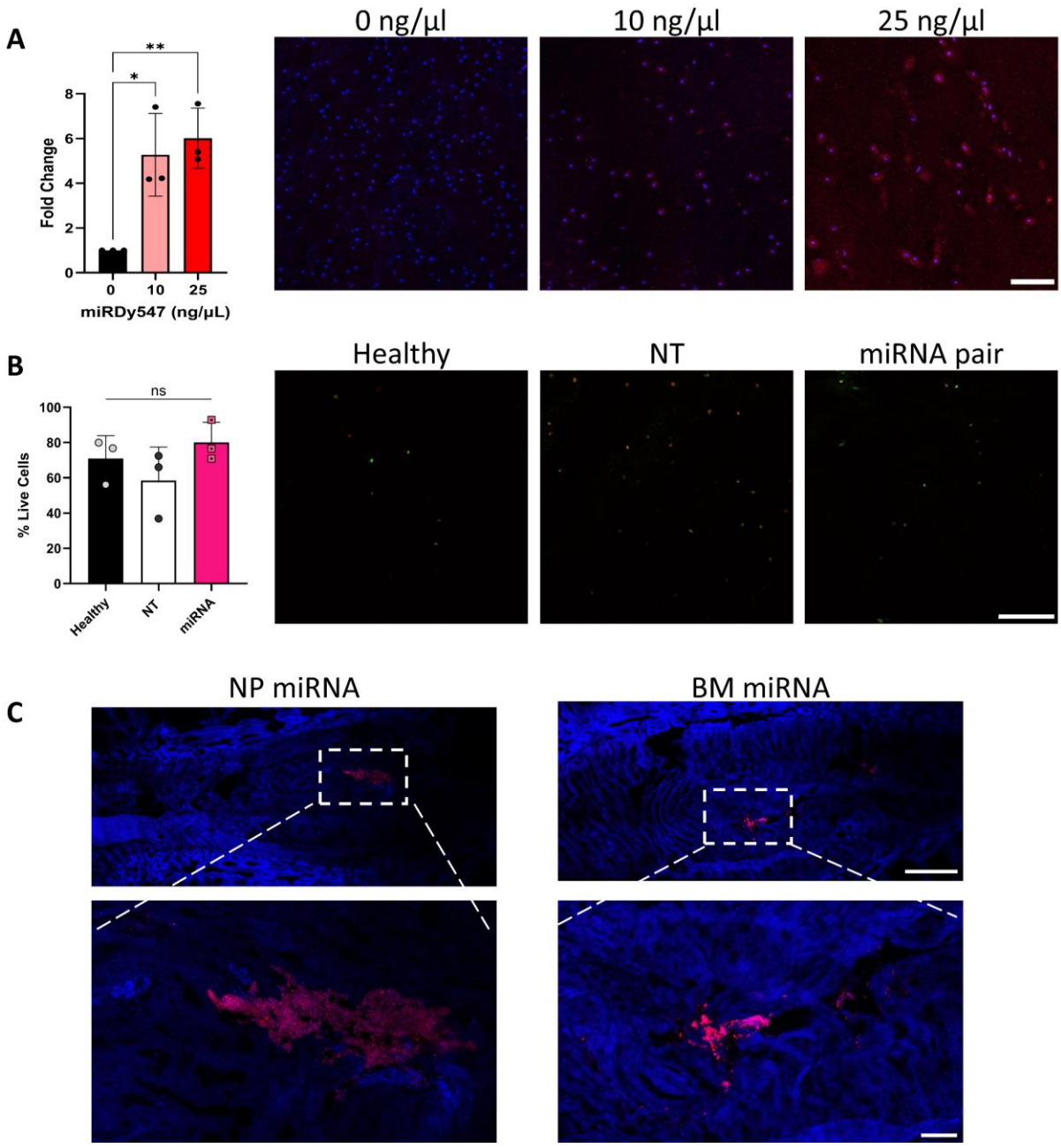

Figure 6.10 Assessment of miRNA delivery efficiency, culture viability, and cell retention in ex vivo organ culture of goat intervertebral discs. (A) Delivery of a fluorescently tagged miRNA demonstrated efficient uptake 3 days post-transfection. (B) Live/dead staining of sections of nucleus pulposus (NP) tissue following 28 days of culture. (C) PKH-26 staining of cells delivered demonstrated retention during the 28-day culture period. Statistical test is one-way ANOVA with Tukey's post-hoc analysis. * $p < 0.05$, ** $p < 0.01$, ns = non-significant. Scale bars for A & B are 100 µm. Scale bars for whole organ view of C are 1mm and 200 µm for inset.

Following treatment with dual-miRNA only or with stimulated cells, histological and biochemical assessment was carried out to assess cell and matrix composition. H&E staining demonstrated maintenance of the cell population despite degeneration and confirmed retention of

delivered NP cells and BMSCs as indicated by the black arrows in Fig. 6.11A. These observations were supported by DNA quantification (Fig. 6.11H). Proteoglycan content was evaluated using AB staining (Fig. 6.11 C). Although modest increases in AB staining were observed in treatment groups, quantitative sGAG measurements revealed no significant differences (Fig. 6.11C & I). Specific markers were assessed to examine potential differences in early (SOX9) and late-stage (aggrecan) matrix protein production. Delivery of dual-miRNA transfected NP cells elevated SOX9 protein expression compared to the healthy, NT, and BMSC miRNA groups (Fig. 6.11D & E, $p = 0.042$, 0.02, and 0.106, respectively). This enhancement of matrix markers was reflected in aggrecan synthesis, which was strongly upregulated in the NP-miRNA group compared to controls (Fig. 6.11F & G, $p = 0.038$). Collagen content assessed by PSR showed no substantial changes consistent with biochemical analysis (Fig. 6.11B & J). Finally, no differences in the sGAG to collagen ratio was observed for any of the groups investigated (Fig. 6.11H).

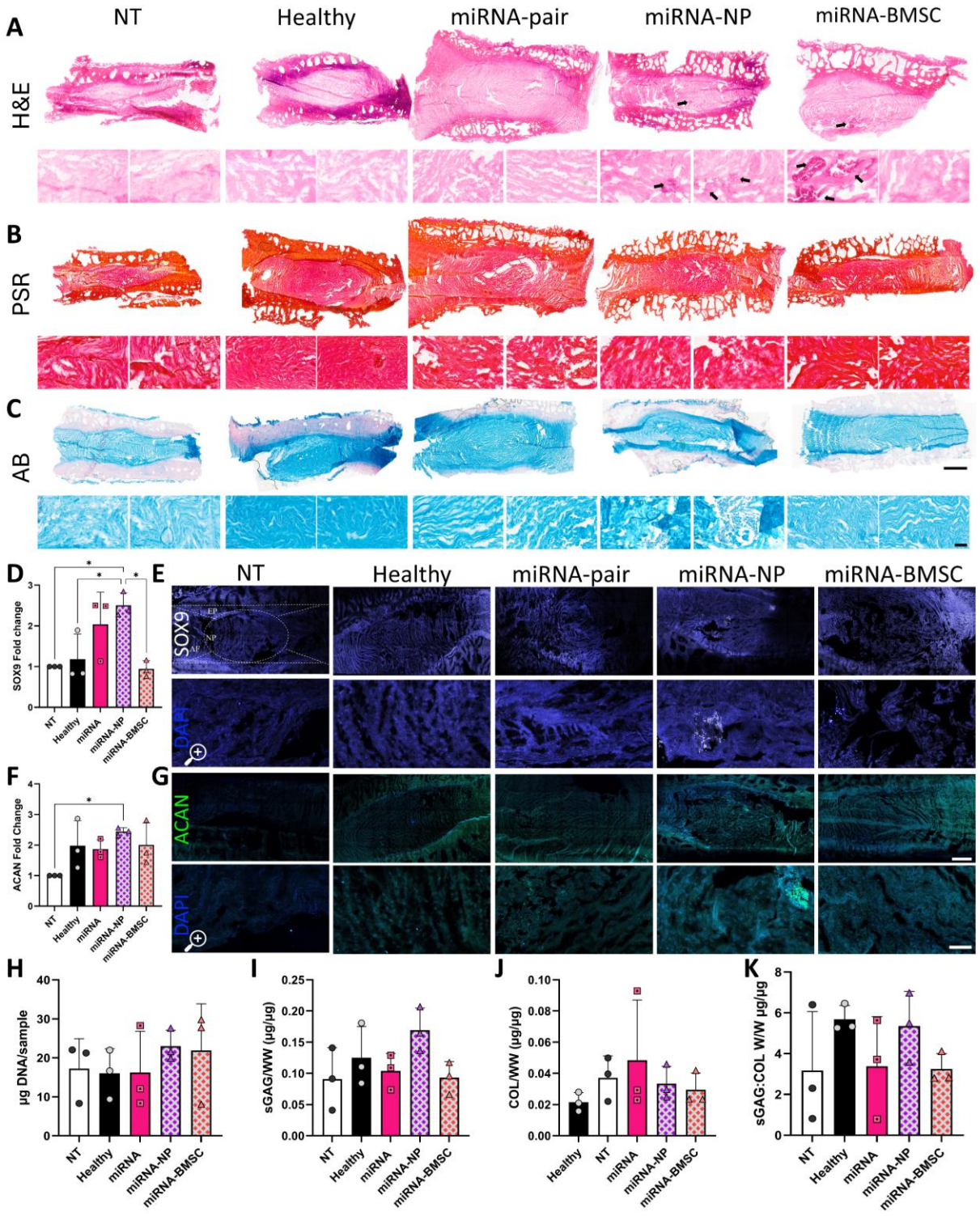

Figure 6.11 Histological and biochemical evaluation of goat ex vivo organ culture following dual delivery of miRNA-149-5p mimic and 221-3p inhibitor, or dual-miRNA stimulated goat nucleus pulposus (NP) and bone marrow-derived stem cells (BMSC) following 28 days of culture. (A) Representative images of histological staining for haematoxylin & eosin (H&E), (B) Picrosirius red (PSR) (C) Alcian blue (AB). (D & E) Sox9 expression was elevated in NP miRNA cells compared to controls (healthy and non-transfected, NT). (F & G) ACAN expression was also higher in the NP-miRNA treated group compared to NT control. (H) Biochemical quantification of

DNA (µg/sample), (I) sGAGs (µg/µg), (J) collagen (COL, µg/µg) production and (K) sGAG:COL (µg/µg) ratio during the 14-day culture period. Statistical test is one-way ANOVA with Tukey's post-hoc analysis. N = 3 independent biological donors. * $p < 0.05$ indicates statistical significance. Scale bars for whole organ view = 2 mm, magnified images 400 µm, indicated by magnifying glass.

Given the variety of approaches available for normalising biochemical data obtained from organ culture, all biochemical results are presented in Fig. 6.12. The parameters shown include tissue hydration, total DNA content, sGAG content, and collagen content, together with values normalised to both wet and dry tissue weight.

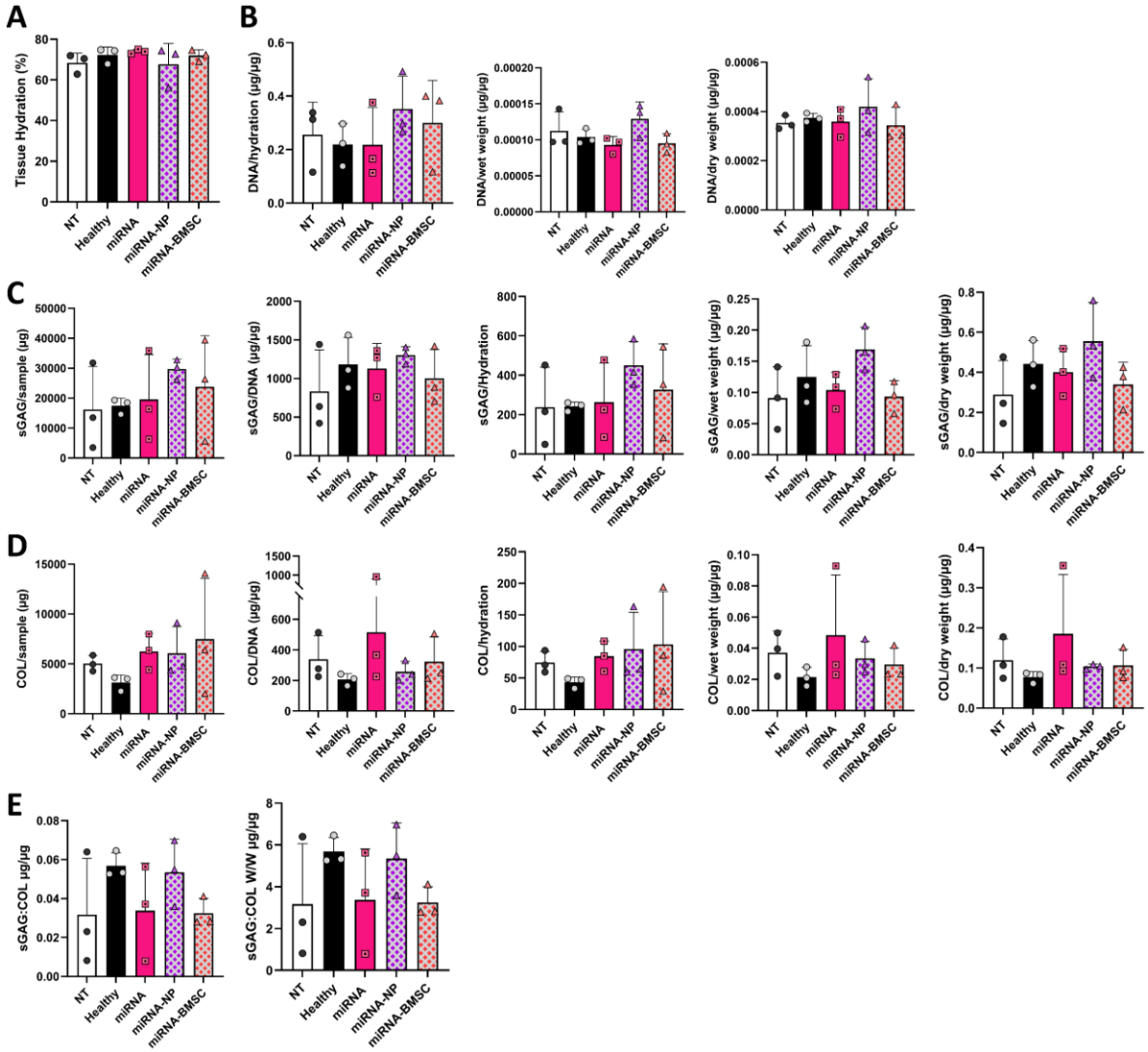

Figure 6.12 Supplementary biochemical analysis of goat intervertebral discs following ex vivo organ culture. (A) Tissue hydration, (B) DNA content, (C) sulphated glycosaminoglycans (sGAGs), (D) collagen content, and (E) sGAG to collagen ratio. N = 3 independent biological replicates.

Following evaluation of discogenic markers, the effects of dual-miRNA and dual-miRNA transfected cells on the protein expression of catabolic and inflammatory targets was evaluated. cABC-induced degeneration in the NT group elicited a substantial increase for all targets when compared to the healthy non-degenerated controls. ADAMTS5 expression was significantly suppressed by dual-miRNA delivery (Fig. 6.13A & B $p = 0.0088$). MMP13 levels were significantly attenuated across all treatments groups compared to the degenerated NT control (Fig. 6.13C & D $p = 0.0082$, $p = 0.007$, and $p = 0.0239$, for dual-miRNA, NP-miRNA, and BMSC-miRNA vs NT, respectively). Similarly, IL-1β activity was strongly diminished following treatment compared with NT controls (Fig. 6.13E & F $p = 0.0002$ for dual-miRNA, $p < 0.0001$ for both NP-miRNA and BMSC-miRNA). Finally, TNF-α production was supressed across all treatment groups when compared to the degenerated NT controls (Fig. 6.13G & H $p = 0.001$, $p = 0.0004$, $p = 0.0007$, for dual-miRNA, NP-miRNA, and BMSC-miRNA, respectively). Aside from the reduction of ADAMTS5, which was specific to dual-miRNA delivery, no notable differences were observed between groups suggesting no clear advantage of NP cells versus BMSCs for supressing these degradative factors in the NP region.

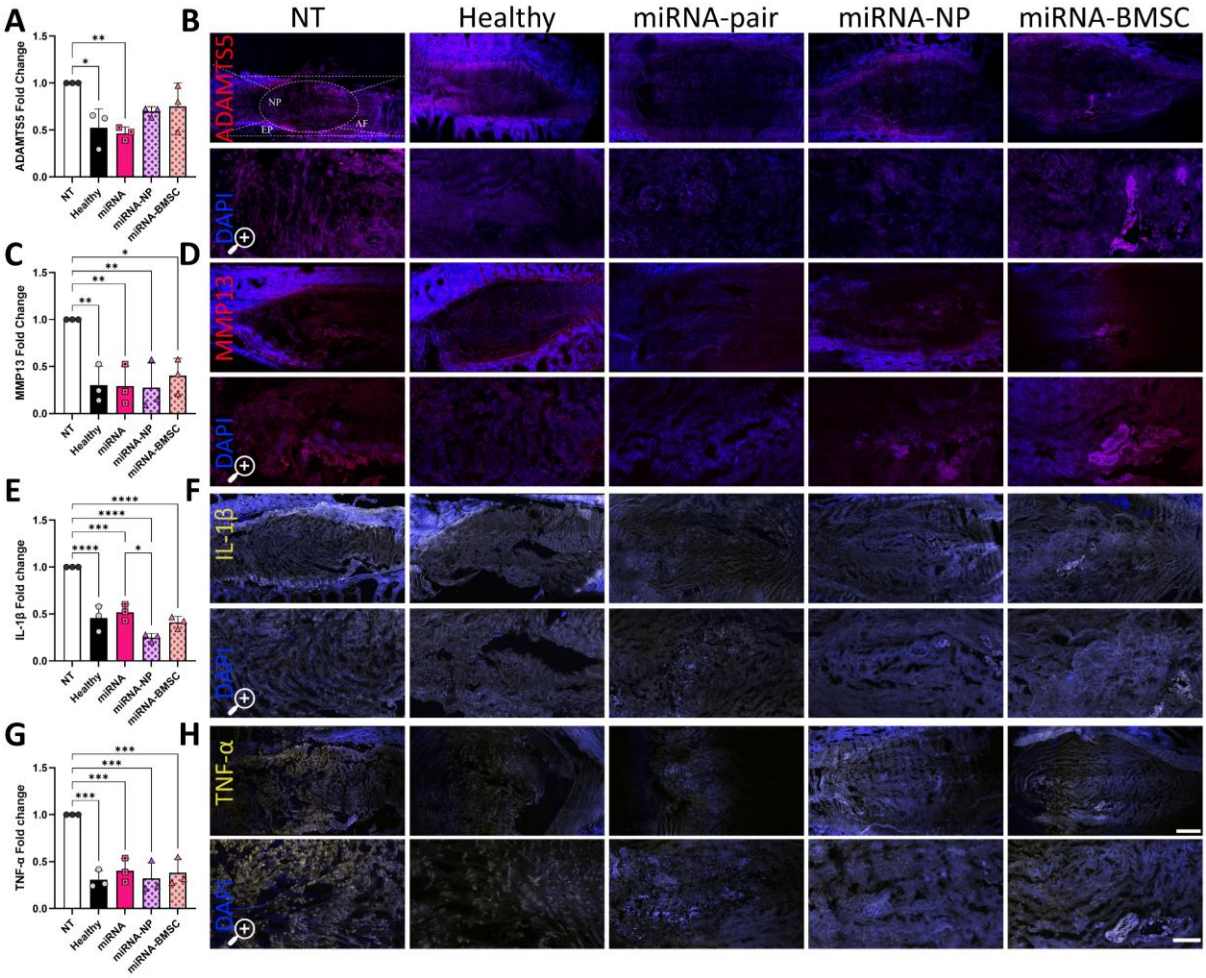

Figure 6.13 Immunofluorescence analysis and representative images of catabolic enzyme and pro-inflammatory cytokine protein levels in ex vivo organ culture following dual-miRNA delivery alone, or transfected nucleus pulposus (NP) and bone marrow-derived stem cell (BMSC), post-28 days in culture. (A & B) ADAMTS5 protein expression was markedly reduced following dual-miRNA delivery. (C & D) MMP13 was significantly downregulated across all treatment groups. (E & F) Protein production of IL-1β was supressed post-treatment delivery. (G & H) TNF-α activity was strongly diminished by all treatments. Statistical test is one-way ANOVA with Tukey's post-hoc analysis. N = 3 independent biological donors. * $p < 0.05$, ** $p < 0.01$, *** $p < 0.001$, ****$p < 0.0001$ indicates statistical significance. Scale bars = 1 mm for whole organ view and 400 µm for magnified image, indicated by magnifying glass.

6.4 Discussion

The therapeutic potency of miRNA-guided augmentation of cellular phenotypes has gained significant appreciation in recent years. Similarly, the efficacy of cell transplantation to promote IVD anabolism while curbing catabolism has been debated. While some studies report increased

ECM production and improvements to disc height, others have observed no changes in disc height, and minimal regeneration.[19,274-276,278,288] In this study, the delivery of two cell populations following dual-miRNA stimulation was explored, to determine whether the delivery of a transfected cell source offers advantages over administering the dual-miRNA only. Central to this chapters' results was the sustained anti-catabolic effect previously attributed to the dual delivery of FLR-miRNA-149-5p mimic + miRNA-221-3p inhibitor.[241,242] Furthermore, the evidence presented suggests the upregulation of discogenic markers following the delivery of dual-miRNA transfected NP cells in a goat ex vivo organ culture model of mild IVD degeneration. Taken together, these results highlight the potency of dual-miRNA delivery while also identifying encouraging restorative trends post-miRNA-NP cell transplantation.

The onset of degeneration and decline of IVD health is characterised by the amplification of the catabolic and inflammatory milieu. In agreement with previous work from Chapter 4 and 5, dual-miRNA delivery strongly inhibited degradative protein markers. miRNA-149-5p in particular has been highlighted as an anti-inflammatory miRNA, eliciting positive effects both in vitro and in vivo. Specifically, Lang *et al* demonstrated that protein expression of IL-1α, IL-1β, and IL-6 were significantly reduced in miRNA-transfected versus non-transfected wounds during healing and these effects persisted even under a TNF-α challenge. [289] Furthermore, in chondrocytes, cells that closely resemble NP cells in both morphology and behaviour, miRNA-149 delivery has been shown to markedly suppress the inflammatory cytokine IL-6 and degradative enzyme MMP-3 at both the mRNA and protein levels.[191] A recent study demonstrated that the inhibition of miRNA-149-5p in tert-Butyl hydroperoxide (TBHP)-challenged NP cells exacerbated the inflammatory response through Nod-like receptor Pyrin domain containing 1 (NLRP1) activation, [290] a critical inflammation mediator, further emphasising the anti-catabolic utility of this miRNA. These findings support the anti-degradative effects mediated by miRNA-149 when delivered in tandem with miRNA-221-3p inhibitor.

In both two- and three-dimensional culture, NP cells exhibited greater resilience when exposed to cytokine challenges. Expression of ADAMTS5, MMP13, IL-1β, and TNF-α in NP cells tended to be lower than in BMSCs, regardless of transfection. This may reflect an inherent adaptive advantage, as NP cells secrete low levels of TNF-α and IL-1β, even in a healthy state. [42,291] Serum starvation and cytokine challenges were applied in monolayer, which may have disproportionately affected BMSCs. Redondo-Castro and colleagues identified a strong up-regulation of anti-inflammatory factors; granulocyte-colony stimulating factors (GCSF), and IL-1 receptor antagonist in cytokine-stimulated spheroids in comparison to their monolayer counterparts, suggesting BMSCs are sensitive to challenges based on their culture dimensionality. [292] Conversely, cervical

derived NP cells did not elicit an immunogenic response when co-cultured with peripheral blood mononuclear cells (PBMCs) in monolayer, with no discernible increase in T cell markers or pro-inflammatory cytokines. [293] These observations suggest that NP cells exhibit a comparatively lower inflammatory response to challenges, particularly in vitro.

The suppression of degradative factors was most pronounced in the ex vivo model of mild degeneration, further supporting the implementation of physiologically relevant culture systems. A strong catabolic upregulation was observed between the healthy and degenerative controls, validating the model, with both miRNA only and transfected cells strongly supressing these elevated levels of catabolic expression. Encouragingly, this mirrors previous chapters in rat ex vivo organ culture, demonstrating the utility of dual-miRNA+149-5p and 221-3p inhibitor across species.[241,242] Interestingly, and contrary to the in vitro experiments, miRNA-BMSCs exhibited an anti-catabolic effect in the ex vivo model. BMSCs rely upon microenvironmental factors to exert immunomodulatory effects, which may have been further enhanced when delivered directly to an organ. In vitro, application of conditioned media from BMSCs has been shown to reduce cytokine expression in NP cells. [294] Moreover, MSC encapsulated hydrogels have demonstrated immunomodulatory potential, curbing inflammation and promoting an anti-inflammatory state through macrophage polarisation. [295] Taken together, these findings highlight the importance of culture model, with the immunomodulatory effect being supressed in vitro, but enhanced ex vivo.

In the context of IVD degeneration, catabolic suppression may represent the gateway to regeneration, but this must occur concurrently with matrix accumulation to restore lost tissue components. Minor increases in sGAGs were identified histologically and biochemically following treatment with miRNA-NP cells. However, analysis of specific markers was particularly encouraging, with both SOX9 and aggrecan showing significant upregulation. Feng *et al* delivered NP cells and BMSCs to degenerated rabbit discs, which halted DHI decline, and resulted in improvements to histological scoring compared to the sham control. [288] Consistent with this study, albeit at the gene rather than protein level, aggrecan was significantly upregulated in both treatment groups compared to the degenerated control. Moreover, Chen and colleagues delivered NP cells and NP-derived mesenchymal stem cells to rabbit IVDs, finding no regenerative differences between the treatment groups, although both showed improvement compared to the degenerated control. [274] In this work, the detection of both early and late-stage ECM production markers following delivery of transfected NP cells is encouraging, indicating a shift towards a regenerative response that may not have had sufficient time to fully mature.

Ex vivo organ degeneration was induced by delivering the enzyme chondroitinase ABC (cABC), which degrades chondroitin sulphate GAG chains of proteoglycans, [296] and is widely recognised for reducing GAG content whilst eliciting a catabolic response in both ex vivo and in

vivo models of disc degeneration. [148,267,268] As the principal sulphated proteoglycan within the disc ECM, regulation of aggrecan catabolism is key to restoring homeostasis. In bovine cartilage explants, aggrecan has been shown to be rapidly cleaved by cABC into numerous smaller core peptides, [297] suggesting these core fragments must be replenished and modified prior to the reformation of the total proteoglycan. [298,299] The observed increase in SOX9, considered a discogenic master regulator, [300,301] and aggrecan in the NP-miRNA group suggests the early establishment of a regenerative phenotype. Full glycosylation may not yet have been achieved, likely reflecting a limitation of the ex vivo organ culture model, in which maintaining cultures beyond 4 weeks is currently not feasible. Truncated aggrecan molecules lacking chondroitin sulphate chains are characteristic of ageing and degenerative pathology, [302,303] and may potentially explain the disparity observed between sGAG and aggrecan levels.

The upregulation of discogenic factors observed in this work is likely to be primarily influenced by the inhibition of miRNA-221-3p, the chondroinductive element of the dual-miRNA therapy. In cartilage regeneration, silencing of miRNA-221 has been shown to enhance the production of matrix markers. As early as 2010, microtissue cultures of MSCs demonstrated enhanced chondrogenesis and cell proliferation through degradation of Slug protein in cells treated with miRNA-221 inhibitor. [304] More recently, the loading of collagen hydrogels with miRNA-221 inhibitor similarly led to significant increases in collagen type II and aggrecan at the mRNA level and sGAGs at the protein level. [256] In the context of disc regeneration, Sheng and colleagues reported a protective effect of miRNA-221 inhibition in cartilaginous endplate (CEP) cells, with significant upregulation of aggrecan and collagen type II protein expression. [305] Similar upward trends were observed here, particularly in more sophisticated culture models, reinforcing the potential of miRNA-221 silencing as a strategy to counter intervertebral disc degeneration.

The combined delivery of dual-miRNAs produced a beneficial effect, enhancing pro-anabolic and suppressing catabolic signals, reflecting the inherent biological complexity of simultaneously targeting multiple degenerative pathways. This combinatorial approach has been successful in other fields, including the treatment of various cancers [306-308], where it proved both therapeutically effective and non-toxic. Similarly, in this study, dual-miRNA delivery showed no adverse effects on cell viability in ex vivo organ culture. In Chapter 4 it was shown that dual delivery of miRNA-149-5p + miRNA-221-3p inhibitor outperformed single miRNA treatment, both in terms of ECM molecule accumulation and in the suppression of matrix degrading enzymes. [241] A similar effect was reported by Castaño *et al*, whereby combined delivery of miRNA-210 + miRNA-16 inhibitor loaded scaffolds significantly enhanced the osteogenic potential of MSCs when compared to individual-miRNA transfection. [184] The synergistic effect of dual-miRNA therapy likely arises from the modulation of complementary signalling pathways. For example, miRNA-149 is known to target molecules involved in the NF-κB pathway, [191,309] while miRNA-221 has been shown to

modulate members of the TIMP signalling family. [257,310] These distinct targets may be responsible for the modulation of both anabolic and catabolic factors, which further investigations could better elucidate given the multitude of pathways potentially involved.

Although a range of culture models were utilised here, certain limitations should be acknowledged. While mechanical loading within the human physiological range [136] was applied in the bioreactor system, more sophisticated models could be utilised to better simulate the diurnal and complex loading pattern experienced through daily life. Recent studies using such dynamic systems have demonstrated modulation of the microenvironment, whereby anabolic genes were downregulated and catabolic genes upregulated following a regime of dynamic and static loading, perpetuating degeneration even in the absence of enzymatic insult.[311] Furthermore, dynamic loading may increase the diffusivity of treatments throughout the NP region. [312] However, the simplified model incorporating static loading and cABC enzyme delivery successfully induced degeneration while maintaining viability comparable to that observed in more complex dynamic systems over the same culture period.[313] Furthermore, PKH26 positive staining confirmed the presence of injected cells within the NP region, demonstrating their retention within the disc and supporting the utility of this approach as an accessible model.

Whilst aligning with the 3R principles, [314] organ culture inherently limits the duration of experiments compared to in vivo studies, typically to a maximum of 4 weeks,[315,316] which restricts assessment of longer term effects. Regeneration of the in vivo GAG matrix to a healthy level has been predicted to require 12 months in a goat following delivery of 5.5 x 10^6 cells,[287] which is not feasible when using organ culture models. Nonetheless, organ culture models provide valuable insights into the early stages of treatment, and the use of goat discs offers strong translational relevance for human IVD therapies due to their anatomical and matrix compositional similarity to human discs.[148]

One aspect of degeneration not addressed in this study but warrants further investigation is nociceptive pain. Elevated levels of markers such as β-nerve growth factor (β-NGF) and brain derived neurotrophic factor (BDNF) are associated with increasing degeneration severity and substantially affect quality of life in patients with degenerated discs. In a clinical study of platelet lysate delivery to the IVD, no measurable improvement in disc height was observed, yet both the visual analogue scale (VAS) and Roland-Morris disability questionnaire showed significant pain reduction.[239] This highlights that modulation of pain perception is a key factor in rehabilitation, and should be considered alongside regenerative strategies. TNF-α has been shown in vitro to upregulate BDNF and β-NGF expression, [317-319] suggesting that a TNF-α silencing approach may potentially impact pain perception, although this remains to be explored in future studies.

In this study, the effect of dual delivery of the anti-inflammatory miRNA-149-5p mimic and the pro-matrix miRNA-221-3p inhibitor with the cell penetrating peptide FLR was examined to stimulate two candidate cell populations, NP and BMSCs to determine the most efficacious for delivery to a mildly degenerated IVD. The findings highlight the potential of a dual-miRNA transfected cell delivery approach to exert both anti-catabolic and anti-inflammatory effects in vitro and in ex vivo goat organ culture models, while demonstrating positive upregulation of matrix promoting markers. Stimulation of both NP and BMSCs with FLR-miRNA-149-5p mimic + 221-3p inhibitor elicited positive effects, primarily through the suppression of key catabolic factors, ADAMTS5, MMP13, and the pro-inflammatory cytokines TNF-α and IL-1β. Notably, delivery of dual-miRNA treated NP cells to goat organs demonstrated particularly promising improvements in matrix-related markers, SOX9 and aggrecan, suggesting the potential of this strategy as a cell therapy for IVD degeneration when combined with the dual-miRNA. Furthermore, these results suggest that NP cells are more suited than BMSCs for delivery to the IVD post-miRNA transfection, as they demonstrated combined anti-catabolic and pro-restorative activity. Collectively, these findings support further longer-term investigations to assess the feasibility and efficacy of a dual-miRNA NP cell-based delivery strategy to target and attenuate the degradative cascade promoting IVD degeneration and the development of LBP.

6.5 Conclusion

In this chapter the response of NP and BMSCs to the therapeutic dual-miRNA, miRNA-149-5p mimic and miRNA-221-3p inhibitor was investigated, with the goal identifying the optimal cellular vehicle for IVD delivery. Suppression was demonstrated of key catabolic enzymes, ADAMTS5 and MMP13, alongside inflammatory mediators, TNF-α and IL-1β across all delivery groups, confirming the establishment of a robust anti-catabolic microenvironment. Importantly, only the delivery of dual-miRNA stimulated NP cells into organ culture elicited a significant anabolic response, evidence by the upregulation of matrix markers SOX9 and aggrecan, an effect not replicated by miRNA-BMSC delivery. Overall, the work presented in this chapter suggests NP cells as the more suitable regenerative cell source when delivered with FLR-miRNA-149-5p and 221-3p inhibitor as a treatment of IVD degeneration.

Chapter 7. In vivo assessment of miRNA and miRNA stimulated cells

7.1 Introduction

While dual-miRNA delivery has shown promise in Chapter 4, pre-conditioning cells with miRNAs prior to transplantation could provide a stimulatory and enhanced therapeutic effect, suggested in Chapter 6. As degeneration progresses, the proportion of necrotic cells increases, therefore replenishing the resident cell population may also restore regenerative capacity.[320] NP cells have been widely investigated due to their innate ability to withstand and survive the harsh NP microenvironment of low pH, glucose, and oxygen. This intrinsic adaptability has made them a promising candidate for transplantation to the IVD, and they have been explored in preclinical models. Nukaga et al delivered autologous NP cells co-cultured with bone marrow derived stem cells (BMSCs) in a canine model of induced IVD degeneration, observing increased proteoglycan staining, preserved disc height and reduced histological scores compared to untreated controls.[275] Following promising preclinical results,[19,20] the biotech startup Discgenics have progressed to human clinical trials (NCT03955315 and NCT03347708). Using a canine IVD model, they demonstrated that transplanted human disc progenitor cells improved histological grading and disc height compared to untreated controls. [20] Furthermore, in a rabbit model of IVD degeneration they observed significant restoration of disc height in comparison to the untreated controls, with evidence of deeper ECM staining in treated discs. [19]

However, contradictory findings have emerged following cell delivery to degenerated IVDs. In a prospective human trial, autologous NP cells and BMSCs were co-cultured prior to the NP cells being delivered to an adjacent disc with evidence of moderate degeneration. [321] While the treatment was well tolerated, at a three-year follow up, only one of the nine patients showed mild improvement on magnetic resonance imaging (MRI). Similarly, with stem cell delivery, Haufe et al reported no improvements in patient outcomes after a 1-year follow up. [322] Collectively, these studies highlight the potential of cell-based therapies for IVD regeneration, but their efficacy has yet to be fully elucidated. Furthermore, the choice of cell source is also critical; NP cells may have limited regenerative potential particularly if derived from herniated tissue, [323] while healthy cells, often cadaveric, raises possible ethical issues. Consequently, strategies that optimise the therapeutic potential of delivered cells may elicit meaningful functional responses. Similar strategies have been employed with promising effects through delivery of nucleic acid engineered extracellular vesicles (EVs) to IVDs.[90,324] Accordingly, the inclusion of dual-miRNA-stimulated cells has, to the best of our knowledge, not been evaluated in animal or human studies, offering the potential to introduce a pre-programmed cell population capable of restoring the degenerated IVD niche.

In vivo evaluation remains a powerful tool for assessing the translatability of potential therapies. For IVD degeneration, large animal models such as goats closely replicate the geometry and biochemical composition of the human disc, making them well-suited for bridging preclinical findings to human clinical trials. [287,325] Degeneration can be induced via NP aspiration,[326] annular injury,[327] mechanical disruption,[328] or chemonucleolysis.[329] Chemonucleolysis, often using chondroitinase ABC (cABC), enzymatically degrades proteoglycans, breaking down ECM, [296] inducing inflammation,[149] and allowing tuneable degeneration levels, as demonstrated in goat models. [148,330-332]

The overall aim of this chapter was to preclinically evaluate the safety and efficacy of dual-miRNA-149-5p mimic and 221-3p inhibitor delivery in a goat model of mild IVD degeneration. Building on the potential of cell delivery from chapter 6, both miRNA- transfected, and non-transfected NP cells were also delivered to determine the most effective injectable treatment. The findings presented here highlight the therapeutic promise of dual-FLR-miRNA-149-5p mimic and 221-3p delivery, while revealing that cell delivery, regardless of transfection, negatively affected sGAG content, catabolic enzyme activity and pro-inflammatory cytokine expression.

7.2 Materials and methods

7.2.1 Animals and study design

The aim of this study was to assess the regenerative potential of dual-miRNA delivery alone, or through dual-miRNA transfected NP cell delivery as a treatment for mild degeneration of the IVD. All animal experiments were carried out in accordance with the recommendations of the Irish Health Products Regulatory Authority (HPRA) following Directive 2010/63/EU on the protection of animals used for scientific purposes, outlined in the requirements of the Statutory Instrument No. 543 of 2012. This study was approved by the University College Dublin Animal Research Ethics Committee (Approval number – AREC-23-20) and the HPRA (Approval number – AE18982/P241). Six skeletally mature male goats were used in the study, as determined by power analysis to detect significance at the 0.05 level. The study comprised of two surgeries performed 8 weeks apart: the first to induce degeneration and the second to administer the investigational treatments (Fig. 7.1). Treatments consisted of 1. A degenerated control (DC), which received the vehicle OptiMEM, 2. Dual-miRNA, 3. NP cells, and 4. Dual-miRNA transfected NP cells. Four disc levels (L1-L5) were designated to receive treatment, while T13-L1 and L5-6 were maintained as intact, untreated healthy controls.

Animals were housed indoors under standard husbandry conditions, and weather permitting, were returned to pasture 2 weeks after surgeries. Grass hay was available ad libitum and where appropriate supplemented with concentrates. The veterinary team performed daily welfare checks and completed scoresheets to assess pain, behavioural changes, gait abnormalities, and neurological deficits. Experimental outcomes included disc height measurements as evaluated from radiographs, MRI of select spines to examine disc condition, and computed tomography (CT) to assess changes to the vertebrae structure. Furthermore, biochemical characterisation of key matrix components was performed, alongside histological scoring, and semi-quantitative immunohistochemical analysis of specific extracellular matrix constituents, matrix degrading enzymes, and pro-inflammatory cytokines.

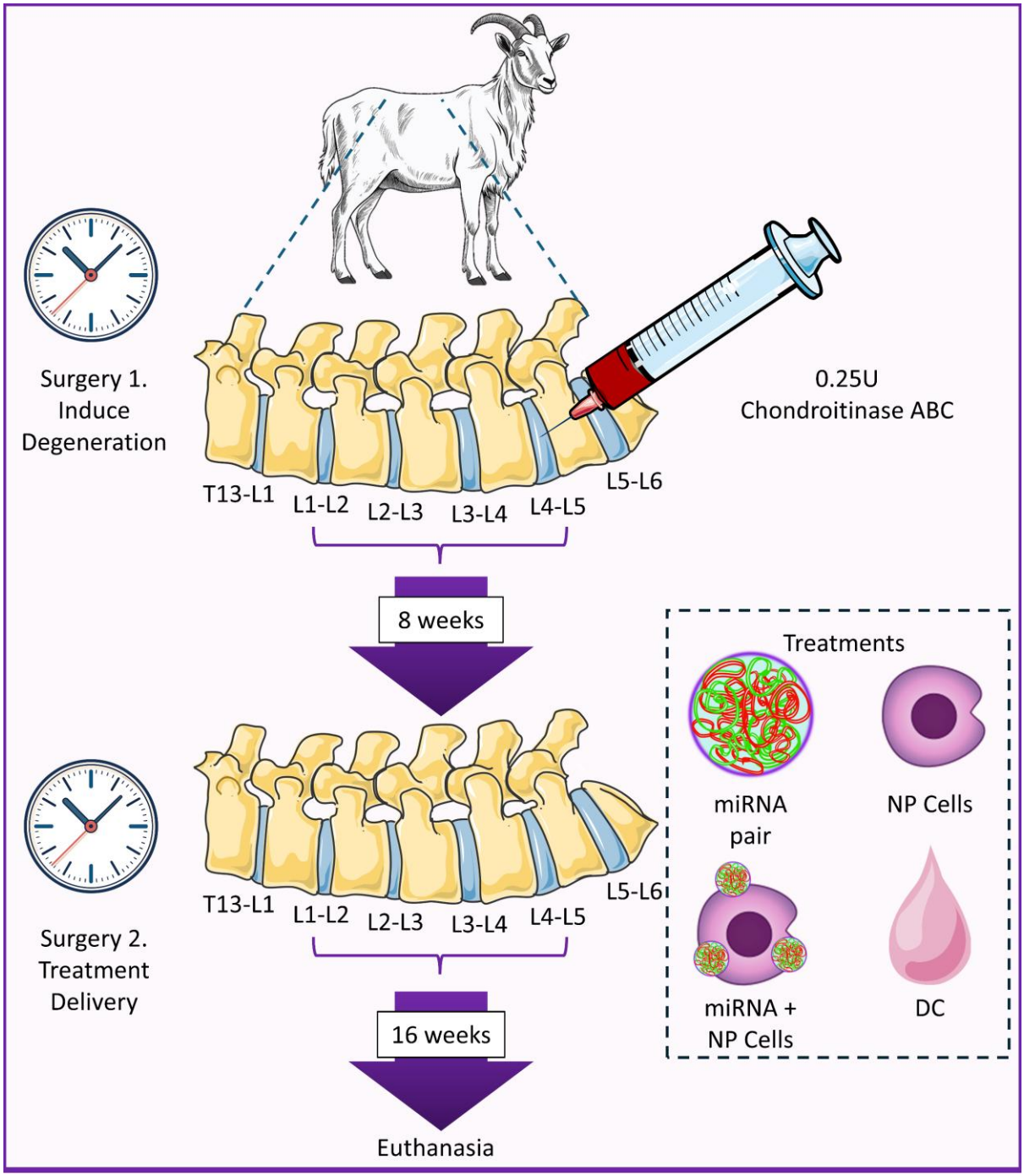

Figure 7. 1 Study design. Surgery 1 induced degeneration with the delivery of 0.25U chondroitinase ABC (cABC) to lumbar (L) levels L1-L5. Thoracic (T)13-L1 and L5-L6 were maintained as intact healthy controls. Treatments were delivered during the second surgery. NP: nucleus pulposus. NT: non-treated.

7.2.2 Surgical approach and enzymatic degeneration of IVDs

Degeneration was induced by injecting the enzyme chondroitinase ABC into four disc levels (L1-L5). Animals were sedated by administration of intravenous Diazepam (0.3-0.4 mg/kg) and intramuscular Morphine (0.4 mg/kg). Anaesthesia was then induced with propofol to effect (maximum dose 4mg/kg), followed by endotracheal intubation and maintenance with an oxygen-isoflurane mixture. An ultrasound-guided retrolaminar nerve block was performed with lidocaine (2 mg/kg) to allow for an optimal balanced anaesthesia. A right lateral retroperitoneal surgical approach was used to access the IVDs via a retropsoas exposure. A metal marker (cerclage 0.6 mm diameter) was placed at the transverse process of L3 to secure correct location of injections. A 200µl dose of 0.25 U cABC (Sigma-Aldrich) was injected to L1-L2, L2-L3, L3-L4, and L4-L5 using a 23G 5/8-inch needle. Incisions were closed with sutures in three layers, and an aseptic stent dressing was applied before animals were returned to their pre-surgery housing. Animals were administered intramuscular morphine (0.1-0.2 mg/kg) and subcutaneous non-steroidal anti-inflammatory drugs (NSAID, Meloxicam 0.5 mg/kg) at the end of anaesthesia. NSAID treatment was continued daily for 5 days postoperatively, stents were removed at day 3 and skin sutures were removed at day 14.

7.2.3 miRNA and cell preparation

Dual-miRNA-149-5p mimic + 221-3p inhibitor complexes were prepared with the FLR peptide (Dixon Lab., Nottingham, United Kingdom) in OptiMEM reduced serum media (Gibco) at a charge ratio of N:P 5. For direct dual-miRNA delivery, complexes at a dose of 25 ng/µl were formed via electrostatic interactions for 30 minutes at room temperature. In preparation for intradiscal delivery, goat NP cells were cultured in low glucose DMEM (LG DMEM, Sigma-Aldrich) supplemented with 2% penicillin/streptomycin (pen/strep, Gibco), 10% foetal bovine serum (FBS, Gibco), and 2.5 mg/mL Amphotericin B (Sigma-Aldrich), dubbed XPAN media. Cells were maintained until confluency under physioxic conditions (5% O_2 and 5% CO_2, 37°C) up to passage 3, where they were trypsinised and resuspended in OptiMEM reduced serum media, or prepared for transfection. NP + miRNA cells were transfected with dual-miRNA complexes prepared as above at a dose of 10 ng/µl. Transfection proceeded for 6 hours at 5% O_2 at 37°C, whereupon complexes were removed and replaced with XPAN media. Transfected cells recovered overnight prior to trypsinisation and surgical delivery. In total, 5.5 x 10^6 transfected or non-transfected cells were delivered to each disc, a dose predicted to restore matrix synthesis in goat disc to healthy levels. [287]

7.2.5 Disc height assessment

Disc height changes were assessed at three timepoints during the study period: Before degeneration (week 0), post-degeneration (week 8), and post-treatment (week 24). Lateral radiographs were acquired in standing, fully weight-bearing positions. To assess degenerative changes and account for preferential height loss in specific regions disc height was measured separately across the ventral, dorsal, and central regions, by three blinded assessors. As an evaluation of the whole disc, disc height index (DHI) was likewise determined by the methods proposed by Sasaki et al. [333]

7.2.6 Magnetic resonance imaging

Following euthanasia, the lumbar spines of two randomly selected goats were imaged using MRI to gain further insights into disc condition post-treatment. Spines were imaged using a 1.5 T clinical MRI scanner (GE SIGNA Artist, GE Healthcare). T1-weighted transverse fast spin echo (FSE), T2-weighted transverse FSE, T1-weighted sagittal FSE, T2-weighted sagittal FSE and dorsal SPIN images were obtained.

7.2.7 Immunofluorescence and immunocytochemistry

Tissue sections were permeabilised in 0.1% Triton X-100 and blocked for 1 hour in 5% bovine serum albumin (BSA) in PBS-Tween. All antibodies and dilutions used are presented in Table 1. Primary antibodies were incubated overnight at 4°C, followed by incubation with species-matched Alex Fluor secondaries for 2 hours at room temperature. An IgG control was included for all staining conditions. Nuclear counterstaining was performed using Hoechst Bisbenzimide 33342. Imaging was conducted on a Leica SP8 Gated STED microscope. Corrected total cell fluorescence was quantified for regions of interest specific to the NP and normalised to cell number.

Table 7. 1 Primary and secondary antibodies used for immunofluorescence.

Antigen	Species	Concentration	Supplier & Code
Aggrecan	Rabbit	1:250	Invitrogen, MA532695
SOX9	Rabbit	1:250	Invitrogen, PA586301
ADAMTS5	Rabbit	1:250	Invitrogen, PA532142

MMP13	Mouse	1:125	Invitrogen, MA514247
TNF-α	Rabbit	1:100	Invitrogen, PA519810
IL-1β	Rabbit	1:200	Invitrogen, P420B
Anti-Rabbit Alexa Fluor 488	Goat	1:500	Invitrogen, A27034
Anti-Mouse Alexa Fluor 488	Goat	1:2000	Invitrogen, A11001

7.2.8 mRNA isolation, sequencing, and data analysis

Total RNA was extracted from approximately 50 mg of NP tissue using TRIzol reagent (Thermo Fisher) according to manufacturers' instructions. Samples were submitted to Novogene Co. (Cambridge, U.K.) for library preparation and sequencing using the Illumina NovaSeq platform. For bioinformatic analysis, cleaned data reads were obtained and aligned to the ARS1.2 GCA_001704415.2 reference genome using HISAT2 (v2.2.1). Mapped reads of each sample were assembled by StringTie (v2.2.3), and gene expression levels calculated using featureCounts (v2.0.6). Differential gene expression analysis was obtained using DESeq2, using an adjusted p-value (padj) < 0.05 and $|\log2(\text{foldchange})| \geq 1$. Gene ontology (GO) enrichment was performed using clusterProfiler (v4.8.1) with a correction for gene length bias, a corrected p-value of < 0.05 was accepted as significant.

7.2.9 Statistical analysis

Statistical analyses were carried out using GraphPad Prism (version 10.42). Normality testing and ROUT outlier testing was performed on each dataset. Changes in disc height over time were evaluated using a two-way ANOVA with Tukey's post-hoc tests. Biochemical differences were analysed using Brown-Forsythe and Welch ANOVA with Dunnett's post-hoc testing. Immunohistochemical differences were established using a one-way ANOVA followed by Tukey's post-hoc test with data for these tests displayed as mean ± standard deviation. For glucose and lactate assays, differences were assessed with a Kruskal-Wallis test followed by Dunn's multiple comparisons test, with data displayed as median ± interquartile range. Each disc was considered as being an experimental unit and is identified as an individual datapoint, and statistical significance denoted as $p < 0.05$.

7.3 Results

7.3.1 Radiographic assessment of disc height demonstrated trending increases post-cell delivery

To fully assess the changes occurring at each disc level the DHI was evaluated as a measure of the full disc, alongside measurements of the ventral, dorsal, and central regions to distinguish preferential height loss that may occur. These measurements were assessed at each point of the study, at Week 0, pre-degeneration induction, Week 8 where treatments were delivered, and Week 24 prior to euthanasia. DHI was mildly affected by the induction of degeneration, likely due to the low cABC doses utilised in this study. A restorative trend was identified in the DC and miRNA-NP group at the study endpoint compared to the degeneration at Week 8 (Fig. 7.2A, $p = 0.097$, and $p = 0.104$, respectively). For all other groups DHI returned to that of the pre-degeneration levels or exceeded them in the case of the untouched healthy control.

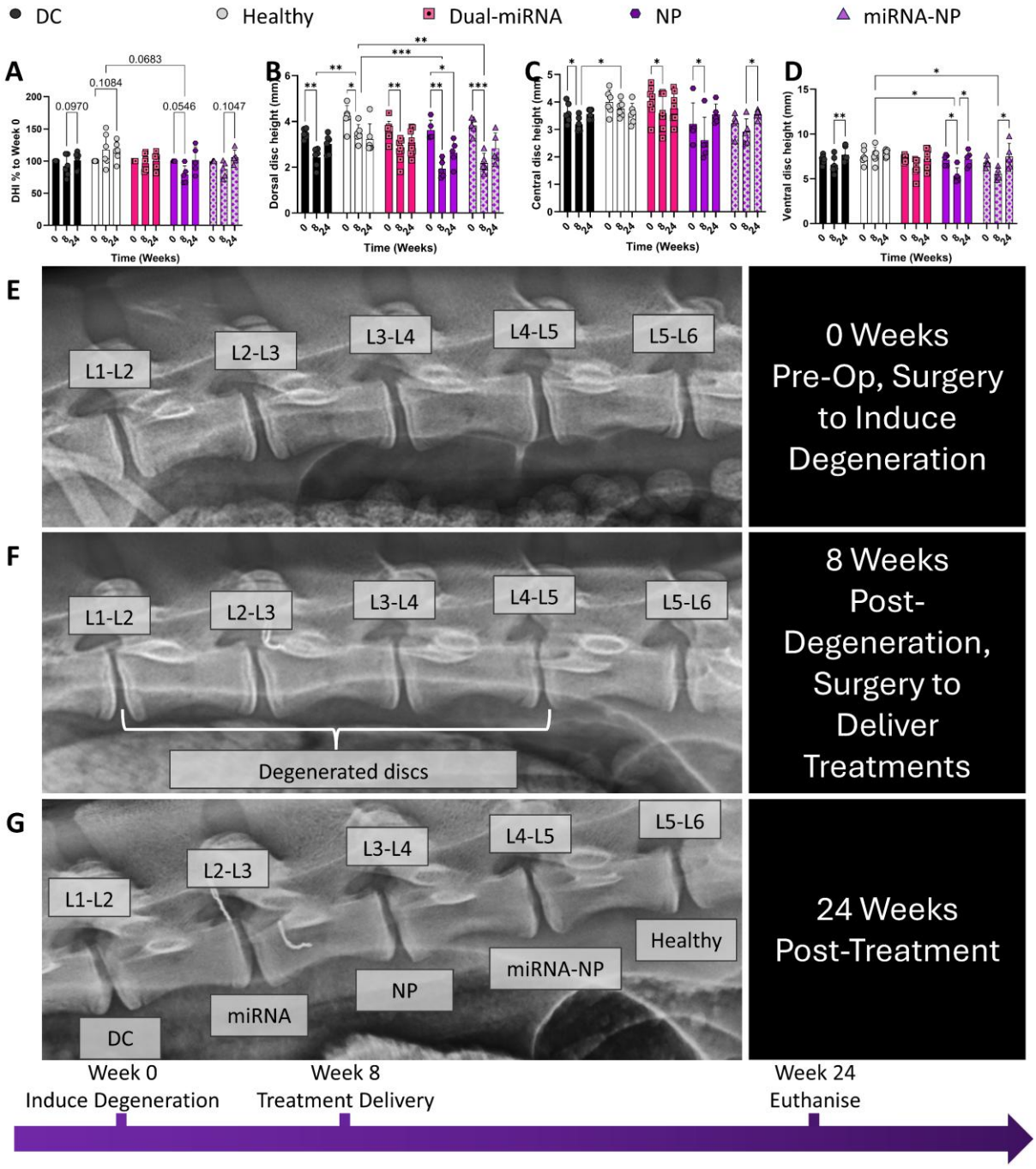

Figure 7.2 Quantitative disc height analysis and representative in vivo radiographs throughout study. (A) Percentage change in disc height index (DHI) calculated from measurements taken at Weeks 0, 8, and 24. Regional measurements are shown for (B) dorsal (C) central and (D) ventral regions. (E-G) Representative radiographs acquired during the study period. * $p < 0.05$, ** $p < 0.01$, *** $p < 0.001$, indicates statistical significance, $N \geq 5$.

Region-specific analysis revealed more pronounced changes with the dorsal region exhibiting the most severe degenerative. At the Week 24 endpoint, none of the groups showed

restoration of disc height in this region (Fig. 7.2B). Dorsal disc height was significantly reduced at Week 24 for NP ($p = 0.042$). With respect to central disc height, the healthy, dual-miRNA, and NP groups saw significant decreases following degeneration induction (Fig. 7.2C, $p \leq 0.05$ for all), with the miRNA-NP demonstrating a significant increase at Week 24 when compared to Week 8 (Fig. 7.2C, $p = 0.032$). Ventral disc height was restored by Week 24 for healthy, NP, and miRNA-NP treatments (Fig. 2D, all $p \leq 0.05$). Each group was also plotted separately in Figure 7.3 to illustrate changes in DHI and regional variations across the three study periods.

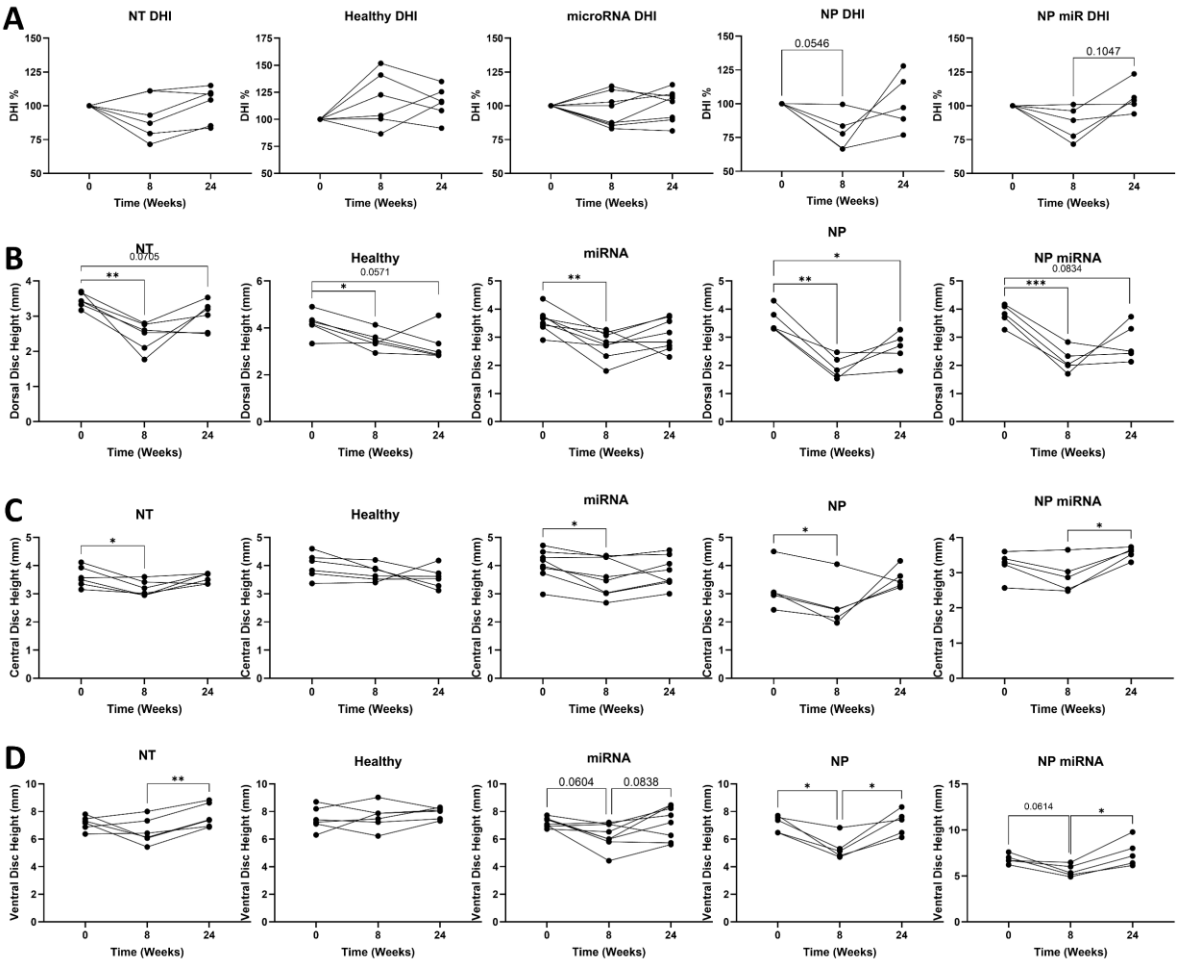

Figure 7.3 All radiographic quantifications plotted per group. (A) Disc height index (DHI), (B) Dorsal (C) Central and (D) Ventral measurements for each treatment group across the three radiographic imaging timepoints. Week 0: initiation of study and cABC-induced degeneration. Week 8: treatment delivery. Week 24: study endpoint. The healthy control group did not undergo cABC treatment and served as an untouched control. Each point represents an individual IVD, * $p < 0.05$, ** $p < 0.01$ indicates statistical significance, $N \geq 5$.

7.3.2 Qualitative assessment of IVDs by MRI

A representative MRI image was acquired at the study endpoint, to allow for qualitative evaluation of IVD hydration. On T2-weighted images, hydration, reflected by hyperintense signal was most prominent in the dual-miRNA and healthy discs in the dorsal view, with comparatively reduced yet detectable regions in the NP group (Fig. 7.4A, white arrows). A similar pattern was observed in the sagittal plane, where the dual-miRNA and healthy discs again exhibited higher T2 signal intensity, while only limited focal hyperintensity was present in the DC group (Fig. 7.4B). Structural irregularities indicative of disc disruption and adjacent bony changes were observed in the miRNA-NP and DC groups (Fig. 7.4A, red arrows). In these regions, decreased T2 signal intensity was observed, suggesting reduced hydration and potential degenerative changes. Additionally, hypointense signal along the endplate on the T1-weighted image of the miRNA-NP may indicate endplate alterations (Fig. 7.4C, yellow arrow). However, definitive interpretation would require further imaging and analysis in a larger cohort.

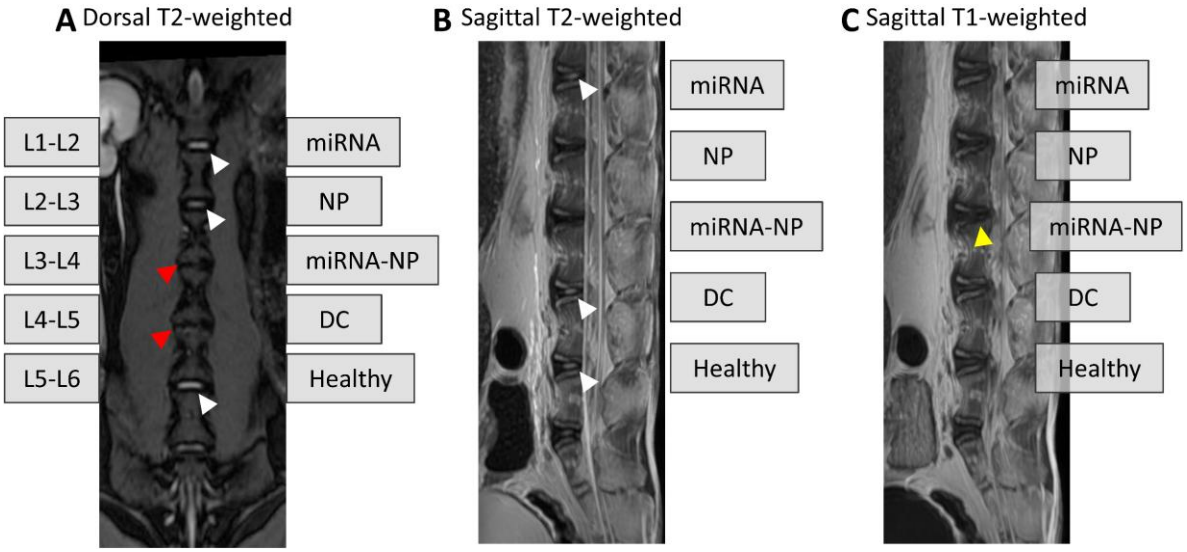

Figure 7.4 Representative magnetic resonance imaging (MRI) scan obtained at the study endpoint (Week 24). (A) Dorsal T2-weighted image, (B) Sagittal T2-weighted image and (C) Sagittal T1-weighted image.

7.3.3 Cell delivery negatively impacts cellularity and metabolic activity

Biochemical assessment of DNA content revealed a significant increase in DNA following dual-miRNA treatment compared to the healthy control (Fig. 7.5B, $p = 0.016$). The miRNA-NP treated group showed a trend toward increased DNA content, although this did not reach statistical significance (Fig. 7.5B, $p = 0.062$). Histological grading was performed according to the

methodology described by Lee et al, where higher scores indicate a greater degree of degeneration.[334] The combined total histological score was significantly increased in NT, NP, and miRNA-NP groups when compared to the healthy control (Fig. 7.5C, p = 0.01, p = 0.002, and p = 0.003, respectively). Similarly, NP cellularity scores demonstrated significantly greater degeneration in the NT, NP, and miRNA-NP groups relative to both the healthy control (p = 0.0007, 0.002, and <0.0001 Healthy vs, NT, NP, miRNA-NP, respectively) and dual-miRNA treatment (p = 0.013, 0.031, and 0.0004, dual-miRNA vs NT, NP, miRNA-NP, respectively) (Fig. 7.5D). These findings are supported by the presence of large cell clusters indicated by black arrows (Fig. 7.5A). To evaluate metabolic changes associated with treatment, glucose and lactate concentrations were measured in digested NP tissue. Interstitial glucose levels were significantly reduced in the miRNA-NP group compared to the dual-miRNA group (Fig. 7.5E, p = 0.022). Conversely, lactate concentrations were significantly elevated in the miRNA-NP group (Fig. 7.5F, p = 0.015).

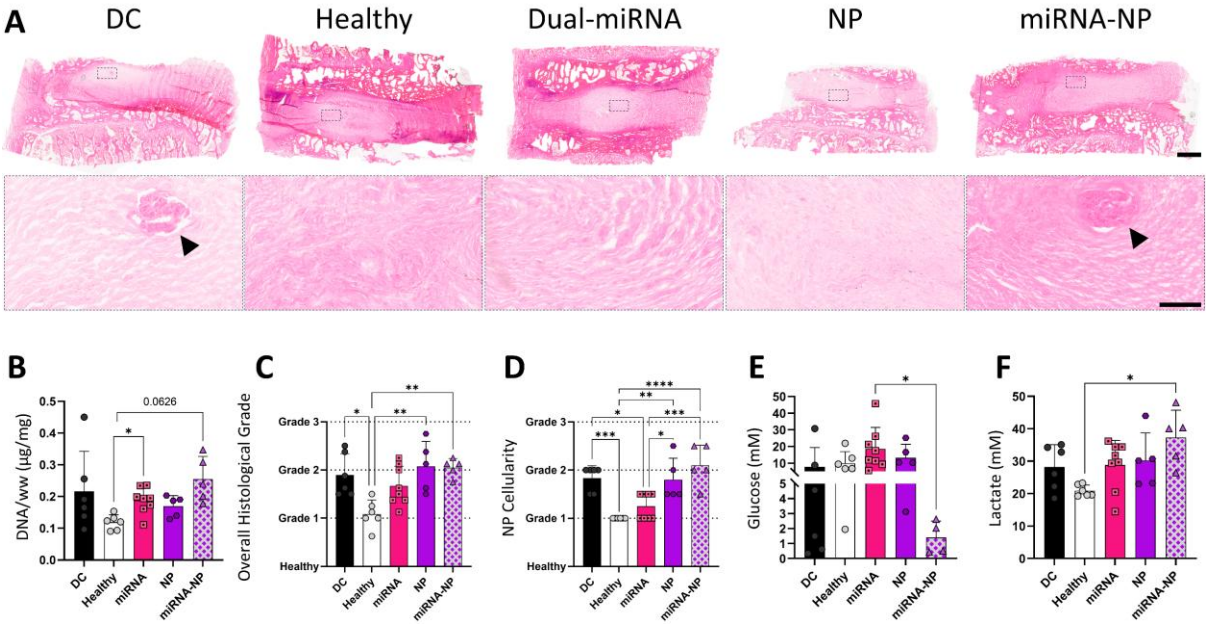

Figure 7.5 Evaluation of cellularity and metabolic activity by histological and biochemical analyses. (A) Representative haematoxylin and eosin (H&E) staining of mid-sagittal sections. (B) Biochemical quantification of DNA content normalised to tissue wet weight (ww, µg/mg) in nucleus pulposus (NP) tissue. (C) Overall histological grade and (D) NP cellularity grading. Quantification of interstitial (E) glucose (mM) and (F) lactate concentrations (mM). Black arrows indicate cell clusters associated with degenerative changes in cellularity. Scale bars are 2 mm for whole disc and 300 µm for insets. * $p < 0.05$, ** $p < 0.01$, *** $p < 0.001$, **** $p < 0.0001$, indicates statistical significance, $N \geq 5$.

7.3.4 Dual-miRNA delivery enhances proteoglycan extracellular matrix constituents

Degenerative changes in the IVD are characterised by depletion of upon proteoglycan constituents within the ECM. Therefore, restoration of these components is a key therapeutic objective. Total sGAGs were quantified biochemically from the NP tissue. In comparison to the healthy control, sGAG content was significantly lower in the miRNA-NP treatment group (Fig. 7.6F, $p = 0.016$), while NP only groups demonstrated a downward trend that did not reach statistical significance (Fig. 7.6F $p = 0.104$). This finding was consistent with reduced Alcian blue staining intensity in the cell-treated groups, particularly when compared to the healthy control (Fig. 7.6A). The early matrix-associated marker SOX9 was evaluated by immunofluorescence. Dual-miRNA treatment significantly upregulated SOX9 expression compared to NP delivery alone (Fig. 7.6B & C, $p = 0.006$) and showed a strong upward trend relative to DC, Healthy, and miRNA-NP (Fig. 7.6B & C, $p = 0.058$, 0.0501, 0.102, respectively). Expression of the later-stage matrix marker aggrecan was significantly upregulated following dual-miRNA treatment compared to all other treatment groups (Fig. 7.6D & E, $p \leq 0.01$ for all comparisons). Collectively, these changes suggest a shift towards matrix anabolism following dual-miRNA delivery, whereas NP cell delivery (with or without transfection) appears to have had no beneficial effect in restoring matrix composition. Histological grading revealed no significant changes in NP matrix or CEP structural scores (Fig. 7.6G & H), although a high degree of donor-to-donor variability was observed.

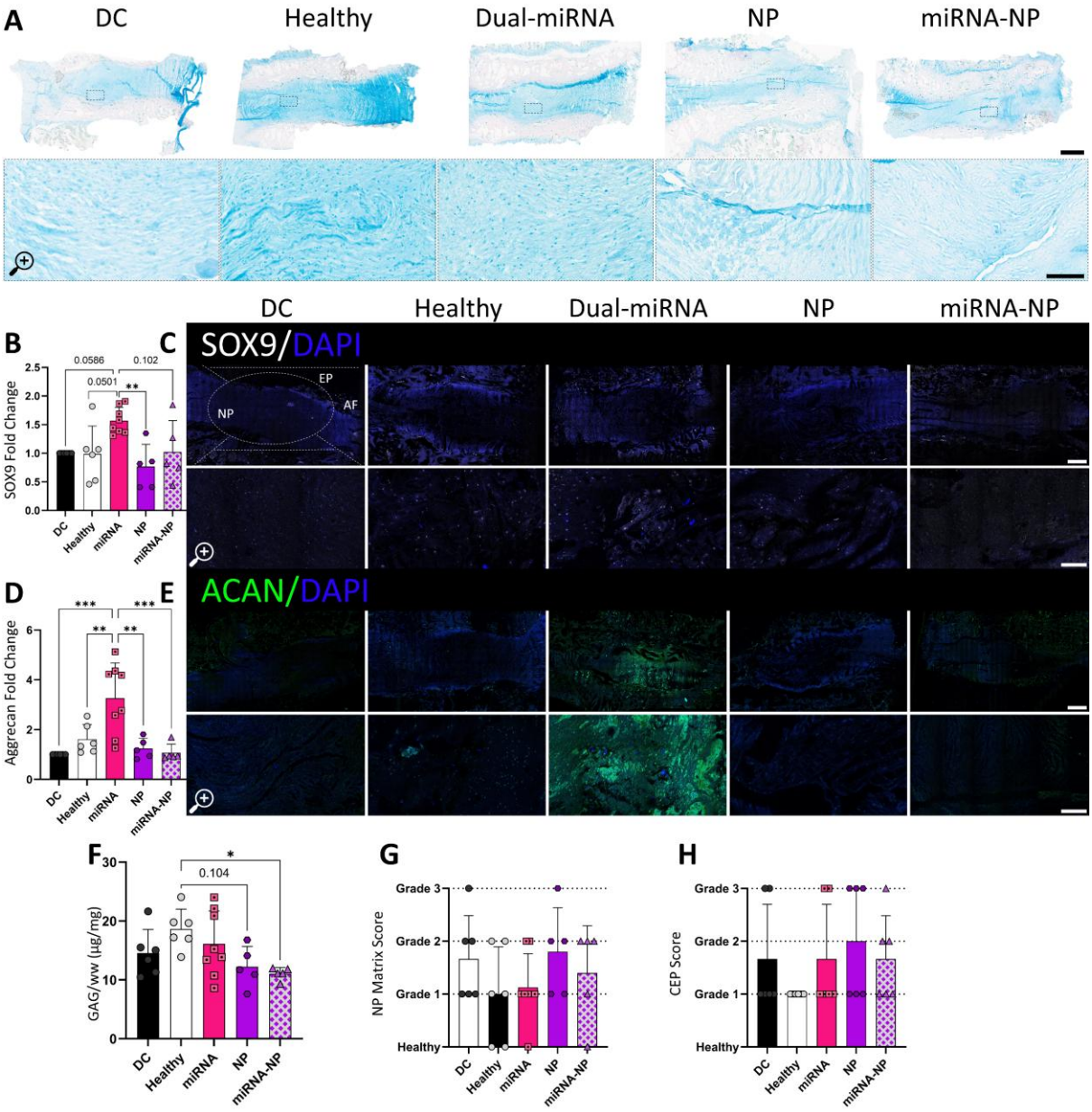

Figure 7. 6 Quantification of proteoglycan matrix constituents in nucleus pulposus (NP) tissue using histological, immunofluorescent, and biochemical analyses. (A) Representative Alcian blue staining for glycosaminoglycans. (B & C) Semi-quantitative immunofluorescence and representative images of SOX9 and (D & E) aggrecan. (F) Biochemical quantification of sulphated glycosaminoglycans, normalised to tissue wet weight (ww, µg/mg). (G) Histological scoring for NP matrix and (H) cartilage endplate (CEP) structure. Scale bars are 2 mm for whole disc and 300 µm for insets and magnified images. Immunofluorescence data was normalised to the degenerated control (DC), AF: Annulus fibrosus, * $p < 0.05$, ** $p < 0.01$, *** $p < 0.001$, indicates statistical significance, $N \geq 5$.

7.3.5 Alterations in collagen composition and structure following cell delivery

Changes in collagen composition can inform a switch towards a more fibrotic and degenerative phenotype. Therefore, collagen content and structural organisation were evaluated both biochemically and histologically (Fig. 7.7). Total collagen content within the NP tissue was significantly increased following NP delivery (Fig. 7.7B, $p = 0.041$). Histological assessment of AF demonstrated a trend toward greater structural disruption in the DC and NP groups to the healthy control (Fig. 7.7C, $p = 0.102$ and $p = 0.059$). The integrity of the NP and AF boundary was significantly more compromised in NT, NP, and miRNA-NP groups relative to the healthy control (Fig. 7.7D, $p = 0.037$, $p = 0.033$, and $p = 0.033$, respectively). Collectively, these findings suggest a shift toward a more fibrotic matrix architecture, consistent with a degenerative response following cell delivery.

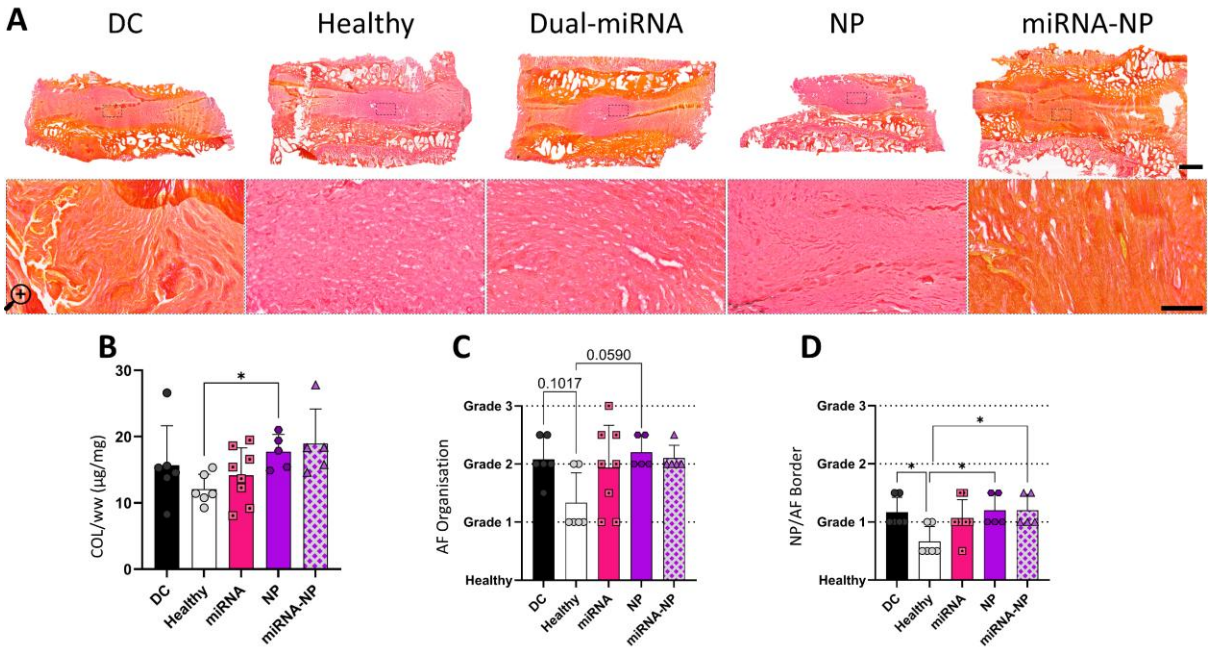

Figure 7. 7 Histological and biochemical assessment of collagen within the intervertebral disc (IVD). (A) Representative picrosirius red staining of mid-sagittal sections. (B) Biochemical quantification of total collagen content in the nucleus pulposus (NP) tissue, normalised to tissue wet weight (ww, µg/mg). Histological scoring of (C) Annulus fibrosus (AF) organisation and (D) integrity of the NP/AF interface. Scale bars are 2 mm for whole disc and 300 µm for insets, * $p < 0.05$, indicates statistical significance, $N \leq 5$.

All hydration and biochemical data are presented below in Figure 7.8, with the total overall content, and normalisations by wet weight (ww), dry weight (dw), and DNA.

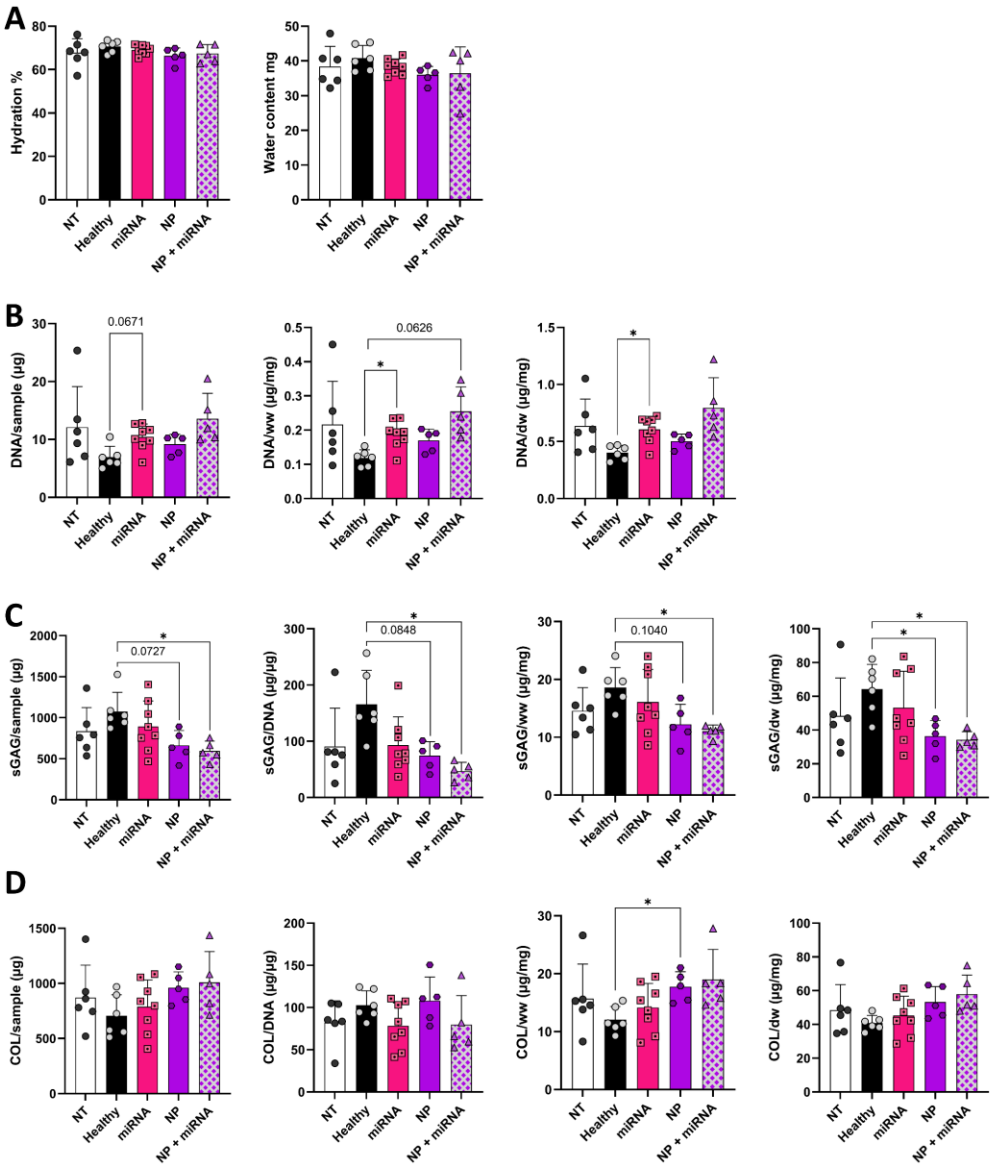

Figure 7. 8 Biochemical measurements from nucleus pulposus (NP) tissue. (A) hydration (%), (B) DNA content , (C) sulphated glycosaminoglycan content (sGAG), and (D) collagen (COL). ww: wet weight, dw: dry weight, * p , 0.05, indicates statistical significance, N ≤ 5.

7.3.6 Cell delivery increases expression of catabolic enzymes and pro-inflammatory cytokines compared to healthy control and dual-miRNA treatment

Effective regeneration of the IVD requires suppression of key mediators within the degradative cascade. Protein expression of catabolic enzymes and pro-inflammatory cytokines was therefore evaluated by immunofluorescence staining. MMP13, a collagenase commonly upregulated during disc degeneration, was significantly downregulated in both the healthy and dual-miRNA groups compared to NP cell delivery (Fig. 7.9A & B, p = 0.037 and p = 0.013, respectively).

Similarly, expression of the aggrecanase ADAMTS5 (Fig. 7.9C & D) was substantially reduced in the healthy and dual-miRNA groups when compared to both NP ($p = 0.039$ and $p = 0.018$ Healthy vs NP and miRNA-NP, respectively) and miRNA-NP treatments ($p = 0.039$ and $p = 0.018$ dual-miRNA vs NP and miRNA-NP, respectively).

Moreover, proinflammatory cytokine dysregulation plays a central role in initiating and sustaining the degenerative cascade, particularly through upregulation of TNF-α and IL-1β. Both the healthy and dual-miRNA groups exhibited significantly reduced expression of these cytokines compared to the DC control (Fig. 7.9E & F, $p = 0.006$ and $p = < 0.001$, respectively). Furthermore, cell delivery exacerbated TNF-α protein expression, with expression significantly upregulated in the NP cell treatment group in comparison to dual-miRNA treatment (Fig. 7.9E & F, $p = 0.028$). Similarly, miRNA-NP cell transplantation resulted in overexpression of TNF-α compared to both healthy and dual-miRNA groups (Fig. 7.9E & F, $p = 0.011$ and $p = < 0.001$, respectively). A comparable trend was observed for IL-1β expression. NP cell significantly increased IL-1β expression relative to both healthy and dual-miRNA groups (Fig. 7.9G & H, $p = 0.026$ and $p = 0.029$, respectively). Similarly, miRNA-NP treatment resulted in overexpression of IL-1β compared with healthy and dual-miRNA groups (Fig. 7.9G & H, $p = 0.02$ and $p = 0.02$, respectively). Taken together, these findings indicate that cell transplantation may potentiate a catabolic and pro-inflammatory response, in contrast to the suppressive effects observed following dual-miRNA delivery.

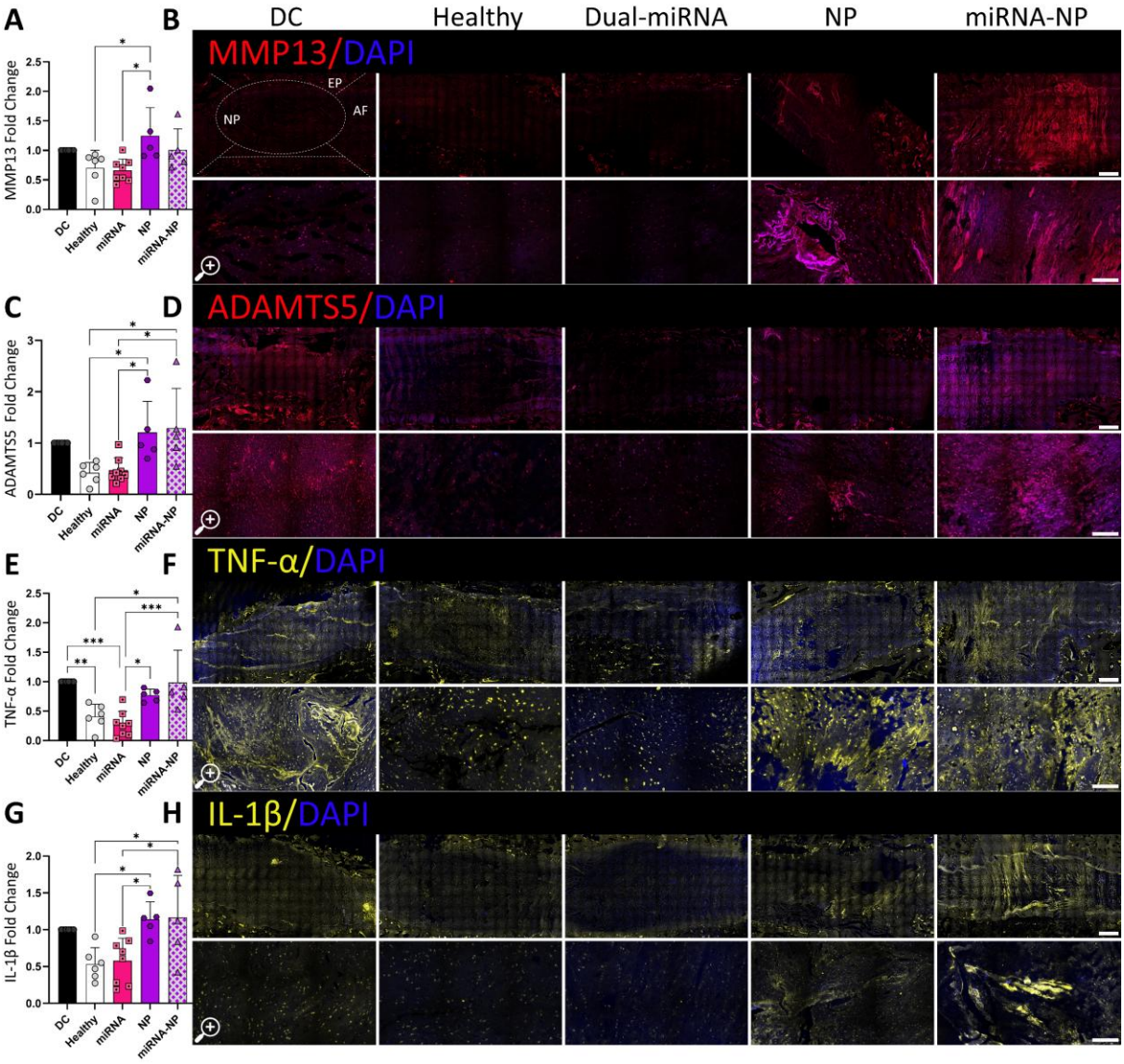

Figure 7. 9 Semi-quantitative immunofluorescent assessment of catabolic and pro-inflammatory marker expression in nucleus pulposus (NP) tissue. Quantification and representative images of (A & B) MMP13, (C & D) ADAMTS5, (E & F) TNF-α, and (G & H) IL-1β. All values are normalised to the degenerated control (DC). Scale bars are 2 mm for whole disc and 300 μm for and magnified images. * $p < 0.05$, ** $p < 0.01$, *** $p < 0.001$, indicates statistical significance, $N \geq 5$.

7.3.7 Biochemical, matrix, and inflammatory markers correlate with histological grading of intervertebral disc degeneration

Associations between biochemical parameters, histological grading, and semi-quantitative immunofluorescence measurements were analysed using Pearson's correlation coefficient, with

results summarised in Figure 7.10. Glucose concentration exhibited a weak but statistically significant negative correlation with total histological score (Fig. 7.10A, r = -0.156, p = 0.041). In contrast, lactate tissue concentrations demonstrated multiple significant associations. Lactate levels were moderately positively correlated with DNA content (r = 0.648, p = 0.0001), collagen content (r = 0.500, p = 0.005), and histological score (r = 0.367, p = 0.046) (Fig. 7.10B). Additionally, lactate concentration showed a moderate negative correlation with total sGAG levels (r = -0.508, p = 0.004) (Fig. 7.10B).

Significant associations were also identified among matrix-related biochemical markers. DNA content showed a moderate negative correlation with sGAG levels (Fig. 7.10C, r = -0.406, p = 0.026). Similarly , sGAG content was moderately negatively correlated with both collagen content (Fig. 7.10C, r = -0.556, p = 0.001), and total histological score (Fig. 7.10D, r = -0.502, p = 0.005). In contrast, moderate positive correlations were observed between DNA and collagen content (Fig. 7.10C, r = 0.366, p = 0.047), as well as between collagen content and histological score (Fig. 7.10D, r = 0.468, p = 0.009).

No significant correlations were observed between the expression of the matrix-associated markers, SOX9 and aggrecan and histological score (Fig. 7.10E). However, catabolic and pro-inflammatory markers quantified from immunofluorescence staining demonstrated significant positive relationships with increasing degeneration severity. The matrix degrading enzymes MMP13 (Fig. 7.10F, r = 0.491, p = 0.006) and ADAMTS5 (Fig. 7.10F, r = 0.585, p = 0.0007) displayed moderate positive correlations with histology score. Similarly, TNF-α (Fig. 7.10F, r = 0.522, p = 0.003) and IL-1β (Fig. 7.10F, r = 0.590, p = 0.0006) were moderately positively correlated with more advanced grades of degeneration.

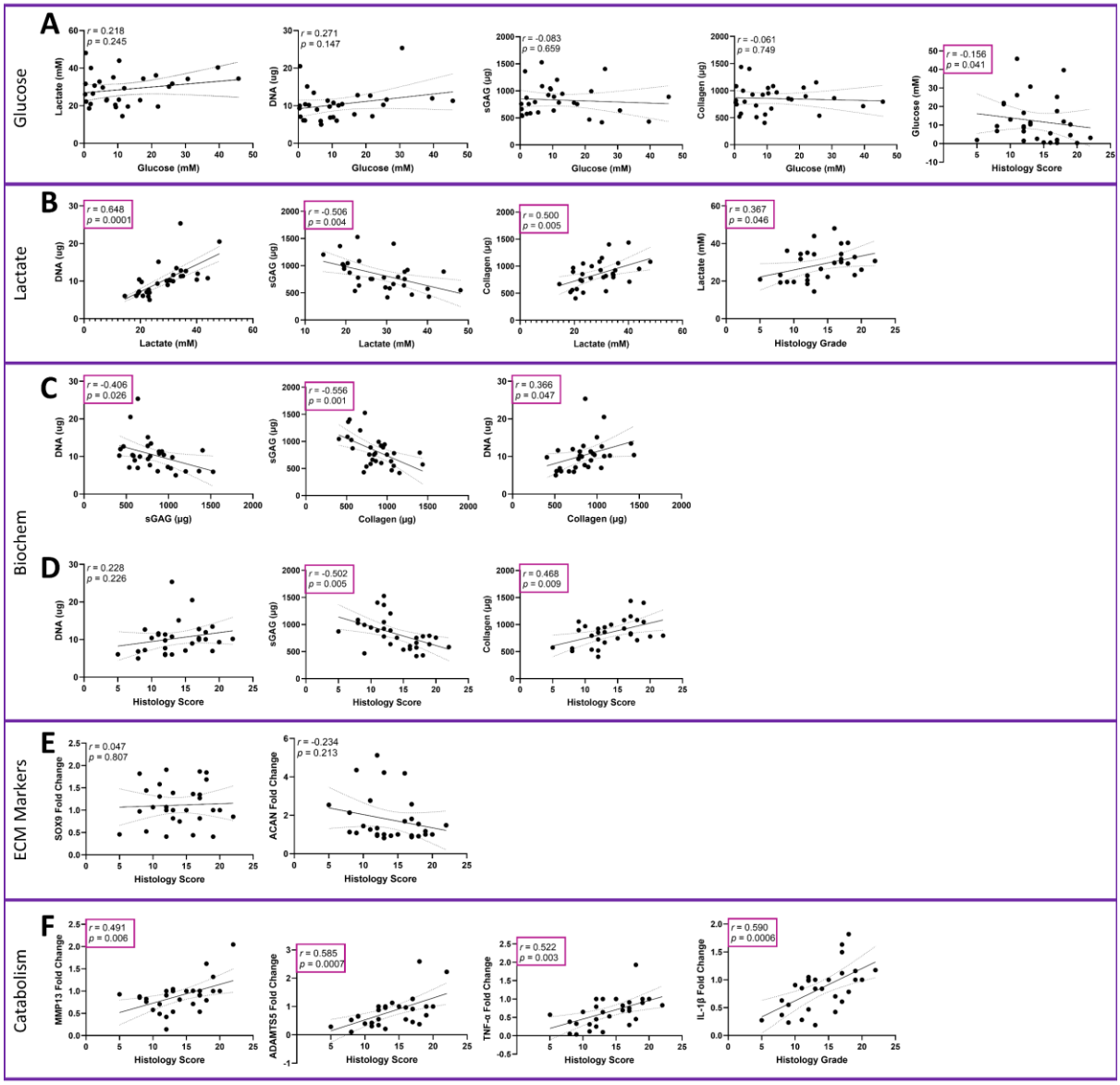

Figure 7. 10 Correlation analysis between biochemical, histological score, and semi-quantitative immunofluorescence measurements of catabolic and pro-inflammatory markers in nucleus pulposus (NP) tissue. Correlations are shown for (A) glucose concentration, (B) lactate concentration, (C & D) matrix related biochemical parameters, (E) semi-quantitative immunofluorescent analysis of extracellular matrix (ECM) markers, and (F) catabolic and pro-inflammatory markers. Boxes denote statistically significant correlations; dotted lines represent 95% confidence intervals.

7.3.8 Hierarchical clustering revealed distinct transcriptional profiles among treatment groups

Hierarchical cluster analysis was performed on all differentially expressed genes across treatment groups, with row-wise scaled (z-score normalised) (Figure 7.11A). To further interrogate genes of particular relevance to IVD biology, a curated panel of 70 genes was selected for focused analysis. These genes were categorised into four functional groups based on their roles within the disc: ECM/Anabolism, Catabolism, Inflammation, and Stress & Pain (Fig. 7.11B). Heatmap visualisation revealed that the DC and miRNA-NP groups exhibited comparatively elevated expression across genes within all four functional categories. In contrast, the healthy and dual-miRNA groups displayed reduced relative expression of genes associated with catabolism, inflammation, and stress/pain responses, consistent with trends observed in immunofluorescence analyses. Notably, these groups also displayed lower relative expression of ECM- and anabolism-related genes compared to the DC and miRNA-NP groups.

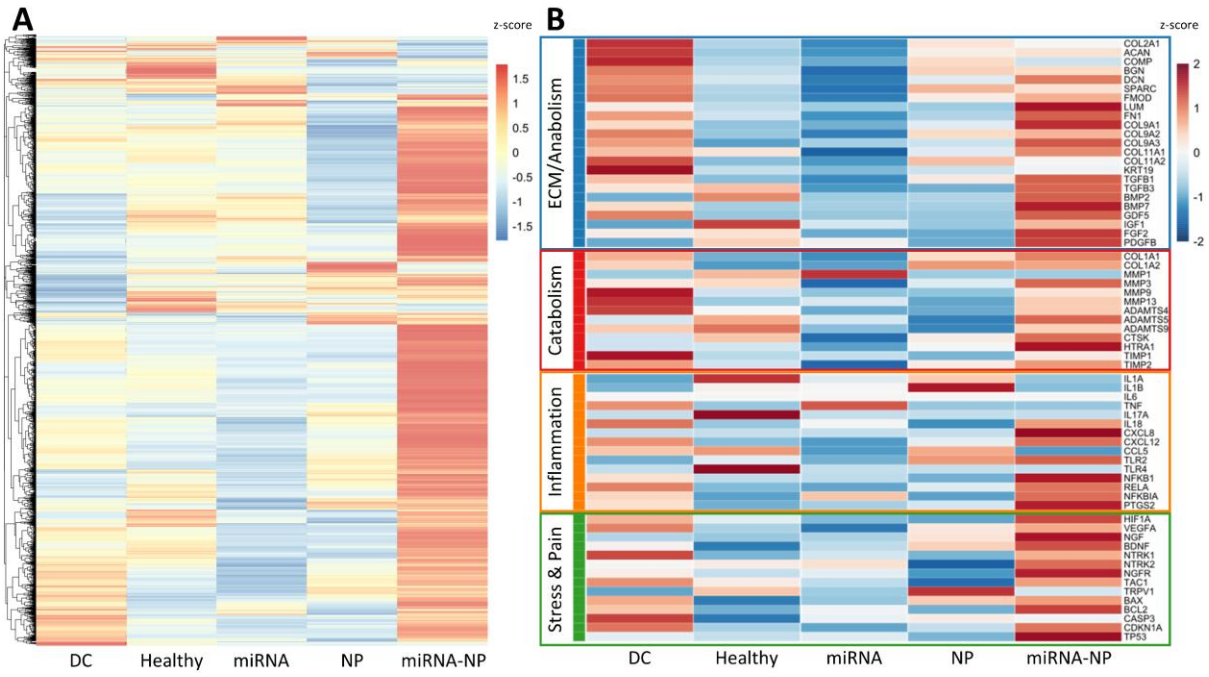

Figure 7. 11 Heatmaps showing expression patterns across (A) all groups and (B) a set of 70 intervertebral disc (IVD) related genes, functionally classified into extracellular matrix (ECM)/anabolism, catabolism, inflammation, and stress & pain categories. Gene expression values were normalised and scaled per gene (row z-score) before plotting. Heatmap colours indicate the z-scored expression relative to the mean of each group. DC: degenerated control.

7.3.9 Differential gene expression and pathway enrichment reveal divergent treatment responses

To directly compare the five experimental groups, predicted or poorly characterised genes were first removed. Genes showing significant differential expression (adjusted p-value < 0.05, |log2FC| > 1) were visualised as a heatmap (Fig. 7.12A). Several metabolism-related genes (ATP5A1, MDH2, TKT, TPI1, PGAM1, PHB2, GALE, GUKI) were differentially expressed, with the most pronounced effect being their downregulation in the dual-miRNA group relative to DC. In contrast, following cell delivery, many of these metabolic genes were strongly upregulated, suggesting metabolic adaptation and shifts in energy requirements depending on the treatment. Inflammatory genes also exhibited differential expression. NFATC1, CEBPD, ARID5A, SPP1, and PRDX2 were significantly reduced in the dual-miRNA versus DC group but upregulated in NP and miRNA-NP groups compared to dual-miRNA. Interestingly, LGALS1, S100A4, S100A13, and VEGF-b were significantly decreased in dual-miRNA relative to DC. Contrastingly they were overexpressed when comparing cell delivery to dual-miRNA (LGALS1, S100A4, S100A13: NP and miRNA-NP vs miRNA, VEGF-b: miRNA-NP vs miRNA), highlighting treatment-specific transcriptional responses.

To further explore potential treatment responses, significantly enriched GO pathways were analysed (Fig. 7.12B & C), revealing distinct enrichment patterns across groups. Among the upregulated pathways, two comparisons, NP vs dual-miRNA and miRNA-NP vs dual-miRNA showed significant enrichment. These pathways were primarily associated with membrane dynamics and trafficking, including cellular membranes, the endomembrane system, and vesicles, reflecting activation of cellular stress and proteostatic mechanisms. In the same comparisons, inflammatory and stress-response pathways were also enriched, including proteasome complex, peptidase complex, endopeptidase complex, regulation of intracellular signal transduction, and response to stimulus. Metabolic disruption pathways demonstrated consistent enrichment patterns, with ATP production, mitochondrial function, and nucleotide metabolism being upregulated. Conversely, in dual-miRNA vs DC and NP vs DC comparisons, similar membrane-related systems particularly involving the endoplasmic reticulum were significantly downregulated, alongside suppression of proteasome core complex and peptidase complexes. Metabolic pathways showed an opposing trend, with ATP and mitochondrial processes significantly downregulated.

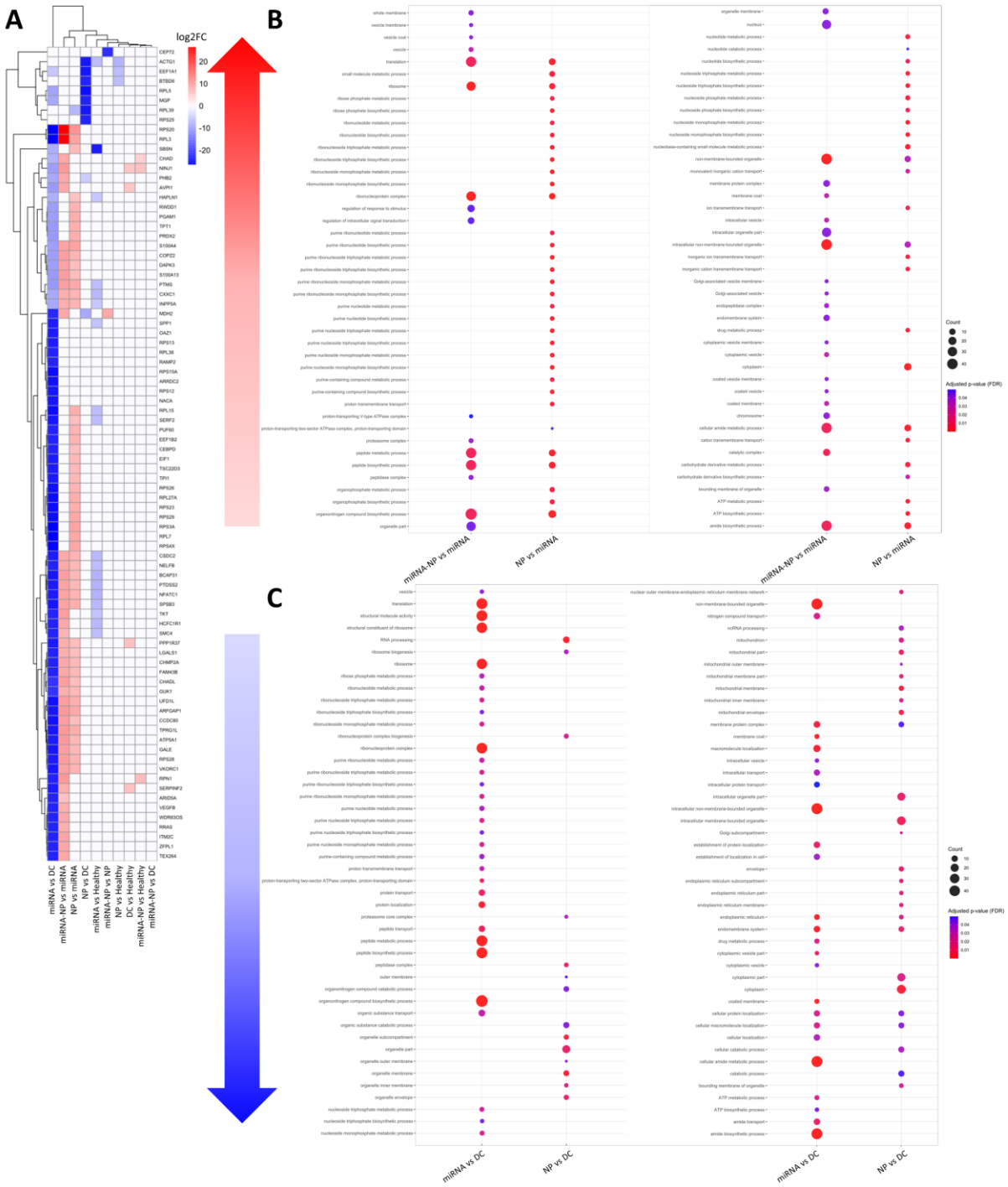

Figure 7. 12 Differential gene expression and functional pathway enrichment across treatment groups. (A) Heatmaps of genes showing significant differential expression across all group comparisons. (B) Significantly enriched upregulated gene ontology (GO) pathways in miRNA-NP vs dual-miRNA and NP vs dual-miRNA. (C) Significantly enriched downregulated GO pathways in dual-miRNA vs DC and NP vs DC. DC: Degenerated control.

7.4 Discussion

Despite its central role in the progression of LBP, IVD degeneration lacks effective treatments, particularly those to target the homeostatic dysregulation that augment the degradative cascade. As LBP prevalence continues to rise there is a pressing need for early-stage interventions that mitigate degeneration. Injectable therapies have therefore gained increasing attention, with miRNA and cell-based approaches offering the potential to dampen the immune response while stimulating the resident cell population. In the context of cell transplantation, an additional objective is to restore the local disc cell population that has been diminished due to degeneration. Consequently, this study aimed to explore the dual delivery of FLR-149-5p mimic and miRNA-221-3p inhibitor alone, and also to assess the delivery of NP cells, transfected or non-transfected, in a goat model of mild IVD degeneration. We found that the introduction of cells induced a pronounced inflammatory and catabolic response, accompanied by metabolic disruption, and significantly enriched stress-associated pathways identified through mRNA sequencing. Furthermore, cell transplantation did not restore sGAG content and was associated with increased histological severity scores. Contrary to this, dual-miRNA delivery attenuated the catabolic and inflammatory response in comparison to the cell groups, while simultaneously demonstrating a strong trend towards the upregulation of ECM markers. Together, these findings implicate metabolic stress as a potential consequence of cell transplantation, whereas dual-miRNA delivery mitigated this response, highlighting its promise as a clinically relevant and translational therapeutic approach for early-stage IVD degeneration.

Consistent with previous work from our laboratory, the dual delivery of FLR-149-5p mimic and 221-3p inhibitor demonstrated a strong anti-catabolic and anti-inflammatory response. [241,242] This action is crucial in suppressing the amplified catabolic and inflammatory milieu that is characteristic of IVD degeneration. Dual-miRNA delivery reduced TNF-α expression compared with the DC control as well as NP cell or miRNA-NP transfected cell delivery, highlighting its functionally relevant therapeutic potential. As a key mediator of inflammation in the IVD, TNF-α drives degenerative changes by upregulating cytokines, recruiting ECM-degrading factors, such as ADAMTS-4 and -5, and MMPs-1, -2, -3, -4, -13, and -14, and inducing cellular senescence.[194,335,336] Similarly, IL-1β, which we found to be significantly downregulated in the dual-miRNA compared to both cell groups, acts a key regulator of inflammation and progressive degeneration, promoting ECM-degradative factors. [193,337] Among the dual-miRNA cargo, miRNA-149-5p in particular has proven effective at suppressing the inflammatory response. An in vivo wound healing study showed that IL-1α, IL-1β, and IL-6 protein levels were markedly downregulated in miRNA-149 transfected wounds, even in the presence of a TNF-α challenge. [289] Recently, inhibition of miRNA-149-5p was found to enhance inflammatory signalling through the Nod-like receptor Pyrin domain containing

1 (NLRP1) activation in tert-Butyl hydroperoxide (TBHP)-challenged NP cells. [290] NLRP1, a key component of the inflammasome responsible for triggering IL-1β expression,[43] may play a mechanistic role in the IL-1β suppression observed in this study. Moreover, given the strong correlation identified between higher TNF-α and IL-1β expression and increasing degeneration grade, dual-miRNA delivery may hold significant promise as an anti-inflammatory strategy.

Alongside effective suppression of inflammatory mediators, downregulating catabolic enzymes could promote IVD restoration and help reverse the degenerative cascade. The metalloproteinases, MMP13 and ADAMTS5 are of particular interest due to their central role in degrading the native ECM, and their association with progressively severe degeneration in patients.[39,221] We observed a significant reduction in MMP13 protein expression in the dual-miRNA group compared with the NP group. Furthermore, ADAMTS5 was significantly downregulated in dual-miRNA samples relative to both cell delivery groups, highlighting the anti-catabolic effect previously demonstrated with dual-miRNA delivery in rat ex vivo organ cultures. [241,242] Although MMP13 and ADAMTS5 induction has been reported in large animal models of IVD degeneration,[149,331] their therapeutic inhibition, particularly in NP tissue, remains less explored. Given their central role in perpetuating degeneration, suppressing MMP13 and ADAMTS5 is critical, and the dual-miRNA results observed here are particularly promising as a therapeutic strategy.

Alongside the reductions to protein expression of critical catabolic and inflammatory markers, transcriptomic analysis revealed distinct inflammatory gene expression profiles across treatment groups. Genes associated with catabolism and inflammation demonstrated a pattern of upregulated z-scores in the DC and miRNA-NP groups, whereas dual-miRNA delivery exhibited the opposite trend. Certain genes were downregulated in the dual-miRNA group relative to DC but were upregulated in both NP and miRNA-NP groups compared to the dual-miRNA group, indicating a divergent biological response. Among these, *NFATC1*, a TNF-α-responsive regulator of cytokine expression linked to increased degeneration severity in human IVD tissue samples, [338] was significantly downregulated by dual-miRNA delivery compared to DC. [339] *CEBPD* was similarly implicated, with its silencing shown to reduce MMP13, TNF-α, and IL-1β expression in a rat model of IVD degeneration. [340] Reduced expression of *LGASLS1,* a modulator of NF-κB signalling associated with increasing severity of IVD degeneration was also observed.[341] Collectively, the pronounced downregulation of these genes in dual-miRNA treatment versus DC, followed by their significant upregulation in NP and miRNA-NP relative to dual-miRNA, supports dual-miRNA as an anti-inflammatory treatment. Alongside the concomitant reduction in catabolic and inflammatory protein markers, these findings reinforce the therapeutic promise of dual-miRNA delivery for attenuating inflammatory signalling in mild IVD degeneration.

Evidence of metabolic perturbation was observed within the NP tissue region following delivery of miRNA-NP cells, with both glucose and lactate concentrations significantly altered compared to healthy controls. This was accompanied by a marked reduction in NP cellularity on histological grading after NP and miRNA-NP delivery, indicating disruption of resident cell homeostasis. Notably, glucose levels were negatively correlated with worsening histological scores, whereas lactate levels exhibited a positive correlation, reinforcing the association between metabolic imbalance and degenerative severity. The administered dose of 5.5 x 10^6 cells was selected based on predictive modelling [287] and a previous in vivo study in goat, [342] which suggested that while nutrient concentrations may decline slightly compared to a healthy disc, it would not severely compromise the microenvironment. However, as glucose serves as the primary substrate for glycolysis in the avascular disc, even modest reductions in its availability may have significant consequences, as we report here. [343] In vitro, reductions in glucose levels have been shown to significantly decrease both NP cell viability and proteoglycan production.[344,345] Supporting these findings, transcriptomic analysis revealed significant upregulation of *GALE* in NP and miRNA-NP groups in comparison to dual-miRNA. *GALE* overexpression has been implicated in glucose homeostasis in the liver by impairing glucose tolerance,[346] consistent with the observed perturbation of glucose levels following miRNA-NP delivery. Collectively, these results suggest that introducing additional cells may increase metabolic demand within the limited-nutrient NP microenvironment, potentially creating a glucose deficit that exacerbates degenerative processes.

Lactate, the primary metabolic byproduct of glycolysis in the disc, accumulates readily, leading to acidification of the disc microenvironment, which can adversely affect disc health.[347] In vitro studies have demonstrated that reduced pH, directly associated with increased lactate production, [320] significantly impairs cell survival and matrix accumulation.[348] Similarly, lactate measurements in goat models of degeneration show significantly elevated levels in degenerated tissues compared to healthy controls, correlating with degeneration grade as determined by MRI.[349] These findings are consistent with our observations, as increased lactate concentrations coincided with higher histological grades following miRNA-NP delivery, and overall lactate levels were significantly correlated with degeneration severity. Transcriptomic analysis further supported these biochemical results. GO pathways related to ATP biosynthesis, mitochondrial function, and ribose phosphate metabolism were significantly enriched in both cell-treated groups compared to dual-miRNA treatment, indicating metabolic dysregulation and a shift in energy demands following cell delivery to the NP. Additionally, *MDH2*, a mitochondrial enzyme whose overexpression has been linked to cellular senescence,[350] was significantly upregulated in miRNA-NP groups relative to dual-miRNA and NP. Notably, *MDH2* was strongly downregulated in dual-miRNA groups compared to DC, further highlighting the divergent metabolic effects across treatment groups and reinforcing the shifts in metabolic requirements observed biochemically and histologically.

Beyond suppressing degradative pathways, injectable therapeutics also aim to restore ECM integrity, which is critical for rebuilding damaged IVD tissue. Contrary to this objective, both cell-treated groups exhibited downwards trends in sGAG content compared to healthy controls and marked downregulation of ECM markers SOX9 and aggrecan relative to dual-miRNA delivery. These reductions likely result from metabolic disruption following cell delivery, which may compromise matrix synthesis. Supporting this interpretation, GO analysis revealed significant enrichment of pathways related to the endomembrane system, vesicles, and membrane trafficking in NP and miRNA-NP groups compared to dual-miRNA treatment. This may indicate altered protein secretion and folding and potential impairment of proteostasis, a feature associated with progressive degeneration.[351] In contrast, dual-miRNA delivery promoted upregulation of SOX9 and aggrecan protein expression. Specifically, silencing miRNA-221-3p has been linked to increased ECM marker expression in chondrocytes and cartilage models.[352,353] In the IVD context, miRNA-221 inhibition was shown to protect CEP cells and strongly enhance aggrecan protein expression, [305] supporting its inclusion in this dual-miRNA strategy.

Cell transplantation to the IVD has demonstrated considerable preclinical promise,[19,20,275] however, the present findings indicate metabolic stress, catabolic disruption, decreased matrix marker expression and increased collagen disorganisation. One possible explanation is that degeneration induced by cABC administration may more closely resemble a chronic degenerative state rather than an acute injury model. Supporting this, Detiger et al reported that 0.25 U cABC followed by stromal vascular fraction (SVF) administration caused severe adverse inflammatory effects, evidenced by pronounced immune cell infiltration.[354] Interestingly, when degeneration was induced via partial nucleotomy, mimicking herniation, no adverse effects were observed following SVF delivery. Similarly, a prospective clinical study treating naturally occurring canine IVD degeneration with MSC-seeded collagen microcarriers reported no regenerative improvements on MRI. [355] A subsequent study from the same group injected autologous BMSCs in naturally degenerated discs; while no adverse effects were observed, regenerative outcomes were also not achieved. [356] Chronic IVD degeneration is characterised by a sustained inflammatory cascade and progressive ECM breakdown, Notably, cABC administration induces a cytokine response, and has been correlated with neuronal and inflammatory markers in goats. [149,357] In such a hostile microenvironment, transplanted cells may experience nutrient depreviation and heightened inflammatory stress, limiting their regenerative potential. In contrast, many of the most encouraging studies involving cell delivery target IVDs degenerated through mechanical disruption or injury,[133,358-360] suggesting that cell therapies may be more effective in acute or herniated pathologies, whereas chronically degenerated discs may require prior modulation of the inflammatory-metabolic milieu to support regenerative strategies.

Beyond establishing safety and biological efficacy, the translatability from bench to bedside is paramount. The most compelling findings from this preclinical evaluation position dual-miRNA as a potential injectable treatment for IVD degeneration. Compared to cell-based approaches, dual-miRNA offers several practical advantages that enhances clinical feasibility. Firstly, it eliminates the need for a viable regenerative cell source and avoids potential ethical concerns associated with cadaveric tissue use. The dual-miRNA cargo can be reproducibly manufactured and modified, providing a flexible therapeutic platform. Furthermore, it can be combined with adjunctive stimuli such as growth factor cocktails,[59,361] or incorporated into biomaterials or scaffolds.[184,229,256] Such combinatorial strategies may be particularly valuable in degenerative environments, where cell transplantation imposes metabolic stress. Incorporating regenerative cues that synergise with dual-miRNA could further enhance therapeutic efficacy and increase the clinical relevance of this approach.

Several limitations of this study should be acknowledged. First, comprehensive quantitative profiling of pro-inflammatory cytokines and catabolic enzymes would have strengthened comparisons with human clinical datasets. However, given the limited tissue yield from a single disc, priority was given to maximising outputs across biochemical and histological analyses, while adhering to the 3R principles to minimise animal numbers.[362] Second, the follow-up duration may have constrained the assessment of regenerative outcomes. Previous work involving in silico modelling predicted that restoration of sGAG content in the goat disc may require extended timeframes. [287] As dual-miRNA delivery has to the best of our knowledge not been previously evaluated in large animal models of IVD degeneration, there was no established to guide study duration. While the shorter timeframe was appropriate for an initial proof-of-concept, future studies extending beyond one year may better capture long-term matrix remodelling and functional recovery. Finally, the cell dose employed likely contributed to observed cellular perturbations. Although the selected dose was within ranges reported in the literature and did not elicit adverse effects in prior ex vivo organ culture experiments, the in vivo environment appears more sensitive to cellular loading. Future studies aiming for cell transplantation may benefit from reduced cell numbers, as exemplified by Discgenics, which adjusted from an initial preclinical cell dose of 10 $x10^6$ cells delivered intradiscally, to 3 x 10^6 and 6 $x10^6$ cells in their clinical trial (NCT03347708). [19]

In summary, dual-miRNA delivery in a goat model of mild IVD degeneration enhanced ECM marker expression while suppressing inflammatory and catabolic signalling. In contrast, NP and miRNA-NP cell transplantation induced metabolic perturbations and exacerbated degenerative features, emphasising the critical role of the microenvironment in regenerative interventions. Collectively, these results position dual-miRNA therapy as a promising molecular strategy for targeting the key pathological hallmarks of IVD degeneration.

7.5 Conclusion

This study provides the first evaluation of the safety and efficacy of dual-miRNA delivery in a large-animal model of mild IVD degeneration, demonstrating its ability to enhance ECM marker expression while suppressing catabolic and inflammatory signalling. In contrast, both NP and miRNA-transfected NP cell delivery were associated with metabolic perturbations, reduced matrix integrity, and exacerbation of degenerative features, highlighting the critical influence of the microenvironment in the context of cell-based therapies. Collectively, these results identify dual-miRNA therapy as a promising molecular strategy for targeting the key hallmarks of IVD degeneration, specifically inflammation, metabolic dysregulation, and ECM breakdown. By modulating resident cell behaviour without imposing additional metabolic burden, dual-miRNA delivery offers a clinically translatable and potentially scalable therapeutic avenue for treating degenerative disc disease.

Chapter 8. Final Discussion

8.1 Discussion

The prevalence of LBP is increasing globally, currently affecting 600 million people and imposing a growing socioeconomic burden, particularly in ageing populations. [363,364] Though multi-factorial in nature, the predominant cause of LBP is degeneration of the IVD, characterised by breakdown of the ECM of the NP tissue, and loss of essential proteoglycan and GAG components. [9,25] Specifically, this matrix disruption leads to reduced expression of key matrix-associated TFs, such as SOX9, and structural proteins such as aggrecan and collagen type II. [34] Concurrently, there is a significant increase in the activity of matrix degrading enzymes, such as those from the MMP and ADAMTS families, alongside pro-inflammatory cytokine overexpression, perpetuating the degradative cascade. [39,194,221] Taken together, this creates a harsh microenvironment in the avascular IVD, presenting a challenging environment for regenerative approaches. Current treatments do not extent beyond surgical interventions such as discectomy or spinal fusion, and pain management, leaving the underlying homeostatic disturbance untreated. [1] This has led to investigations into injectable strategies that would target the anabolic : catabolic imbalance, such as biomaterials, [228-230] cell delivery, [225-227] growth factors, [58,231,232] and gene therapy. [73,74,79] miRNAs, short, non-coding nucleotides that regulate the expression of multiple genes simultaneously, have garnered considerable attention in regenerative medicine and represent promising candidates for further examination. [156-159] Considering this, the work presented in this thesis aimed to develop miRNA-based therapies that would elicit anti-catabolic and pro-regenerative effects, providing a clinically relevant treatment strategy for IVD degeneration applications.

Therefore, the aim of Chapter 4 was to screen miRNAs identified as being regeneratively promising, evaluating them individually and in pairs. Simultaneously, two CPPs were assessed to uncover the most suitable for delivering cargo to the IVD, a proteoglycan-rich tissue. Central to the findings of this chapter were significant reductions to ADAMTS5 and MMP13, enzymes well established in the onset of degradation, following FLR-miRNA-149-5p mimic and miRNA-221-3p inhibitor dual delivery. This attenuation possibly reflects the generation of a regenerative niche in rat ex vivo organ culture, whereby regeneration could take place. Staining for sGAGs revealed deeper staining post-dual-miRNA delivery, supporting this shift towards strengthening matrix integrity.

Of note, a synergistic effect was identified when delivering the miRNAs in pairs rather than individually, suggesting the targeting of discrete yet complementary molecular networks. Similar strategies of utilising miRNA combinations have been demonstrated across other fields, though none were found in the IVD field while preparing this work, underpinning its novelty. In diabetic

wound healing, Wang and colleagues reported that although individual transfection with miRNA-129 or miRNA-335 enhanced repair, co-delivery of both miRNAs produced a more pronounced effect. [180] Similarly, combined administration of let-7b and miRNA-34a suppressed proliferation of non-small cell lung cancer cell lines more effectively than either miRNA alone, leading to a greater reduction in tumour size. [365] Extending findings from earlier work, Mariner et al. showed that co-delivery of a miRNA-148b mimic with a miRNA-489 inhibitor promoted osteogenic differentiation of human mesenchymal stem cells (MSCs) more robustly than single-miRNA treatments. [183] Furthermore, incorporation of a miRNA-210 mimic and miRNA-16 inhibitor into collagen–nanohydroxyapatite scaffolds significantly enhanced vascularisation and bone density in a rat calvarial defect model, further supporting the efficacy of dual miRNA strategies. [184] Collectively, these studies highlight the potential for synergistic effects through carefully selected miRNA pairings, underscoring the cooperative impact that combinatorial miRNA delivery can achieve.

The enhanced regenerative effects observed following dual-miRNA-149-5p mimic and 221-3p inhibitor delivery may be attributed to their modulation of distinct pathways with functional cooperation. Bioinformatics analysis of enriched and experimentally validated miRNA target interactions revealed that each miRNA regulates discrete networks relevant to IVD degeneration. miRNA-149-5p was predominantly associated with inflammatory signalling pathways. Validated targets included IL-6, FASLG, MyD88, all of which are strongly linked to inflammatory activity within the extracellular compartment. A meta-analysis by Deng et al. demonstrated significantly elevated IL-6 protein levels in patients with IDD compared to healthy controls. [195] Furthermore, IL-6 concentrations have been shown to correlate with low back pain severity, [196] and increased systemic IL-6 levels have been clinically associated with higher reported pain incidence. [197] Through suppressing IL-6 associated signalling, miRNA-149-5p may disrupt the inflammatory-catabolic feedback loop characteristic of progressive degeneration.

FASLG, a member of the TNF superfamily, has been increasingly implicated in disc degeneration, with gene polymorphisms associated with heightened susceptibility to IVD degeneration. [198] Mechanistically, FASLG promotes NP cell apoptosis via FAS receptor binding and subsequent recruitment of pro-inflammatory cytokines. [199] Similarly, MyD88, a key adaptor protein in toll-like receptor signalling, has previously been linked to miRNA-149 in LPS-stimulated NP models. [201] Silencing of MyD88 attenuated inflammatory signalling and promoted restoration of anabolic markers such as aggrecan and collagen type II. MyD88 expression within the disc is driven by pro-inflammatory cytokines, and it is also implicated in immune-mediated cardiovascular and neurological disorders. [167] Given the pivotal contribution of inflammation to IDD pathogenesis, the capacity of miRNA-149-5p to modulate these mediators presents considerable therapeutic promise.

In contrast to miRNA-149-5ps anti-inflammatory roles, miRNA-221-3p, commonly associated with chondrogenic regulation, was enriched for ECM-related pathways. Highly expressed targets included MMP2, TIMP3, and CXCL12. Dysregulation of MMPs and their respective TIMP inhibitors disrupts the anabolic–catabolic equilibrium central to IDD progression. [11,37] MMP2 contributes directly to collagen degradation and ECM remodelling, and gene polymorphisms have been linked to increased IVD degeneration risk. [205] TIMP3 is unique among the TIMP family in its ability to inhibit all MMPs as well as several ADAMTS enzymes, including ADAMTS-4 and -5, which are key mediators of aggrecan degradation. [12,41,206] Notably, stimulation with TIMP3 reduced expression of the discogenic pain marker Substance P in a rodent model, potentially through suppression of aberrant vascularisation. [207] Therapeutic upregulation of TIMP3 may therefore confer both structural and symptomatic benefits. CXCL12 presents a more complex profile. Circulating levels have been reported to increase in serum with advancing IVD degeneration and correlate with pain severity. [208] In CEP cells it has been shown to regulate MMP2 expression in a dose-dependent manner. [209] However, when delivered directly to the NP in a rat tail model, CXCL12 enhanced proteoglycan deposition, potentially via recruitment of progenitor cells. [210] Despite this regenerative observation, CXCL12 is more commonly associated with inflammation-induced apoptosis and matrix degradation.

Taken together, these interconnected pathways illustrate a complex regulatory network governing ECM turnover. Modulation of these targets by miRNA-221-3p inhibition, in combination with the anti-inflammatory actions of miRNA-149-5p, may therefore offer a complementary and potentially synergistic strategy for restoring regenerative capacity within the degenerated intervertebral disc. Importantly, the identification of this novel pair acts as a strong framework to build miRNA-based strategies upon, which was further explored in the subsequent chapters.

While the development of an anti-catabolic niche was promising, one of the shortcomings of the work presented in Chapter 4 was the lack of a robust pro-regenerative response post-dual-miRNA delivery. Ultimately effective IVD therapies will require strategies that encompass a multimodal approach, stimulating ECM synthesis and attenuating inflammatory and catabolic processes. To this end, Chapter 5 aimed to combine dual-miRNA treatment with an adjunct stimulus in the form of HPL, as a novel therapeutic approach for IVD degeneration treatment. HPL, a growth factor cocktail rich in regenerative GFs and anti-inflammatory cytokines, has demonstrated great promise not only in driving ECM production, but also being safe and generally well tolerated in both in vivo and clinical settings.

Central to the aim of this study was to amplify the anabolic effect of dual-miRNA delivery. Notably, combining the dual-miRNA approach with human platelet lysate (HPL) elicited a cooperative response, resulting in greater upregulation of matrix-associated markers than miRNA

delivery alone in rat ex vivo organ culture, and in a human NP cell-laden NP-ECM gel analogue. HPL is rich in GFs, with proteomic profiling having identified over 1,400 proteins, emphasising g its regenerative capacity. Prominent among these are members of the TGF superfamily, VEGF, PDGF, FGFs, EGF, and bone morphogenetic BMPs, all of which are implicated in matrix synthesis, cell survival, and tissue repair. [59] Consistent with the matrix-promoting effects observed in this chapter, previous work with platelet-derived therapies have demonstrated regenerative potential in NP cells. For example, treatment with 2.5% platelet-rich plasma (PRP) significantly increased collagen type II, aggrecan, and SOX9 expression in rat NP cells. [253] Similarly, pure PRP enhanced aggrecan and collagen type II protein expression in IL-1β–stimulated rat NP cells. [254] In a porcine ex vivo organ culture model, PRP administration also resulted in significantly elevated glycosaminoglycan (GAG) content compared to degenerated controls, [255] further supporting the results presented in this work. Importantly, dual-miRNA + HPL delivery sustained the anti-catabolic effects identified in Chapter 4, presenting evidence of ADAMTS4, ADAMTS5, MMP3, and MMP13 protein downregulation. Therefore, these findings suggest a dual-miRNA + HPL as a promising combinatorial therapy that can modulate catabolic factors while concurrently enhancing production of ECM markers.

In tandem with exploring the therapeutic suitability of dual-miRNA + HPL administration, Chapter 5 established the usage of a biomimetic NP-ECM gel analogue laden with patient NP cells as a high throughput method of screening treatment strategies. The use of physiologically relevant in vitro systems is essential for accurately interrogating cellular responses to regenerative strategies. NP cells are known to exhibit phenotype-dependent variability when cultured in two-dimensional (2D) versus 3D environments, with 3D systems promoting enhanced expression of discogenic markers and maintenance of a more native NP-like phenotype. [219,259] Accordingly, a decellularised NP-ECM hydrogel was employed here, designed to recapitulate the matrix composition of a mildly degenerated (Pfirrmann Grade III) disc. This approach facilitated modelling of the structural and biochemical microenvironment characteristic of early-stage degeneration. However, for future work, this system could be altered to represent milder or more severe degeneration grades based on the target application through modification of the ECM and CS proportions.

Evidence from the wider field supports the use of such biomimetic culture models. Fibroblasts seeded onto a rabbit-derived NP matrix exhibited increased collagen type II and reduced collagen type I expression, indicating a phenotypic shift toward NP-like behaviour. [366] Rashidi et al. similarly demonstrated that NP cell morphology and surface marker expression are sensitive to matrix composition. [264] They demonstrated that collagen–proteoglycan gels mimicking aged matrix promoted increased ITGB1 expression consistent with a degenerated phenotype. [265] Although our model recapitulated a mildly degenerated matrix, further modulation of ECM and chondroitin sulphate content could enable the generation of more advanced degenerative states. Indeed, Peng

et al. reported that bone marrow–derived stem cells cultured within decellularised NP gels upregulated collagen type II, aggrecan, and NP-associated markers including CD24 and KRT19, reinforcing the capacity of NP-derived matrices to promote a pro-regenerative, NP-like phenotype in 3D culture. [266] The inclusion of a cABC challenge further strengthened the model. A well-established inducer of sGAG degradation and matrix remodelling through the stimulation of ADAMTS and MMP proteins, two of the critical target families of the dual-miRNA treatment. [149,367] Through incorporating this catabolic stimulus, the model presented here provides a meaningful platform not only to characterise dual-miRNA-based strategies, but other injectable biologics.

While the stimulation of the resident NP cell population is promising therapeutically, progressive IVD degeneration is associated with an increase in cell necrosis as degeneration worsens. Consequently, replenishing the NP with a healthy cell population may strengthen restorative approaches. Among candidate cell types, delivery of NP and BMSCs are the most commonly investigated. NP cells with their innate adaptations to the harsh IVD microenvironment, [151,272,273] and BMSCs with their differentiation potentiality, [276,277] both offer potential advantages in conferring restorative function. Therefore, Chapter 6 aimed to investigate dual-miRNA stimulation of these cell populations, characterising their pro-anabolic and anti-catabolic effects in culture models progressing from monolayer to goat ex vivo organ culture. Identified were divergent responses between the two cell groups, with BMSCs evidencing a stronger catabolic particularly in in vitro cultures. Protein expression levels of ADAMTS5, MMP13, IL-1β, and TNF-α were consistently lower in NP cells compared with BMSCs, irrespective of transfection status. This distinction may reflect an inherent adaptive phenotype, as NP cells are known to constitutively secrete low levels of TNF-α and IL-1β even under non-degenerative conditions. [291,368] It is also important to consider the influence of culture conditions. Serum starvation and cytokine stimulation were performed in monolayer, which may have disproportionately sensitised BMSCs to inflammatory challenge. Supporting this, Redondo-Castro et al. reported significant upregulation of anti-inflammatory mediators, including G-CSF and IL-1Ra, in cytokine-stimulated BMSC spheroids compared with monolayer cultures, indicating that BMSC immunomodulatory behaviour is strongly influenced by culture dimensionality. [292] Contrastingly, cervical-derived NP cells have been shown to exhibit minimal immunogenicity when co-cultured with peripheral blood mononuclear cells (PBMCs) in monolayer, with no significant increase in T cell activation markers or pro-inflammatory cytokine production. [293] Together this suggests that BMSCs may be more sensitive to inflammatory challenges in vitro, whereas NP cells were more resilient.

Interestingly, this catabolic disparity was mitigated in ex vivo organ culture, potentially due to the influence of microenvironmental factors that were retained in the culture set up. The immunomodulatory effect has been demonstrated by MSCs encapsulated in hydrogels, where they can influence macrophage polarisation towards an anti-inflammatory state. [295] However, of the two

cell types, NP cells revealed to be more advantageous than BMSCs. Dual-miRNA transfection once again maintained an anti-catabolic and inflammatory response, further justifying its utility as a therapy to treat degeneration of the IVD. However, dual-miRNA transfected NP cells when delivered in ex vivo organ culture revealed the strongest upregulation of matrix markers, SOX9 and aggrecan, suggesting its therapeutic benefit over dual-miRNA stimulated BMSCs. It should be noted that overall sGAGs were not significantly impacted upon by any treatments. This is potentially as a result of the degeneration method employing cABC, which cleaves the CS GAG chains of proteoglycans, disrupting the whole protein. [296] In bovine cartilage explants, aggrecan is rapidly cleaved by cABC into multiple smaller core protein fragments, indicating that these fragments must subsequently be regenerated and fully modified before restoration of intact proteoglycan structure can occur. [297-299] In Chapter 6, increased expression of SOX9, a recognised master regulator of discogenic differentiation, [300,301] together with elevated aggrecan expression in the NP-miRNA group, suggests early initiation of a regenerative phenotype. Furthermore, given the inherent time restriction with organ culture studies, limited to approximately four weeks, it is likely that full matrix regeneration could not possible have taken place. Through in silico modelling it has been predicted that in vivo functional restoration of sGAGs would require 1 year following cell transplantation at our delivered dose, [287] a timeline that cannot be replicated in organ culture systems. Nonetheless this chapter provides insights for the first time as to the most suitable cell group for delivery to the IVD following dual-miRNA stimulation.

Given the inherent constraints described with ex vivo organ culture systems, to best evaluate the potential full restoration of the ECM, extended culture periods and in vivo models prevail as the best method of assessment. Therefore, the objective of Chapter 7 was to evaluate for the first time the safety and efficacy of dual-miRNA delivery in a large animal in vivo model of mild intervertebral disc degeneration. It was observed that cell introduction elicited a pronounced inflammatory and catabolic response, accompanied by metabolic dysregulation and significant enrichment of stress-associated pathways identified through mRNA sequencing. These molecular changes were paralleled by a reduction in sGAG content and worsening histological scores, indicating exacerbation of degenerative features. In contrast, dual-miRNA delivery attenuated both inflammatory and catabolic signalling relative to the cell-treated groups. Notably, this intervention was also associated with a strong trend toward upregulation of ECM markers, suggesting a shift toward a more regenerative phenotype.

As was demonstrated throughout this thesis, dual-miRNA administration elicited a potent anti-catabolic and inflammatory effect, contrasted by a sharp rise in these factors following cell delivery. This was observed at both protein and transcriptomic levels, with ADAMTS5, MMP13, TNF-α, and IL-1β being significantly suppressed, alongside genes such as *NFATC1, CEBPD,* and *LGASLS1*, all of which have been implicated in IVD degeneration. [338-341] Collectively, the marked

downregulation of these genes in the dual-miRNA group, together with their significant upregulation in NP and miRNA-NP groups relative to dual-miRNA treatment, supports the role of dual-miRNA delivery as an anti-inflammatory strategy. When considered alongside the concomitant reduction in catabolic and inflammatory protein markers, these findings further strengthen the therapeutic potential of dual-miRNA delivery as an approach to attenuate inflammatory signalling in early-stage intervertebral disc degeneration.

A particularly striking observation was the metabolic disruption associated with cell delivery. Both glucose and lactate concentrations were significantly altered following NP and miRNA-NP cell delivery compared with healthy controls, coinciding with reduced NP cellularity and worsened histological scores, indicative of disrupted cellular homeostasis. Glucose levels negatively correlated with degeneration severity, whereas lactate showed a positive correlation, reinforcing the association between metabolic imbalance and progressive disc pathology. Although the administered dose of 5.5×10^6 cells was predicted to only modestly impact nutrient availability, [287] even moderate reductions in glucose evidently can substantially impair NP cell viability and proteoglycan synthesis. Concordantly, transcriptomic analysis revealed upregulation of GALE in NP and miRNA-NP groups, consistent with perturbed glucose homeostasis. [346] Elevated lactate accumulation, known to promote microenvironmental acidification and compromise cell survival and matrix production, further aligned with increased degeneration severity and enrichment of metabolic and mitochondrial pathways, including upregulation of the senescence-associated enzyme MDH2. [350] Collectively, these findings suggest that exogenous cell delivery may impose excessive metabolic demand within the nutrient-restricted disc niche, exacerbating glucose depletion, lactate accumulation, and downstream degenerative processes, whereas dual-miRNA treatment appears to mitigate these metabolically disruptive effects.

Although cell transplantation to the IVD has demonstrated considerable preclinical promise, our findings indicate that, within the present model, cell delivery was associated with metabolic strain, heightened catabolic activity, reduced matrix marker expression, and increased collagen disorganisation. One explanation may lie in the nature of degeneration induced by cABC, which likely more closely recapitulates a chronic degenerative state rather than an acute injury. Supporting this notion, Detiger et al. reported pronounced inflammatory responses and immune cell infiltration following SVF delivery to discs degenerated with 0.25 U cABC, whereas no adverse effects were observed when degeneration was induced via partial nucleotomy, a model more reflective of herniation. [354] Similarly, clinical studies treating naturally occurring canine IVD degeneration with MSC-based therapies reported no significant regenerative improvements, despite an absence of major adverse effects. [355,356] Chronic IVD degeneration is characterised by sustained inflammation and progressive extracellular matrix breakdown, and cABC administration itself is known to trigger cytokine upregulation and inflammatory signalling. [149] In such a hostile, nutrient-

restricted microenvironment, transplanted cells may experience exacerbated metabolic and inflammatory stress, limiting their regenerative potential. In contrast, many of the most encouraging outcomes in the literature arise from models of mechanically induced or acute injury–related degeneration, suggesting that cell-based therapies may be better suited to early or herniated pathologies. [19,20,275,321] Chronically degenerated discs may require prior modulation of the inflammatory and metabolic milieu, such as through dual-miRNA delivery to enable effective regeneration.

8.2 Limitations and future perspectives

While the findings reported in this thesis show promise and offer a meaningful contribution to the field, they are not without limitations. The goal of this section is therefore to examine the constraints and highlight areas where future endeavours could develop the work, to continue the development of miRNA-based therapies.

One of the limitations of Chapters 4 and 5 was the use of rat cells and IVD organs. In the context of the IVD, it is well recognised that NP cells rapidly lose their native phenotype when expanded in monolayer culture. [213] Moreover, rats belong to a subset of species that retain a population of NP progenitor-like notochordal cells into adulthood. However, previous studies have demonstrated that porcine notochordal cells decrease with passaging, such that NP and notochordal cells become phenotypically indistinguishable in vitro. [214] In a rat ex vivo organ culture model, notochordal cells are present and may constitute up to 30% of the NP cell population, although degenerative injury reduces this proportion. [215] Notochordal cells have been associated with enhanced regenerative capacity, and their presence may have contributed to some of the beneficial effects observed following miRNA delivery. [30,216] Despite these considerations, the use of whole-organ culture confers several advantages. Maintaining the intact disc preserves the native ECM and associated paracrine signalling, creating a more physiologically relevant niche for therapeutic assessment. [135] Ex vivo organ culture systems also better recapitulate the disc's metabolic microenvironment, offering a more representative platform for evaluating candidate treatments. [137] Notably, the response between rat ex vivo organs and the cell-laden NP-ECM gel analogue in Chapter 5 was comparable, suggesting that while notochordal cells may persist, the model itself is applicable for the development of therapeutics.

In Chapter 4, four candidate miRNAs and six miRNA pairings were screened based on selections from the literature. [164,166,167,169,189,369-371] While this targeted approach enabled focused mechanistic evaluation, it necessarily represented only a subset of potentially relevant miRNAs. Numerous additional miRNAs remain to be explored, and alternative combinatorial pairings may yield equally or more effective outcomes. Though dual-miRNA delivery has been trialled in oncology and regenerative medicine, IVD research has thus far focused largely on single-miRNA

modulation, with several promising candidates reported. miRNA-338-3p has been shown to be significantly upregulated in NP tissue from patients suffering from IVD degeneration, with expression levels positively correlating with disease severity. [372] Its inhibition in human NP cells markedly increased the expression of anabolic markers COL2 and ACAN and reduced catabolic enzymes MMP9 and ADAMTS4, attenuated degeneration in a mouse in vivo model. Given the detrimental effect that degeneration has upon the resident cell population, preserving their viability would be particularly relevant. miRNA-125-5p has also been shown to be substantially overexpressed in degenerated tissue, however its suppression reduces IL-1β expression and apoptotic mediators including APAF1 and caspases-3, -7, and -9. [114] Furthermore, miRNA-206 has been implicated as a regulator of inflammatory processes. Its activity functions by silencing GJA1, reducing the expression of IL-1β, TNF-α, and IL-6 in human NP cells. [132] As recognition of the role miRNAs play in the progression of IVD degeneration expands, their potential utility as diagnostic or prognostic biomarkers of disease grows. Integration of transcriptomic profiling with functional validation may facilitate identification of miRNA signatures, enabling both therapeutic targeting and disease stratification. The miRNAs explored in this thesis represent only a fraction of the broader regulatory landscape governing IVD degeneration. The field remain in an exploratory phase, with substantial untapped potential for the discovery of novel miRNA targets and rational combinatorial strategies. Continued systematic investigation, incorporating multi-omics approaches and experimental validation, will be essential to full harness miRNA-based therapeutics for IVD regeneration.

An critical aspect of disc degeneration not addressed in this thesis, but warranting further investigation, is nociceptive pain. Elevated levels of mediators such as β-NGF and BDNF have been associated with increasing severity of degeneration and are known to substantially impair quality of life in patients with degenerated discs. Notably, in a clinical study evaluating platelet lysate delivery to the intervertebral disc, no significant improvement in disc height was observed; however, both VAS and Roland–Morris Disability Questionnaire scores demonstrated significant reductions in pain. [239] These findings underscore that modulation of pain perception represents a critical component of rehabilitation and should be considered alongside structural regenerative strategies. Mechanistically, TNF-α has been shown in vitro to upregulate BDNF and β-NGF expression, suggesting that TNF-α silencing approaches may have the potential to influence pain signalling pathways. [317-319] ELISAs to quantitatively measure β-NGF, TNF-α, and IL-1β were trialled for Chapter 5, however expression levels did not meet the minimal threshold to be read. Achieving measurable concentrations would likely require supraphysiological challenges not representative of the microenvironments being modelled. Furthermore, this would negatively impact any meaningful conclusions being drawn about other aspects of the treatments, reflecting the inherent trade off in designing physiologically relevant in vitro culture models.

Therefore, to better understand these nociceptive mechanisms, new models should be developed that would facilitate a greater understanding into pain mechanisms and the cellular response to potential new treatments. Recent advances in tissue engineering offer promising avenues in this regard, particularly in modelling the whole intervertebral disc in vitro. Kim et al presented a whole disc model incorporating NP and AF spheroids, demonstrated region-specific characteristics. Here, AF spheroids began to develop lamellar structures, and NP spheroids being more amorphous and demonstrating translocation of HIF-1α expression, reflecting native phenotypes. [373] Similarly, employing bioprinting approaches has likewise shown great potential. Moxon and colleagues utilised suspended layer additive manufacturing (SLAM) to print IVD analogues with distinct NP and AF regions that could be used as a platform to advance translational research. [374] The use of scaffolds to create a disc model have also been demonstrated by combining both NP and AF cells, exhibiting regional expression of cartilage and bone like tissue based upon their internal cues, reflecting in vivo patterns. [375] By employing more complex in vitro models such as the ones described, it could mean being able to better study the mechanisms of pain that couldn't be achieved here. Transcriptomic analysis from Chapter 7 suggested the relative downregulation of pain-related genes following dual-miRNA delivery, therefore further investigations in a suitable model may yield meaningful results. Validation of this observation within dedicated pain-modelling systems would be of considerable translational interest. Given the widespread reliance on analgesic medications for the management of LBP, [376,377] further studies evaluating the pain response, particularly when combined with a regenerative treatment such as dual-miRNA ,would be a valuable approach for patients.

In the development of new therapeutics, ensuring the most suitable patient cohort is targeted is of the utmost importance, and an area that would strengthen future works. Findings from Chapter 7 highlight this necessity, the metabolic and matrix disruptions we observed following cell delivery were not predicted by ex vivo organ culture studies in Chapter 6. As previously discussed, this discrepancy is likely due to the inherently short culture times with ex vivo organ culture, it reinforces the complexity of translating regenerative interventions in clinical settings. Published literature supports the therapeutic promise of cell-based delivery, particularly in injury models reflective of herniation. This distinction suggests that patient stratification, distinguishing inflammatory, mechanical, or chronic degenerative states, may be best to optimise outcomes. From a clinical standpoint, evidence of inflammatory disc degeneration relies heavily on imaging. Modic changes as ascertained by MRI being commonly used indicators, with type I changes are associated with bone marrow oedema and inflammatory changes. Type II are reflective of degeneration to the fatty bone marrow, and type III indicative of subchondral bone sclerosis. [378] Though informative, abnormal readings from MRIs have been reported, particularly in older individuals, and given the prevalence of IVD degeneration in the ageing population,[379] additional imaging modalities should

be considered. Single photon emission computed tomography with computed tomography (SPECT-CT) may add further insights into painful IVD degeneration driven by inflammation. [380] [381] SPECT-CT, though at present less widely implemented clinically, has been reported to identify painful LBP associated with chronic degeneration, potentially reflecting inflammatory processes. [382,383] SPECT-CT has demonstrated this utility in atherosclerotic plaques, suggesting it could be similarly implemented in the spine field. [384] Future work, correlating imaging findings with biological markers of inflammation, could optimise patient outcomes by providing a precision-based approach, identifying the most suitable treatment for each patient.

A parallel consideration arises when incorporating additional supplemental with factors such as HPL as explored in Chapter 5. Donor-specific responsiveness to GFs would greatly impact upon the successful outcome of a treatment. A recent study identified variable responses between microtissues generated from patient NP cells to GDF-5 stimulation, presumed to be an effect of the presence or absence of its requisite receptor. [58] Therefore, future endeavours may benefit from better patient matching to treatments. Ongoing identification of biomarkers associated with disease onset and progression may further refine therapeutic matching, although the regulatory landscape of IVD degeneration remains incompletely defined. [22,123] As regenerative medicine continues to transition toward personalised approaches, integration of biomarker profiling with computational modelling could further enhance predictive capacity and optimise therapy selection.

Further to this, deeper interrogation into the effect of cABC on cell metabolism may likewise improve the design of new treatment approaches. In the case of dual-miRNA delivery, the alterations were mitigated, however for cell delivery they were exacerbated, negatively impacting upon matrix production, as presented in Chapter 7. While the impact on catabolic and inflammatory pathways in a large animal model post-cABC administration has been reported,[149] its impact on cellular metabolism has not, to the best of my knowledge, been investigated. A clearer understanding of these metabolic consequences may prove valuable in informing future therapeutic strategies, revealing how cABC alters nutrient diffusion, glycolytic flux, and mitochondrial function. Given the complexity of IVD degeneration this was not within the remit of this work, however more in-depth investigations would give greater insight when developing models and again ensuring appropriate treatment development and selection.

Finally, in Chapter 7, the treatment duration time of 4 months could be extended beyond 1 year to gain a better understanding of long-term matrix remodelling in response to dual-miRNA administration, which was unable to be captured in the shorter timeframe. Extended longitudinal studies are required to realise these matrix modulation effects. Computational modelling predicts that following delivery of cells a year would be necessary to elicit functional changes sGAGs and the ECM. [287] In a study in humans, 10 years post-MSC and PL delivery patients reported significant

reductions to pain and functional impairments, and a 78.1% improvement to their overall feeling post-treatment. [385] A study of BMSCs delivered intradiscally followed patients up 4-6 years on from treatment. [386] They reported that all five patients exhibited overall improvements, with 80% reporting an improvement to mobility. In a study following patients three years on from BMSC delivery to degenerated IVDs likewise reported improvements to pain and disability scores which persisted over the follow-up time. [387] However, miRNA-based approaches are in their infancy comparative to cell delivery, hench currently no experimental or in silico data exists to suggest a regenerative timeframe. The field as a whole would considerably benefit from such additions, supporting better experimental design ultimately leading to the most efficacious therapies that would treat IVD degeneration.

Overall, this thesis highlights the clinical promise of miRNA-based therapeutics for the treatment of IVD degeneration. Through exploring the delivery of miRNAs alone, in pairs, with adjunct stimulus, and in cell-based approaches, the work presented here identifies dual-miRNA treatment as a promising therapeutic component for injectable strategies. Their efficacy was explored both as single and dual combinations, and in conjunction with adjunctive approaches including HPL and cell delivery. Through the integration of a rigorous experimental design with physiologically relevant in vitro and preclinical models, these findings strengthen the translational rationale for miRNA-based therapies as clinically viable interventions for IVD degeneration. Future developments incorporating additional stimuli, personalised medication approaches, and sophisticated computational modelling will only reinforce miRNA-based strategies, hopefully resulting in meaningful therapies that will significantly improve the quality of life of those suffering from LBP as a result of degeneration of the IVD.

Chapter 9. Concluding Remarks

The main goal of this thesis was to evaluate miRNA-based approaches to treat degeneration of the IVD, the main causative agent of LBP. Given the prevalence of LBP and the paucity of treatments, the work presented here demonstrates the developmental pipeline for novel miRNA-based strategies. This thesis reinforces the importance of clinically relevant models, building in complexity from in vitro two-dimensional culture to large animal in vivo models. Key contributions to the biomedical field stemming from this research are summarised below:

- I comprehensively screened miRNAs identified from the literature as being potentially pro-regenerative for IVD applications, utilising in vitro and ex vivo models to evaluate their promise individually and in pairs.
- I evaluated two cell penetrating peptides with the specific aim of identifying the vector most suitable for miRNA delivery to the IVD.
- I explored additional regenerative stimuli by combining dual-miRNA delivery with HPL, identifying a promising clinically relevant strategy to target IVD degeneration.
- I employed a tuneable, biomimetic culture system where patient cells can be incorporated, offering a platform to assess the therapeutic translatability of dual-miRNA-based approaches. This system could be scaled up and adjusted to encompass different degrees of degeneration, making it suitable for multiple applications within the field.
- I investigated the dual-miRNA-stimulation of two commonly transplanted cell types to identify the most appropriate for delivery to the IVD, characterising the pro-regenerative and anti-catabolic response.
- I assessed, for the first time, the safety and efficacy of dual-miRNA delivery in a large animal model of IVD degeneration, delivering dual-miRNA, NP cells, and dual-miRNA cells.
- Through this in vivo model, I identified dual-miRNA treatment as a clinically relevant and translatable approach to treat IVD degeneration, revealing promising therapeutic outcomes from gene and protein expression data.

References

1. Simon J, McAuliffe M, Shamim F, Vuong N, Tahaei A. Discogenic Low Back Pain. *Physical Medicine and Rehabilitation Clinics of North America*. 2014/05/01/ 2014;25(2):305-317. doi:https://doi.org/10.1016/j.pmr.2014.01.006
2. Lorio M, Kim C, Araghi A, Inzana J, Yue JJ. International Society for the Advancement of Spine Surgery Policy 2019-Surgical Treatment of Lumbar Disc Herniation with Radiculopathy. *Int J Spine Surg*. Feb 2020;14(1):1-17. doi:10.14444/7001
3. Gray DT, Deyo RA, Kreuter W, et al. Population-based trends in volumes and rates of ambulatory lumbar spine surgery. *Spine (Phila Pa 1976)*. Aug 1 2006;31(17):1957-63; discussion 1964. doi:10.1097/01.brs.0000229148.63418.c1
4. Mani K, Kleinbart E, Goldman SN, et al. Projections of Single-level and Multilevel Spinal Instrumentation Procedure Volume and Associated Costs for Medicare Patients to 2050. *J Am Acad Orthop Surg Glob Res Rev*. May 1 2024;8(5)doi:10.5435/JAAOSGlobal-D-24-00053
5. Sherman J, Cauthen J, Schoenberg D, Burns M, Reaven NL, Griffith SL. Economic impact of improving outcomes of lumbar discectomy. *Spine J*. Feb 2010;10(2):108-16. doi:10.1016/j.spinee.2009.08.453
6. Kibble MJ, Domingos M, Hoyland JA, Richardson SM. Importance of Matrix Cues on Intervertebral Disc Development, Degeneration, and Regeneration. *Int J Mol Sci*. Jun 21 2022;23(13)doi:10.3390/ijms23136915
7. Gruber HE, Norton HJ, Ingram JA, Hanley EN, Jr. The SOX9 transcription factor in the human disc: decreased immunolocalization with age and disc degeneration. *Spine (Phila Pa 1976)*. Mar 15 2005;30(6):625-30. doi:10.1097/01.brs.0000155420.01444.c6
8. Buckwalter JA. Aging and degeneration of the human intervertebral disc. *Spine (Phila Pa 1976)*. Jun 1 1995;20(11):1307-14. doi:10.1097/00007632-199506000-00022
9. Yaltirik CK, Timirci-Kahraman Ö, Gulec-Yilmaz S, Ozdogan S, Atalay B, Isbir T. The Evaluation of Proteoglycan Levels and the Possible Role of ACAN Gene (c.6423T>C) Variant in Patients with Lumbar Disc Degeneration Disease. *In Vivo*. Mar-Apr 2019;33(2):413-417. doi:10.21873/invivo.11488
10. Pockert AJ, Richardson SM, Le Maitre CL, et al. Modified expression of the ADAMTS enzymes and tissue inhibitor of metalloproteinases 3 during human intervertebral disc degeneration. *Arthritis & Rheumatism*. 2009;60(2):482-491. doi:https://doi.org/10.1002/art.24291
11. Vo NV, Hartman RA, Yurube T, Jacobs LJ, Sowa GA, Kang JD. Expression and regulation of metalloproteinases and their inhibitors in intervertebral disc aging and degeneration. *Spine J*. Mar 2013;13(3):331-41. doi:10.1016/j.spinee.2012.02.027
12. Gendron C, Kashiwagi M, Lim NH, et al. Proteolytic activities of human ADAMTS-5: comparative studies with ADAMTS-4. *J Biol Chem*. Jun 22 2007;282(25):18294-18306. doi:10.1074/jbc.M701523200
13. Agarwal V, Bell GW, Nam JW, Bartel DP. Predicting effective microRNA target sites in mammalian mRNAs. *Elife*. Aug 12 2015;4doi:10.7554/eLife.05005
14. Bushati N, Cohen SM. microRNA functions. *Annu Rev Cell Dev Biol*. 2007;23:175-205. doi:10.1146/annurev.cellbio.23.090506.123406
15. Shirley JL, de Jong YP, Terhorst C, Herzog RW. Immune Responses to Viral Gene Therapy Vectors. *Mol Ther*. Mar 4 2020;28(3):709-722. doi:10.1016/j.ymthe.2020.01.001
16. Wivel NA, Wilson JM. METHODS OF GENE DELIVERY. *Hematology/Oncology Clinics of North America*. 1998/06/01/ 1998;12(3):483-501. doi:https://doi.org/10.1016/S0889-8588(05)70004-6

17. Jalal AR, Dixon JE. Efficient Delivery of Transducing Polymer Nanoparticles for Gene-Mediated Induction of Osteogenesis for Bone Regeneration. Original Research. *Frontiers in Bioengineering and Biotechnology*. 2020-August-05 2020;8doi:10.3389/fbioe.2020.00849
18. McCarthy HO, McCaffrey J, McCrudden CM, et al. Development and characterization of self-assembling nanoparticles using a bio-inspired amphipathic peptide for gene delivery. *J Control Release*. Sep 10 2014;189:141-9. doi:10.1016/j.jconrel.2014.06.048
19. Silverman LI, Dulatova G, Tandeski T, et al. In vitro and in vivo evaluation of discogenic cells, an investigational cell therapy for disc degeneration. *Spine J*. Jan 2020;20(1):138-149. doi:10.1016/j.spinee.2019.08.006
20. Hiraishi S, Schol J, Sakai D, et al. Discogenic cell transplantation directly from a cryopreserved state in an induced intervertebral disc degeneration canine model. *JOR Spine*. Jun 2018;1(2):e1013. doi:10.1002/jsp2.1013
21. Amirdelfan K, Bae H, McJunkin T, et al. Allogeneic mesenchymal precursor cells treatment for chronic low back pain associated with degenerative disc disease: a prospective randomized, placebo-controlled 36-month study of safety and efficacy. *Spine J*. Feb 2021;21(2):212-230. doi:10.1016/j.spinee.2020.10.004
22. Yang F, Wang J, Chen Z, et al. Role of microRNAs in intervertebral disc degeneration (Review). *Exp Ther Med*. Aug 2021;22(2):860. doi:10.3892/etm.2021.10292
23. Dieleman JL, Baral R, Birger M, et al. US Spending on Personal Health Care and Public Health, 1996-2013. *JAMA*. 2016;316(24):2627-2646. doi:10.1001/jama.2016.16885
24. Humzah MD, Soames RW. Human intervertebral disc: Structure and function. *The Anatomical Record*. 1988;220(4):337-356. doi:https://doi.org/10.1002/ar.1092200402
25. Lundon K, Bolton K. Structure and function of the lumbar intervertebral disk in health, aging, and pathologic conditions. *J Orthop Sports Phys Ther*. Jun 2001;31(6):291-303; discussion 304-6. doi:10.2519/jospt.2001.31.6.291
26. Mirza SK, White AA, 3rd. Anatomy of intervertebral disc and pathophysiology of herniated disc disease. *J Clin Laser Med Surg*. Jun 1995;13(3):131-42. doi:10.1089/clm.1995.13.131
27. Torre OM, Mroz V, Bartelstein MK, Huang AH, Iatridis JC. Annulus fibrosus cell phenotypes in homeostasis and injury: implications for regenerative strategies. *Ann N Y Acad Sci*. Apr 2019;1442(1):61-78. doi:10.1111/nyas.13964
28. Horner HA, Roberts S, Bielby RC, Menage J, Evans H, Urban JP. Cells from different regions of the intervertebral disc: effect of culture system on matrix expression and cell phenotype. *Spine (Phila Pa 1976)*. May 15 2002;27(10):1018-28. doi:10.1097/00007632-200205150-00004
29. Maroudas A, Stockwell RA, Nachemson A, Urban J. Factors involved in the nutrition of the human lumbar intervertebral disc: cellularity and diffusion of glucose in vitro. *J Anat*. Sep 1975;120(Pt 1):113-30.
30. Aguiar DJ, Johnson SL, Oegema TR. Notochordal Cells Interact with Nucleus Pulposus Cells: Regulation of Proteoglycan Synthesis. *Experimental Cell Research*. 1999/01/10/ 1999;246(1):129-137. doi:https://doi.org/10.1006/excr.1998.4287
31. Hunter CJ, Matyas JR, Duncan NA. The notochordal cell in the nucleus pulposus: a review in the context of tissue engineering. *Tissue Eng*. Aug 2003;9(4):667-77. doi:10.1089/107632703768247368
32. Pattappa G, Li Z, Peroglio M, Wismer N, Alini M, Grad S. Diversity of intervertebral disc cells: phenotype and function. *J Anat*. Dec 2012;221(6):480-96. doi:10.1111/j.1469-7580.2012.01521.x

33. Erwin WM, Islam D, Inman RD, Fehlings MG, Tsui FW. Notochordal cells protect nucleus pulposus cells from degradation and apoptosis: implications for the mechanisms of intervertebral disc degeneration. *Arthritis Res Ther*. 2011;13(6):R215. doi:10.1186/ar3548
34. Silagi ES, Shapiro IM, Risbud MV. Glycosaminoglycan synthesis in the nucleus pulposus: Dysregulation and the pathogenesis of disc degeneration. *Matrix Biol*. Oct 2018;71-72:368-379. doi:10.1016/j.matbio.2018.02.025
35. Chen S, Liu S, Ma K, Zhao L, Lin H, Shao Z. TGF-β signaling in intervertebral disc health and disease. *Osteoarthritis Cartilage*. Aug 2019;27(8):1109-1117. doi:10.1016/j.joca.2019.05.005
36. Gandhi SD, Maerz T, Mitchell S, et al. Intradiscal Delivery of Anabolic Growth Factors and a Metalloproteinase Inhibitor in a Rabbit Acute Lumbar Disc Injury Model. *Int J Spine Surg*. Aug 2020;14(4):585-593. doi:10.14444/7078
37. Wang WJ, Yu XH, Wang C, et al. MMPs and ADAMTSs in intervertebral disc degeneration. *Clin Chim Acta*. Aug 25 2015;448:238-46. doi:10.1016/j.cca.2015.06.023
38. Adams MA, Stefanakis M, Dolan P. Healing of a painful intervertebral disc should not be confused with reversing disc degeneration: implications for physical therapies for discogenic back pain. *Clin Biomech (Bristol, Avon)*. Dec 2010;25(10):961-71. doi:10.1016/j.clinbiomech.2010.07.016
39. Aripaka SS, Bech-Azeddine R, Jørgensen LM, Mikkelsen JD. The expression of metalloproteinases in the lumbar disc correlates strongly with Pfirrmann MRI grades in lumbar spinal fusion patients. *Brain and Spine*. 2022/01/01/ 2022;2:100872. doi:https://doi.org/10.1016/j.bas.2022.100872
40. Lv FJ, Peng Y, Lim FL, et al. Matrix metalloproteinase 12 is an indicator of intervertebral disc degeneration co-expressed with fibrotic markers. *Osteoarthritis and Cartilage*. 2016/10/01/ 2016;24(10):1826-1836. doi:https://doi.org/10.1016/j.joca.2016.05.012
41. Tortorella MD, Burn TC, Pratta MA, et al. Purification and cloning of aggrecanase-1: a member of the ADAMTS family of proteins. *Science*. Jun 4 1999;284(5420):1664-6. doi:10.1126/science.284.5420.1664
42. Le Maitre CL, Hoyland JA, Freemont AJ. Catabolic cytokine expression in degenerate and herniated human intervertebral discs: IL-1beta and TNFalpha expression profile. *Arthritis Res Ther*. 2007;9(4):R77. doi:10.1186/ar2275
43. Wang Y, Che M, Xin J, Zheng Z, Li J, Zhang S. The role of IL-1β and TNF-α in intervertebral disc degeneration. *Biomed Pharmacother*. Nov 2020;131:110660. doi:10.1016/j.biopha.2020.110660
44. Xia Y, Shen S, Verma IM. NF-κB, an active player in human cancers. *Cancer Immunol Res*. Sep 2014;2(9):823-30. doi:10.1158/2326-6066.Cir-14-0112
45. Schneider-Brachert W, Tchikov V, Neumeyer J, et al. Compartmentalization of TNF Receptor 1 Signaling: Internalized TNF Receptosomes as Death Signaling Vesicles. *Immunity*. 2004/09/01/ 2004;21(3):415-428. doi:https://doi.org/10.1016/j.immuni.2004.08.017
46. Cabal-Hierro L, Artime N, Iglesias J, et al. A TRAF2 binding independent region of TNFR2 is responsible for TRAF2 depletion and enhancement of cytotoxicity driven by TNFR1. *Oncotarget*. Jan 15 2014;5(1):224-36. doi:10.18632/oncotarget.1492
47. Lee S, Moon CS, Sul D, et al. Comparison of growth factor and cytokine expression in patients with degenerated disc disease and herniated nucleus pulposus. *Clin Biochem*. Oct 2009;42(15):1504-11. doi:10.1016/j.clinbiochem.2009.06.017
48. Le Maitre CL, Freemont AJ, Hoyland JA. The role of interleukin-1 in the pathogenesis of human intervertebral disc degeneration. *Arthritis Res Ther*. 2005;7(4):R732-45. doi:10.1186/ar1732

49. Rousseau MA, Ulrich JA, Bass EC, Rodriguez AG, Liu JJ, Lotz JC. Stab incision for inducing intervertebral disc degeneration in the rat. *Spine (Phila Pa 1976)*. Jan 1 2007;32(1):17-24. doi:10.1097/01.brs.0000251013.07656.45
50. Tolofari SK, Richardson SM, Freemont AJ, Hoyland JA. Expression of semaphorin 3A and its receptors in the human intervertebral disc: potential role in regulating neural ingrowth in the degenerate intervertebral disc. *Arthritis Res Ther*. 2010;12(1):R1. doi:10.1186/ar2898
51. Gruber HE, Ingram JA, Hoelscher G, Zinchenko N, Norton HJ, Hanley EN, Jr. Brain-derived neurotrophic factor and its receptor in the human and the sand rat intervertebral disc. *Arthritis Res Ther*. 2008;10(4):R82. doi:10.1186/ar2456
52. Lee JM, Song JY, Baek M, et al. Interleukin-1β induces angiogenesis and innervation in human intervertebral disc degeneration. *J Orthop Res*. Feb 2011;29(2):265-9. doi:10.1002/jor.21210
53. Du J, Pfannkuche JJ, Lang G, et al. Proinflammatory intervertebral disc cell and organ culture models induced by tumor necrosis factor alpha. *JOR Spine*. Sep 2020;3(3):e1104. doi:10.1002/jsp2.1104
54. Sun ZY, Liu YT, Liang H, Li Y, Wang DG, Tian JW. Interleukin-1β exacerbates the catabolic effects of human nucleus pulposus cells through activation of the Nuclear Factor kappa B signaling pathway under hypoxic conditions. *Eur Rev Med Pharmacol Sci*. Nov 2018;22(21):7129-7139. doi:10.26355/eurrev_201811_16244
55. Wang X, Meng Q, Qiu C, et al. Potential therapeutic role of Co-Q10 in alleviating intervertebral disc degeneration and suppressing IL-1β-mediated inflammatory reaction in NP cells. *International Immunopharmacology*. 2018/11/01/ 2018;64:424-431. doi:https://doi.org/10.1016/j.intimp.2018.09.029
56. Miyamoto K, Masuda K, Kim JG, et al. Intradiscal injections of osteogenic protein-1 restore the viscoelastic properties of degenerated intervertebral discs. *The Spine Journal*. 2006/11/01/ 2006;6(6):692-703. doi:https://doi.org/10.1016/j.spinee.2006.04.014
57. Yan J, Yang S, Sun H, et al. Effects of releasing recombinant human growth and differentiation factor-5 from poly(lactic-co-glycolic acid) microspheres for repair of the rat degenerated intervertebral disc. *J Biomater Appl*. Jul 2014;29(1):72-80. doi:10.1177/0885328213515034
58. McDonnell EE, Ní Néill T, Wilson N, Darwish SL, Butler JS, Buckley CT. In silico modeling the potential clinical effect of growth factor treatment on the metabolism of human nucleus pulposus cells. *JOR SPINE*. 2024;7(3):e1352. doi:https://doi.org/10.1002/jsp2.1352
59. Wang S-z, Chang Q, Lu J, Wang C. Growth factors and platelet-rich plasma: promising biological strategies for early intervertebral disc degeneration. *International Orthopaedics*. 2015/05/01 2015;39(5):927-934. doi:10.1007/s00264-014-2664-8
60. Yang H, Gao F, Li X, Wang J, Liu H, Zheng Z. TGF-β1 antagonizes TNF-α induced up-regulation of matrix metalloproteinase 3 in nucleus pulposus cells: role of the ERK1/2 pathway. *Connect Tissue Res*. Nov 2015;56(6):461-8. doi:10.3109/03008207.2015.1054030
61. Qu Z, Zhang F, Chen W, Lin T, Sun Y. High-dose TGF-β1 degrades human nucleus pulposus cells via ALK1-Smad1/5/8 activation. *Exp Ther Med*. Oct 2020;20(4):3661-3668. doi:10.3892/etm.2020.9088
62. Chen WH, Liu HY, Lo WC, et al. Intervertebral disc regeneration in an ex vivo culture system using mesenchymal stem cells and platelet-rich plasma. *Biomaterials*. Oct 2009;30(29):5523-33. doi:10.1016/j.biomaterials.2009.07.019
63. Dhollander AA, De Neve F, Almqvist KF, et al. Autologous matrix-induced chondrogenesis combined with platelet-rich plasma gel: technical description and a five

pilot patients report. *Knee Surg Sports Traumatol Arthrosc*. Apr 2011;19(4):536-42. doi:10.1007/s00167-010-1337-4
64. Duymus TM, Mutlu S, Dernek B, Komur B, Aydogmus S, Kesiktas FN. Choice of intra-articular injection in treatment of knee osteoarthritis: platelet-rich plasma, hyaluronic acid or ozone options. *Knee Surg Sports Traumatol Arthrosc*. Feb 2017;25(2):485-492. doi:10.1007/s00167-016-4110-5
65. Pirvu TN, Schroeder JE, Peroglio M, et al. Platelet-rich plasma induces annulus fibrosus cell proliferation and matrix production. *Eur Spine J*. Apr 2014;23(4):745-53. doi:10.1007/s00586-014-3198-x
66. Crespo-Diaz R, Behfar A, Butler GW, et al. Platelet Lysate Consisting of a Natural Repair Proteome Supports Human Mesenchymal Stem Cell Proliferation and Chromosomal Stability. *Cell Transplantation*. 2011;20(6):797-812. doi:10.3727/096368910x543376
67. Rodrigues RM, Valim VS, Berger M, et al. The proteomic and particle composition of human platelet lysate for cell therapy products. *J Cell Biochem*. Sep 2022;123(9):1495-1505. doi:10.1002/jcb.30310
68. Levi D, Horn S, Tyszko S, Levin J, Hecht-Leavitt C, Walko E. Intradiscal Platelet-Rich Plasma Injection for Chronic Discogenic Low Back Pain: Preliminary Results from a Prospective Trial. *Pain Med*. Jun 2016;17(6):1010-22. doi:10.1093/pm/pnv053
69. Akeda K, An HS, Pichika R, et al. Platelet-rich plasma (PRP) stimulates the extracellular matrix metabolism of porcine nucleus pulposus and anulus fibrosus cells cultured in alginate beads. *Spine (Phila Pa 1976)*. Apr 20 2006;31(9):959-66. doi:10.1097/01.brs.0000214942.78119.24
70. Temin HM. Mixed infection with two types of Rous sarcoma virus. *Virology*. 1961/02/01/ 1961;13(2):158-163. doi:https://doi.org/10.1016/0042-6822(61)90049-6
71. Blaese RM, Culver KW, Miller AD, et al. T Lymphocyte-Directed Gene Therapy for ADA[−] SCID: Initial Trial Results After 4 Years. *Science*. 1995;270(5235):475-480. doi:doi:10.1126/science.270.5235.475
72. Tang R, Xu Z. Gene therapy: a double-edged sword with great powers. *Molecular and Cellular Biochemistry*. 2020/11/01 2020;474(1):73-81. doi:10.1007/s11010-020-03834-3
73. Wehling P, Schulitz K-P, Robbins PD, Evans CH, Reinecke JA. Transfer of Genes to Chondrocytic Cells of the Lumbar Spine: Proposal for a Treatment Strategy of Spinal Disorders by Local Gene Therapy. *Spine*. 1997;22(10):1092-1097.
74. Nishida K, Kang JD, Suh JK, Robbins PD, Evans CH, Gilbertson LG. Adenovirus-mediated gene transfer to nucleus pulposus cells. Implications for the treatment of intervertebral disc degeneration. *Spine (Phila Pa 1976)*. Nov 15 1998;23(22):2437-42; discussion 2443. doi:10.1097/00007632-199811150-00016
75. Paul R, Haydon RC, Cheng H, et al. Potential use of Sox9 gene therapy for intervertebral degenerative disc disease. *Spine (Phila Pa 1976)*. Apr 15 2003;28(8):755-63.
76. Zhao J, Jia L, Chen D, Xiao J, Pan X, Jing X. Adenovirus-mediated TGF-beta(1) gene transfer to human degenerative lumbar intervertebral disc cells. *Chin Med J (Engl)*. Mar 2002;115(3):409-12.
77. Nishida K, Kang JD, Gilbertson LG, et al. Modulation of the biologic activity of the rabbit intervertebral disc by gene therapy: an in vivo study of adenovirus-mediated transfer of the human transforming growth factor beta 1 encoding gene. *Spine (Phila Pa 1976)*. Dec 1 1999;24(23):2419-25. doi:10.1097/00007632-199912010-00002
78. Le Maitre CL, Freemont AJ, Hoyland JA. A preliminary in vitro study into the use of IL-1Ra gene therapy for the inhibition of intervertebral disc degeneration. *Int J Exp Pathol*. Feb 2006;87(1):17-28. doi:10.1111/j.0959-9673.2006.00449.x

79. Le Maitre CL, Hoyland JA, Freemont AJ. Interleukin-1 receptor antagonist delivered directly and by gene therapy inhibits matrix degradation in the intact degenerate human intervertebral disc: an in situ zymographic and gene therapy study. *Arthritis Res Ther*. 2007;9(4):R83. doi:10.1186/ar2282
80. Wallach CJ, Sobajima S, Watanabe Y, et al. Gene transfer of the catabolic inhibitor TIMP-1 increases measured proteoglycans in cells from degenerated human intervertebral discs. *Spine (Phila Pa 1976)*. Oct 15 2003;28(20):2331-7. doi:10.1097/01.Brs.0000085303.67942.94
81. Moon SH, Nishida K, Gilbertson LG, et al. Biologic response of human intervertebral disc cells to gene therapy cocktail. *Spine (Phila Pa 1976)*. Aug 1 2008;33(17):1850-5. doi:10.1097/BRS.0b013e31817e1cd7
82. Ren S, Liu Y, Ma J, et al. Treatment of rabbit intervertebral disc degeneration with co-transfection by adeno-associated virus-mediated SOX9 and osteogenic protein-1 double genes in vivo. *Int J Mol Med*. Nov 2013;32(5):1063-8. doi:10.3892/ijmm.2013.1497
83. Liu Y, Yu T, Ma XX, Xiang HF, Hu YG, Chen BH. Lentivirus-mediated TGF-β3, CTGF and TIMP1 gene transduction as a gene therapy for intervertebral disc degeneration in an in vivo rabbit model. *Exp Ther Med*. Apr 2016;11(4):1399-1404. doi:10.3892/etm.2016.3063
84. Ren XF, Diao ZZ, Xi YM, et al. Adeno-associated virus-mediated BMP-7 and SOX9 in vitro co-transfection of human degenerative intervertebral disc cells. *Genetics and molecular research : GMR*. 2015;14(2):3736-3744. doi:10.4238/2015.april.22.1 Accessed 2015/04//. http://europepmc.org/abstract/MED/25966142

https://doi.org/10.4238/2015.April.22.1
85. Wallach CJ, Kim JS, Sobajima S, et al. Safety assessment of intradiscal gene transfer: a pilot study. *Spine J*. Mar-Apr 2006;6(2):107-12. doi:10.1016/j.spinee.2005.05.002
86. Snuggs JW, Senter RK, Whitt JP, Jackson JD, Le Maitre CL. PCRX-201, a novel IL-1Ra gene therapy treatment approach for low back pain resulting from intervertebral disc degeneration. *Gene Therapy*. 2025/03/01 2025;32(2):93-105. doi:10.1038/s41434-024-00504-7
87. Kim CH, Oliver C, Dar H, Drissi H, Presciutti SM. AAV6 as an effective gene delivery vector for prolonged transgene expression in intervertebral disc cells in vivo. *Genes & Diseases*. 2022/07/01/ 2022;9(4):1074-1085. doi:https://doi.org/10.1016/j.gendis.2020.12.009
88. Bernardi S, Balbi C. Extracellular Vesicles: From Biomarkers to Therapeutic Tools. *Biology (Basel)*. Aug 31 2020;9(9)doi:10.3390/biology9090258
89. Elsharkasy OM, Nordin JZ, Hagey DW, et al. Extracellular vesicles as drug delivery systems: Why and how? *Advanced Drug Delivery Reviews*. 2020/01/01/ 2020;159:332-343. doi:https://doi.org/10.1016/j.addr.2020.04.004
90. Tang S, Salazar-Puerta A, Richards J, et al. Non-viral reprogramming of human nucleus pulposus cells with FOXF1 via extracellular vesicle delivery: an in vitro and in vivo study. *Eur Cell Mater*. Jan 19 2021;41:90-107. doi:10.22203/eCM.v041a07
91. Tang SN, Salazar-Puerta AI, Heimann MK, et al. Engineered extracellular vesicle-based gene therapy for the treatment of discogenic back pain. *Biomaterials*. 2024/07/01/ 2024;308:122562. doi:https://doi.org/10.1016/j.biomaterials.2024.122562
92. Liao Z, Ou Z, Tong B, Li S, Yang C. Customized extracellular vesicles targeting lysosomal biogenesis deliver therapeutic cargo for intervertebral disc degeneration treatment. *J Nanobiotechnology*. Oct 11 2025;23(1):659. doi:10.1186/s12951-025-03772-6

93. Chen W, Zhao T, Ren Y, et al. Dual-pathological cascade delivery of apoptotic vesicles for targeted therapy in intervertebral disc degeneration. *Materials Today Bio*. 2025/10/01/ 2025;34:102200. doi:https://doi.org/10.1016/j.mtbio.2025.102200
94. Ma W, Wang W, Zhao L, et al. Reprogramming to restore youthful epigenetics of senescent nucleus pulposus cells for mitigating intervertebral disc degeneration and alleviating low back pain. *Bone Research*. 2025/03/12 2025;13(1):35. doi:10.1038/s41413-025-00416-1
95. Kozomara A, Griffiths-Jones S. miRBase: annotating high confidence microRNAs using deep sequencing data. *Nucleic Acids Res*. Jan 2014;42(Database issue):D68-73. doi:10.1093/nar/gkt1181
96. Friedman RC, Farh KK, Burge CB, Bartel DP. Most mammalian mRNAs are conserved targets of microRNAs. *Genome Res*. Jan 2009;19(1):92-105. doi:10.1101/gr.082701.108
97. Tsekoura EK, K.C RB, Uludag H. Biomaterials to Facilitate Delivery of RNA Agents in Bone Regeneration and Repair. *ACS Biomaterials Science & Engineering*. 2017/07/10 2017;3(7):1195-1206. doi:10.1021/acsbiomaterials.6b00387
98. Zhou X, Chen L, Grad S, et al. The roles and perspectives of microRNAs as biomarkers for intervertebral disc degeneration. *J Tissue Eng Regen Med*. Dec 2017;11(12):3481-3487. doi:10.1002/term.2261
99. Macfarlane LA, Murphy PR. MicroRNA: Biogenesis, Function and Role in Cancer. *Curr Genomics*. Nov 2010;11(7):537-61. doi:10.2174/138920210793175895
100. O'Carroll D, Schaefer A. General Principals of miRNA Biogenesis and Regulation in the Brain. *Neuropsychopharmacology*. 2013/01/01 2013;38(1):39-54. doi:10.1038/npp.2012.87
101. Eichhorn SW, Guo H, McGeary SE, et al. mRNA destabilization is the dominant effect of mammalian microRNAs by the time substantial repression ensues. *Mol Cell*. Oct 2 2014;56(1):104-15. doi:10.1016/j.molcel.2014.08.028
102. Huntzinger E, Izaurralde E. Gene silencing by microRNAs: contributions of translational repression and mRNA decay. *Nature Reviews Genetics*. 2011/02/01 2011;12(2):99-110. doi:10.1038/nrg2936
103. Meijer HA, Kong YW, Lu WT, et al. Translational repression and eIF4A2 activity are critical for microRNA-mediated gene regulation. *Science*. Apr 5 2013;340(6128):82-5. doi:10.1126/science.1231197
104. Vasudevan S. Posttranscriptional upregulation by microRNAs. *Wiley Interdiscip Rev RNA*. May-Jun 2012;3(3):311-30. doi:10.1002/wrna.121
105. Vasudevan S, Tong Y, Steitz JA. Cell-cycle control of microRNA-mediated translation regulation. *Cell Cycle*. Jun 1 2008;7(11):1545-9. doi:10.4161/cc.7.11.6018
106. Vasudevan S, Tong Y, Steitz JA. Switching from Repression to Activation: MicroRNAs Can Up-Regulate Translation. *Science*. 2007;318(5858):1931-1934. doi:doi:10.1126/science.1149460
107. Mollaei H, Safaralizadeh R, Rostami Z. MicroRNA replacement therapy in cancer. *Journal of Cellular Physiology*. 2019;234(8):12369-12384. doi:https://doi.org/10.1002/jcp.28058
108. Gantier MP, Williams BR. The response of mammalian cells to double-stranded RNA. *Cytokine Growth Factor Rev*. Oct-Dec 2007;18(5-6):363-71. doi:10.1016/j.cytogfr.2007.06.016
109. Verdera HC, Kuranda K, Mingozzi F. AAV Vector Immunogenicity in Humans: A Long Journey to Successful Gene Transfer. *Mol Ther*. Mar 4 2020;28(3):723-746. doi:10.1016/j.ymthe.2019.12.010

110. Goswami R, Subramanian G, Silayeva L, et al. Gene Therapy Leaves a Vicious Cycle. Review. *Frontiers in Oncology*. 2019-April-24 2019;9doi:10.3389/fonc.2019.00297
111. Tripathy SK, Black HB, Goldwasser E, Leiden JM. Immune responses to transgene-encoded proteins limit the stability of gene expression after injection of replication-defective adenovirus vectors. *Nat Med*. May 1996;2(5):545-50. doi:10.1038/nm0596-545
112. Goodwin T, Huang L. Chapter One - Nonviral Vectors: We Have Come a Long Way. In: Huang L, Liu D, Wagner E, eds. *Advances in Genetics*. Academic Press; 2014:1-12.
113. Liu W, Zhang Y, Feng X, et al. Inhibition of microRNA-34a prevents IL-1β-induced extracellular matrix degradation in nucleus pulposus by increasing GDF5 expression. *Exp Biol Med (Maywood)*. Nov 2016;241(17):1924-1932. doi:10.1177/1535370216657444
114. Jie J, Xu X, Li W, Wang G. Regulation of Apoptosis and Inflammatory Response in Interleukin-1β-Induced Nucleus Pulposus Cells by miR-125b-5p Via Targeting TRIAP1. *Biochem Genet*. Apr 2021;59(2):475-490. doi:10.1007/s10528-020-10009-8
115. Wang B, Xu N, Cao L, et al. miR-31 from Mesenchymal Stem Cell-Derived Extracellular Vesicles Alleviates Intervertebral Disc Degeneration by Inhibiting NFAT5 and Upregulating the Wnt/β-Catenin Pathway. *Stem Cells Int*. 2022;2022:2164057. doi:10.1155/2022/2164057
116. Lonez C, Vandenbranden M, Ruysschaert J-M. Cationic lipids activate intracellular signaling pathways. *Advanced Drug Delivery Reviews*. 2012/12/01/ 2012;64(15):1749-1758. doi:https://doi.org/10.1016/j.addr.2012.05.009
117. Dass CR. Cytotoxicity issues pertinent to lipoplex-mediated gene therapy in-vivo. *J Pharm Pharmacol*. May 2002;54(5):593-601. doi:10.1211/0022357021778817
118. Fischer D, Li Y, Ahlemeyer B, Krieglstein J, Kissel T. In vitro cytotoxicity testing of polycations: influence of polymer structure on cell viability and hemolysis. *Biomaterials*. 2003/03/01/ 2003;24(7):1121-1131. doi:https://doi.org/10.1016/S0142-9612(02)00445-3
119. Saqafi B, Rahbarizadeh F. Effect of PEI surface modification with PEG on cytotoxicity and transfection efficiency. *Micro & Nano Letters*. 2018;13(8):1090-1095. doi:https://doi.org/10.1049/mnl.2017.0457
120. Cao Y, Tan YF, Wong YS, Liew MWJ, Venkatraman S. Recent Advances in Chitosan-Based Carriers for Gene Delivery. *Mar Drugs*. Jun 25 2019;17(6)doi:10.3390/md17060381
121. Milletti F. Cell-penetrating peptides: classes, origin, and current landscape. *Drug Discovery Today*. 2012/08/01/ 2012;17(15):850-860. doi:https://doi.org/10.1016/j.drudis.2012.03.002
122. Farkhani SM, Valizadeh A, Karami H, Mohammadi S, Sohrabi N, Badrzadeh F. Cell penetrating peptides: efficient vectors for delivery of nanoparticles, nanocarriers, therapeutic and diagnostic molecules. *Peptides*. Jul 2014;57:78-94. doi:10.1016/j.peptides.2014.04.015
123. Nir S, Nicol F, Szoka FC, Jr. Surface aggregation and membrane penetration by peptides: relation to pore formation and fusion. *Mol Membr Biol*. Jan-Mar 1999;16(1):95-101. doi:10.1080/096876899294814
124. Plank C, Zatloukal K, Cotten M, Mechtler K, Wagner E. Gene transfer into hepatocytes using asialoglycoprotein receptor mediated endocytosis of DNA complexed with an artificial tetra-antennary galactose ligand. *Bioconjugate Chemistry*. 1992/11/01 1992;3(6):533-539. doi:10.1021/bc00018a012
125. Abu-Awwad HAM, Thiagarajan L, Dixon JE. Controlled release of GAG-binding enhanced transduction (GET) peptides for sustained and highly efficient intracellular delivery. *Acta Biomater*. Jul 15 2017;57:225-237. doi:10.1016/j.actbio.2017.04.028

126. Dixon JE, Osman G, Morris GE, et al. Highly efficient delivery of functional cargoes by the synergistic effect of GAG binding motifs and cell-penetrating peptides. *Proc Natl Acad Sci U S A*. Jan 19 2016;113(3):E291-9. doi:10.1073/pnas.1518634113
127. Jiang H, Moro A, Wang J, Meng D, Zhan X, Wei Q. MicroRNA-338-3p as a novel therapeutic target for intervertebral disc degeneration. *Exp Mol Med*. Sep 2021;53(9):1356-1365. doi:10.1038/s12276-021-00662-3
128. Zhang H-J, Liao H-Y, Bai D-Y, Wang Z-Q, Xie X-W. MAPK /ERK signaling pathway: A potential target for the treatment of intervertebral disc degeneration. *Biomedicine & Pharmacotherapy*. 2021/11/01/ 2021;143:112170. doi:https://doi.org/10.1016/j.biopha.2021.112170
129. Dai S, Shi X, Qin R, Zhang X, Xu F, Yang H. Sodium Tanshinone IIA Sulfonate Ameliorates Injury-Induced Oxidative Stress and Intervertebral Disc Degeneration in Rats by Inhibiting p38 MAPK Signaling Pathway. *Oxid Med Cell Longev*. 2021;2021:5556122. doi:10.1155/2021/5556122
130. Zhang S, Liang W, Abulizi Y, et al. Quercetin Alleviates Intervertebral Disc Degeneration by Modulating p38 MAPK-Mediated Autophagy. *BioMed Research International*. 2021/05/12 2021;2021:6631562. doi:10.1155/2021/6631562
131. Yu X, Liu Q, Wang Y, et al. Depleted Long Noncoding RNA GAS5 Relieves Intervertebral Disc Degeneration via microRNA-17-3p/Ang-2. *Oxid Med Cell Longev*. 2022;2022:1792412. doi:10.1155/2022/1792412
132. Zhou P, Xu P, Yu W, Li H. MiR-206 improves intervertebral disk degeneration by targeting GJA1. *J Orthop Surg Res*. Mar 12 2022;17(1):157. doi:10.1186/s13018-022-03044-1
133. Oehme D, Ghosh P, Goldschlager T, et al. Reconstitution of degenerated ovine lumbar discs by STRO-3–positive allogeneic mesenchymal precursor cells combined with pentosan polysulfate. *Journal of Neurosurgery: Spine SPI*. 01 May. 2016 2016;24(5):715-726. doi:10.3171/2015.8.Spine141097
134. Parliament E, Council E. DIRECTIVE 2010/63/EU on the protection of animals used for scientific purposes. *EU Official Journal*. 10/20 2010;L276
135. Rijal G, Li W. Native-mimicking in vitro microenvironment: an elusive and seductive future for tumor modeling and tissue engineering. *Journal of Biological Engineering*. 2018/09/12 2018;12(1):20. doi:10.1186/s13036-018-0114-7
136. Chan SC, Ferguson SJ, Gantenbein-Ritter B. The effects of dynamic loading on the intervertebral disc. *Eur Spine J*. Nov 2011;20(11):1796-812. doi:10.1007/s00586-011-1827-1
137. McDonnell EE, Buckley CT. Investigating the physiological relevance of ex vivo disc organ culture nutrient microenvironments using in silico modeling and experimental validation. *JOR SPINE*. 2021;4(2):e1141. doi:https://doi.org/10.1002/jsp2.1141
138. Krupkova O, Hlavna M, Amir Tahmasseb J, et al. An Inflammatory Nucleus Pulposus Tissue Culture Model to Test Molecular Regenerative Therapies: Validation with Epigallocatechin 3-Gallate. *Int J Mol Sci*. Sep 27 2016;17(10)doi:10.3390/ijms17101640
139. Salzer E, Mouser VHM, Tryfonidou MA, Ito K. A bovine nucleus pulposus explant culture model. *J Orthop Res*. Sep 2022;40(9):2089-2102. doi:10.1002/jor.25226
140. Teixeira GQ, Boldt A, Nagl I, et al. A Degenerative/Proinflammatory Intervertebral Disc Organ Culture: An Ex Vivo Model for Anti-inflammatory Drug and Cell Therapy. *Tissue Eng Part C Methods*. Jan 2016;22(1):8-19. doi:10.1089/ten.tec.2015.0195
141. Gu SX, Li X, Hamilton JL, et al. MicroRNA-146a reduces IL-1 dependent inflammatory responses in the intervertebral disc. *Gene*. Jan 25 2015;555(2):80-7. doi:10.1016/j.gene.2014.10.024

142. Bucher C, Gazdhar A, Benneker LM, Geiser T, Gantenbein-Ritter B. Nonviral Gene Delivery of Growth and Differentiation Factor 5 to Human Mesenchymal Stem Cells Injected into a 3D Bovine Intervertebral Disc Organ Culture System. *Stem Cells International*. 2013/12/23 2013;2013:326828. doi:10.1155/2013/326828
143. Setton LA, Chen J. Mechanobiology of the Intervertebral Disc and Relevance to Disc Degeneration. *JBJS*. 2006;88(suppl_2)
144. Jin L, Balian G, Li XJ. Animal models for disc degeneration-an update. *Histol Histopathol*. Jun 2018;33(6):543-554. doi:10.14670/hh-11-910
145. Willems N, Tellegen AR, Bergknut N, et al. Inflammatory profiles in canine intervertebral disc degeneration. *BMC Veterinary Research*. 2016/01/13 2016;12(1):10. doi:10.1186/s12917-016-0635-6
146. Daly C, Ghosh P, Jenkin G, Oehme D, Goldschlager T. A Review of Animal Models of Intervertebral Disc Degeneration: Pathophysiology, Regeneration, and Translation to the Clinic. *Biomed Res Int*. 2016;2016:5952165. doi:10.1155/2016/5952165
147. Showalter BL, Beckstein JC, Martin JT, et al. Comparison of animal discs used in disc research to human lumbar disc: torsion mechanics and collagen content. *Spine (Phila Pa 1976)*. Jul 1 2012;37(15):E900-7. doi:10.1097/BRS.0b013e31824d911c
148. Gullbrand SE, Malhotra NR, Schaer TP, et al. A large animal model that recapitulates the spectrum of human intervertebral disc degeneration. *Osteoarthritis Cartilage*. Jan 2017;25(1):146-156. doi:10.1016/j.joca.2016.08.006
149. Zhang C, Gullbrand SE, Schaer TP, et al. Inflammatory cytokine and catabolic enzyme expression in a goat model of intervertebral disc degeneration. *J Orthop Res*. Nov 2020;38(11):2521-2531. doi:10.1002/jor.24639
150. Lai A, Gansau J, Gullbrand SE, et al. Development of a standardized histopathology scoring system for intervertebral disc degeneration in rat models: An initiative of the ORS spine section. *JOR Spine*. Jun 2021;4(2):e1150. doi:10.1002/jsp2.1150
151. Sadowska A, Kameda T, Krupkova O, Wuertz-Kozak K. Osmosensing, osmosignalling and inflammation: how intervertebral disc cells respond to altered osmolarity. *Eur Cell Mater*. Nov 19 2018;36:231-250. doi:10.22203/eCM.v036a17
152. Blokpoel Ferreras LA, Chan SY, Vazquez Reina S, Dixon JE. Rapidly Transducing and Spatially Localized Magnetofection Using Peptide-Mediated Non-Viral Gene Delivery Based on Iron Oxide Nanoparticles. *ACS Applied Nano Materials*. 2021/01/22 2021;4(1):167-181. doi:10.1021/acsanm.0c02465
153. Udhayakumar VK, De Beuckelaer A, McCaffrey J, et al. Arginine-Rich Peptide-Based mRNA Nanocomplexes Efficiently Instigate Cytotoxic T Cell Immunity Dependent on the Amphipathic Organization of the Peptide. *Adv Healthc Mater*. Jul 2017;6(13)doi:10.1002/adhm.201601412
154. Bennett R, Yakkundi A, McKeen HD, et al. RALA-mediated delivery of FKBPL nucleic acid therapeutics. *Nanomedicine (Lond)*. Oct 2015;10(19):2989-3001. doi:10.2217/nnm.15.115
155. Ignat'eva NY, Danilov NA, Averkiev SV, Obrezkova MV, Lunin VV, Sobol' EN. Determination of hydroxyproline in tissues and the evaluation of the collagen content of the tissues. *Journal of Analytical Chemistry*. 2007/01/01 2007;62(1):51-57. doi:10.1134/S106193480701011X
156. Zheng L, Chen Y, Ye L, et al. miRNA-584-3p inhibits gastric cancer progression by repressing Yin Yang 1- facilitated MMP-14 expression. *Sci Rep*. Aug 21 2017;7(1):8967. doi:10.1038/s41598-017-09271-5
157. Hoang DH, Zhao D, Branciamore S, et al. MicroRNA networks in FLT3-ITD acute myeloid leukemia. *Proceedings of the National Academy of Sciences*. 2022;119(16):e2112482119. doi:doi:10.1073/pnas.2112482119

158. Eulalio A, Mano M, Ferro MD, et al. Functional screening identifies miRNAs inducing cardiac regeneration. *Nature*. 2012/12/01 2012;492(7429):376-381. doi:10.1038/nature11739
159. Gabisonia K, Prosdocimo G, Aquaro GD, et al. MicroRNA therapy stimulates uncontrolled cardiac repair after myocardial infarction in pigs. *Nature*. 2019/05/01 2019;569(7756):418-422. doi:10.1038/s41586-019-1191-6
160. Miyaki S, Nakasa T, Otsuki S, et al. MicroRNA-140 is expressed in differentiated human articular chondrocytes and modulates interleukin-1 responses. *Arthritis Rheum*. Sep 2009;60(9):2723-30. doi:10.1002/art.24745
161. Yang J, Qin S, Yi C, et al. MiR-140 is co-expressed with Wwp2-C transcript and activated by Sox9 to target Sp1 in maintaining the chondrocyte proliferation. *FEBS Lett*. Oct 3 2011;585(19):2992-7. doi:10.1016/j.febslet.2011.08.013
162. Miyaki S, Sato T, Inoue A, et al. MicroRNA-140 plays dual roles in both cartilage development and homeostasis. *Genes Dev*. Jun 1 2010;24(11):1173-85. doi:10.1101/gad.1915510
163. Si HB, Zeng Y, Liu SY, et al. Intra-articular injection of microRNA-140 (miRNA-140) alleviates osteoarthritis (OA) progression by modulating extracellular matrix (ECM) homeostasis in rats. *Osteoarthritis Cartilage*. Oct 2017;25(10):1698-1707. doi:10.1016/j.joca.2017.06.002
164. Ji ML, Jiang H, Wu F, et al. Precise targeting of miR-141/200c cluster in chondrocytes attenuates osteoarthritis development. *Ann Rheum Dis*. Mar 2021;80(3):356-366. doi:10.1136/annrheumdis-2020-218469
165. Ji M-l, Jiang H, Zhang X-j, et al. Preclinical development of a microRNA-based therapy for intervertebral disc degeneration. *Nature Communications*. 2018/11/28 2018;9(1):5051. doi:10.1038/s41467-018-07360-1
166. Xu Q, Xing H, Wu J, Chen W, Zhang N. miRNA-141 Induced Pyroptosis in Intervertebral Disk Degeneration by Targeting ROS Generation and Activating TXNIP/NLRP3 Signaling in Nucleus Pulpous Cells. Original Research. *Frontiers in Cell and Developmental Biology*. 2020-August-31 2020;8doi:10.3389/fcell.2020.00871
167. Qin C, Lv Y, Zhao H, Yang B, Zhang P. MicroRNA-149 Suppresses Inflammation in Nucleus Pulposus Cells of Intervertebral Discs by Regulating MyD88. *Med Sci Monit*. Jul 2 2019;25:4892-4900. doi:10.12659/msm.915858
168. Wang Z, Hu J, Pan Y, et al. miR-140-5p/miR-149 Affects Chondrocyte Proliferation, Apoptosis, and Autophagy by Targeting FUT1 in Osteoarthritis. *Inflammation*. Jun 2018;41(3):959-971. doi:10.1007/s10753-018-0750-6
169. Penolazzi L, Lambertini E, Bergamin LS, et al. MicroRNA-221 silencing attenuates the degenerated phenotype of intervertebral disc cells. *Aging (Albany NY)*. Aug 20 2018;10(8):2001-2015. doi:10.18632/aging.101525
170. Penolazzi L, Lambertini E, Scussel Bergamin L, et al. Reciprocal Regulation of TRPS1 and miR-221 in Intervertebral Disc Cells. *Cells*. Sep 28 2019;8(10)doi:10.3390/cells8101170
171. Bennie LA, Feng J, Emmerson C, et al. Formulating RALA/Au nanocomplexes to enhance nanoparticle internalisation efficiency, sensitising prostate tumour models to radiation treatment. *Journal of Nanobiotechnology*. 2021/09/19 2021;19(1):279. doi:10.1186/s12951-021-01019-8
172. McCrudden CM, McBride JW, McCaffrey J, et al. Gene therapy with RALA/iNOS composite nanoparticles significantly enhances survival in a model of metastatic prostate cancer. *Cancer Nanotechnol*. 2018;9(1):5. doi:10.1186/s12645-018-0040-x

173. Wang J, Tian Y, Phillips KL, et al. Tumor necrosis factor α- and interleukin-1β-dependent induction of CCL3 expression by nucleus pulposus cells promotes macrophage migration through CCR1. *Arthritis Rheum*. Mar 2013;65(3):832-42. doi:10.1002/art.37819
174. Wang J, Markova D, Anderson DG, Zheng Z, Shapiro IM, Risbud MV. TNF-α and IL-1β promote a disintegrin-like and metalloprotease with thrombospondin type I motif-5-mediated aggrecan degradation through syndecan-4 in intervertebral disc. *J Biol Chem*. Nov 18 2011;286(46):39738-49. doi:10.1074/jbc.M111.264549
175. Huang H-Y, Lin Y-C-D, Cui S, et al. miRTarBase update 2022: an informative resource for experimentally validated miRNA–target interactions. *Nucleic Acids Research*. 2021;50(D1):D222-D230. doi:10.1093/nar/gkab1079
176. Licursi V, Conte F, Fiscon G, Paci P. MIENTURNET: an interactive web tool for microRNA-target enrichment and network-based analysis. *BMC Bioinformatics*. 2019/11/04 2019;20(1):545. doi:10.1186/s12859-019-3105-x
177. Shannon P, Markiel A, Ozier O, et al. Cytoscape: a software environment for integrated models of biomolecular interaction networks. *Genome Res*. Nov 2003;13(11):2498-504. doi:10.1101/gr.1239303
178. Snel B, Lehmann G, Bork P, Huynen MA. STRING: a web-server to retrieve and display the repeatedly occurring neighbourhood of a gene. *Nucleic Acids Res*. Sep 15 2000;28(18):3442-4. doi:10.1093/nar/28.18.3442
179. Szklarczyk D, Kirsch R, Koutrouli M, et al. The STRING database in 2023: protein-protein association networks and functional enrichment analyses for any sequenced genome of interest. *Nucleic Acids Res*. Jan 6 2023;51(D1):D638-d646. doi:10.1093/nar/gkac1000
180. Wang W, Yang C, Wang Xy, et al. MicroRNA-129 and -335 Promote Diabetic Wound Healing by Inhibiting Sp1-Mediated MMP-9 Expression. *Diabetes*. 2018;67(8):1627-1638. doi:10.2337/db17-1238
181. Kasinski AL, Kelnar K, Stahlhut C, et al. A combinatorial microRNA therapeutics approach to suppressing non-small cell lung cancer. *Oncogene*. Jul 2015;34(27):3547-55. doi:10.1038/onc.2014.282
182. Schoolmeesters A, Eklund T, Leake D, et al. Functional Profiling Reveals Critical Role for miRNA in Differentiation of Human Mesenchymal Stem Cells. *PLOS ONE*. 2009;4(5):e5605. doi:10.1371/journal.pone.0005605
183. Mariner PD, Johannesen E, Anseth KS. Manipulation of miRNA activity accelerates osteogenic differentiation of hMSCs in engineered 3D scaffolds. *J Tissue Eng Regen Med*. Apr 2012;6(4):314-24. doi:10.1002/term.435
184. Castaño IM, Raftery RM, Chen G, et al. Dual Scaffold Delivery of miR-210 Mimic and miR-16 Inhibitor Enhances Angiogenesis and Osteogenesis to Accelerate Bone Healing. *Acta Biomater*. Oct 3 2023;doi:10.1016/j.actbio.2023.09.049
185. Jensen C, Teng Y. Is It Time to Start Transitioning From 2D to 3D Cell Culture? Review. *Frontiers in Molecular Biosciences*. 2020-March-06 2020;7doi:10.3389/fmolb.2020.00033
186. Ndikung J, Storm D, Violet N, et al. Restoring circadian synchrony in vitro facilitates physiological responses to environmental chemicals. *Environment International*. 2020/01/01/ 2020;134:105265. doi:https://doi.org/10.1016/j.envint.2019.105265
187. Kaeffer B, Pardini L. Clock genes of Mammalian cells: practical implications in tissue culture. *In Vitro Cell Dev Biol Anim*. Nov-Dec 2005;41(10):311-20. doi:10.1007/s11626-005-0001-7
188. Yang M, Zhang L, Gibson GJ. Chondrocyte miRNAs 221 and 483-5p respond to loss of matrix interaction by modulating proliferation and matrix synthesis. *Connect Tissue Res*. Jun 2015;56(3):236-43. doi:10.3109/03008207.2015.1018384

189. Lolli A, Narcisi R, Lambertini E, et al. Silencing of Antichondrogenic MicroRNA-221 in Human Mesenchymal Stem Cells Promotes Cartilage Repair In Vivo. *Stem Cells*. Jul 2016;34(7):1801-11. doi:10.1002/stem.2350
190. Lambertini E, Penolazzi L, Notarangelo MP, et al. Pro-differentiating compounds for human intervertebral disc cells are present in Violina pumpkin leaf extracts. *Int J Mol Med*. May 2023;51(5)doi:10.3892/ijmm.2023.5242
191. Chen Q, Wu S, Wu Y, Chen L, Pang Q. MiR-149 suppresses the inflammatory response of chondrocytes in osteoarthritis by down-regulating the activation of TAK1/NF-κB. *Biomed Pharmacother*. May 2018;101:763-768. doi:10.1016/j.biopha.2018.02.133
192. Santini P, Politi L, Vedova PD, Scandurra R, Scotto d'Abusco A. The inflammatory circuitry of miR-149 as a pathological mechanism in osteoarthritis. *Rheumatol Int*. May 2014;34(5):711-6. doi:10.1007/s00296-013-2754-8
193. Li H, Wang X, Pan H, et al. The mechanisms and functions of IL-1β in intervertebral disc degeneration. *Exp Gerontol*. Jun 15 2023;177:112181. doi:10.1016/j.exger.2023.112181
194. Johnson ZI, Schoepflin ZR, Choi H, Shapiro IM, Risbud MV. Disc in flames: Roles of TNF-α and IL-1β in intervertebral disc degeneration. *Eur Cell Mater*. Sep 21 2015;30:104-16; discussion 116-7. doi:10.22203/ecm.v030a08
195. Deng X, Zhao F, Kang B, Zhang X. Elevated interleukin-6 expression levels are associated with intervertebral disc degeneration. *Exp Ther Med*. Apr 2016;11(4):1425-1432. doi:10.3892/etm.2016.3079
196. Weber KT, Alipui DO, Sison CP, et al. Serum levels of the proinflammatory cytokine interleukin-6 vary based on diagnoses in individuals with lumbar intervertebral disc diseases. *Arthritis Research & Therapy*. 2016/01/07 2016;18(1):3. doi:10.1186/s13075-015-0887-8
197. Haddadi K, Abediankenari S, Alipour A, et al. Association between Serum Levels of Interleukin-6 on Pain and Disability in Lumbar Disc Herniation Surgery. *Asian J Neurosurg*. Jul-Sep 2020;15(3):494-498. doi:10.4103/ajns.AJNS_71_20
198. Huang D, Xiao J, Deng X, et al. Association between Fas/FasL gene polymorphism and musculoskeletal degenerative diseases: a meta-analysis. *BMC Musculoskelet Disord*. May 7 2018;19(1):137. doi:10.1186/s12891-018-2057-z
199. Han D, Ding Y, Liu S-L, et al. Double role of Fas ligand in the apoptosis of intervertebral disc cells in vitro. *Acta Biochimica et Biophysica Sinica*. 2009;41(11):938-947. doi:10.1093/abbs/gmp087
200. Yamamoto J, Maeno K, Takada T, et al. Fas ligand plays an important role for the production of pro-inflammatory cytokines in intervertebral disc nucleus pulposus cells. *Journal of Orthopaedic Research*. 2013;31(4):608-615. doi:https://doi.org/10.1002/jor.22274
201. Qin C, Zhang B, Zhang L, et al. MyD88-dependent Toll-like receptor 4 signal pathway in intervertebral disc degeneration. *Exp Ther Med*. Aug 2016;12(2):611-618. doi:10.3892/etm.2016.3425
202. Bayer AL, Alcaide P. MyD88: At the heart of inflammatory signaling and cardiovascular disease. *Journal of Molecular and Cellular Cardiology*. 2021/12/01/ 2021;161:75-85. doi:https://doi.org/10.1016/j.yjmcc.2021.08.001
203. Zheng C, Chen J, Chu F, Zhu J, Jin T. Inflammatory Role of TLR-MyD88 Signaling in Multiple Sclerosis. Review. *Frontiers in Molecular Neuroscience*. 2020-January-10 2020;12doi:10.3389/fnmol.2019.00314
204. Rastogi A, Kim H, Twomey JD, Hsieh AH. MMP-2 mediates local degradation and remodeling of collagen by annulus fibrosus cells of the intervertebral disc. *Arthritis Res Ther*. Apr 27 2013;15(2):R57. doi:10.1186/ar4224

205. Zhang Y, Gu Z, Qiu G. Association of the polymorphism of MMP2 with the risk and severity of lumbar disc degeneration in the Chinese Han population. *Eur Rev Med Pharmacol Sci*. Jul 2013;17(13):1830-4.
206. Fan D, Kassiri Z. Biology of Tissue Inhibitor of Metalloproteinase 3 (TIMP3), and Its Therapeutic Implications in Cardiovascular Pathology. Review. *Frontiers in Physiology*. 2020-June-16 2020;11doi:10.3389/fphys.2020.00661
207. He M, Pang J, Sun H, Zheng G, Lin Y, Ge W. Overexpression of TIMP3 inhibits discogenic pain by suppressing angiogenesis and the expression of substance P in nucleus pulposus. *Mol Med Rep*. Mar 2020;21(3):1163-1171. doi:10.3892/mmr.2020.10922
208. Er ZJ, Yin CF, Wang WJ, Chen XJ. Serum CXCL12/SDF-1 level is positively related with lumbar intervertebral disc degeneration and clinical severity. *Innate Immun*. Jul 2020;26(5):341-350. doi:10.1177/1753425919895086
209. Zhang H, Zhu T, Zhang L, Wu Q. Stromal cell-derived factor-1 induces matrix metalloproteinase expression in human endplate chondrocytes, cartilage endplate degradation in explant culture, and the amelioration of nucleus pulposus degeneration in vivo. *Int J Mol Med*. Feb 2018;41(2):969-976. doi:10.3892/ijmm.2017.3278
210. Liu Z, Ma C, Shen J, Wang D, Hao J, Hu Z. SDF-1/CXCR4 axis induces apoptosis of human degenerative nucleus pulposus cells via the NF-κB pathway. *Mol Med Rep*. 2016/07/01 2016;14(1):783-789. doi:10.3892/mmr.2016.5341
211. Liu Z-c, Wang Z-l, Huang C-y, et al. Duhuo Jisheng Decoction inhibits SDF-1-induced inflammation and matrix degradation in human degenerative nucleus pulposus cells in vitro through the CXCR4/NF-κB pathway. *Acta Pharmacologica Sinica*. 2018/06/01 2018;39(6):912-922. doi:10.1038/aps.2018.36
212. Zhong H, Zhou Z, Guo L, et al. The miR-623/CXCL12 axis inhibits LPS-induced nucleus pulposus cell apoptosis and senescence. *Mech Ageing Dev*. Mar 2021;194:111417. doi:10.1016/j.mad.2020.111417
213. Kluba T, Niemeyer T, Gaissmaier C, Gründer T. Human anulus fibrosis and nucleus pulposus cells of the intervertebral disc: effect of degeneration and culture system on cell phenotype. *Spine (Phila Pa 1976)*. Dec 15 2005;30(24):2743-8. doi:10.1097/01.brs.0000192204.89160.6d
214. Gantenbein B, Calandriello E, Wuertz-Kozak K, Benneker LM, Keel MJB, Chan SCW. Activation of intervertebral disc cells by co-culture with notochordal cells, conditioned medium and hypoxia. *BMC Musculoskeletal Disorders*. 2014/12/11 2014;15(1):422. doi:10.1186/1471-2474-15-422
215. Liu Z, Zheng Z, Qi J, et al. CD24 identifies nucleus pulposus progenitors/notochordal cells for disc regeneration. *Journal of Biological Engineering*. 2018/12/22 2018;12(1):35. doi:10.1186/s13036-018-0129-0
216. Gantenbein-Ritter B, Chan SC. The evolutionary importance of cell ratio between notochordal and nucleus pulposus cells: an experimental 3-D co-culture study. *Eur Spine J*. Aug 2012;21 Suppl 6(Suppl 6):S819-25. doi:10.1007/s00586-011-2026-9
217. Dou Y, Sun X, Ma X, Zhao X, Yang Q. Intervertebral Disk Degeneration: The Microenvironment and Tissue Engineering Strategies. Review. *Frontiers in Bioengineering and Biotechnology*. 2021-July-20 2021;9doi:10.3389/fbioe.2021.592118
218. Frapin L, Clouet J, Delplace V, Fusellier M, Guicheux J, Le Visage C. Lessons learned from intervertebral disc pathophysiology to guide rational design of sequential delivery systems for therapeutic biological factors. *Advanced Drug Delivery Reviews*. 2019/09/01/ 2019;149-150:49-71. doi:https://doi.org/10.1016/j.addr.2019.08.007
219. Guerrero J, Häckel S, Croft AS, Hoppe S, Albers CE, Gantenbein B. The nucleus pulposus microenvironment in the intervertebral disc: the fountain of youth? *Eur Cell Mater*. Jun 15 2021;41:707-738. doi:10.22203/eCM.v041a46

220. Altun I. Cytokine profile in degenerated painful intervertebral disc: variability with respect to duration of symptoms and type of disease. *Spine J*. Jul 2016;16(7):857-61. doi:10.1016/j.spinee.2016.03.019
221. Bachmeier BE, Nerlich A, Mittermaier N, et al. Matrix metalloproteinase expression levels suggest distinct enzyme roles during lumbar disc herniation and degeneration. *Eur Spine J*. Nov 2009;18(11):1573-86. doi:10.1007/s00586-009-1031-8
222. Raftery RM, Walsh DP, Blokpoel Ferreras L, et al. Highly versatile cell-penetrating peptide loaded scaffold for efficient and localised gene delivery to multiple cell types: From development to application in tissue engineering. *Biomaterials*. Sep 2019;216:119277. doi:10.1016/j.biomaterials.2019.119277
223. Lee S, Millecamps M, Foster DZ, Stone LS. Long-term histological analysis of innervation and macrophage infiltration in a mouse model of intervertebral disc injury-induced low back pain. *J Orthop Res*. Jun 2020;38(6):1238-1247. doi:10.1002/jor.24560
224. Wuertz K, Haglund L. Inflammatory Mediators in Intervertebral Disk Degeneration and Discogenic Pain. *Global Spine Journal*. 2013;3(3):175-184. doi:10.1055/s-0033-1347299
225. Sakai D, Mochida J, Yamamoto Y, et al. Transplantation of mesenchymal stem cells embedded in Atelocollagen gel to the intervertebral disc: a potential therapeutic model for disc degeneration. *Biomaterials*. Sep 2003;24(20):3531-41. doi:10.1016/s0142-9612(03)00222-9
226. Henriksson HB, Svanvik T, Jonsson M, et al. Transplantation of human mesenchymal stems cells into intervertebral discs in a xenogeneic porcine model. *Spine (Phila Pa 1976)*. Jan 15 2009;34(2):141-8. doi:10.1097/BRS.0b013e31818f8c20
227. Schol J, Sakai D. Comprehensive narrative review on the analysis of outcomes from cell transplantation clinical trials for discogenic low back pain. *N Am Spine Soc J*. Mar 2023;13:100195. doi:10.1016/j.xnsj.2022.100195
228. Li C, Bai Q, Lai Y, et al. Advances and Prospects in Biomaterials for Intervertebral Disk Regeneration. Review. *Frontiers in Bioengineering and Biotechnology*. 2021-October-22 2021;9doi:10.3389/fbioe.2021.766087
229. Ma T, Liu C, Zhao Q, Zhang Y, Xiao L. Decellularized nucleus pulposus matrix/chitosan hybrid hydrogel combined with nucleus pulposus stem cells and GDF5-loaded microspheres for intervertebral disc degeneration prevention. *Molecular Medicine*. 2024/01/10 2024;30(1):7. doi:10.1186/s10020-024-00777-z
230. Koo YW, Lim CS, Darai A, et al. Shape-memory collagen scaffold combined with hyaluronic acid for repairing intervertebral disc. *Biomaterials Research*. 2023/03/29 2023;27(1):26. doi:10.1186/s40824-023-00368-9
231. Hodgkinson T, Shen B, Diwan A, Hoyland JA, Richardson SM. Therapeutic potential of growth differentiation factors in the treatment of degenerative disc diseases. *JOR Spine*. Mar 2019;2(1):e1045. doi:10.1002/jsp2.1045
232. Guo S, Cui L, Xiao C, et al. The Mechanisms and Functions of GDF-5 in Intervertebral Disc Degeneration. *Orthopaedic Surgery*. 2021;13(3):734-741. doi:https://doi.org/10.1111/os.12942
233. THOMPSON JP, OEGEMA TR, BRADFORD D. Stimulation of Mature Canine Intervertebral Disc by Growth Factors. *Spine*. 1991;16(3):253-260.
234. Walsh AJ, Bradford DS, Lotz JC. In vivo growth factor treatment of degenerated intervertebral discs. *Spine (Phila Pa 1976)*. Jan 15 2004;29(2):156-63. doi:10.1097/01.Brs.0000107231.67854.9f
235. Willems N, Bach FC, Plomp SG, et al. Intradiscal application of rhBMP-7 does not induce regeneration in a canine model of spontaneous intervertebral disc degeneration. *Arthritis Res Ther*. May 27 2015;17(1):137. doi:10.1186/s13075-015-0625-2

236. Mitchell AC, Briquez PS, Hubbell JA, Cochran JR. Engineering growth factors for regenerative medicine applications. *Acta Biomater*. Jan 2016;30:1-12. doi:10.1016/j.actbio.2015.11.007
237. Doucet C, Ernou I, Zhang Y, et al. Platelet lysates promote mesenchymal stem cell expansion: A safety substitute for animal serum in cell-based therapy applications. *Journal of Cellular Physiology*. 2005;205(2):228-236. doi:https://doi.org/10.1002/jcp.20391
238. Tuakli-Wosornu YA, Terry A, Boachie-Adjei K, et al. Lumbar Intradiskal Platelet-Rich Plasma (PRP) Injections: A Prospective, Double-Blind, Randomized Controlled Study. *Pm r*. Jan 2016;8(1):1-10; quiz 10. doi:10.1016/j.pmrj.2015.08.010
239. Akeda K, Ohishi K, Masuda K, et al. Intradiscal Injection of Autologous Platelet-Rich Plasma Releasate to Treat Discogenic Low Back Pain: A Preliminary Clinical Trial. *Asian Spine J*. Jun 2017;11(3):380-389. doi:10.4184/asj.2017.11.3.380
240. McDonnell EE, Buckley CT. Consolidating and re-evaluating the human disc nutrient microenvironment. *JOR SPINE*. 2022;5(1):e1192. doi:https://doi.org/10.1002/jsp2.1192
241. Barcellona MN, Ní Néill T, O'Brien FJ, Dixon JE, Curtin CM, Buckley CT. Modulation of Inflammation and Regeneration in the Intervertebral Disc Using Enhanced Cell-Penetrating Peptides for MicroRNA Delivery. *Advanced NanoBiomed Research*. 2024;4(7):2300112. doi:https://doi.org/10.1002/anbr.202300112
242. Ní Néill T, Barcellona MN, Wilson N, et al. In vitro and ex vivo screening of microRNA combinations with enhanced cell penetrating peptides to stimulate intervertebral disc regeneration. *JOR Spine*. Dec 2024;7(4):e1366. doi:10.1002/jsp2.1366
243. Zhang J, Liu D, Gong Q, Chen J, Wan L. Intradiscal Autologous Platelet-Rich Plasma Injection for Discogenic Low Back Pain: A Clinical Trial. *Biomed Res Int*. 2022;2022:9563693. doi:10.1155/2022/9563693
244. Xie S-c, Yang L, Shu T, Liu Q, Wang W. miR-149-5p mitigates tumor necrosis factor-α-induced chondrocyte apoptosis by inhibiting TRADD. journal article. *Archives of Medical Science*. 2024;20(2):602-611. doi:10.5114/aoms.2020.92324
245. Jiang Y, Zhang L, Tian H. MicroRNA-149 improves osteoarthritis via repression of VCAM-1 and inactivation of PI3K/AKT pathway. *Experimental Gerontology*. 2023/04/01/ 2023;174:112103. doi:https://doi.org/10.1016/j.exger.2023.112103
246. Backly RE, Ulivi V, Tonachini L, Cancedda R, Descalzi F, Mastrogiacomo M. Platelet Lysate Induces In Vitro Wound Healing of Human Keratinocytes Associated with a Strong Proinflammatory Response. *Tissue Engineering Part A*. 2011/07/01 2011;17(13-14):1787-1800. doi:10.1089/ten.tea.2010.0729
247. Pereira RC, Scaranari M, Benelli R, et al. Dual effect of platelet lysate on human articular cartilage: a maintenance of chondrogenic potential and a transient proinflammatory activity followed by an inflammation resolution. *Tissue Eng Part A*. Jun 2013;19(11-12):1476-88. doi:10.1089/ten.TEA.2012.0225
248. Pan X, Yuan S, Xun X, et al. Long-Term Recruitment of Endogenous M2 Macrophages by Platelet Lysate-Rich Plasma Macroporous Hydrogel Scaffold for Articular Cartilage Defect Repair. *Advanced Healthcare Materials*. 2022;11(6):2101661. doi:https://doi.org/10.1002/adhm.202101661
249. Filardo G, Di Matteo B, Di Martino A, et al. Platelet-Rich Plasma Intra-articular Knee Injections Show No Superiority Versus Viscosupplementation: A Randomized Controlled Trial. *Am J Sports Med*. Jul 2015;43(7):1575-82. doi:10.1177/0363546515582027
250. Khoshbin A, Leroux T, Wasserstein D, et al. The Efficacy of Platelet-Rich Plasma in the Treatment of Symptomatic Knee Osteoarthritis: A Systematic Review With

Quantitative Synthesis. *Arthroscopy: The Journal of Arthroscopic & Related Surgery*. 2013/12/01/ 2013;29(12):2037-2048. doi:https://doi.org/10.1016/j.arthro.2013.09.006
251. Le NTN, Han CL, Delila L, et al. Proteomics of human platelet lysates and insight from animal studies on platelet protein diffusion to hippocampus upon intranasal administration. *APL Bioeng*. Jun 2024;8(2):026111. doi:10.1063/5.0196553
252. Delila L, Wu Y-W, Nebie O, et al. Extensive characterization of the composition and functional activities of five preparations of human platelet lysates for dedicated clinical uses. *Platelets*. 2021/02/17 2021;32(2):259-272. doi:10.1080/09537104.2020.1849603
253. Yang H, Yuan C, Wu C, et al. The role of TGF-β1/Smad2/3 pathway in platelet-rich plasma in retarding intervertebral disc degeneration. *Journal of Cellular and Molecular Medicine*. 2016;20(8):1542-1549. doi:https://doi.org/10.1111/jcmm.12847
254. Huang J, Lian S-l, Han J-h, Lu Z-c, Ding Y. Pure platelet-rich plasma promotes semaphorin-3A expression: a novel insight to ameliorate intervertebral disk degeneration in vitro. *Journal of Orthopaedic Surgery and Research*. 2023/10/20 2023;18(1):789. doi:10.1186/s13018-023-04290-7
255. Nikkhoo M, Wang JL, Abdollahi M, Hsu YC, Parnianpour M, Khalaf K. A regenerative approach towards recovering the mechanical properties of degenerated intervertebral discs: Genipin and platelet-rich plasma therapies. *Proc Inst Mech Eng H*. Feb 2017;231(2):127-137. doi:10.1177/0954411916681597
256. An S, Intini C, O'Shea D, Dixon JE, Zheng Y, O'Brien FJ. A miR-activated hydrogel for the delivery of a pro-chondrogenic microRNA-221 inhibitor as a minimally invasive therapeutic approach for articular cartilage repair. *Materials Today Bio*. 2025/02/01/ 2025;30:101382. doi:https://doi.org/10.1016/j.mtbio.2024.101382
257. Xu YQ, Zhang ZH, Zheng YF, Feng SQ. MicroRNA-221 Regulates Hypertrophy of Ligamentum Flavum in Lumbar Spinal Stenosis by Targeting TIMP-2. *Spine (Phila Pa 1976)*. Feb 2016;41(4):275-82. doi:10.1097/brs.0000000000001226
258. Guerrero J, Häckel S, Croft AS, Albers CE, Gantenbein B. The effects of 3D culture on the expansion and maintenance of nucleus pulposus progenitor cell multipotency. *JOR Spine*. Mar 2021;4(1):e1131. doi:10.1002/jsp2.1131
259. Sun Y, Lv M, Zhou L, et al. Enrichment of committed human nucleus pulposus cells expressing chondroitin sulfate proteoglycans under alginate encapsulation. *Osteoarthritis Cartilage*. Jul 2015;23(7):1194-203. doi:10.1016/j.joca.2015.02.166
260. Prudnikova K, Lightfoot Vidal SE, Sarkar S, et al. Aggrecan-like biomimetic proteoglycans (BPGs) composed of natural chondroitin sulfate bristles grafted onto a poly(acrylic acid) core for molecular engineering of the extracellular matrix. *Acta Biomaterialia*. 2018/07/15/ 2018;75:93-104. doi:https://doi.org/10.1016/j.actbio.2018.05.013
261. Borrelli C, Buckley CT. Injectable Disc-Derived ECM Hydrogel Functionalised with Chondroitin Sulfate for Intervertebral Disc Regeneration. *Acta Biomater*. Nov 2020;117:142-155. doi:10.1016/j.actbio.2020.10.002
262. Xing H, Zhang Z, Mao Q, et al. Injectable exosome-functionalized extracellular matrix hydrogel for metabolism balance and pyroptosis regulation in intervertebral disc degeneration. *J Nanobiotechnology*. Sep 6 2021;19(1):264. doi:10.1186/s12951-021-00991-5
263. Yuan M, Pai PJ, Liu X, Lam H, Chan BP. Proteomic Analysis of Nucleus Pulposus Cell-derived Extracellular Matrix Niche and Its Effect on Phenotypic Alteration of Dermal Fibroblasts. *Sci Rep*. Jan 24 2018;8(1):1512. doi:10.1038/s41598-018-19931-9
264. Rashidi N, Dowell N, Covill D, Shepperd J, Santin M. Biomimetic Hydrogels for In Vitro Modelling of Nucleus Pulposus Degeneration: Effects of Extracellular Matrix

Compositional Change on Physicochemical Properties and Cell Phenotype. *Journal of Functional Biomaterials*. 2025;16(7):253.
265. Xia M, Zhu Y. Expression of integrin subunits in the herniated intervertebral disc. *Connect Tissue Res*. 2008;49(6):464-9. doi:10.1080/03008200802325425
266. Peng Y, Qing X, Lin H, et al. Decellularized Disc Hydrogels for hBMSCs tissue-specific differentiation and tissue regeneration. *Bioact Mater*. Oct 2021;6(10):3541-3556. doi:10.1016/j.bioactmat.2021.03.014
267. Rustenburg CM, Snuggs JW, Emanuel KS, et al. Modelling the catabolic environment of the moderately degenerated disc with a caprine ex vivo loaded disc culture system. *Eur Cell Mater*. Jul 16 2020;40:21-37. doi:10.22203/eCM.v040a02
268. Hoogendoorn RJ, Helder MN, Kroeze RJ, Bank RA, Smit TH, Wuisman PI. Reproducible long-term disc degeneration in a large animal model. *Spine (Phila Pa 1976)*. Apr 20 2008;33(9):949-54. doi:10.1097/BRS.0b013e31816c90f0
269. Takahashi H, Suguro T, Okazima Y, Motegi M, Okada Y, Kakiuchi T. Inflammatory cytokines in the herniated disc of the lumbar spine. *Spine (Phila Pa 1976)*. Jan 15 1996;21(2):218-24. doi:10.1097/00007632-199601150-00011
270. Guo Z, Qiu C, Mecca C, et al. Elevated lymphotoxin-α (TNFβ) is associated with intervertebral disc degeneration. *BMC Musculoskeletal Disorders*. 2021/01/13 2021;22(1):77. doi:10.1186/s12891-020-03934-7
271. Lv J, He J, Ni Y, et al. Immune cell infiltration and inflammatory response in nucleus pulposus following annular disruption in degenerative disc disease. *BMC Musculoskelet Disord*. Nov 28 2025;26(1):1080. doi:10.1186/s12891-025-09340-1
272. Kodama J, Wilkinson KJ, Otsuru S. Nutrient metabolism of the nucleus pulposus: A literature review. *N Am Spine Soc J*. Mar 2023;13:100191. doi:10.1016/j.xnsj.2022.100191
273. Johnston SN, Silagi ES, Madhu V, Nguyen DH, Shapiro IM, Risbud MV. GLUT1 is redundant in hypoxic and glycolytic nucleus pulposus cells of the intervertebral disc. *JCI Insight*. 04/24/ 2023;8(8)doi:10.1172/jci.insight.164883
274. Chen X, Zhu L, Wu G, Liang Z, Yang L, Du Z. A comparison between nucleus pulposus-derived stem cell transplantation and nucleus pulposus cell transplantation for the treatment of intervertebral disc degeneration in a rabbit model. *Int J Surg*. Apr 2016;28:77-82. doi:10.1016/j.ijsu.2016.02.045
275. Nukaga T, Sakai D, Tanaka M, Hiyama A, Nakai T, Mochida J. Transplantation of activated nucleus pulposus cells after cryopreservation: efficacy study in a canine disc degeneration model. *Eur Cell Mater*. Jan 27 2016;31:95-106. doi:10.22203/ecm.v031a07
276. Williams RJ, Tryfonidou MA, Snuggs JW, Le Maitre CL. Cell sources proposed for nucleus pulposus regeneration. *JOR Spine*. Dec 2021;4(4):e1175. doi:10.1002/jsp2.1175
277. Wang W, Wang Y, Deng G, et al. Transplantation of Hypoxic-Preconditioned Bone Mesenchymal Stem Cells Retards Intervertebral Disc Degeneration via Enhancing Implanted Cell Survival and Migration in Rats. *Stem Cells International*. 2018;2018(1):7564159. doi:https://doi.org/10.1155/2018/7564159
278. Orozco L, Soler R, Morera C, Alberca M, Sánchez A, García-Sancho J. Intervertebral disc repair by autologous mesenchymal bone marrow cells: a pilot study. *Transplantation*. Oct 15 2011;92(7):822-8. doi:10.1097/TP.0b013e3182298a15
279. Zhang YG, Guo X, Xu P, Kang LL, Li J. Bone mesenchymal stem cells transplanted into rabbit intervertebral discs can increase proteoglycans. *Clin Orthop Relat Res*. Jan 2005;(430):219-26. doi:10.1097/01.blo.0000146534.31120.cf
280. Zhang Y, Drapeau S, Howard SA, Thonar EJ, Anderson DG. Transplantation of goat bone marrow stromal cells to the degenerating intervertebral disc in a goat disc injury

model. *Spine (Phila Pa 1976)*. Mar 1 2011;36(5):372-7. doi:10.1097/BRS.0b013e3181d10401
281. Li W, Zhao H, Xiong Z, et al. Evaluation of the Efficacy of Stem Cell Therapy in Animal Models of Intervertebral Disc Degeneration Based on Imaging Indicators: A Systematic Review and Meta-Analysis. *Stem Cells Int*. 2022;2022:2482653. doi:10.1155/2022/2482653
282. Pittenger MF, Mackay AM, Beck SC, et al. Multilineage Potential of Adult Human Mesenchymal Stem Cells. *Science*. 1999;284(5411):143-147. doi:doi:10.1126/science.284.5411.143
283. Johnstone B, Hering TM, Caplan AI, Goldberg VM, Yoo JU. In VitroChondrogenesis of Bone Marrow-Derived Mesenchymal Progenitor Cells. *Experimental Cell Research*. 1998/01/10/ 1998;238(1):265-272. doi:https://doi.org/10.1006/excr.1997.3858
284. Gómez-Leduc T, Hervieu M, Legendre F, et al. Chondrogenic commitment of human umbilical cord blood-derived mesenchymal stem cells in collagen matrices for cartilage engineering. *Scientific Reports*. 2016/09/08 2016;6(1):32786. doi:10.1038/srep32786
285. Blokpoel Ferreras LA, Scott D, Vazquez Reina S, et al. Enhanced Cellular Transduction of Nanoparticles Resistant to Rapidly Forming Plasma Protein Coronas. *Advanced Biosystems*. 2020;4(10):2000162. doi:https://doi.org/10.1002/adbi.202000162
286. Paul CP, Zuiderbaan HA, Zandieh Doulabi B, et al. Simulated-physiological loading conditions preserve biological and mechanical properties of caprine lumbar intervertebral discs in ex vivo culture. *PLoS One*. 2012;7(3):e33147. doi:10.1371/journal.pone.0033147
287. McDonnell EE, Wilson N, Barcellona MN, et al. Preclinical to clinical translation for intervertebral disc repair: Effects of species-specific scale, metabolism, and matrix synthesis rates on cell-based regeneration. *JOR SPINE*. 2023;6(3):e1279. doi:https://doi.org/10.1002/jsp2.1279
288. Feng G, Zhao X, Liu H, et al. Transplantation of mesenchymal stem cells and nucleus pulposus cells in a degenerative disc model in rabbits: a comparison of 2 cell types as potential candidates for disc regeneration. *J Neurosurg Spine*. Mar 2011;14(3):322-9. doi:10.3171/2010.11.Spine10285
289. Lang H, Zhao F, Zhang T, et al. MicroRNA-149 contributes to scarless wound healing by attenuating inflammatory response. *Mol Med Rep*. Aug 2017;16(2):2156-2162. doi:10.3892/mmr.2017.6796
290. Li T, Peng Y, Chen Y, et al. Long intergenic non-coding RNA -00917 regulates the proliferation, inflammation, and pyroptosis of nucleus pulposus cells via targeting miR-149-5p/NOD-like receptor protein 1 axis. *Bioengineered*. 2022/03/01 2022;13(3):6036-6047. doi:10.1080/21655979.2022.2043100
291. Liu XG, Hou HW, Liu YL. Expression levels of IL-17 and TNF-α in degenerated lumbar intervertebral discs and their correlation. *Exp Ther Med*. 2016/06/01 2016;11(6):2333-2340. doi:10.3892/etm.2016.3250
292. Redondo-Castro E, Cunningham CJ, Miller J, Brown H, Allan SM, Pinteaux E. Changes in the secretome of tri-dimensional spheroid-cultured human mesenchymal stem cells in vitro by interleukin-1 priming. *Stem Cell Res Ther*. Jan 17 2018;9(1):11. doi:10.1186/s13287-017-0753-5
293. Stich S, Stolk M, Girod PP, et al. Regenerative and Immunogenic Characteristics of Cultured Nucleus Pulposus Cells from Human Cervical Intervertebral Discs. *PLOS ONE*. 2015;10(5):e0126954. doi:10.1371/journal.pone.0126954

294. Miguélez-Rivera L, Pérez-Castrillo S, González-Fernández ML, et al. Immunomodulation of mesenchymal stem cells in discogenic pain. *The Spine Journal*. 2018;18(2):330-342. doi:10.1016/j.spinee.2017.09.002
295. Saldaña L, Bensiamar F, Vallés G, Mancebo FJ, García-Rey E, Vilaboa N. Immunoregulatory potential of mesenchymal stem cells following activation by macrophage-derived soluble factors. *Stem Cell Res Ther*. Feb 13 2019;10(1):58. doi:10.1186/s13287-019-1156-6
296. Yamagata T, Saito H, Habuchi O, Suzuki S. Purification and Properties of Bacterial Chondroitinases and Chondrosulfatases. *Journal of Biological Chemistry*. 1968/04/10/ 1968;243(7):1523-1535. doi:https://doi.org/10.1016/S0021-9258(18)93574-X
297. Ilic MZ, Robinson HC, Handley CJ. Characterization of Aggrecan Retained and Lost from the Extracellular Matrix of Articular Cartilage: INVOLVEMENT OF CARBOXYL-TERMINAL PROCESSING IN THE CATABOLISM OF AGGRECAN*. *Journal of Biological Chemistry*. 1998/07/10/ 1998;273(28):17451-17458. doi:https://doi.org/10.1074/jbc.273.28.17451
298. Ghiselli G. Drug-Mediated Regulation of Glycosaminoglycan Biosynthesis. *Med Res Rev*. Sep 2017;37(5):1051-1094. doi:10.1002/med.21429
299. Prydz K. Determinants of Glycosaminoglycan (GAG) Structure. *Biomolecules*. Aug 21 2015;5(3):2003-22. doi:10.3390/biom5032003
300. Bi W, Deng JM, Zhang Z, Behringer RR, de Crombrugghe B. Sox9 is required for cartilage formation. *Nature Genetics*. 1999/05/01 1999;22(1):85-89. doi:10.1038/8792
301. Tsingas M, Ottone OK, Haseeb A, et al. Sox9 deletion causes severe intervertebral disc degeneration characterized by apoptosis, matrix remodeling, and compartment-specific transcriptomic changes. *Matrix Biol*. Dec 2020;94:110-133. doi:10.1016/j.matbio.2020.09.003
302. Sivan SS, Wachtel E, Roughley P. Structure, function, aging and turnover of aggrecan in the intervertebral disc. *Biochimica et Biophysica Acta (BBA) - General Subjects*. 2014/10/01/ 2014;1840(10):3181-3189. doi:https://doi.org/10.1016/j.bbagen.2014.07.013
303. Hayes AJ, Hughes CE, Ralphs JR, Caterson B. Chondroitin sulphate sulphation motif expression in the ontogeny of the intervertebral disc. *Eur Cell Mater*. Jan 7 2011;21:1-14.
304. Kim D, Song J, Jin EJ. MicroRNA-221 regulates chondrogenic differentiation through promoting proteosomal degradation of slug by targeting Mdm2. *J Biol Chem*. Aug 27 2010;285(35):26900-26907. doi:10.1074/jbc.M110.115105
305. Sheng B, Yuan Y, Liu X, et al. Protective effect of estrogen against intervertebral disc degeneration is attenuated by miR-221 through targeting estrogen receptor α. *Acta Biochim Biophys Sin (Shanghai)*. Apr 1 2018;50(4):345-354. doi:10.1093/abbs/gmy017
306. Yue R, Chen M, Ma N. Dual MicroRNA-Triggered Drug Release System for Combined Chemotherapy and Gene Therapy with Logic Operation. *ACS Applied Materials & Interfaces*. 2020/07/22 2020;12(29):32493-32502. doi:10.1021/acsami.0c09494
307. Liu Y, Zheng M, Jiao M, et al. Polymeric nanoparticle mediated inhibition of miR-21 with enhanced miR-124 expression for combinatorial glioblastoma therapy. *Biomaterials*. Sep 2021;276:121036. doi:10.1016/j.biomaterials.2021.121036
308. Shang M, Wu Y, Wang Y, Cai Y, Jin J, Yang Z. Dual antisense oligonucleotide targeting miR-21/miR-155 synergize photodynamic therapy to treat triple-negative breast cancer and inhibit metastasis. *Biomed Pharmacother*. Feb 2022;146:112564. doi:10.1016/j.biopha.2021.112564

309. Xu G, Zhang Z, Xing Y, et al. MicroRNA-149 negatively regulates TLR-triggered inflammatory response in macrophages by targeting MyD88. *J Cell Biochem*. May 2014;115(5):919-27. doi:10.1002/jcb.24734
310. Xu Q, Li P, Chen X, et al. miR-221/222 induces pancreatic cancer progression through the regulation of matrix metalloproteinases. *Oncotarget*. Jun 10 2015;6(16):14153-64. doi:10.18632/oncotarget.3686
311. Zhang Y, Xu J, Zhou Z, et al. Diurnal Asymmetric Loading Modulates Cell Phenotype in Intervertebral Disc. *JOR Spine*. Jun 2025;8(2):e70068. doi:10.1002/jsp2.70068
312. Gantenbein B, Grünhagen T, Lee CR, van Donkelaar CC, Alini M, Ito K. An in vitro organ culturing system for intervertebral disc explants with vertebral endplates: a feasibility study with ovine caudal discs. *Spine (Phila Pa 1976)*. Nov 1 2006;31(23):2665-73. doi:10.1097/01.brs.0000244620.15386.df
313. Šećerović A, Ristaniemi A, Cui S, et al. Toward the Next Generation of Spine Bioreactors: Validation of an Ex Vivo Intervertebral Disc Organ Model and Customized Specimen Holder for Multiaxial Loading. *ACS Biomaterials Science & Engineering*. 2022/09/12 2022;8(9):3969-3976. doi:10.1021/acsbiomaterials.2c00330
314. Prescott MJ, Lidster K. Improving quality of science through better animal welfare: the NC3Rs strategy. *Lab Animal*. 2017/04/01 2017;46(4):152-156. doi:10.1038/laban.1217
315. Parolin M, Gawri R, Mwale F, et al. Development of a whole disc organ culture system to study human intervertebral disc. *Evid Based Spine Care J*. Aug 2010;1(2):67-8. doi:10.1055/s-0028-1100919
316. Gawri R, Mwale F, Ouellet J, et al. Development of an organ culture system for long-term survival of the intact human intervertebral disc. *Spine (Phila Pa 1976)*. Oct 15 2011;36(22):1835-42. doi:10.1097/BRS.0b013e3181f81314
317. Bałkowiec-Iskra E, Vermehren-Schmaedick A, Balkowiec A. Tumor necrosis factor-α increases brain-derived neurotrophic factor expression in trigeminal ganglion neurons in an activity-dependent manner. *Neuroscience*. Apr 28 2011;180:322-33. doi:10.1016/j.neuroscience.2011.02.028
318. Saha RN, Liu X, Pahan K. Up-regulation of BDNF in astrocytes by TNF-alpha: a case for the neuroprotective role of cytokine. *J Neuroimmune Pharmacol*. 2006/09// 2006;1(3):212-222. doi:10.1007/s11481-006-9020-8
319. Takano S, Uchida K, Miyagi M, et al. Nerve Growth Factor Regulation by TNF-α and IL-1β in Synovial Macrophages and Fibroblasts in Osteoarthritic Mice. *J Immunol Res*. 2016;2016:5706359. doi:10.1155/2016/5706359
320. Urban JP, Roberts S. Degeneration of the intervertebral disc. *Arthritis Res Ther*. 2003;5(3):120-30. doi:10.1186/ar629
321. Mochida J, Sakai D, Nakamura Y, Watanabe T, Yamamoto Y, Kato S. Intervertebral disc repair with activated nucleus pulposus cell transplantation: a three-year, prospective clinical study of its safety. *Eur Cell Mater*. Mar 20 2015;29:202-12; discussion 212. doi:10.22203/ecm.v029a15
322. Haufe SM, Mork AR. Intradiscal injection of hematopoietic stem cells in an attempt to rejuvenate the intervertebral discs. *Stem Cells Dev*. Feb 2006;15(1):136-7. doi:10.1089/scd.2006.15.136
323. Hegewald AA, Endres M, Abbushi A, et al. Adequacy of herniated disc tissue as a cell source for nucleus pulposus regeneration: Laboratory investigation. *Journal of Neurosurgery: Spine*. 01 Feb. 2011 2011;14(2):273-280. doi:https://doi.org/10.3171/2010.10.SPINE10223
324. Cui S, Zhang L. microRNA-129-5p shuttled by mesenchymal stem cell-derived extracellular vesicles alleviates intervertebral disc degeneration via blockade of LRG1-

mediated p38 MAPK activation. *J Tissue Eng*. Jan-Dec 2021;12:20417314211021679. doi:10.1177/20417314211021679
325. Beckstein JC, Sen S, Schaer TP, Vresilovic EJ, Elliott DM. Comparison of animal discs used in disc research to human lumbar disc: axial compression mechanics and glycosaminoglycan content. *Spine (Phila Pa 1976)*. Mar 15 2008;33(6):E166-73. doi:10.1097/BRS.0b013e318166e001
326. Nishimura K, Mochida J. Percutaneous reinsertion of the nucleus pulposus. An experimental study. *Spine (Phila Pa 1976)*. Jul 15 1998;23(14):1531-8; discussion 1539. doi:10.1097/00007632-199807150-00006
327. Osti OL, Vernon-Roberts B, Fraser RD. 1990 Volvo Award in experimental studies. Anulus tears and intervertebral disc degeneration. An experimental study using an animal model. *Spine (Phila Pa 1976)*. Aug 1990;15(8):762-7. doi:10.1097/00007632-199008010-00005
328. Adams MA, Freeman BJ, Morrison HP, Nelson IW, Dolan P. Mechanical initiation of intervertebral disc degeneration. *Spine (Phila Pa 1976)*. Jul 1 2000;25(13):1625-36. doi:10.1097/00007632-200007010-00005
329. Smith L. ENZYME DISSOLUTION OF THE NUCLEUS PULPOSUS IN HUMANS. *Jama*. Jan 11 1964;187:137-40. doi:10.1001/jama.1964.03060150061016
330. Hoogendoorn RJ, Wuisman PI, Smit TH, Everts VE, Helder MN. Experimental intervertebral disc degeneration induced by chondroitinase ABC in the goat. *Spine (Phila Pa 1976)*. Aug 1 2007;32(17):1816-25. doi:10.1097/BRS.0b013e31811ebac5
331. Hoogendoorn R, Doulabi BZ, Huang CL, Wuisman PI, Bank RA, Helder MN. Molecular changes in the degenerated goat intervertebral disc. *Spine (Phila Pa 1976)*. Jul 15 2008;33(16):1714-21. doi:10.1097/BRS.0b013e31817d2468
332. Detiger SE, Holewijn RM, Hoogendoorn RJ, et al. MRI T2* mapping correlates with biochemistry and histology in intervertebral disc degeneration in a large animal model. *Eur Spine J*. Sep 2015;24(9):1935-43. doi:10.1007/s00586-014-3498-1
333. Sasaki M, Takahashi T, Miyahara K, Hirose, Tsuneo. Effects of Chondroitinase ABC on Intradiscal Pressure in Sheep: An: In Vivo: Study. *Spine*. 2001;26(5):463-468.
334. Lee NN, Salzer E, Bach FC, et al. A comprehensive tool box for large animal studies of intervertebral disc degeneration. *JOR Spine*. Jun 2021;4(2):e1162. doi:10.1002/jsp2.1162
335. Purmessur D, Walter BA, Roughley PJ, Laudier DM, Hecht AC, Iatridis J. A role for TNFα in intervertebral disc degeneration: a non-recoverable catabolic shift. *Biochem Biophys Res Commun*. Mar 29 2013;433(1):151-6. doi:10.1016/j.bbrc.2013.02.034
336. Yang S, Li L, Zhu L, et al. Aucubin inhibits IL-1β- or TNF-α-induced extracellular matrix degradation in nucleus pulposus cell through blocking the miR-140-5p/CREB1 axis. *Journal of Cellular Physiology*. 2019;234(8):13639-13648. doi:https://doi.org/10.1002/jcp.28044
337. Phillips KLE, Cullen K, Chiverton N, et al. Potential roles of cytokines and chemokines in human intervertebral disc degeneration: interleukin-1 is a master regulator of catabolic processes. *Osteoarthritis and Cartilage*. 2015/07/01/ 2015;23(7):1165-1177. doi:https://doi.org/10.1016/j.joca.2015.02.017
338. Yarilina A, Xu K, Chen J, Ivashkiv LB. TNF activates calcium-nuclear factor of activated T cells (NFAT)c1 signaling pathways in human macrophages. *Proc Natl Acad Sci U S A*. Jan 25 2011;108(4):1573-8. doi:10.1073/pnas.1010030108
339. Notarangelo MP, Penolazzi L, Lambertini E, et al. The NFATc1/P2X7 receptor relationship in human intervertebral disc cells. *Front Cell Dev Biol*. 2024;12:1368318. doi:10.3389/fcell.2024.1368318

340. Liu M, Duan X, Lou C. Quercetin alleviates intervertebral disc degeneration by disrupting CEBPB-HMGA1 interaction to suppress TNFA production and reduce ECM degradation. *Int Immunopharmacol*. Dec 10 2025;167:115654. doi:10.1016/j.intimp.2025.115654
341. Elshamly M, Kinslechner K, Grohs JG, et al. Galectins-1 and -3 in Human Intervertebral Disc Degeneration: Non-Uniform Distribution Profiles and Activation of Disease Markers Involving NF-κB by Galectin-1. *J Orthop Res*. Oct 2019;37(10):2204-2216. doi:10.1002/jor.24351
342. Zhang C, Gullbrand SE, Schaer TP, et al. Combined Hydrogel and Mesenchymal Stem Cell Therapy for Moderate-Severity Disc Degeneration in Goats. *Tissue Eng Part A*. Jan 2021;27(1-2):117-128. doi:10.1089/ten.TEA.2020.0103
343. Holm S, Maroudas A, Urban JP, Selstam G, Nachemson A. Nutrition of the intervertebral disc: solute transport and metabolism. *Connect Tissue Res*. 1981;8(2):101-19. doi:10.3109/03008208109152130
344. Yin X, Motorwala A, Vesvoranan O, Levene HB, Gu W, Huang C-Y. Effects of Glucose Deprivation on ATP and Proteoglycan Production of Intervertebral Disc Cells under Hypoxia. *Scientific Reports*. 2020/06/01 2020;10(1):8899. doi:10.1038/s41598-020-65691-w
345. Bibby SR, Urban JP. Effect of nutrient deprivation on the viability of intervertebral disc cells. *Eur Spine J*. Dec 2004;13(8):695-701. doi:10.1007/s00586-003-0616-x
346. Zhu Y, Zhao S, Deng Y, et al. Hepatic GALE Regulates Whole-Body Glucose Homeostasis by Modulating Tff3 Expression. *Diabetes*. Nov 2017;66(11):2789-2799. doi:10.2337/db17-0323
347. Zhang T, Feng P, Alexander PG, Lee JY, Sowa GA, Vo NV. Lactate Metabolism in the Intervertebral Disc: Mechanistic Insights and Pathological Implications. *Biomolecules*. 2026;16(1):170.
348. Wilson N, Ní Néill T, McDonnell J, McDonnell E, Brama PAJ, Buckley CT. Influence of the Intervertebral Disc Microenvironment on Matrix Synthesis and Metabolism in Goat Nucleus Pulposus Cells. *JOR Spine*. Mar 2026;9(1):e70160. doi:10.1002/jsp2.70160
349. Rajagopal K, Schaer TP, Meadows KD, et al. In Vivo Measurements Reveal Increased Nucleus Pulposus Lactate and Oxygen Concentrations in a Goat Model of Intervertebral Disc Degeneration. *JOR Spine*. Jun 2025;8(2):e70076. doi:10.1002/jsp2.70076
350. Mao Z, Liu W, Zou R, et al. Glibenclamide targets MDH2 to relieve aging phenotypes through metabolism-regulated epigenetic modification. *Signal Transduction and Targeted Therapy*. 2025/02/17 2025;10(1):67. doi:10.1038/s41392-025-02157-3
351. Chen X, Shi C, He M, Xiong S, Xia X. Endoplasmic reticulum stress: molecular mechanism and therapeutic targets. *Signal Transduction and Targeted Therapy*. 2023/09/15 2023;8(1):352. doi:10.1038/s41392-023-01570-w
352. Lolli A, Sivasubramaniyan K, Vainieri ML, et al. Hydrogel-based delivery of antimiR-221 enhances cartilage regeneration by endogenous cells. *Journal of Controlled Release*. 2019/09/10/ 2019;309:220-230. doi:https://doi.org/10.1016/j.jconrel.2019.07.040
353. Intini C, Ferreras LB, Casey S, Dixon JE, Gleeson JP, O'Brien FJ. An Innovative miR-Activated Scaffold for the Delivery of a miR-221 Inhibitor to Enhance Cartilage Defect Repair. *Advanced Therapeutics*. 2023;6(7):2200329. doi:https://doi.org/10.1002/adtp.202200329
354. Detiger SEL, Helder MN, Smit TH, Hoogendoorn RJW. Adverse effects of stromal vascular fraction during regenerative treatment of the intervertebral disc: observations in a

goat model. *European Spine Journal*. 2015/09/01 2015;24(9):1992-2000. doi:10.1007/s00586-015-3803-7
355. Steffen F, Bertolo A, Affentranger R, Ferguson SJ, Stoyanov J. Treatment of Naturally Degenerated Canine Lumbosacral Intervertebral Discs with Autologous Mesenchymal Stromal Cells and Collagen Microcarriers: A Prospective Clinical Study. *Cell Transplant*. Feb 2019;28(2):201-211. doi:10.1177/0963689718815459
356. Steffen F, Smolders LA, Roentgen AM, Bertolo A, Stoyanov J. Bone Marrow-Derived Mesenchymal Stem Cells as Autologous Therapy in Dogs with Naturally Occurring Intervertebral Disc Disease: Feasibility, Safety, and Preliminary Results. *Tissue Eng Part C Methods*. Nov 2017;23(11):643-651. doi:10.1089/ten.TEC.2017.0033
357. Augustin JA, Burt KG, Barrett C, et al. Neuroimmune Activation in a Goat Model of Intervertebral Disc Degeneration. *Cells*. 2026;15(3):286.
358. Yuan Q, Du L, Xu H, et al. Autologous Mesenchymal Stromal Cells Combined with Gelatin Sponge for Repair Intervertebral Disc Defect after Discectomy: A Preclinical Study in a Goat Model. *Front Biosci (Landmark Ed)*. 2022-04-19 2022;27(4):131-. doi:10.31083/j.fbl2704131
359. Freeman BJC, Kuliwaba JS, Jones CF, et al. Allogeneic Mesenchymal Precursor Cells Promote Healing in Postero-lateral Annular Lesions and Improve Indices of Lumbar Intervertebral Disc Degeneration in an Ovine Model. *Spine (Phila Pa 1976)*. Sep 2016;41(17):1331-1339. doi:10.1097/brs.0000000000001528
360. Schmitt C, Radetzki F, Stirnweiss A, et al. Long-term pre-clinical evaluation of an injectable chitosan nanocellulose hydrogel with encapsulated adipose-derived stem cells in an ovine model for IVD regeneration. *J Tissue Eng Regen Med*. Jul 2021;15(7):660-673. doi:10.1002/term.3216
361. Alsousou J, Ali A, Willett K, Harrison P. The role of platelet-rich plasma in tissue regeneration. *Platelets*. 2013;24(3):173-82. doi:10.3109/09537104.2012.684730
362. Russell W, Burch R. The Principles of Humane Experimental. *Technique London: Methuen*. 1959;
363. Fatoye F, Gebrye T, Ryan CG, Useh U, Mbada C. Global and regional estimates of clinical and economic burden of low back pain in high-income countries: a systematic review and meta-analysis. *Front Public Health*. 2023;11:1098100. doi:10.3389/fpubh.2023.1098100
364. Global, regional, and national burden of low back pain, 1990-2020, its attributable risk factors, and projections to 2050: a systematic analysis of the Global Burden of Disease Study 2021. *Lancet Rheumatol*. Jun 2023;5(6):e316-e329. doi:10.1016/s2665-9913(23)00098-x
365. Shu J, Xia Z, Li L, et al. Dose-dependent differential mRNA target selection and regulation by let-7a-7f and miR-17-92 cluster microRNAs. *RNA Biology*. 2012/10/01 2012;9(10):1275-1287. doi:10.4161/rna.21998
366. Yuan M, Pai P-J, Liu X, Lam H, Chan BP. Proteomic Analysis of Nucleus Pulposus Cell-derived Extracellular Matrix Niche and Its Effect on Phenotypic Alteration of Dermal Fibroblasts. *Scientific Reports*. 2018/01/24 2018;8(1):1512. doi:10.1038/s41598-018-19931-9
367. Bautista CA, Park HJ, Mazur CM, Aaron RK, Bilgen B. Effects of Chondroitinase ABC-Mediated Proteoglycan Digestion on Decellularization and Recellularization of Articular Cartilage. *PLoS One*. 2016;11(7):e0158976. doi:10.1371/journal.pone.0158976
368. Le Maitre CL, Hoyland JA, Freemont AJ. Catabolic cytokine expression in degenerate and herniated human intervertebral discs: IL-1β and TNFα expression profile. *Arthritis Research & Therapy*. 2007/08/09 2007;9(4):R77. doi:10.1186/ar2275

369. Sun Z, Liu B, Liu ZH, et al. Notochordal-Cell-Derived Exosomes Induced by Compressive Load Inhibit Angiogenesis via the miR-140-5p/Wnt/β-Catenin Axis. *Mol Ther Nucleic Acids*. Dec 4 2020;22:1092-1106. doi:10.1016/j.omtn.2020.10.021
370. Mahboudi H, Soleimani M, Enderami SE, et al. Enhanced chondrogenesis differentiation of human induced pluripotent stem cells by MicroRNA-140 and transforming growth factor beta 3 (TGFβ3). *Biologicals*. Mar 2018;52:30-36. doi:10.1016/j.biologicals.2018.01.005
371. Nakamura Y, He X, Kato H, et al. Sox9 is upstream of microRNA-140 in cartilage. *Appl Biochem Biotechnol*. Jan 2012;166(1):64-71. doi:10.1007/s12010-011-9404-y
372. Jiang H, Moro A, Wang J, Meng D, Zhan X, Wei Q. MicroRNA-338-3p as a novel therapeutic target for intervertebral disc degeneration. *Experimental & Molecular Medicine*. 2021/09/01 2021;53(9):1356-1365. doi:10.1038/s12276-021-00662-3
373. Kim T-W, Kim A-G, Hwang M-H, Choi H. Intervertebral disc spheroids as an in vitro multicellular platform for recapitulating the microenvironment of intervertebral disc degeneration. *Biofabrication*. 2025/06/26 2025;17(3):035023. doi:10.1088/1758-5090/ade56c
374. Moxon SR, McMurran Z, Kibble MJ, Domingos M, Gough JE, Richardson SM. 3D bioprinting of an intervertebral disc tissue analogue with a highly aligned annulus fibrosus via suspended layer additive manufacture. *Biofabrication*. Oct 24 2024;17(1)doi:10.1088/1758-5090/ad8379
375. Zhu Y, Liu Q, Yu C, et al. An Intervertebral Disc (IVD) Regeneration Model Using Human Nucleus Pulposus Cells (iHNPCs) and Annulus Fibrosus Cells (iHAFCs). *Adv Healthc Mater*. Apr 2025;14(10):e2403742. doi:10.1002/adhm.202403742
376. Deyo RA, Von Korff M, Duhrkoop D. Opioids for low back pain. *Bmj*. Jan 5 2015;350:g6380. doi:10.1136/bmj.g6380
377. Mohd Isa IL, Teoh SL, Mohd Nor NH, Mokhtar SA. Discogenic Low Back Pain: Anatomy, Pathophysiology and Treatments of Intervertebral Disc Degeneration. *Int J Mol Sci*. Dec 22 2022;24(1)doi:10.3390/ijms24010208
378. Teichtahl AJ, Urquhart DM, Wang Y, et al. Modic changes in the lumbar spine and their association with body composition, fat distribution and intervertebral disc height - a 3.0 T-MRI study. *BMC Musculoskelet Disord*. Feb 19 2016;17:92. doi:10.1186/s12891-016-0934-x
379. Boden SD, McCowin PR, Davis DO, Dina TS, Mark AS, Wiesel S. Abnormal magnetic-resonance scans of the cervical spine in asymptomatic subjects. A prospective investigation. *J Bone Joint Surg Am*. Sep 1990;72(8):1178-84.
380. García-Cosamalón J, del Valle ME, Calavia MG, et al. Intervertebral disc, sensory nerves and neurotrophins: who is who in discogenic pain? *J Anat*. Jul 2010;217(1):1-15. doi:10.1111/j.1469-7580.2010.01227.x
381. Hirsch BP, Sossamon J, Khan MA, et al. Applications of SPECT/CT in the Evaluation of Spinal Pathology: A Review. *Int J Spine Surg*. Mar 4 2024;18(1):9-23. doi:10.14444/8552
382. Varga M, Kantorová L, Langaufová A, et al. Role of Single-Photon Emission Computed Tomography Imaging in the Diagnosis and Treatment of Chronic Neck or Back Pain Caused by Spinal Degeneration: A Systematic Review. *World Neurosurgery*. 2023/05/01/ 2023;173:65-78. doi:https://doi.org/10.1016/j.wneu.2023.02.058
383. Russo VM, Dhawan RT, Dharmarajah N, Baudracco I, Lazzarino AI, Casey AT. Hybrid Bone Single Photon Emission Computed Tomography Imaging in Evaluation of Chronic Low Back Pain: Correlation with Modic Changes and Degenerative Disc Disease. *World Neurosurg*. Aug 2017;104:816-823. doi:10.1016/j.wneu.2017.03.107

384. Van der Heiden K, Barrett HE, Meester EJ, et al. SPECT/CT imaging of inflammation and calcification in human carotid atherosclerosis to identify the plaque at risk of rupture. *J Nucl Cardiol*. Oct 2022;29(5):2487-2496. doi:10.1007/s12350-021-02745-0
385. Hooper N, Ierulli J, Demarest C, Pitts J, Olufade OA, Williams C. Long-Term Effectiveness of Intradiscal Culture-Expanded Mesenchymal Stem Cells (MSCs) with Platelet Products for Discogenic Low Back Pain. *Biomedicines*. Sep 26 2025;13(10)doi:10.3390/biomedicines13102365
386. Elabd C, Centeno CJ, Schultz JR, Lutz G, Ichim T, Silva FJ. Intra-discal injection of autologous, hypoxic cultured bone marrow-derived mesenchymal stem cells in five patients with chronic lower back pain: a long-term safety and feasibility study. *J Transl Med*. Sep 1 2016;14(1):253. doi:10.1186/s12967-016-1015-5
387. Pettine KA, Suzuki RK, Sand TT, Murphy MB. Autologous bone marrow concentrate intradiscal injection for the treatment of degenerative disc disease with three-year follow-up. *International Orthopaedics*. 2017/10/01 2017;41(10):2097-2103. doi:10.1007/s00264-017-3560-9

Appendices

Appendix A. Standard operating protocols (SOPs) established within this thesis.

A.1 miRNA transfection with cell penetrating peptides RALA and FLR in 2D

Background:

FLR is used at a concentration of 0.1 M, RALA 30.04 nmol (ie 60 µl 1X TE Buffer to 0.1mg aliquot). RALA is synthesised by Genscript custom peptide synthesis. The charge ratios of 10 for RALA and 5 for FLR have been previously optimised, as has 10 ng/µl miRNA for rat and goat nucleus pulposus (NP), bone marrow derived stem cells (BMSCs), and monocytes. However, if attempting transfection with a new cell type, a dosage study using a fluorescently tagged miRNA may be required.

Procedure:

miRNA from Miridian Dharmacon have been trialled, and prepared to aliquots of 30 ng/µl, ie 1.25 mL 1X TE Buffer per 5 nmol of miRNA, aliquoted into a suitable amount to reduce the amount of freeze/thaw cycles.

Seed cells at an appropriate density, ex 5000/well of ibidi 18-well chamber slide for NP and BMSCs and allow overnight to attach.

On the day of transfection, prepare the complexes as follows, using Lipofectamine RNAiMAX Transfection reagent as a control for transfection. A negative or scrambled control should be used in initial experiments to ensure transfection does not have any effects on cell function. Each experiment should also have a non-transfected (NT) control that receives OptiMEM only.

To prepare 65 µl of complexes:

	µl
RALA	4.97
miRNA	21.51
OptiMEM	38.33
FLR	3.31

miRNA	21.51
OptiMEM	41.11
Lipofectamine	3.9
miRNA	21.51
OptiMEM	39.59

Combine and mix well, allow complexes to form for 30 minutes at room temperature.

Remove media from wells, wash once with PBS, and add complexes or OptiMEM for the NT controls as appropriate. Return cells to the incubator.

Allow transfection to continue for 6 hours, after this, remove complexes and replace with your culture media, culturing for your given timepoint for functional analysis. As an example, uptake of a fluorescently tagged miRNA could be a time-course ranging from 24 hours to 7 days, protein expression generally is from 3 to 7 days, though this should be tailored to the cell type and output.

A.2 miRNA transfection with cell penetrating peptides RALA and FLR in rat and goat ex vivo organ culture

FLR is used at a concentration of 0.1 M, RALA 30.04 nmol (ie 60 µl 1X TE Buffer to 0.1mg aliquot). RALA is synthesised by Genscript custom peptide synthesis. The charge ratios of 10 for RALA and 5 for FLR have been previously optimised, as has 25 ng/µl miRNA for direct delivery into rat and goat IVD organs.

miRNA from Miridian Dharmacon have been trialled, and prepared to aliquots of 30 ng/µl, ie 1.25 mL 1X TE Buffer per 5 nmol of miRNA, aliquoted into a suitable amount to reduce the amount of freeze/thaw cycles.

Culture organs for a suitable amount of time to allow degeneration to occur, ex. 7 days of 0.0025 U cABC for mild degeneration in rat, 14 days 2U or 4U for mild or severe degeneration respectively for goat.

Rat organs can have 2 µl of complexes injected, goats 200 µl via a Hamilton syringe, use 31 G needle for rat and 22G for goat.

To prepare 200 µl of 25 ng/µl complexes, adjust as needed:

	µl
RALA	12.8
miRNA	156
OptiMEM	31.2
FLR	25.54
miRNA	156
OptiMEM	18.46

A.3 Live/dead assessment of rat ex vivo organ culture

Caudal rat organs are cultured up to the relevant timepoints, for example, T0 taken on day of isolation, T7 for 1 week degeneration, and T21 for end of culture period following two weeks of treatment. Using this method, viability of the nucleus pulpous (NP) region can be estimated.

Procedure:

Remove the discs from culture, label glass Superfrost slides or confocal dishes.

Prepare live/dead assay solution: 20µL EthD-1 (stock: 2 mM, Biotium BT40014) + 5µL Calcein (stock: 4mM, Biotium BT80011-1) + 10mL PBS in a 15ml Falcon tube. This makes a 4uM EthD-1 and 2uM Calcein concentration. Shield from light.

Make an incision along the bounding endplate to open the IVE along the transverse plane, exposing the disc. Scoop out the NP using a needle point tweezers and place onto the slide or confocal dish.

Add live/dead solution, cover with tin foil and incubate at 37°C for 30 minutes to 1 hour.

Wash three times with PBS.

Image on the confocal or fluorescent microscope, excitation/emission wavelengths:

Calcein 485 nm/515 nm

EthD-1 525 nm/590 nm

A.4 Live/dead assessment of goat ex vivo organ culture

This SOP is based off Paul *et al* 2012.[286]

Goat organs are cultured up to the relevant timepoints, for example, T0 taken on day of isolation, T14 for 2 weeks degeneration, and T28 for end of culture period. Using this method, viability of both the annulus fibrosus (AF) and nucleus pulpous (NP) regions can be estimated.

Dissect intact disc from IVD, maintaining the AF and NP regions. Do for both sides of the disc as below:

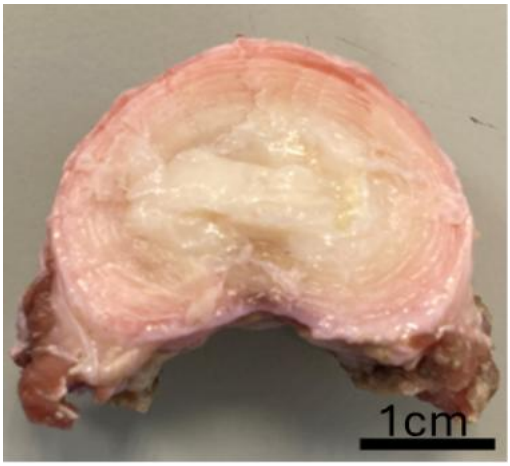

Prepare live/dead assay solution: 20µL EthD-1 (stock: 2 mM, Biotium BT40014) + 5µL Calcein (stock: 4mM, Biotium BT80011-1) + 10mL PBS in a 15ml Falcon tube. This makes a 4uM EthD-1 and 2uM Calcein concentration.

Place solution and disc in a 6-well plate, cover with tin foil and incubate in an oven at 37°C for 1 hour.

Wash three times with PBS.

Place in the largest size mould and cover with OCT medium, put inside an empty 20 µl or 200 µl tip container. Fill an empty 1000 µl tip container with liquid nitrogen in the fume hood. Using the surgical clamp to grip the smaller of the tip containers, gently place in the liquid nitrogen filled container.

Allow for the OCT to freeze, approximately 5 minutes, and remove with the surgical clamp. Leave the remaining liquid nitrogen to in the hood to sublimate, with a sign to let others know there is liquid nitrogen in the hood.

Slice on the cryostat at a thickness of 10 µm, keep the mounted slides shielded from light.

Image on the confocal or fluorescent microscope, excitation/emission wavelengths:

Calcein 485 nm/515 nm

EthD-1 525 nm/590 nm

Appendix B. Chapter 4

B.1 List of gene name abbreviations for miRNA-149-5p enrichment analysis

Abbreviation	Full Name
BBC3	Bcl-2-binding component 3
FASLG	Fas ligand
FOXM1	Forkhead box protein M1
GIT1	G protein-coupled receptor kinase interacting ArfGAP1
GPC1	Glypician 1
IL6	Interleukin-6
MYD88	Myeloid differentiation primary response protein 88
PTGER2	Prostaglandin E Receptor 2
ZBTB2	Zinc Finger and BTB Domain Containing 2

B.2 List of gene abbreviations for miRNA-221-3p enrichment analysis

Abbreviation	Full Name
ANXA1	Annexin A1
ARNT	Aryl Hydrocarbon Receptor Nuclear Translocator
BBC3	Bcl-2-binding component 3
BCL2L11	Bcl-2-like 11
BECN1	Beclin 1
BMF	Bcl Modifying Factor
BNIP3	Bcl-2 interacting protein 3
BNIP3L	Bcl-2 interacting protein 3 like
BRAP	BRCA1 associated protein

CDKN1C	Cyclin Dependent Kinase Inhibitor 1C
CORO1A	Coronin 1A
CXCL12	C-X-C Motif Chemokine Ligand 12
DIRAS3	Distinct subgroup of the Ras family member 3
DKK2	Dickkopf WNT Signalling Pathway Inhibitor 2
DVL2	Dishevelled Segment Polarity Protein 2
FMR1	Fragile X messenger ribonucleoprotein 1
MBD2	Methyl-CpG binding domain protein 2
MMP2	Matrix Metallopeptidase 2
PAK1	P21 (RAC1) activated kinase 1
PTEN	Phosphatase and tensin homolog
RB1	RB transcriptional corepressor 1
SELE	Selectin E
SOCS3	Suppressor of cytokine signalling 3
SSX2IP	Synovial sarcoma X breakpoint 2 interacting protein
STAT5A	Signal transducer and activator of transcription 5A
TBK1	TANK binding kinase 1
TICAM1	TIR domain containing adaptor molecule 1
TIMP3	Tissue inhibitor of metalloproteinase 3
TNFSF10	TNF superfamily member 10
USP18	Ubiquitin specific peptidase 18

Appendix C. Abstract

Low back pain is one of the leading causes of disability worldwide, with its prevalence growing. Believed to be predominately caused through degeneration of the intervertebral disc (IVD), current treatments are conservative and do not target the homeostatic imbalance at the core of the degradative cascade. This dysregulation is characterised by a disruption to and loss of key extracellular matrix (ECM) proteins, with a concurrent aggravated inflammatory and catabolic response. microRNAs (miRNAs) can regulate the expression of multiple target genes, making them an attractive treatment option. Subsequently, this thesis aims to explore miRNA approaches with the aim of developing a translationally relevant injectable therapy that will impart a multimodal effect: suppression of the inflammatory milieu and promoting of regenerative ECM factors.

Firstly, this work screened miRNAs identified from the literature with the aim of identifying the most suitable for IVD delivery, systematically evaluating their anti-catabolic and pro-matrix potential. Concurrently two cell penetrating peptides (CPPs) were assessed for optimal delivery to the nucleus pulposus (NP) of the IVD. To enhance therapeutic the miRNAs were co-delivered in pairs to investigate possible synergistic effects. Secondly, this thesis explored adjunct stimulation in combination with dual-miRNA treatment. For this purpose, human platelet lysate (HPL), a clinically established regenerative aid in the orthopaedics and musculoskeletal field, was delivered alongside the selected dual-miRNA. Cell transplantation to the IVD has been suggested as a method to replace the native population that was depleted through degeneration. Therefore, the third aim of this work was to compare dual-miRNA stimulation of NP and bone marrow derived stem cells (BMSCs) to analyse the most appropriate cell source for IVD delivery. Finally, the optimised dual-miRNA formulation was evaluated in a preclinical large animal model of mild IVD degeneration, to determine its safety, efficacy, and translational feasibility.

Overall, this work highlights miRNAs as a promising component to injectable therapies for IVD degeneration, exploring their utility alone, in pairs, and combined with external factors, both HPL and cells. By integrating a robust experimental framework with physiologically relevant culture and preclinical models the findings presented here support the translational potential of miRNA-based therapies for clinical applications to target IVD degeneration.